

Conference Proceedings

Hydrogen and Syngas - Platform for a sustainable future

October 28 - 29, 2025 | Essen



DGMK und Autor(en) haben alle Sorgfalt walten lassen, um vollständige und akkurate Informationen in diesem Buch zu publizieren. Der Verlag übernimmt weder Garantie noch die juristische Verantwortung oder irgendeine Haftung für die Nutzung dieser Informationen, für deren Wirtschaftlichkeit oder fehlerfreie Funktion für einen bestimmten Zweck. Die DGMK übernimmt keine Gewähr dafür, dass die beschriebenen Verfahren, Programme usw. frei von Schutzrechten Dritter sind.

Alle Rechte vorbehalten
© DGMK e.V., Hamburg, 2025

Für Copyright in Bezug auf das verwendete Bildmaterial siehe Quellenangaben in den Abbildungsunterschriften. Abbildungen ohne Quellenangabe sind von den Autoren.

Das Werk einschließlich aller seiner Teile ist urheberrechtlich geschützt. Jede Verwertung außerhalb der engen Grenzen des Urheberrechtsgesetzes ist ohne Zustimmung der DGMK unzulässig und strafbar. Das gilt insbesondere für Vervielfältigungen, Übersetzungen, Mikroverfilmungen und die Einspeicherung und Verarbeitung in elektronischen Systemen.

The work including all its parts is protected by copyright. Any use outside the narrow limits of the German Copyright Law without the consent of the DGMK is prohibited and punishable by law. This applies in particular to reproduction, translation, microfilming and storage and processing in electronic systems.

Umschlaggestaltung: DIE NEUDENKER®, Darmstadt | DGMK e.V., Hamburg Titelfotografie: 2019 FrankHH/Shutterstock.com

ISSN 3052-1629 ISBN 978-3-947716-75-3

CONTENTS	Page
From Ambition to Infrastructure: The Industrial Imperative for Hydrogen and Syngas B. Bergt, T. Kehler	1
Power-to-X in Chile, Namibia, and Saudi Arabia: A Systematic Cross-Regional Assessment of Costs, Emissions, and Land Use U. Langenmayr, V. Slednev, P. Heinzmann	2
Amino Acid based Carbon Capture Technology – from DAC to point sources applications R. Gesthuisen, U. Dietz, J. Nottbohm, T. Bittner	17
Evaluating Electrochemical Mineral Trapping for Carbon Dioxide Removal: Insights from Experiments and Predictive Modeling D. Groh, J. Staudt, K. Kanokkanchana, M. Ibañez, N. Plumeré, J. Burger	25
Pathways to Low Carbon Hydrogen A. Behrens, JP. Bohn, N. Schödel	44
Decarbonization of Syngas and Hydrogen Production M. Marchionna	45
Experimental Investigation of Syngas Purification from Biogenic Residue Gasification L. Hassel, J. Kaltenmorgen, F. Panitz, M. Siodlaczek, P. Eiden, J. Ströhle, B. Epple	53
Novel Joule-heated Reactor based on Radial Current and Flow for the Intensification of Endothermic Catalytic Processes L. Cozzarolo, F. Romanelli, C. Ferroni, M. Ambrosetti, B. Mello Gabbrielleschi, M. Bracconi, M. Maestri, G. Groppi, A. Beretta, B. Williams, E. Tronconi	65
Potential of Dimethylether as a large-scale chemical hydrogen carrier A. Peschel	66
Catalysts for Hydrogen Storage based on Liquid Organic Hydrogen Carriers B. Bong, C. Mebrahtu, R. Palkovits	67
Advanced Catalyst and Reactor Engineering for Efficient Hydrogen Release from Perhydro-Benzyltoluene E. Herzinger, H. Park, J. Weimann, J. Berger, O. Kırlangıçoğlu, J. Biesinger, M. Wolf	86
Light-assisted thermal catalysis for hydrogen storage in a "methanol economy" M. Rehner, K. Blank, J. Huang, J. Strunk	87
CO ₂ methanation as a strategy for green H ₂ storage and distribution: experimental optimisation and process design M. Tommasi, A. Gramegna, S. Romegialli, G. Ramis, I. Rossetti	88

A chemical and engineering analysis of the conversion of biomass to lactic acid using POMs under nitrogen atmosphere E. Hundt , JD. Krueger, A. Pawlig, L. Schidowski, I. Wirth, M. J. Poller, D. Voß, J. Albert	89
Transforming wet biomass waste into sustainable methanol: Concept study of a competitive and mild process route P. Nathrath, F. Kroll, D. Karmann, V. Haagen, D. Weber, T. Franken, M. Geißelbrecht, P. Schühle	90
NET-Fuels – Integrating negative emission technologies in biofuels production M. Meiller, C. Groves, F. Lehner, C. Kick, R. Daschner, B. Kocacenk, A. Apfelbacher, N. Hagemann, D. Chiari, A. Contin, D. Marazza, M. Proniewicz, K. Petela, A. Szlek, M. Vega-Paredes, D. Molognoni, E. Borràs	91
The role of hydrogen and syngas for coupling energy transformation and circular economy F. Scheiff, T. Kolb, S. Bajohr, F. Graf, S. Fleck, U. Santo, T. Jakobs, M. Haas, W. Köppel	108
Excellent T Control in Compact Fischer–Tropsch Reactor with Al Packed POCS M. Panzeri, C.Giorgio Visconti, G. Groppi, E. Tronconi	109
Shaping of a methanol catalyst: Parameter study of the tableting of CuO/ZnO/ZrO₂ F. Neumann, M. Herfet, S. Grewe, L. Warmuth, T.A. Zevaco, T.N. Otto, M. Zimmermann, S. Pitter, M. Wolf	110
Towards Sustainable Ethene Production: Modified Fischer-Tropsch Synthesis from CO ₂ and H ₂ K. Laichter, A. Chowdhury, V. Hagen, T. Liese, M. Doeker, F. Buschsieweke, J. Hannes, F. Heck, HJ. Woelk, I. J. Graef, T. E. Müller	111
Enzyme-Inspired Gel Materials: Tuneable Gels for Hydroformylation P. McNeice, W. Leitner, A. J. Vorholt	128
From Syngas to Alcohol E-fuels –Scale up from lab to miniplant H. Stieber, S. Popp, W. Leitner, G. Prieto, A. J. Vorholt	129
Upstream and Feedstock Requirements for Cost-Competitive Green Methanol Production M. Checinski, R. Krähnert, H. Mehmke, J. von der Ohe	130
Catalyst study for selective catalytic oxidation of residual ammonia for purification of green hydrogen from ammonia cracking A. Sack, A. Gradel, HP. Schmid, J. Wünning, T. Plessing, A. Jess	131
Elevating the C ₂ to C ₄ Chemistry M. Belleflamme, F. S. Heinen, S. Mersmann, A. J. Vorholt	132

Chemical Industry	133
L. Steinwachs, A. Bauer, E. Jodat, Rüdiger Eichel, R. Pastusiak, E. Simon, M. Kristen, R. Franke, A. Vorholt	
Microwave-Assisted Catalytic Polymer Cracking into Hydrogen at Low Temperatures Using Ionic Liquids and Nanoparticles K. Bürner, M. Haumann	134
Tandem Fischer-Tropsch Synthesis and Reductive Hydroformylation under Mild Conditions for Optimized Higher Oxygenate E-Fuels S. Popp, H. Stieber, W. Leitner, G. Prieto, A. J. Vorholt	135
Development and Enhancement of Iron-Based Catalysts to Boost the Conversion of CO ₂ to Liquid Hydrocarbons <i>F. Mai, A. Jess</i>	136
WasteWood2Fuel – Development of a technology for the decentralised synthesis of liquid fuels from solid biogenic residues S. Kolb, C. Kern, A. Jess	137
Homogenous catalyst recovery by nanofiltration for the production of a potential hydrogen carrier such as formic acid from biomass L. Schidowski, D. Voß, M. Poller, J. Albert	138
Advanced biphasic selective glycerol oxidation in a jet loop reactor using polyoxometalates I. C. Wirth, D. Niehaus, D. Voß, J. Albert	139
Carbon-Encapsulated Magnetic Nanoparticles for Magnetocatalytic CO ₂ Hydrogenation to CO J. Hu, W. Leitner, A. Bordet	140
Improving Reactivity in Biphasic Hydroformylation of Long-Chain Olefins F. S. Heinen, Andreas J. Vorholt	141
Continuous Reductive Hydroformylation in a Segmented Slug Flow Reactor Using a Single Catalyst Enabled by CO-Degassing A. Windisch, P. Pey, D. Vogt, T. Seidensticker	142
Synthesis of suitable catalysts to produce synthesis gas through dry reforming of methane for green kerosene M. Bachstädter, A. Jess	143
Development of catalyst recycling strategies for the hydroformylation of olefins using methanol as a syngas source J. T. Groteguth, S. Stahl, J. Mädicke, W. Leitner, A. J. Vorholt	144
Polyoxometalates and strongly non-ideal solvent mixtures (SNISMs) towards boosting acid-catalysed esterification reactions L. Prawitt, P. Figiel, C. Held, M. Poller, J. Albert	145
Photocatalytic processes for energy storage S.N. Degerli, M. Tommasi, A. Gramegna, I. Rossetti, G. Ramis	146

CO ₂ Assisted Primary Amine Isolation and Catalyst Recycling in the Homogeneously Catalyzed Nitrile Hydrogenation and Alcohol Amination B. Rienhoff, N. Oppenberg, F. Zolthoff, D. Vogt, T. Seidensticker	147
Challenges of catalyst development for the load-flexible and integrated production of molecular hydrogen carriers from CO ₂ and water <i>T. Duyster, J. Artz, C. Mebrahtu, R. Palkovits</i>	148
Sustainable Hydrogen Generation via Continuous Dehydrogenation of Biomass-derived Formic Acid T. Hein, P. Schühle	149
Production of Syngas via Dehydration of Biogenic Aqueous Formic Acid coupled with the Water-Gas Shift Reaction E. Hoffmann, P. Schuehle	150
Shaping Methanol Synthesis from CO ₂ : Phase Transitions, Residence Time, and Reactor Design A. Böhmeke, K. Laichter, G. Nell, T. E. Müller	151
Towards Sustainable Ethene: Techno-Environmental Assessment of a Modified Fischer-Tropsch Pathway from CO ₂ and H ₂ M. Hebenbrock, V. Hagen, T. E. Müller	152
Selective Hydrogenation of Renewable Raw Materials Using Commercial Catalyst Systems D. Pietschmann, J. Bernstein, D. Vogt, T. Seidensticker	153
Carbon Capture and Hydrogen Plants - Overcoming Challenges and Optimizing Integration A. Wincierz	154
Operando spectroscopic techniques to investigate molecular catalysts in flow R. S. Medhekar, A. Sobolev, M. Gerlach, C. Hamel, W. Leitner, A. J. Vorholt	172
Linear, Aliphatic Polymer Precursors from Local Plant Oils through Cross Metathesis and Isomerizing Functionalisation J. Hommes, D. Vogt, T. Seidensticker	173
Direct, tandem catalysis synthesis of higher alcohols from syngas: the influence of water on reaction rates and alcohol (regio)selectivity F. Fiore, A. Rodriguez-Gomez, D. De Baker, M. Claeys, A. J. Vorholt, G. Prieto	174
Property-performance relationship assessment of tailored nanoparticles for alkaline water electrolysis T. Simson Sicila Mary, A. Barthelmeß, M. Wolf, J. Schröder	175
Methanolation of Olefins: Versatile low-pressure synthesis of various alcohols from olefins and methanol S. Stahl, J. T. Vossen, J. Mädicke, S. Popp, W. Leitner, A. J. Vorholt	176

From Ambition to Infrastructure: The Industrial Imperative for Hydrogen and Syngas Bengt Bergt, Timm Kehler Die Gas- und Wasserstoffwirtschaft e.V.

Abstract

Europe's energy and climate ambitions are clear – but ambition alone will not build infrastructure, secure competitiveness, or safeguard industrial value chains. Hydrogen and syngas are not niche topics for future scenarios; they are critical elements in a robust industrial policy for the present. While electrification plays a vital role in the energy transition, it cannot decarbonise all sectors. Molecules are indispensable where electrons reach their limits – in high-temperature processes, chemical feedstocks, and energy-dense applications. This keynote will explore the strategic role of gaseous molecules in preserving Europe's industrial core and closing the gap between political vision and infrastructure reality.

Power-to-X in Chile, Namibia, and Saudi Arabia: A Systematic Cross-Regional Assessment of Costs, Emissions, and Land Use

Langenmayr, Uwe^{1,} Slednev, Viktor¹, Heinzmann, Paul^{2,3}

- ¹ Karlsruhe Institute of Technology Institute for Industrial Production Chair of Energy Economics
- ² Karlsruhe Institute of Technology Institute for Industrial Production Chair of Production and Operations Management

³BASF

Abstract

Decarbonizing hard-to-abate sectors such as aviation, shipping, and chemical production requires carbon-neutral energy carriers beyond direct electrification. Power-to-X (PtX) processes, which convert renewable electricity into electricity-based hydrogen and hydrogen derivatives (eFuels), represent a promising solution but face challenges related to high production costs, renewable electricity intermittency, and system integration. This study applies an integrated modelling framework combining flowsheet optimization, technoeconomic assessment (TEA), life cycle analysis (LCA), renewable electricity generation modelling, and multi-objective optimization to evaluate PtX production at three representative locations: Chile, Saudi Arabia, and Namibia. Location-specific renewable resources, financial risks, and infrastructure availability are incorporated to assess production costs and greenhouse gas (GHG) emissions of hydrogen, methanol (MeOH), and Fischer-Tropsch (FT) fuels. The results demonstrate that hydrogen production exhibits lower costs and emissions than MeOH and FT fuels, primarily due to its operational flexibility and reduced need for auxiliary components. Among the locations, Chile shows a clear advantage with high wind capacity factors enabling low-cost, low-emission production. Namibia's mixed renewable profile offers beneficial trade-offs between costs and emissions, while Saudi Arabia faces higher emissions reduction costs due to less favourable renewable conditions. The Pareto analysis highlights the strong dependence of PtX system design on stakeholder preferences regarding cost-emission trade-offs, while the spatial analysis underscores the significant landuse requirements for large-scale deployment. The framework can support site-specific and global assessments of PtX projects, offering valuable insights for planning sustainable fuel production pathways.

Abbreviations

Carbon dioxide: CO₂

Electricity-based hydrogen and hydrogen derivatives: eFuels

Fischer-Tropsch: FT Greenhouse gas: GHG Life cycle analysis: LCA

Methanol: MeOH Power-to-X: PtX

Techno-economic assessment: TEA

Introduction

Anthropogenic climate change is one of the key challenges of our society. The current approach to abating GHG emissions mainly aims at energy efficiency measurements and the replacement of fossil electricity generation by renewable electricity generation. However, neither approach can directly address hard-to-abate sectors like aviation, shipping, or industry, since the electrification of these processes is technically infeasible. For example, the energy density of battery solutions is insufficient for long-distance flights and heavy-duty shipping. Furthermore, some processes, such as the production of chemicals, pharmaceuticals, or fertilisers, require the material application of hydrogen and its derivatives.

The current use of fossil fuels is not sustainable, and a continuation without major adjustments would impede climate change mitigation. Three approaches exist to address this challenge.

Biomass-based energy carriers, like biogas or E10, are already applied, but biomass has limited potential. First-generation biomass requires farmland, which is scarce in densely populated and industrialized countries, and there is competition with food consumption (tank-or-table discussion). An unexploited potential of second-generation biomass, such as residual waste or sewage waters, might exist, but cannot be scaled to cover global eFuels demands [1]. Carbon capture and storage removes the carbon dioxide (CO₂) from the fossil energy carrier and stores it eternally in CO₂ storage [2]. Finally, PtX produces electricity-based hydrogen and hydrogen derivatives (eFuels) by electrolysis. Here, an electrical current splits water into hydrogen and oxygen [3]. This hydrogen can be further synthesised into hydrogen derivatives using captured CO₂ or nitrogen. PtX is less affected by limited potential or the tank-or-table discussion of biomass, and avoids the debate on the ongoing fossil energy carrier dependency or the potential CO₂ leakage of the CO₂ infrastructure in the case of carbon capture and storage. However, the eFuels are only carbon neutral if the electricity is also carbon neutral and the CO₂ is acquired from sustainable sources like the atmosphere or biomass.

Even though it has several advantages, PtX has several challenges to overcome. First, high electricity demand and capital investment into electrolysis units drive hydrogen production costs. The cost disadvantage of eFuels in comparison to conventional energy carriers is one of the main reasons for the current hesitation of suppliers and consumers, which hinders the implementation of a hydrogen market.[4] Second, volatile renewable electricity generation comprises uncertainties that contradict the narrative of the chemical industry. Synthesis units are usually planned to maintain the temperatures, pressures, and contact times, among others, to achieve optimal production conditions [5]. However, the underlying uncertainty of volatility and availability of renewable electricity generation from wind and solar PV increases the demand for auxiliary components like electricity, hydrogen, and CO₂ storage units, and increases the flexibility demand of the system components. This holds especially true for stand-alone PtX plants, which cannot rely on a backup electricity supply.

High production costs, the necessary carbon neutrality, and the complex integration of volatile renewable electricity constitute significant challenges of PtX system planning, and only fully integrated approaches, which consider the technical complexity of the system, the renewable electricity generation, and the interaction between all system components, can address these challenges sufficiently.

Literature review, research gap, and research questions

Planning and assessing PtX plants are conducted in research using different approaches and narratives. The literature review concentrates on approaches that model stand-alone PtX systems to narrow down the literature review.

The first narrative follows the traditional approach, where a steady-state operation of the synthesis is assumed. This narrative is typically applied in methods like flowsheet optimisation in combination with TEA or LCA. The advantage of this approach is the detailed technical modelling and evaluation of the underlying processes regarding technical feasibility, economic performance, and environmental impact. However, the steady-state operation assumption allows only for scalar parameters, and time-dependent parameters like renewable electricity generation are often only considered as levelized costs of electricity and yearly capacity factors. [6–9] provide comprehensive literature reviews on the TEA and LCA of eFuels production.

The second narrative aims to model the temporal availability of renewable electricity generation and its effect on the dimensioning and operation of the PtX plant. The advantage is the detailed operation modelling, including system components, storage operations, and feedstock availability. However, considering that high-resolution temporal data increases the complexity of the model, detailed modelling of the technical, economic, and environmental performance might suffer since modelling trade-offs often exist, which hinder the simultaneous increase in complexity of different dimensions, such as temporal resolution and degree of technical details. Some exemplary publications following this narrative are [10–13]. This single-objective approach can be extended by assessing systems considering different objectives.

The economic or environmental assessment is often conducted after the technical [14] or the economic [15] analysis. Multi-objective optimisation evaluates various objectives simultaneously to assess the trade-off between objectives. For example, [16] determine production costs, land use, and water use, but their focus is a system-level analysis, avoiding detailed technical modelling of the PtX processes. [17] assess production costs and GHG emissions, but omit the modelling of the renewable electricity generation on a high temporal resolution.

So far, a comprehensive analysis including technical, economic, environmental, and multi-objective analysis has only been conducted in [18]. However, while this research considers the local renewable electricity generation as capacity factor profiles, it omits the consideration of geographic information system (GIS)-based information to enrich the PtX system analysis. This research streamlines the planning approach of stand-alone PtX plants. It conducts an integrated modelling approach of the PtX components using flowsheet optimisation to model the technical setup, deriving economic and environmental parameters based on the technical setup and data from literature, and uses multi-objective optimisation to evaluate the trade-off between production costs and GHG emissions. This assessment is complemented by the GIS-based assessment of the production location, including available infrastructure and space for installing renewable capacities.

Methodology

To comprehensively assess stand-alone PtX systems, [18] have developed an integrated approach (Figure 1), which is briefly described here and applied in this case study. This approach first defines the system design and boundaries of the applied methodology, including locations, technologies, feedstocks, and facility setup. Afterward, flowsheet optimisation using process simulation in Aspen Plus is applied to implement the different system components and optimise the technical setup. This method delivers the equipment list, mass and energy balances, and operation parameters required for the following spreadsheet-based TEA and LCA. The TEA quantifies CAPEX and OPEX of each system component based on the results of the process simulation and based on literature data, while the LCA assesses the environmental impact of the plant and derives the GHG emissions of component production, installation, operation, and disposal. The renewable generation is modelled for each location using the open-source software atlite [19] and ERA 5 data [20]. The output of atlite are hourly capacity factor profiles for wind and solar PV generation, covering the period of one year. Finally, the multi-objective optimisation combines technological, economic, environmental, and renewable generation data in an optimisation tool, which optimises the capacity of each component and its hourly operation. The multi-objective approach allows the simultaneous consideration of production costs and GHG emissions, and derives the Pareto front of the investment. This Pareto Front shows the trade-off between production costs and GHG emissions, which allows investors with different preferences to achieve their desired level of costs and emissions, as well as the respective component capacities of this preference. The multi-objective optimization tool is built to allow a general modelling of PtX processes, which includes the implementation of conversions based on mass and energy balances, storage units of all commodities in the system if required, and generators, which generate a commodity based on the hourly capacity factors. This general approach enables the user to build custom PtX systems. In addition, each commodity is adjustable regarding the option to purchase or sell the commodity. The optimization is driven by an exogenously defined commodity demand, which the system will cover by dimensioning and operating all system components while minimizing the total production costs, including investment and operational costs, by minimizing the GHG emissions, which include emissions from production, installation, operation, and disposal, or by minimizing both objectives simultaneously.

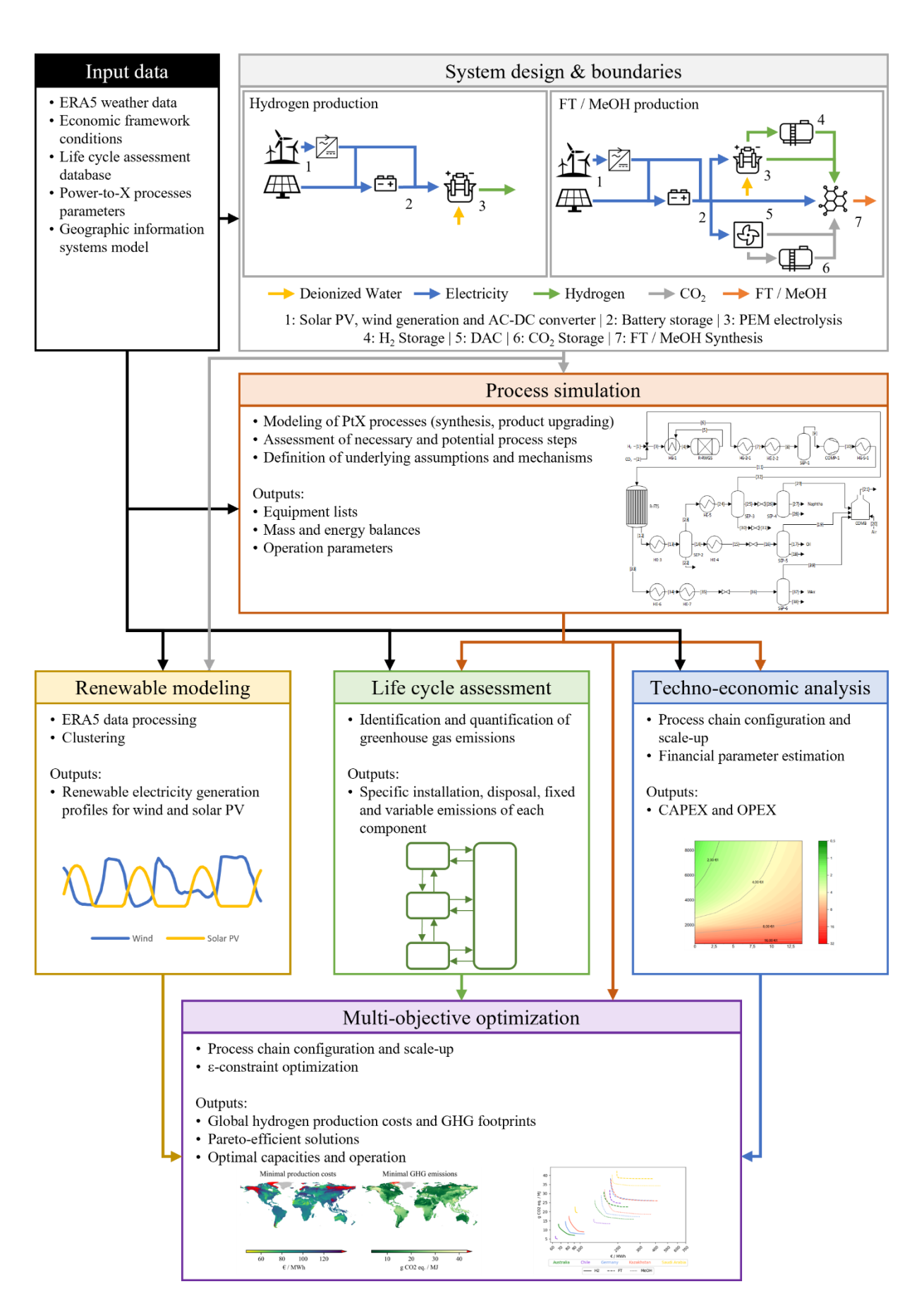


Figure 1: Integrated modelling approach of PtX plants consisting of flowsheet optimisation using process simulation, TEA, LCA, renewable generation modelling, and multi-objective optimisation [18]

While this approach allows the in-depth analysis of single facilities and dimensions the system components based on the local renewable electricity generation conditions, it misses the opportunity to complement critical, location-specific information necessary for comprehensive planning, including the financial risk, available space for renewable generator installations, and existing infrastructure.

Financial risks

Financial risks are affected by several dimensions. Two of them are the political and technological risks of the country. Political risks depend on the country's political stability, including the stability of the government, independence of the judiciary, corruption, trade restrictions, and currency volatility, among others. Next to this kind of risk, technology-specific risks exist and affect technologies with low technology readiness level or maturity, like electrolysis technology. Here, long-term risks exist due to a lack of knowledge on the long-term operation of the technology, like efficiency losses or degradation, as well as CAPEX and OPEX uncertainties, missing purchase certainty of products, or scale-up risks.

The political risks affect each production location differently if different country options exist, and comparing production locations in different countries would be difficult. To address this challenge, researchers of the HYPAT project [21] have derived country-specific weighted costs of capital (WACC) for hydrogen projects, which are applied to the individual case studies.

WACC

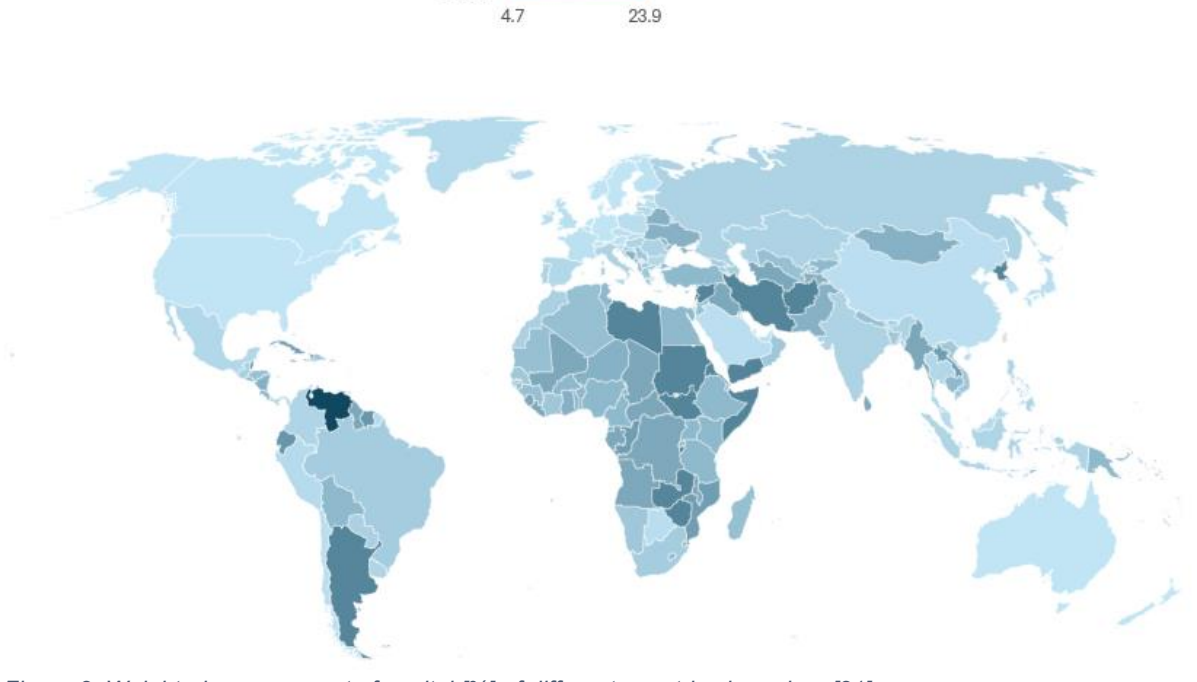


Figure 2: Weighted average cost of capital [%] of different countries based on [21]

Assessment of local renewable generator potentials and infrastructure availability

Another critical factor is sufficient space to install renewable electricity generator capacities, especially for large-scale eFuels production. Land coverage data was used to calculate the available space around the chosen production location for renewable generator capacities. These include urban land use, such as industrial or commercial units or housing, and recreational areas, like green urban areas or sport and leisure facilities. Infrastructures like airports, roads, railways, and electricity transmission grids also affect the available space. Next to human-made exclusion areas, natural areas can exclude the installation of renewable generators, such as national parks, water bodies, and slopes. The applied land coverage data and its processing methods are described in [22] and [23], and assessed on a spatial scale of 100x100 meters.

Infrastructure is another significant component in investment decisions. Production locations with connections to roads, pipelines, or shipping terminals can transport eFuels easily to consumers at low costs. Available infrastructure also affects the general choice of eFuel

products. Hydrogen, for example, requires liquefaction or hydrogen carriers if pipeline infrastructure is not available and large quantities should be transported over long distances. The infrastructure is similarly assessed to the renewable generator potentials by GIS-based identification of gas and oil pipelines, ports, roads, and railroads using OpenStreetMap data [24].

Case Study

The described methodology is applied to three locations, which are being discussed for large-scale eFuels projects. First, the location of the HaruOni project in Chile is considered, where PtX MeOH is already produced. Second, the NEOM project in Saudi Arabia aims to produce hydrogen on a large scale. Third, the Hyphen project seeks to produce ammonia close to Lüderitz, Namibia. The financial risk, renewable generation availability, and infrastructure are derived and applied for each location. Table 1 shows the characteristics of each location and its implications.

Table 1: Information on the locations used in the case study

Location	Chile	Saudi Arabia	Namibia
Coordinates (lat, lon)	-53.15, -70.92	28.14, 34.94	-26.74, 15.16
WACC [%]	5.4	5.4	8.2
Capacity Factor Wind (hours)	5,093	2,481	3,675
Capacity Factor PV (hours)	1,116	1,981	2,018

Even though the projects announced specific eFuels, this study applies the data from [13] to model the production of hydrogen, MeOH, and FT crude production. These different eFuels are chosen since the flexibility of each production process is different, and the impact of the production flexibility can also be assessed. The derived technical, economic, and environmental parameters are transferred to the multi-objective optimisation, which implements the system as shown in Figure 3.

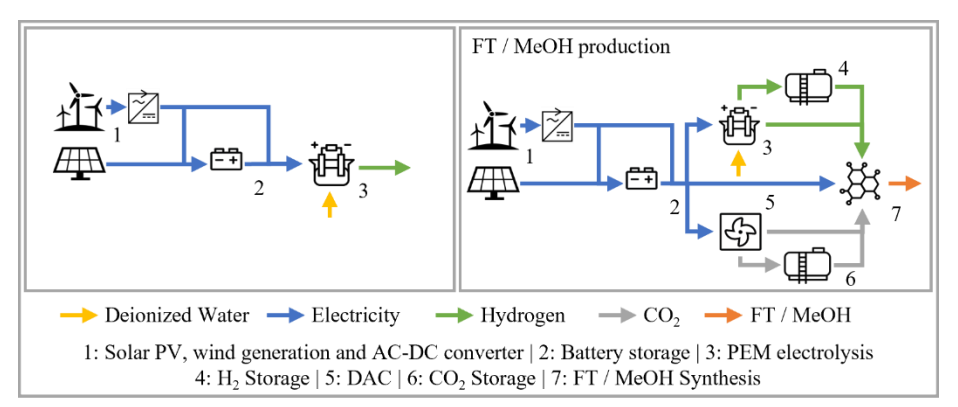


Figure 3: Implemented components of the multi-objective optimisation in the case of hydrogen (left) and FT/MeOH production (right) [18]

Next to analysing these three locations, global hydrogen production costs and GHG emissions are calculated for over 238,479 locations to showcase the model's applicability on global data. However, this large-scale analysis omits location-specific data except for the local weather data since location-specific investigations would be out of scope at this spatial resolution.

Results

Global hydrogen production costs and GHG emissions

The hydrogen production costs and GHG emissions for all onshore locations covered by the ERA5 data have been calculated to showcase the approach's applicability to global data. Low production costs are visible in Northern Africa, central Asia, Australia, Patagonia, and parts of North America. Low GHG emissions are especially possible in locations with high wind

capacity factors, including Patagonia, Australia, Northern Africa, Central Asia, parts of Europe, and parts of North America. This general overview allows for a first identification of favourable locations for PtX systems.

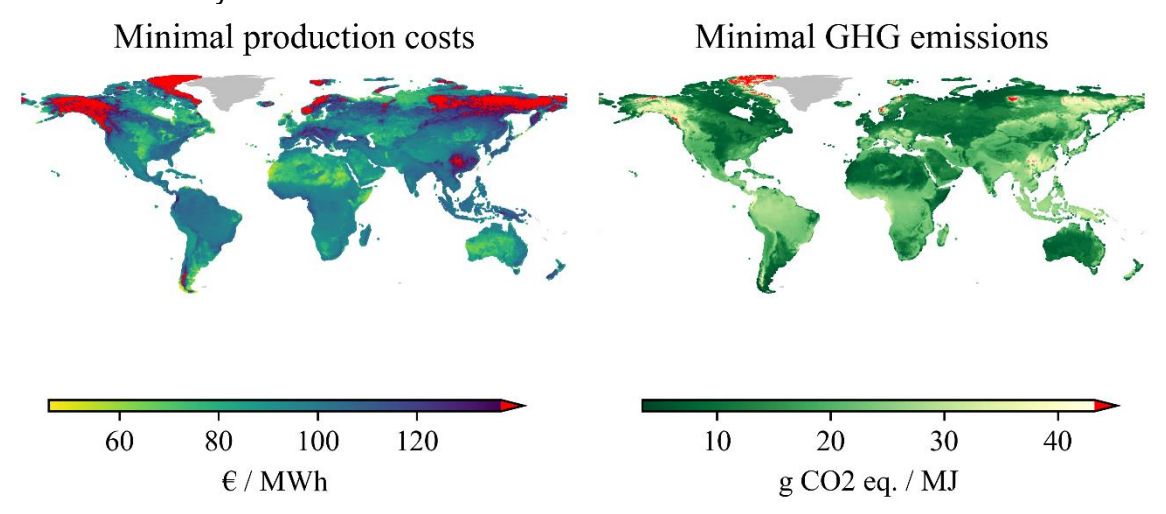


Figure 4: Hydrogen production costs (left) and GHG emissions (right) of each ERA5 weather data grid cell

Comparison of Pareto fronts of different technologies and locations

The comparison of different technologies and locations is based on production costs, GHG emissions, the shape of the Pareto front, and their relation to each other (Figure 5). The lower production costs and GHG emissions of hydrogen production are clearly visible compared to MeOH and FT production. The low costs are based on two advantages of hydrogen production compared to the other two energy carriers. First, auxiliary components like CO₂ supply, synthesis, and hydrogen storage are not required, which reduces the overall investment. Second, the fully flexible PEM electrolysis reduces the demand for battery storage. If battery storage is installed, it is only because of economic advantages and not technical necessity. MeOH and FT production are not entirely flexible, and storage units are required to ensure a steady feedstock supply. The narrow Pareto front of hydrogen production in Chile is of special interest since it shows a high synergy between production costs and GHG emissions, and improving production costs or GHG emissions is difficult.

Comparing the different locations, Chile's clear advantage in terms of costs and GHG emissions is visible. Wind generation achieves high utilization and reduces the demand for storage units since steady electricity generation is possible. Saudi Arabia performs better than Namibia in terms of production costs but worse in terms of GHG emissions. Since worse capacity factors for wind and solar PV are achievable at the chosen location in Saudi Arabia than at the location in Namibia, the higher production costs mainly stem from the higher WACC in Namibia. The Pareto fronts of Saudi Arabia have a flat development, which shows that GHG emissions can be reduced only marginally, while production costs increase significantly. Namibia has the advantage of mixed renewable potentials. The Pareto front is bulbous, showing a significant decrease in GHG emissions while production costs remain constant for the majority of GHG emission reduction. For all Pareto fronts, the marginal production costs to reduce GHG emissions increase significantly with a more ambitious GHG emission reduction. This applies vice versa for the production costs and the marginal GHG emissions.

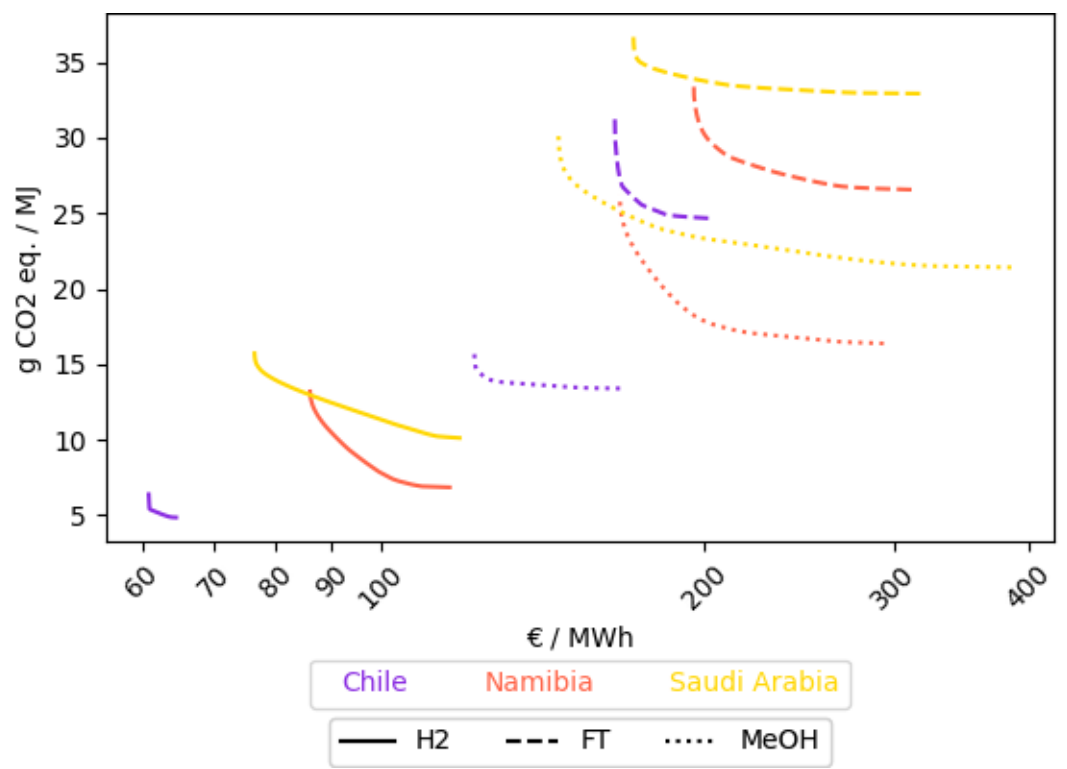


Figure 5: Pareto fronts of the production of hydrogen, FT, and MeOH in Chile, Saudi Arabia, and Namibia. The Pareto fronts show the trade-off between GHG emissions and production costs. Based on personal preference, a stakeholder can decide on the level of production costs and GHG emissions, and derive optimal capacities and operation of these preference levels.

Dimensioning the PtX system based on preferences

The advantage of these Pareto fronts lies in the complete information on the trade-offs between production costs and GHG emissions. Based on their individual preferences, stakeholders can decide which level of production costs and GHG emissions they desire. Obvious decisions include the dimensioning based on minimal production costs or minimal GHG emissions. Another favourable decision is the point on the Pareto front, which is the closest to the origin of the coordinate system. This so-called knee point balances both objectives. The capacities of the individual components of the FT production in Namibia at these three preferences are shown in Figure 6. The *minimize emission* solution installs primarily wind generator capacities and removes almost all solar PV capacities. Most of today's solar PV production capacities are located in China, where the electricity generation mix consists of a large share of coal electricity generation. This circumstance drives the specific GHG emissions per capacity. Combined with the lower total yearly capacity factor, the specific GHG emission per generated kWh of solar PV is significantly higher than that of wind generators, which drives GHG emissions of solutions with high solar PV capacities. The difficulty of an undiversified electricity generation is the full exposure to the generation uncertainty of this single technology. While wind has higher total yearly capacity factors, longer doldrums are possible, requiring large storage unit capacities, as shown by the capacities of CO₂ and hydrogen storage units. As soon as more focus is placed on production costs, electricity generation will be diversified by installing solar PV capacities, reducing exposure to single-generation technology uncertainties, and significantly reducing the need for storage units.

Figure 7 shows the operation of the FT production in Namibia when minimizing GHG emissions (A), aiming for a balanced setup (B), and when minimizing production costs (C). The electricity generation from wind and solar PV is clearly visible, and how the system reacts to this generation in the different cases. Based on this optimal operation, capacities are calculated. Especially during the first hours, the importance of diversified electricity generation is visible. During these hours, almost no wind electricity generation occurs, and storage solutions are required to supply the feedstock to the system. With solar PV capacities, this gap is closed

and storage unit capacities can be reduced. However, these solar PV capacities are not installed when minimizing emissions since installing wind generator capacities in combination with storage units results in lower GHG emissions than using solar PV.

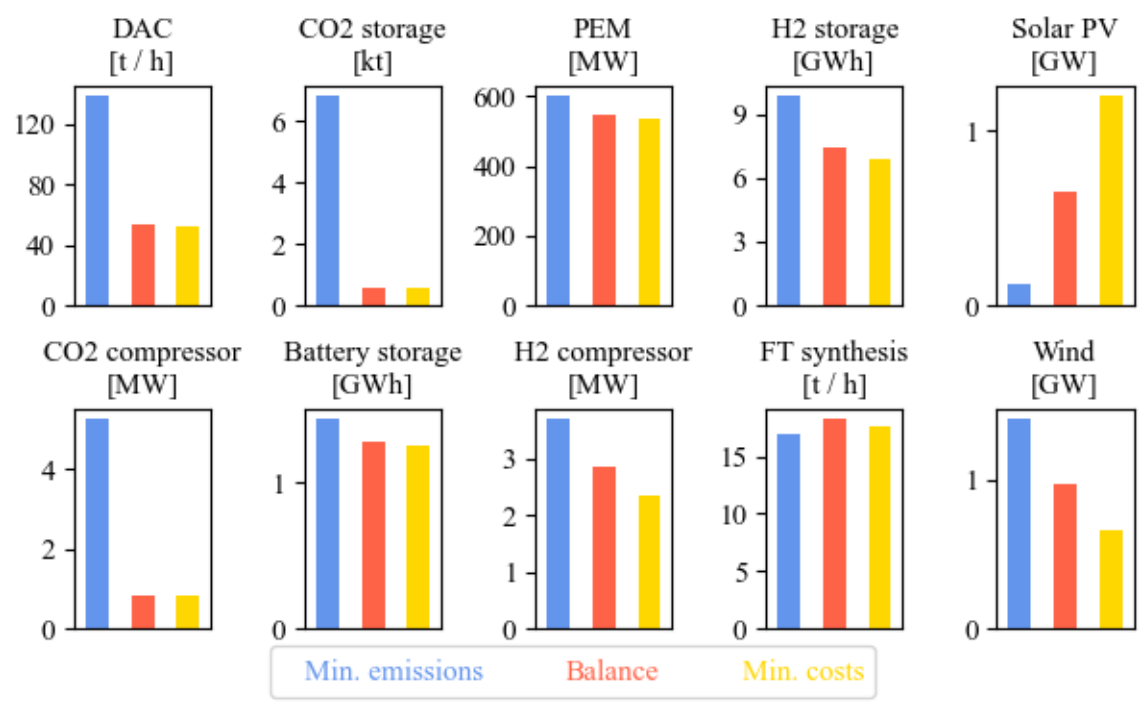


Figure 6: Capacities of the FT production in Namibia when minimizing emissions (blue), at the balanced setup (red), and when minimizing production costs (yellow)

The effect of location-specific renewable electricity generation conditions

The different locations have different renewable electricity generation conditions, which affect the optimal choice of all components of the PtX system. Figure 8 shows the capacities of the FT production in the different locations using the knee point solution. Chile's sole utilization of wind generation is clearly visible, allowing low-cost and low-emission electricity generation. The sole concentration on wind generation requires increased CO_2 and hydrogen storage demand compared to all other locations. Saudi Arabia uses the highest capacities of solar PV and adds wind generation capacities to diversify its electricity generation. The same holds for Namibia; however, fewer solar PV capacities are installed. Saudi Arabia and Namibia require less CO_2 and hydrogen storage capacities, but use higher battery storage capacities. Solar PV has lower total yearly capacity factors, but has high certainty of electricity generation during the daytime. Therefore, these locations focus on short-term storage.

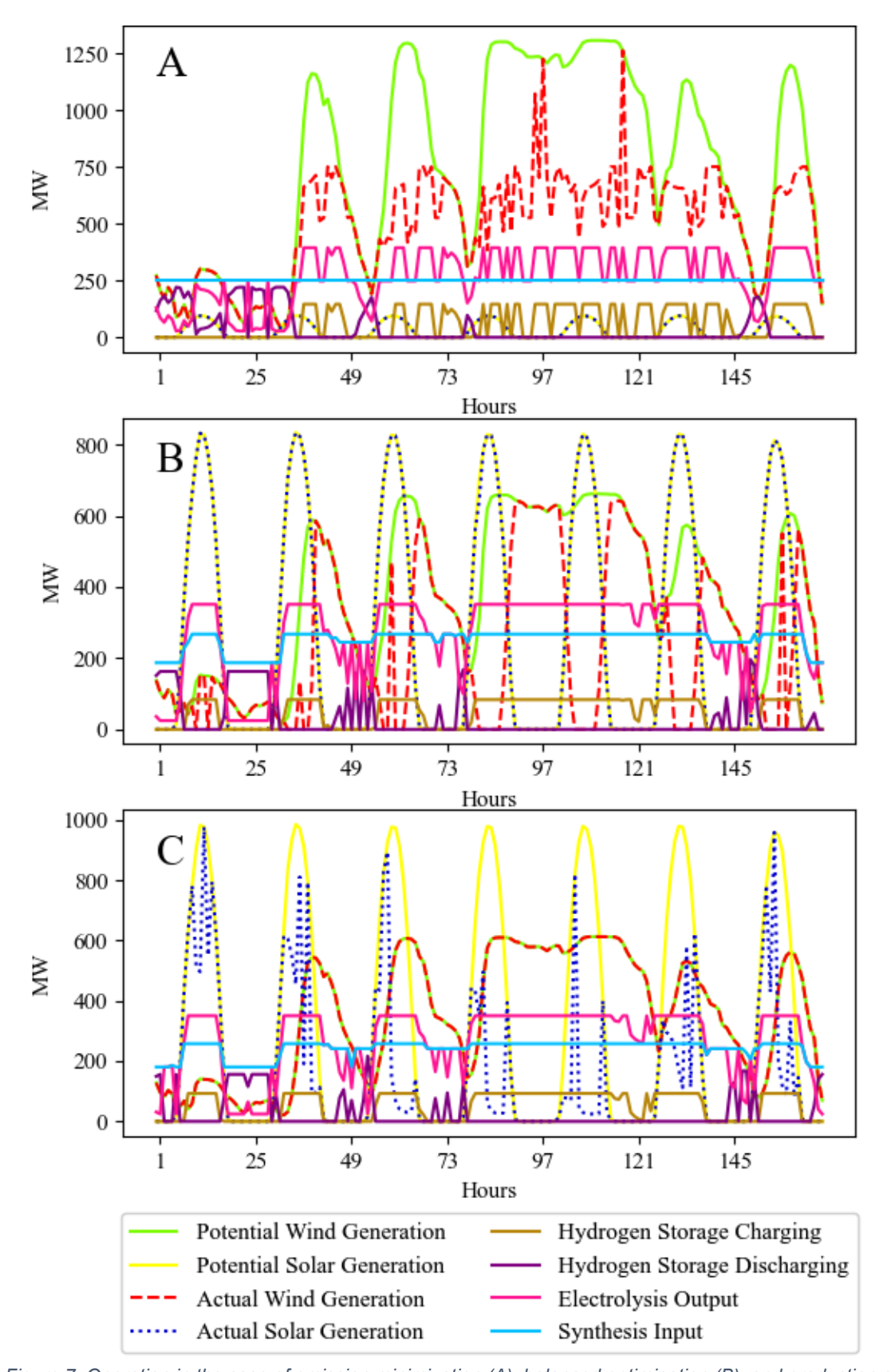


Figure 7: Operation in the case of emission minimization (A), balanced optimisation (B), and production cost minimization (C). Clearly visible is the diversification of the electricity generation in cases B and C, and the interplay of the components with each other based on the renewable electricity generation

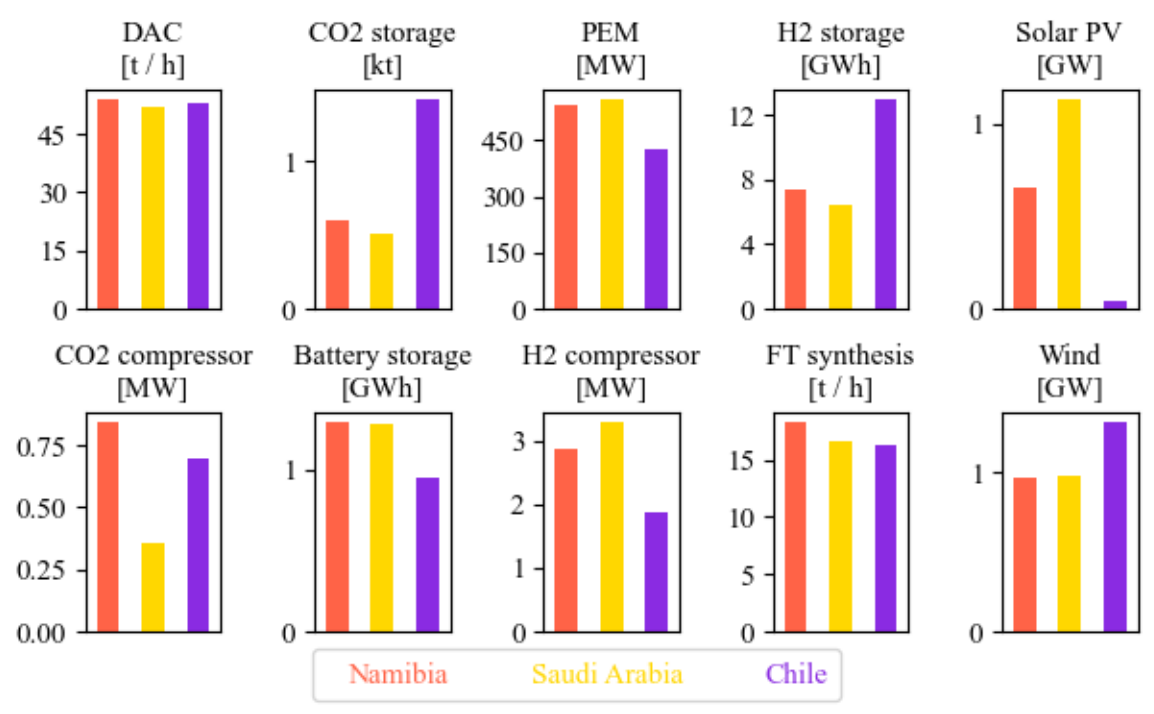


Figure 8: Capacities of the FT production at the knee point of the Pareto front

Identification of a suitable renewable electricity generation location

Based on the capacities derived in the optimisation, the space demand of the renewable generators can be calculated. In Saudi Arabia, around 1 GW of wind generator capacities and around 1.1 GW of solar PV capacities are required in the balanced case to supply the facility. Solar PV modules are tightly packed and do not affect each other significantly. Based on an average space demand of 79.2 MW per km² [25], this would result in a total space demand of 13.89 km². Wind generators are more complex since they affect each other and must not be installed too close together. Based on an assumed 5.5 MW wind turbine with a 135 m rotor diameter [26], 182 turbines are required. Based on a distance to other wind turbines of 6 times the rotor diameter in wind direction and 4 times the rotor diameter vertical to the wind direction, a space demand of 1.75 km² is required. To calculate the total space demand, the overlapping of the individual wind turbine spaces must be considered, resulting in a total wind park space demand of 63.66 km². A hybrid wind and solar PV park is assumed to use the space efficiently since the mutual impact regarding land competition and electricity generation losses is within a low range [27].

The map in Figure 9 shows the potential space available for renewable generators and the required space for the derived hybrid solar PV and wind park capacity. This presentation of required space allows for visualization of the impact of the future PtX production, since large capacities of renewable generators are needed to satisfy the global demand. The map further shows infrastructure like streets, ports, and pipelines required to transport the products to the final destination.

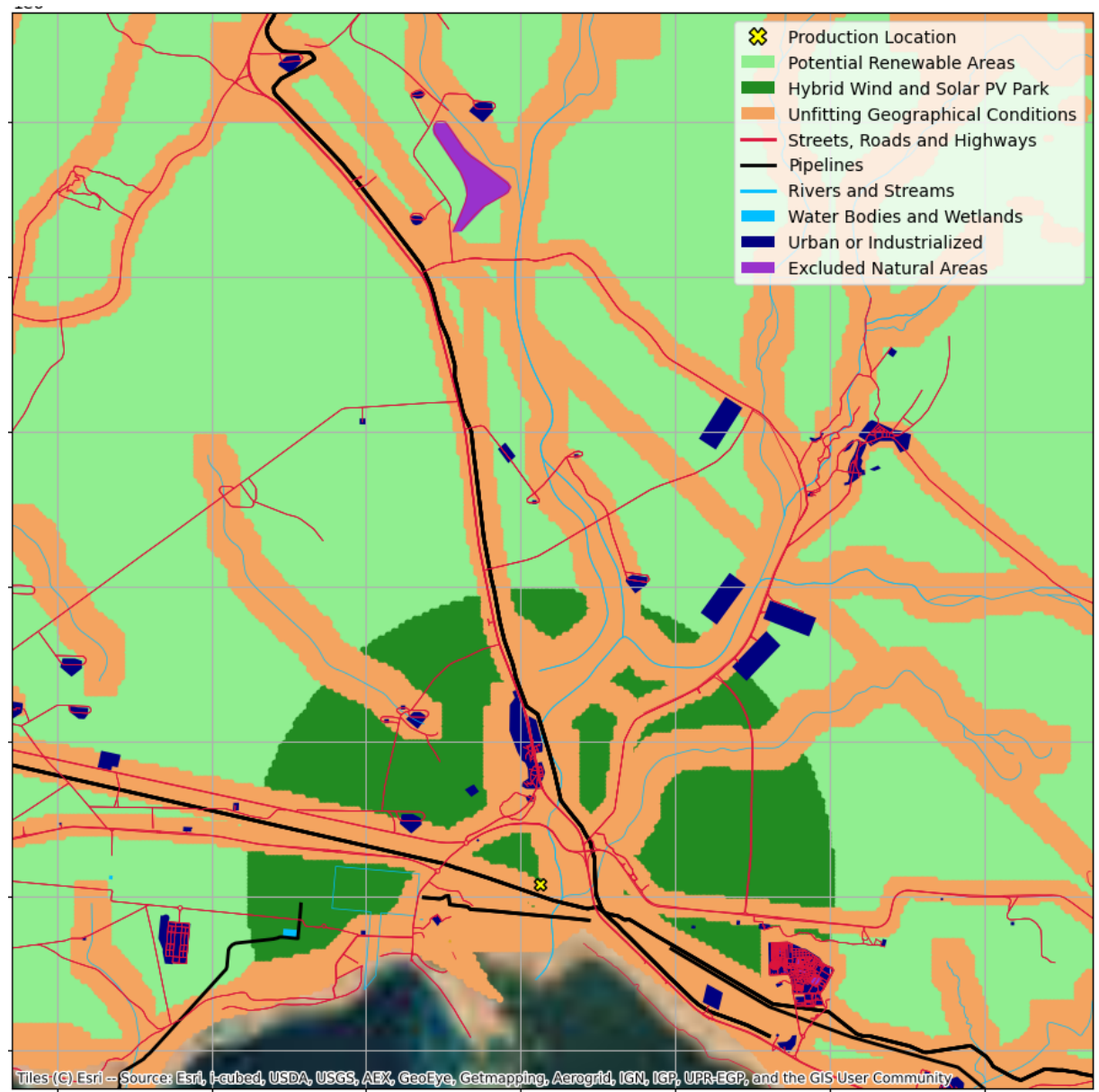


Figure 9: Land coverage and available space for renewable generator capacities

Conclusions

This work presented an integrated framework to evaluate the technical, economic, and environmental performance of stand-alone PtX plants under varying renewable generation conditions. By applying flowsheet optimization, TEA, LCA, and multi-objective optimization, the study provided a comprehensive analysis of hydrogen, MeOH, and FT fuel production across three global case study sites and extended the assessment to a global scale.

The results highlight several key insights. First, hydrogen production achieves the lowest costs and GHG emissions due to its flexibility and reduced system complexity. Second, Chile emerges as a particularly attractive location owing to strong wind resources, while Namibia offers promising trade-offs between cost and emissions through its mixed renewable potential. Despite lower financing costs than Namibia, Saudi Arabia shows limited potential for significant emission reductions without incurring steep cost increases. The Pareto front analysis underscores the value of this framework in informing stakeholder decisions, enabling tailored system designs that balance economic and environmental priorities. Additionally, the land-use assessment emphasizes the substantial spatial requirements of large-scale renewable deployments, an often-overlooked factor in PtX planning.

Nonetheless, the study faces certain limitations. The case study analysis incorporated local renewable availability, infrastructure, and financing risks, but other critical features, like water availability, were not considered. Furthermore, renewable electricity generation includes uncertainty in the form of volatility and availability, which are not considered here. The GIS-based analysis omits potential synergies available in the region, such as CO_2 point sources or heat sources, which could allow low-cost and low-emission production. In addition, some technical properties of the facilities are not modelled, including the utilization-dependent efficiency of the PEM electrolysis. Finally, a more detailed analysis of the renewable generator placement could be conducted to make the approach even more realistic.

Overall, the developed methodology offers a robust and flexible tool for guiding decision-making in the emerging PtX sector, supporting policymakers and industry stakeholders in identifying cost- and emission-efficient strategies for sustainable fuel production.

References

- Sing N, Mahali K, Roy S. An Overview on Biofuels: Advantages and Disadvantages. In: Karaman ProfR, editor. Recent Developments in Chemistry and Biochemistry Research Vol 7 [Internet]. BP International; page 98–1182024 [cited 2025]. Available from: https://stm.bookpi.org/RDCBR-V7/article/view/16014
- 2. Leung DYC, Caramanna G, Maroto-Valer MM. An overview of current status of carbon dioxide capture and storage technologies. Renewable and Sustainable Energy Reviews. Volume 39, Pages: 426–43. [2014].
- 3. Oyewo AS, Lopez G, ElSayed M, Galimova T, Breyer C. Power-to-X Economy: Green e-hydrogen, e-fuels, e-chemicals, and e-materials opportunities in Africa. Energy Reports. Volume 12, Pages: 2026–48. [2024].
- 4. Yap J, McLellan B. Exploring transitions to a hydrogen economy: Quantitative insights from an expert survey. International Journal of Hydrogen Energy. Volume 66, Pages: 371–86. [2024].
- 5. Bielefeld S, Cvetković M, Ramírez A. Should we exploit flexibility of chemical processes for demand response? Differing perspectives on potential benefits and limitations. Frontiers in Energy Research. Volume 11, Pages: 1190174. [2023].
- 6. Ince AC, Colpan CO, Hagen A, Serincan MF. Modeling and simulation of Power-to-X systems: A review. Fuel. Volume 304, Pages: 121354. [2021].
- 7. Koj JC, Wulf C, Zapp P. Environmental impacts of power-to-X systems A review of technological and methodological choices in Life Cycle Assessments. Renewable and Sustainable Energy Reviews. Volume 112, Pages: 865–79. [2019].
- 8. Garcia-Garcia G, Fernandez MC, Armstrong K, Woolass S, Styring P. Analytical Review of Life-Cycle Environmental Impacts of Carbon Capture and Utilization Technologies. ChemSusChem. Volume 14, issue 4. Pages: 995–1015. [2021].
- 9. Ajeeb W, Costa Neto R, Baptista P. Life cycle assessment of green hydrogen production through electrolysis: A literature review. Sustainable Energy Technologies and Assessments. Volume 69, Pages: 103923. [2024].
- 10. Maggi A, Wenzel M, Sundmacher K. Mixed-Integer Linear Programming (MILP) Approach for the Synthesis of Efficient Power-to-Syngas Processes. Frontiers in Energy Research. Volume 8, Pages: 161. [2020].
- 11. Sherwin ED. Electrofuel Synthesis from Variable Renewable Electricity: An Optimization-Based Techno-Economic Analysis. Environmental Science & Technology. Volume 55,

- issue 11. Pages: 7583-94. [2021].
- 12. Berger M, Radu D, Detienne G, Deschuyteneer T, Richel A, Ernst D. Remote Renewable Hubs For Carbon-Neutral Synthetic Fuel Production. Frontiers in Energy Research. Volume 9, Pages: 671279. [2021].
- 13. Fasihi M, Bogdanov D, Breyer C. Techno-Economic Assessment of Power-to-Liquids (PtL) Fuels Production and Global Trading Based on Hybrid PV-Wind Power Plants. Energy Procedia. Volume 99, Pages: 243–68. [2016].
- Heinzmann P, Glöser-Chahoud S, Dahmen N, Langenmayr U, Schultmann F. Technoökonomische Bewertung der Produktion regenerativer synthetischer Kraftstoffe [Internet]. Karlsruher Institut für Technologie (KIT); 2021 [cited 2024]. Available from: https://publikationen.bibliothek.kit.edu/1000140638
- 15. Terlouw T, Rosa L, Bauer C, McKenna R. Future hydrogen economies imply environmental trade-offs and a supply-demand mismatch. Nature Communications. Volume 15, issue 1. Pages: 7043. [2024].
- 16. Farajiamiri M, Meyer JC, Walther G. Multi-objective optimization of renewable fuel supply chains regarding cost, land use, and water use. Applied Energy. Volume 349, Pages: 121652. [2023].
- 17. Kenkel P, Wassermann T, Rose C, Zondervan E. A generic superstructure modeling and optimization framework on the example of bi-criteria Power-to-Methanol process design. Computers & Chemical Engineering. Volume 150, Pages: 107327. [2021].
- 18. Langenmayr U, Heinzmann P, Schneider A, Ruppert M, Rudi A, Fichtner W. Stand-alone power-to-X production dynamics: A multi-method approach to quantify the emission-cost reduction trade-off. Journal of Industrial Ecology. Pages: jiec.70085. [2025].
- 19. Hofmann F, Hampp J, Neumann F, Brown T, Hörsch J. atlite: A Lightweight Python Package for Calculating Renewable Power Potentials and Time Series. Journal of Open Source Software. Volume 6, issue 62. Pages: 3294. [2021].
- 20. Hersbach H, Bell B, Berrisford P, Hirahara S, Horányi A, Muñoz-Sabater J, Nicolas J, Peubey C, Radu R, Schepers D, Simmons A, Soci C, Abdalla S, Abellan X, Balsamo G, Bechtold P, Biavati G, Bidlot J, Bonavita M, De Chiara G, Dahlgren P, Dee D, Diamantakis M, Dragani R, Flemming J, Forbes R, Fuentes M, Geer A, Haimberger L, Healy S, Hogan RJ, Hólm E, Janisková M, Keeley S, Laloyaux P, Lopez P, Lupu C, Radnoti G, De Rosnay P, Rozum I, Vamborg F, Villaume S, Thépaut J. The ERA5 global reanalysis. Quarterly Journal of the Royal Meteorological Society. Volume 146, issue 730. Pages: 1999–2049. [2020].
- 21. Kleinschmitt C, Fragoso García J, Franke K, Teza D, Seidel L, Ebner A, Baier M. Weltweite Potenziale erneuerbarer Energien. HYPAT Working Paper 03/2022 [Internet]. [2022 [cited 2024]]. Available from: https://doi.org/10.24406/publica-177
- 22. Slednev V, Bertsch V, Ruppert M, Fichtner W. Highly resolved optimal renewable allocation planning in power systems under consideration of dynamic grid topology. Computers & Operations Research. Volume 96, Pages: 281–93. [2018].
- 23. Slednev V. Development of a techno-economic energy system model considering the highly resolved conversion and multimodal transmission of energy carriers on a global scale [Internet]. Karlsruher Institut für Technologie (KIT); 2024 [cited 2025]. Available from: https://publikationen.bibliothek.kit.edu/1000170863

- 24. Open Street Map Contributors. Planet dump retrieved from https://planet.osm.org [Internet]. 2017. Available from: https://www.openstreetmap.org
- 25. Maier R, Lütz L, Risch S, Kullmann F, Weinand J, Stolten D. Potential of floating, parking, and agri photovoltaics in Germany. Renewable and Sustainable Energy Reviews. Volume 200, Pages: 114500. [2024].
- 26. Wiser R, Rand J, Seel J, Beiter P, Baker E, Lantz E, Gilman P. Expert elicitation survey predicts 37% to 49% declines in wind energy costs by 2050. Nature Energy. Volume 6, issue 5. Pages: 555–65. [2021].
- 27. McKenna R, Mulalic I, Soutar I, Weinand JM, Price J, Petrović S, Mainzer K. Exploring trade-offs between landscape impact, land use and resource quality for onshore variable renewable energy: an application to Great Britain. Energy. Volume 250, Pages: 123754. [2022].

Amino Acid based Carbon Capture Technology – from Direct Air Capture to Point Sources Applications

Ralf Gesthuisen⁽²⁾, Ulrich Dietz⁽¹⁾, Julien Nottbohm⁽²⁾, Thomas Bittner⁽²⁾

Abstract

Carbon Capture process technologies are gaining more and more interest in the transformation process of various industries. Consequently, existing process technologies are further developed to widen their field of application and to increase their efficiency. Besides, new process technologies are developing. While in the past Carbon Capture in industrial applications was focused on processes like methane steam reforming or flue gas treatment of coal fired power plants more new sources of CO₂ are considered for carbon capture application, from biogas treatment with high CO₂ content to Direct Air Capture (DAC).

The presented Amino-acid based process is a novel technology for Carbon Capture based on the absorption of CO₂ by an aqueous solution containing the natural amino acid L-Arginine, wherein the aqueous derivates of CO₂ can be bound and stored at atmospheric pressure. A nearly complete removal of CO₂ from a carrier gas can be achieved over the full range of applications, from DAC to flue gas treatment to biogas cleaning or respectively from CO2 concentrations of 400 Vppm to 50 V% or higher. The process is capable to reduce the CO₂ content in the off gas below 20Vppm. The absorption process is either based on a membrane contactor or a typical washing tower which leaves the option to optimize the process setup for the specific application. The bounded aqueous derivates of CO₂ can be separated from the acceptor solution by electrodialysis. CO₂ spontaneously flashes out from the receiving solution at high purity. Results from lab experiments for cleaning a flue gas containing contaminants like NO₂ and SO₂ demonstrate the capability and efficiency of the developed process. Although the types of membranes have not yet been optimized the lab experiments show that the absorption efficiency is close to 100% and that the energy efficiency of a further optimized pilot plant has the potential to be below 0.8 MWh/tCO₂ for point sources which is compared to many other technologies quite low. The developed process allows to absorb CO₂ continuously but to run the power consuming desorption discontinuously. This technological option is a trade-off between the invest and the operating cost.

The used chemicals for absorption and as acceptor solution for desorption are not hazardous. The process can be installed even in non-industrial areas Thus, a novel process can be provided to extract, transport and selectively release CO_2 of high purity. The developed process is environmentally harmless, operated electrically at atmospheric pressure with no thermal heat consumption or production and is easy to operate.

Introduction

Climate change is caused largely by anthropogenic greenhouse gas emissions and drives the urgency to mitigate global warming. The Paris Agreement and subsequent international climate frameworks have set ambitious targets to limit global temperature rise to well below 2°C, with efforts to cap it at 1.5°C above pre-industrial levels. Achieving these goals requires not only a rapid transition to low-carbon energy systems but also the deployment of carbon dioxide removal technologies to address residual and historical emissions. Carbon capture technologies, which span from point-source capture—targeting emissions directly from industrial facilities and power plants—to DAC, which extracts CO₂ from the ambient atmosphere are playing an important role for carbon removal. While point-source capture helps prevent new emissions from entering the atmosphere, DAC offers a pathway to negative

¹ CBL – Carbon Beyond Limits GmbH and Co.KG

² INEOS Manufacturing Deutschland GmbH

emissions, essential for offsetting hard-to-abate sectors and reversing emissions. However, the development and scaling of these technologies face significant challenges, including energy intensity, cost, infrastructure requirements, flexibility of e.g. power consumption and public acceptance.

The increasing need for efficient and sustainable Carbon Capture technologies has led to the exploration of novel methods. One such method involves the use of the natural amino acid L-Arginine, which binds CO₂ in aqueous solutions. The process of absorption and desorption operates at ambient pressure and low temperature conditions and is fully electrically driven.

Process Description

The aqueous solution of L-Arginine demonstrates a notable ability to absorb carbon dioxide (CO_2) from gas streams of varying concentrations, including both point sources and ambient air. [1] outlines how L-Arginine, due to its basic guanidino functional group, reacts with CO_2 in aqueous media. This reaction mechanism enables efficient CO_2 uptake even at low partial pressures. This makes the process suitable even for DAC applications or allows to achieve absorption rates of more than 99.5%, respectively. Furthermore, the aqueous L-Arginine solution shows low volatility, biodegradability, and non-toxic properties, positioning it as a sustainable alternative to conventional amine-based solvents.

The mechanism of binding CO_2 is a chemisorption process indicated by the far higher loading of the aqueous L-Arginine solution with CO_2 compared to the theoretically achievable loading via physical absorption [2]. Figure 1 depicts a lab experiment in which a calibration gas with a CO_2 content of 7.5 V% is dispersed through the aqueous L-Arginine solution (1-molar) in two stages. After each stage gas samples were drawn every five minutes and were analysed via gas chromatography.

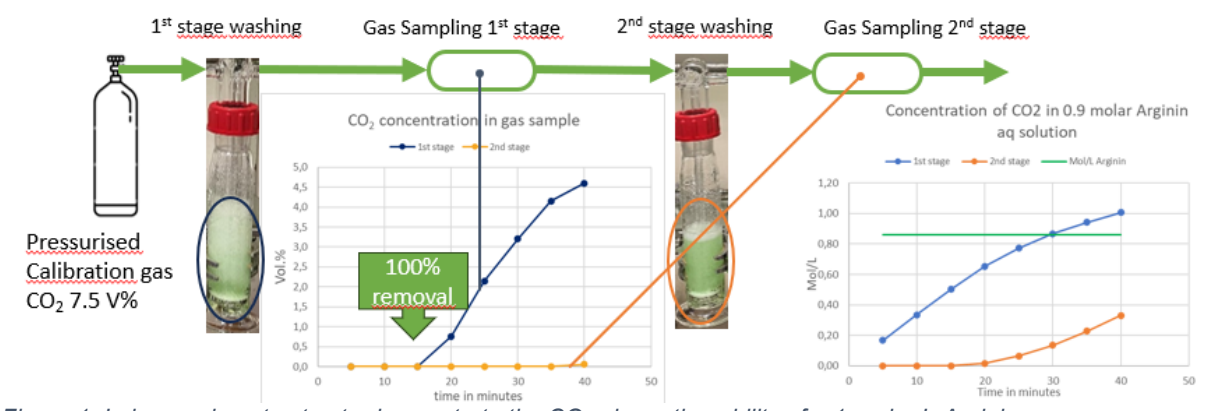
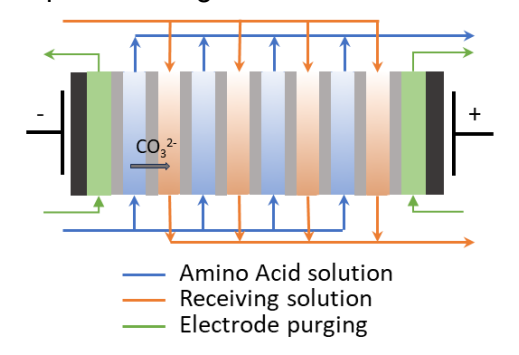


Figure 1: Lab experiment setup to demonstrate the CO₂ absorption ability of a 1-molar L-Arginine aqueous solution

The CO_2 breakthrough occurred at stage 1 after appr. 15 minutes and at a loading of 0.5 moles of CO_2 per mole of L-Arginine. The loading of CO_2 further increased up to levels above 1 mole of CO_2 per mole of L-Arginine. This simple experiments clearly demonstrates the significant ability of L-Arginine to bind CO_2 from gases. Important to note that before the breakthrough of stage 1 and also of stage 2 occurs the concentration of CO_2 in the treated gas was measured below the CO_2 detection limit of 20 Vppm.

Due to the formation of strong electrostatic bonds the recovery of CO₂ is not possible by heating compared to common amine Carbon Capture processes. Recovery of CO₂ from the

aqueous L-Arginine solution is achieved by electrodialysis, where anionic derivatives (e.g.



 ${
m HCO_3^-}$ or ${
m CO_3^{2-}}$) are selectively separated using an anion exchange membrane. L-Arginine remains in the acceptor solution due to its zwitterionic nature at operation around the isoelectric point, ensuring efficient separation and recovery. Figure 2 depicts the setup of an electrodialysis module with a number of membrane stacks.

As receiving solution in the electrodialysis module citric acid can be applied which is another non-hazardous and easy to handle chemical in the proposed process.

Figure 2: Sketch of a electrodialysis module

Technically the absorption process can either be performed in a washing tower with optimized packing [2] or as demonstrated in [3] by membrane modules that keep the gas and the liquid phase separated. Simplified process schemes without break tanks are shown in Figure 3 and Figure 4.

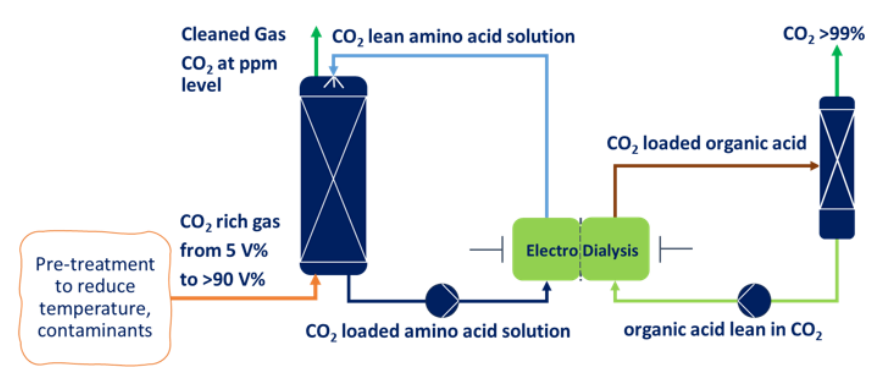


Figure 3: Simplified process scheme with a washing column absorption

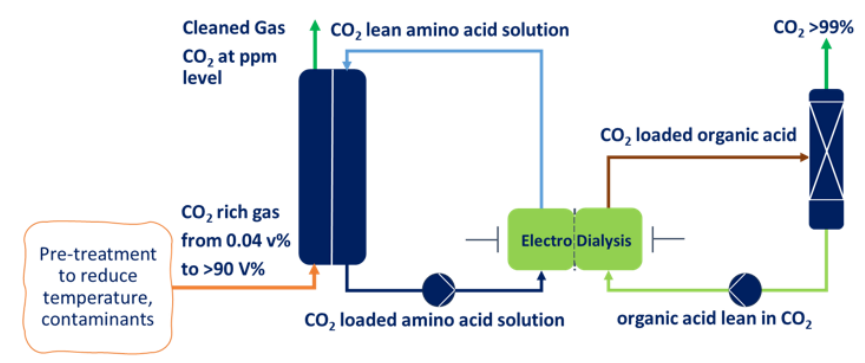


Figure 4: Simplified process scheme with a membrane module system absorption

The latter was successfully applied in the RoKKa Project for the separation of CO₂ from waste water treatment off gases (rotten gas), a type of biogas with a high concentration of CO₂ around 40V% [3].

The entire process is fully electrically operated and does not show a significant heat generation. With a sufficiently large break tank the absorption can be operated independently on the desorption, which is the power consuming process. This flexibility allows the application to continuous processes regarding the absorption with some optimization potential to run the desorption harder when power is cheap.

Experimental results

Due to the strong absorption behavior of L-Arginine the range of application of the technology is wide from low concentrated streams like in DAC to higher CO₂ contents like in biogas or in gases from chemical processes. This chapter discusses experimental results gained for different areas of application of the L-Arginine Carbon Capture process, namely flue gas treatment, rotten gas treatment and DAC.

Flue gas treatment

Flue gas treatment of gas fired processes is an important application for Carbon Capture technologies in general and specifically for the proposed process. A high absorption rate even at medium CO_2 partial pressure in the flue gas is a key feature. Amine based Carbon Capture processes typically achieve a 90-95% absorption rate and thus leave significant residual emissions for large scale industrial processes like steam crackers in the chemical industry. As shown by the absorption experiments the L-Arginine based process has the potential to capture by far more than 95% of the CO_2 in the flue gas. Therefore, experiments in a lab scale plant were performed with the following targets:

- Prove the ability of the L-Arginine process to achieve absorption rates above 99%
- Understand the absorption behavior of other water soluble species present in industrial flue gas streams
- Understand the achievable purity of CO₂ as a product.



Figure 5: Lab plant used for flue gas treatment experiments

Experiments were conducted in the lab skid shown in Figure 5. A calibration gas from a pressurized bottle (composition: CO₂ at 15%, NO₂ at 500 vppm, SO₂ at 500 Vppm, O₂ at 2 V%, and nitrogen) was used to feed the unit at different feed rates. Samples were taken when stationary operation was achieved and the analysis of the different gas and liquid streams was performed as described in

Table 1. The concentration of NO_2 and SO_2 in the calibration gas were chosen by far higher than to be expected in industrial applications just to allow a reasonable analysis of concentrations in the different streams. Just for comparison, in gas fired chemical processes typical NOx concentrations in the flue gas are around 100 to 120 mg/Nm³ (appr. 50 to 60 ppm) and SO_2 is not present at all.

Table 1: Applied analysis methods

Analytical Equipment	Flue gas stream	CO ₂ stream	Arginin solution	Receiving solution	Detect- ion Limit	Comment
Gas Chromatography	CO ₂	CO ₂	-	-	20 Vppm	High accuracy
Ion Chromatography after oxidation with H ₂ O ₂	NO ₂ as Nitrate	NO ₂ as Nitrate	NO ₂ as Nitrate	NO ₂ as Nitrate	0.04 mg/l	Acceptable repeatability of recovery rate qualitative and quantitative analysis ✓
Ion Chromatography after oxidation with H ₂ O ₂	SO ₂ as Sulfate	SO ₂ as Sulfate	SO ₂ as Sulfate	SO ₂ as Sulfate	0.04 mg/l	Recovery rate varies too much qualitative analysis ✓ quantitative analysis (✓)

Figure 6 shows the achieved results for a throughput of 130 and 115 l/h of calibration gas.

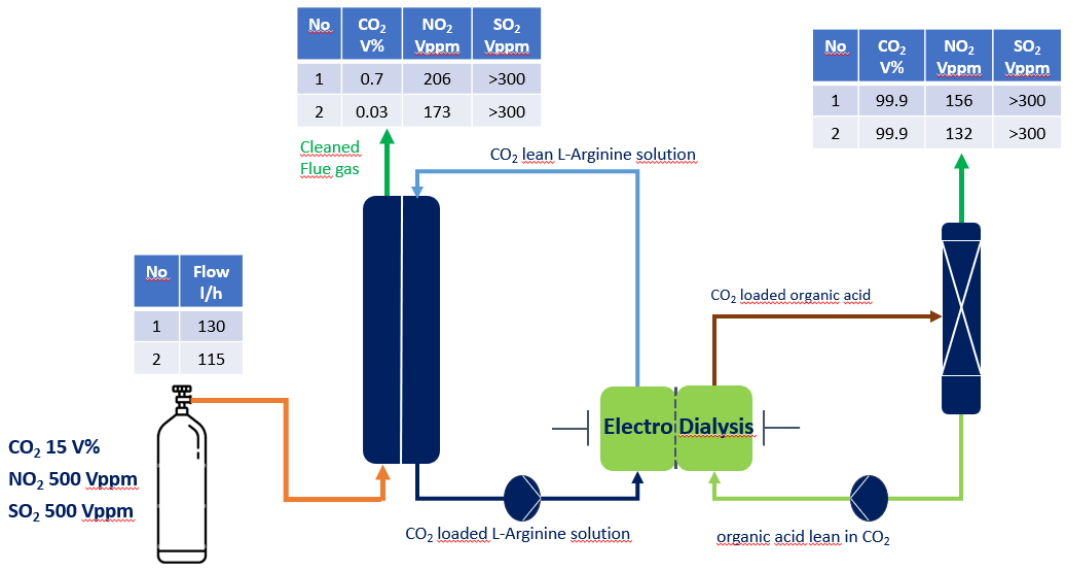


Figure 6: Experimental results for flue gas treatment

The absorption rate depends on the flue gas throughput: At 130 l/h an absorption rate of 95.3~% was achieved which was increased to 99.8% by lowering the feed rate to 115 l/h. SO_2 and NO_2 can be found in both gas fractions, eg the treated gas and the CO_2 stream. The indirect analysis of the content of NO_2 and SO_2 in the gas streams by the oxidised components is difficult and therefore the results need to be considered as a qualitative confirmation that as described in [1] other water soluble components are also absorbed by the aqueous L-Arginine solution and desorbed by the electrodialysis process. Indeed, the dry CO_2 product gas shows a concentration of 99.9%. However, in case of the treatment of a real flue gas from a natural gas fired plant 90-95% of NOx appears to be NO which is not well water soluble. Additionally, typical levels of NOx are below appr. 60 ppm (120 mg/Nm^3) due to strict emission regulation. For a deeper understanding of long term effects a pilot plant project is planned to be started beginning of 2026.

Biogas treatment

Biogas typically consists of methane and CO₂ at high concentration (appr. 50V%). The L-Arginine Carbon Capture process was applied in the RoKKa-Project (Rohstoff Klärschlamm und Klimaschutz auf Kläranlagen, funded by the European Union, and the federal state of Baden Württemberg/EFRE) to separate CO₂ from rotten gas out of a municipal waste water treatment unit to feed an algae production unit [3]. The pilot plant operated in that project is shown in Figure 7. It was operated in an on/off mode throughout the project from 2022 till 2024 without any operational issues at very high availability and without a replacement of the membrane systems.



Figure 7: RoKKa pilot plant for CO2 production from rotten gas from a WWT unit

Figure 8 depicts experimental results achieved for different flow rates of the rotten gas. Note that the purpose of the L-Arginine process was the production of high quality CO_2 for algae production. The target to produce a 99.9% CO_2 quality was always achieved independently on the flow rate of the rotten gas through the absorber. Turning down the flow rate of the biogas shows clearly the impact on the methane quality which increased from 71.4% to 98.5% when changing the flow from 300 to 100 l/h.

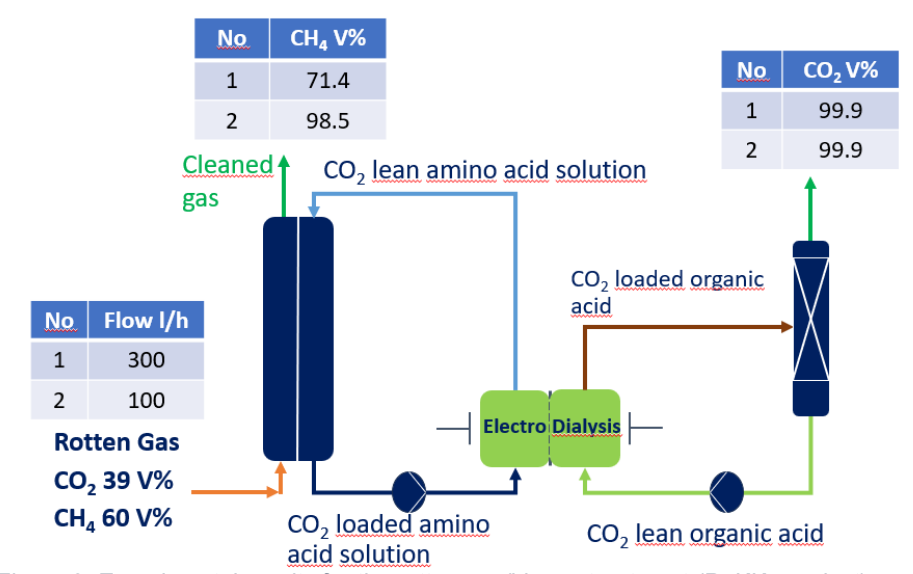


Figure 8: Experimental results for the rotten gas/biogas treatment (RoKKa-project)

Direct Air Capture (DAC)

In lab experiments it was demonstrated that the L-Arginine process is able to extract CO₂ from air down to or below the detection limit of CO₂ at appr. 20 Vppm. It was also observed that due to the low concentration of CO₂ in air at 400 Vppm loading of the L-Arginine solution is limited and not high enough to efficiently remove the CO₂ in the electro dialysis module (see also [2]). Process modifications are in development to overcome this problem and to allow an efficient absorption and desorption at lower power demand than described in [2].

Conclusion

The L-Arginine Carbon Capture process offers several advantages over conventional amine-based solutions. L-Arginine is non-toxic, biodegradable, and chemically stable across a wide pH range. The process is fully electric, allowing desorption to be aligned with renewable energy availability, thus offering the potential of supporting grid stability. It's a modular design and easy to operate process and is suitable for various applications, including DAC, biogas treatment, and industrial offgas purification.

So far an energy consumption of appr. 0.8 MWh/t(CO₂) was achieved in a 400 l/h CO₂ electrodialysis module. Further membrane and module design optimization is highly likely going to improve this energy consumption which makes this process an interesting alternative to state of the art Carbon Capture processes like amine based absorption. The high flexibility to operate the electrodialysis desorber package combined with the ability to operate the absorption independently from the desorption by considering sufficiently large break tanks the process is able to benefit from low power prices induced by the high volatility of renewable power production.

Therefore the amino-acid based Carbon Capture process presents a promising alternative to many other methods. It combines environmental safety, operational simplicity, and high efficiency, making it suitable for a wide range of applications as shown in this paper. Future developments will focus on membrane optimization and scaling up the technology for industrial deployment but also to the long term performance of the technology as well as the impact of NOx contamination.

References

- [1] Dietz, U.: Method for the bonding, transport, reaction activation, conversion, storage and release of water soluble gases; patent WO 2022/023387 A1, 2022, https://patents.google.com/patent/WO2022023387A1/en?oq=WO+2022%2f023387+ A1
- [2] Heß, D. et al: A Novel Approach to Electrochemical Direct Air Capture using aqueous L-Arginine Amino Acid Solutions as an Absorption Solvent: Proof-of-Concept and Technoeconomics, Ind. Eng. Chem. Res, 2025
- [3] Rapp, H.J., Dietz, U.: RoKKa das Update für die Kläranlage; Abschlussbericht, Umwelttechnik BW, Stuttgart, 2024, https://www.umwelttechnik-bw.de/sites/default/files/2024-11/20241111 RoKKa Abschlussbericht barrierefrei web.pdf

Evaluating Electrochemical Mineral Trapping for Carbon Dioxide Removal: Insights from Experiments and Predictive Modeling

Dominik Groh¹, Júnior Staudt¹, Kannasoot Kanokkanchana², Manuel Ibañez¹, Nicolas Plumeré², Jakob Burger¹

¹Technical University of Munich, Campus Straubing for Biotechnology and Sustainability, Laboratory of Chemical Process Engineering, Straubing, Germany

²Technical University of Munich, Campus Straubing for Biotechnology and Sustainability, Professorship for Electrobiotechnology, Straubing, Germany

Abstract

In the efforts of replacing fossil fuels, electrochemical carbon dioxide removal (CDR) is gaining attention.[1] It promises low energy consumption, decentralized operation, and low cost.[2] Utilizing electric current to attain spatially basic and acidic environments in aqueous electrolytes captivates through ease of operation and exploits the direct correlation of alkalinity and dissolved inorganic carbon (DIC).[3] Natural water bodies (e.g., seawater, rivers) are especially interesting since they are saturated in DIC and contain a volumetric carbon content of up to hundreds of times higher than ambient air. Due to kinetic barriers, natural electrolytes are usually supersaturated with carbon-containing minerals like calcite, huntite, and magnesite. A localized increase in alkalinity at the cathode can overcome activation barriers, facilitating the formation of stable minerals and promoting long-term carbon sequestration.^[4] This work investigates the gas-liquid-solid equilibrium of mineral trapping technologies through both modeling and lab-scale experiments. Model implementations use extended Pitzer equations and describe the interplay between alkalinity, CO₂ partial pressure, electrolyte composition, and DIC. The analysis includes water compositions reflecting different natural electrolytes, like rivers or seawater. Salinities are varied from 0.05 g·kg⁻¹ to 46 g·kg⁻¹ and temperatures range from 273.15 K to 313.15 K. The computed values are compared with experimental data. Results show that the mineral trapping yield is a function of the electrolyte composition. Consequently, the process behavior of a specific electrolyte can be better or worse for carbon capture depending on its ion content. Especially, the occurrence of divalent cations highly influences the carbon capture efficiency. This makes specific natural electrolytes more promising for mineral trapping in CDR than others. Environmental considerations highlight that the choice of electrolyte, discharge location, and process configuration is critical to achieving the primary objective: net removal of CO2 from the atmosphere via enhanced reabsorption.

Introduction

Over the past several decades, atmospheric carbon dioxide (CO_2) concentrations have risen from approximately 280 ppm in the pre-industrial era to about 430 ppm today, largely due to anthropogenic emissions. As a major greenhouse gas, human-caused CO_2 disrupts the natural carbon cycle, driving global warming, ocean acidification, and glacier loss. Despite the expansion of renewable energy, the global economy remains heavily dependent on fossil fuels for electricity, transportation, and manufacturing. Consequently, closing the carbon cycle remains one of the greatest engineering challenges of our time. As a result, Carbon Dioxide Removal (CDR) technologies will play a crucial role in humanity's future. At the same time, the growing availability of CO_2 as a feedstock will possibly displace fossil-based alternatives from the market.

The low volumetric concentration of CO₂ in ambient air makes its capture inherently energy-intensive.^[11] Established approaches, such as direct air capture (DAC) by absorption via

chemical looping (ACL), require a high-temperature step to regenerate the sorbent. [12] Similarly, temperature-vacuum swing adsorption (TVSA) demands regeneration via elevated temperatures or reduced pressures. [13] Emerging electrochemical concepts offer an alternative, avoiding thermal or vacuum steps by supplying electrons directly to the absorbent or adsorbent. [2] Among these, pH-modulating methods have attracted growing interest due to their operational simplicity, potentially low energy requirements, and the use of abundant electrolytes as sorbents. [14–18]

In this context, natural water bodies represent promising aqueous electrolytes. These electrolytes contain dissolved inorganic carbon (DIC), defined as the sum of all aqueous carbon species:

$$DIC = \left[CO_3^{2-}\right] + \left[HCO_3^{-}\right] + \left[CO_2\right]$$
 (1)

and total alkalinity (TA), which quantifies the water's acid-neutralizing capacity[19]:

$$TA = 2\left[CO_{3}^{2-}\right] + \left[HCO_{3}^{-}\right] + \left[B(OH)_{4}^{-}\right] + \left[OH^{-}\right] - \left[HSO_{4}^{-}\right] - \left[H^{+}\right]$$
(2)

Surface waters are naturally saturated in DIC through continuous equilibration with atmospheric CO_2 .^[20] The equilibrium DIC is strongly pH-dependent and therefore linked to the alkalinity of the water, which in turn governs the speciation and solubility of carbon. The interplay between TA and DIC is central to understanding marine carbon dioxide removal (mCDR).^[21]

$$CO_2(g) \rightleftharpoons CO_2(aq)$$
 (3)

$$CO_2(aq) + H_2O(I) \rightleftharpoons HCO_3(aq) + H^+(aq)$$
 (4)

$$HCO_3^-(aq) \rightleftharpoons CO_3^{2-}(aq) + H^+(aq)$$
 (5)

Globally and in total numbers, surface waters contain more carbon than the atmosphere, making them an underexploited carbon pool for capture applications (Figure 1A). [22] Among the carbon contained in surface waters, DIC is the predominant contributor (Figure 1B). ph-modulating methods can exploit this: decreasing pH drives CO_2 desorption while increasing pH enhances CO_2 dissolution according to the equilibria above (Equation (3)-(5)). The Bjerrum plot (Figure 1C) illustrates these dynamics and highlights two key concepts of electrochemical approaches for carbon capture: (i) cathodic reduction reactions raise pH, shifting carbon speciation (Figure 1C), increasing the overall amount of DIC (Figure 1D), promoting supersaturation, and driving mineral precipitation from background ions, and (ii) anodic oxidation reactions can release CO_2 at the counter electrode. [4]

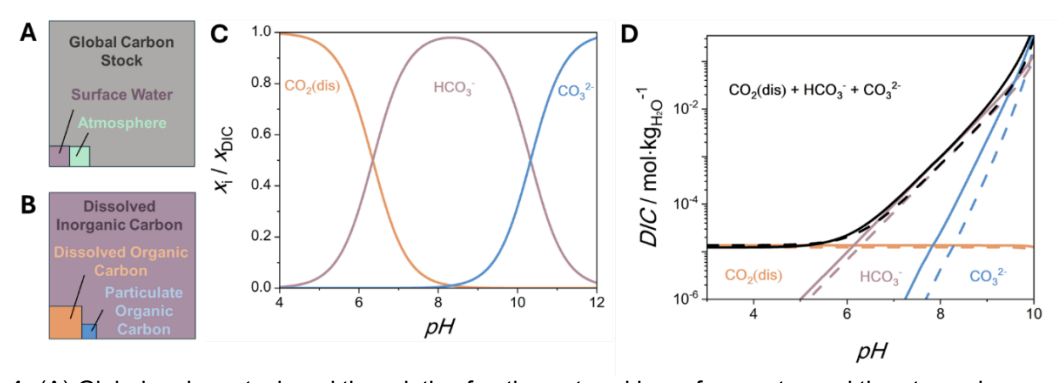


Figure 1: (A) Global carbon stock and the relative fractions stored in surface water and the atmosphere compared to the total carbon reservoir on Earth. [22] (B) Carbon stock of surface waters and the qualitative distribution among dissolved inorganic carbon (DIC), dissolved organic carbon (DOC), and particulate organic carbon (POC). [22] (C) Relationship between carbon speciation in aqueous electrolytes and pH, illustrated by a Bjerrum plot. (D) Carbon speciation and total carbon content in seawater compared to freshwater (dashed line) as a function of pH. Increasing pH levels favor enhanced carbon uptake.

A prominent electrochemical approach that can be exploited for this purpose is water electrolysis. It is important to consider that seawater typically has a pH between 7.5 and 9, whereas freshwater can span a much wider range, from 2.5 to above $10.^{[23,24]}$ Natural electrolytes are often complex, containing a variety of dissolved ions that influence the activity of individual species. Since the formation of carbonaceous minerals is rather slow and often kinetically hindered, this also leads to supersaturation of certain mineral species (e.g., calcite, magnesite, dolomite, ...). During electrolysis, the supply of electrons primarily reduces water at the cathode to produce hydrogen (HER, Equation (6)), whereas the anode either oxidizes water to form oxygen (OER, Equation (7)) or, in the presence of chloride and unselective catalysis, generates chlorine (CIER, Equation (8)). The ionic composition also introduces additional effects, including potential side reactions (e.g., involving Cr^{2+} , Fe^{2+} , Sr^{2+} , and other redox-active species) and the formation of scale on electrode surfaces. Moreover, the locally generated acidic or alkaline environments can chemically attack electrode materials, impacting durability and performance. In property in the property of the same property of the sequence of the same property of the sa

HER:
$$2H_2O(I) + 2e^- \rightarrow H_2(g) + 2 OH^-(aq), E_{red}^0 = -0.828 \text{ V vs SHE}$$
 (6)

OER:
$$2 H_2O(I) \rightarrow O_2(g) + 4 H^+(aq) + 4 e^-, E_{red}^0 = +0.401 V vs SHE$$
 (7)

CIER:
$$2CI^{-}(aq) \rightarrow CI_{2}(g) + 2 e^{-}, E_{red}^{0} = +1.396 \text{ V vs SHE}$$
 (8)

With this background, it is possible to describe how different unit operations influence TA and DIC in aqueous electrolyte solutions. Equilibration with a CO₂-containing gas primarily alters DIC while leaving TA constant (Figure 2A). Electrochemical addition of alkalinity, as schemed by HER, ideally increases TA without affecting DIC (Figure 2B). Precipitation of sparingly soluble minerals can modify both TA and DIC, with the magnitude of change largely dependent on the specific ions forming the solid phase (Figure 2C). Finally, mixing of two electrolyte streams generally leads to an averaging of TA and DIC, unless chemical reactions occur that perturb the composition of the combined solution (Figure 2D).^[21,35]

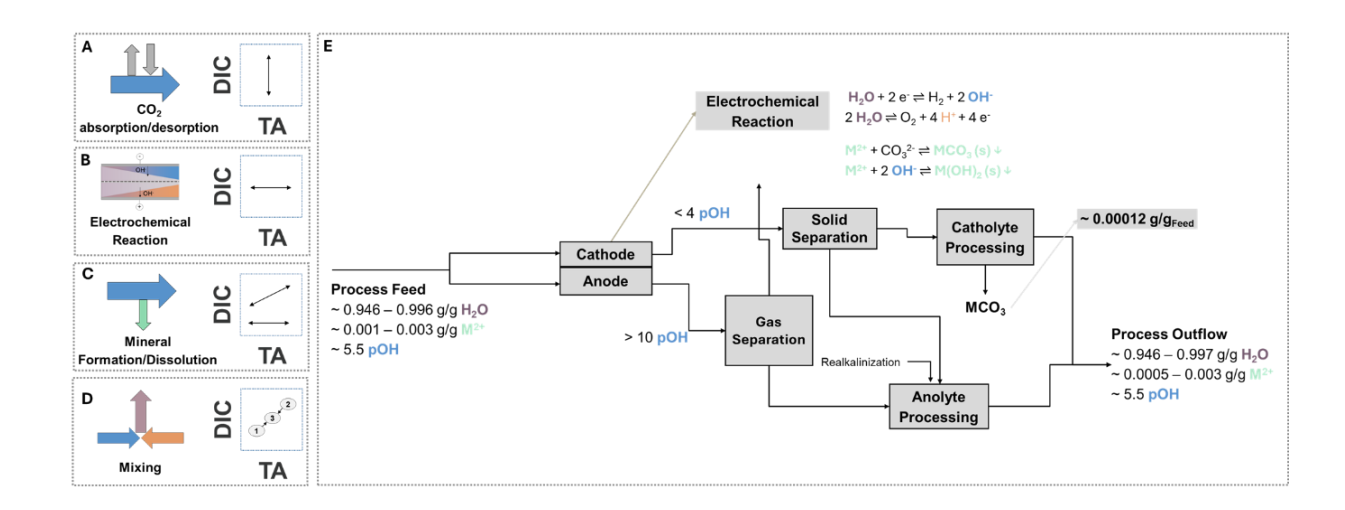


Figure 2: (A) CO₂ absorption or desorption alters the concentration of dissolved inorganic carbon (DIC) but does not affect total alkalinity (TA). (B) Electrochemical generation or consumption of alkalinity modifies TA without changing DIC. (C) Mineral dissolution or precipitation can influence both TA and DIC, depending on the mineral phase and its chemical composition. (D) Mixing of two electrolyte streams results in the averaging of DIC and TA, provided no reactions are ongoing. (E) Process overview of a single-step carbon capture and sequestration strategy, including additional process options building on the concept proposed by LaPlante et al. (2021).

Building on this foundation, several processes can be thought of that can be used for mCDR. One particularly interesting candidate is electrochemical mineral-trapping (Figure 2E). For the process description, we are focusing on aqueous electrolytes that are abundant in nature, e.g., river- or seawater. Within electrochemical mineral trapping, a quasi-neutral aqueous electrolyte containing various dissolved ions enters the electrochemical reactor. At the cathode, water electrolysis locally increases pH, shifts DIC speciation, and potentially triggers precipitation of sparingly soluble minerals, including Mg(OH)₂ (Brucite).^[3] At the same time, hydrogen is being produced as a valuable by-product. At the anode, DIC is shifted toward CO₂, and chlorine or oxygen may be generated depending on electrolyte composition and the catalytic activity and selectivity of the electrode. The catholyte then flows into an absorber unit, where mineral precipitation removes solids and alters both DIC and TA.[4] Mg(OH)₂ is particularly important, as it supplies OH- upon partial dissolution, sustaining CO₂ uptake, and enabling secondary mineralization pathways. [36,37] The analyte passes through a desorber unit, lowering DIC through controlled CO₂ release. Process intensification of alkalinization and absorption, as well as acidification and desorption, is thought of and holds promise for reducing energy demand. [11] After these separation steps, the analyte undergoes realkalinization, typically via silicate dissolution, restoring alkalinity without altering natural water chemistry. Finally, the catholyte and anolyte streams are recombined in a carefully controlled manner to preserve ecosystem integrity and to ensure that the process accelerates natural weathering without adverse environmental impacts. [38-40] Electrochemical mineral trapping offers a unique technique to control alkalinity and carbon speciation at the electrode-electrolyte interface directly. The precise tuning of supplied electrons governs local pH, ion availability, and precipitation kinetics, determining the efficiency and selectivity of mineral formation. [41-44] The dynamic interaction between the cathode-generated alkalinity, Mg(OH)₂ dissolution in the absorber, and subsequent mineralization pathways enables stable, long-term CO₂ sequestration in solid form with minimal environmental impact. [45,46]

So far, research has primarily focused on whether electrochemical mineral trapping with onestep mineralization in plants is a viable technology, what the process design should look like, and how its theoretical energy demand compares to established methods, such as Direct Air Capture (DAC). However, open questions remain, especially regarding the actual energy use in lab- and process-scale setups,^[47,48] the mineralization pathways that occur under these conditions,^[35] their time dependency, how supersaturation affects the solution's chemistry, and its potential environmental impact.^[49]

The present work establishes a thermodynamic and kinetic baseline for electrochemical mineral-trapping processes in mCDR. This is achieved through activity-based modeling, implementing Pitzer equations. Model predictions are validated against experimental data, confirming the accuracy of the underlying assumptions. Experiments and model results presented herein investigate the impact of externally added or withdrawn alkalinity on aqueous electrolytes and their tendency to form stable, carbon-containing minerals.

Experimental Methodology

General Overview

To achieve the given objectives, mineralization experiments and their simulation have been carried out within this work. However, the thermodynamic equilibrium of CO₂ and H₂O, as well as its dissolution kinetics, has already been measured in numerous experimental studies. ^[20,50,51] Therefore, the scope of this study is to investigate specific electrolyte compositions and their influence on the CO₂ gas absorption as well as the subsequent mineralization pathway. Altogether, the analysis should provide information about the

suitability of a natural, aqueous electrolyte for mCDR. Testing whether the model results align with experimentally determined datapoints opens the possibility to apply the findings to other natural electrolytes (e.g., seawater).

For this, the precipitation and dissolution of carbonaceous minerals in a homogeneously stirred setup were investigated. Overall, four aqueous electrolyte solutions were prepared and stimulated to track the dissolution or precipitation process. The initial composition of the aqueous electrolytes, as determined gravimetrically, are listed in Table 1.

Table 1: Initial molalities of the aqueous electrolyte solutions used within the mineralization experiments.

		Molality / mol·kg ⁻¹					Seed	
ID	Salts	Na⁺	K ⁺	Ca ²⁺	Mg ²⁺	Cl-	SO ₄ ² -	Added
SynF1	NaCl, MgSO₄, CaCl₂·2H₂O, KOH	1.2·10-4	1.7·10 ⁻⁵	1.8·10 ⁻³	6.1·10-4	3.8·10 ⁻³	6.1·10-4	-
SynF1-M1	NaCl, MgSO₄, CaCl₂·2H₂O, KOH NaCl,	1.2·10-4	1.7·10 ⁻⁵	1.8·10 ⁻³	6.1·10-4	3.8·10 ⁻³	6.1·10 ⁻⁴	CaCO ₃
SynS1	MgCl ₂ ·6H ₂ O, MgSO ₄ , CaCl ₂ ·2H ₂ O, KCl	6.7·10 ⁻¹	1.5·10 ⁻²	1.6·10-2	7.5·10 ⁻²	7.5·10 ⁻¹	4.0·10-2	-
SynS2	NaCl	6.3·10 ⁻¹	0	0	0	6.3·10 ⁻¹	0	-

Three general types of electrolytes were investigated: a) solutions mimicking freshwater (SynF), b) solutions mimicking seawater (SynS), and c) the interaction of electrolyte solutions with an initial surplus of sparingly soluble carbonaceous minerals.

Chemicals and Preparation

The suppliers and quality of chemicals used for the preparation of the aqueous electrolyte solutions are listed in Table 2. All deionized water used was drawn from a Millipore water purification system (resistivity 18.2 M Ω ·cm). All salts were dried at ambient pressure and 60 °C overnight before use.

Table 2: Suppliers and purities of the chemicals used in the absorption and mineralization experiments.

Solid or Aqueous Solution	Supplier	Purity/Concentration
CaCl ₂ ·2 H ₂ O	Sigma Aldrich	>99%
CaCO₃	Sigma Aldrich	>99.95%
CaMg(CO ₃) ₂	S3 Chemicals	>99%
KCI	Chemsolute	>99.5%
КОН	Sigma Aldrich	>85%
MgSO ₄	ITW Reagents	>98%
MgCl₂·6 H₂O	ITW Reagents	>99%
NaCl	Carl Roth GmbH	>99.5%
NaOH	Merck KGaA	1 M

Analysis

The aqueous electrolyte solutions investigated were analyzed for cations via a METROHM IC 930 Flex ion chromatograph equipped with a conductivity detector. Within the system, a Metrosep C6-250/4.0 column was used. The eluent consisted of 1.7 mM nitric acid and 1.7 mM Pyridine-2,6-dicarboxylic acid. A flow rate of 0.9 mL·min⁻¹ was used while thermostating the measurement chamber to 30 °C. With this setup, the retention times are: Na⁺ 11.9 min, K⁺ 21.9 min, Ca²⁺ 27.7 min, Mg²⁺ 37.2 min. Where necessary, anions were determined mathematically by applying the electroneutrality condition and mass balancing. Calibration of the system was carried out with a 6-component multi-element standard from Carl Roth GmbH. The relative uncertainty for freshly prepared standard solutions was determined to be better than 5% for all ion species.

Proton activity was determined via a pH-Combination Electrode (N 62 Glass Shaft, Pt Diaphragm) from SI Analytics. A 5-point calibration (pH = 4, pH = 7, pH = 9, pH = 10, pH = 12) at 25° C was determined for each measurement day to guarantee Nernst slopes better than 95% (actual/theoretical slope x 100°).

Batch Mineralization Experiments

For the batch mineralization experiments, aqueous electrolyte mixtures were prepared in 40 mL vials, each containing 20 mL of solution. Stock solutions (1 L) of water and the respective salts were prepared in advance. Each vial contained a stirring bar and was placed on a multi-position magnetic stirrer within a thermostated silicone oil bath, maintaining the temperature at the setpoint (±0.1 K) (Figure 3). Mineralization was initiated by adding 1 M NaOH solution, with the amount varied from 4 to 40 µmol in 4 µmol increments. Reaction progress was monitored for two representative cases (20 µmol and 40 µmol NaOH) using continuous syringe sampling at defined time intervals. CO₂ concentrations were measured with a Vaisala CARBOCAP® GMP343 probe, while temperature was recorded with a calibrated Pt100 thermometer connected to a digital multimeter (Keithley DAQ6510). All experiments were performed in triplicate to ensure statistical significance. Based on previous experiments and model results, a minimum equilibration time of 3 days was sufficient to reach equilibrium.

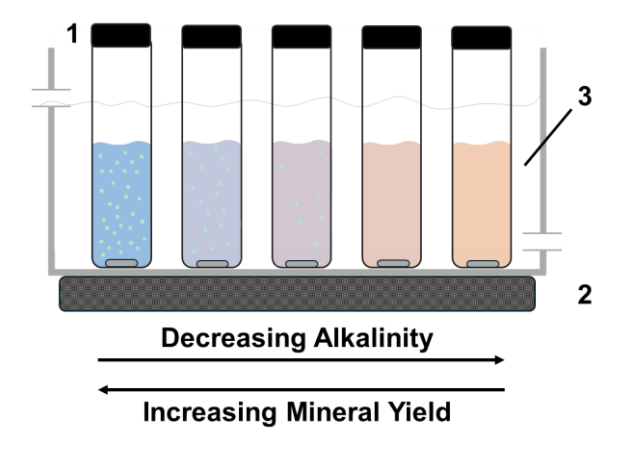


Figure 3: Batch mineralization experiment setup. Blue color indicates higher alkalinity, while orange color displays lower alkalinity. (1) Vials for the equilibration of the samples. (2) Multi-position magnetic stirrer. (3) Silicon oil bath at constant temperature.

After equilibration, samples were withdrawn from each flask using a syringe and immediately filtered through disposable syringe filters (CHROMAFIL® Xtra RC-10/25). Where necessary, samples were gravimetrically diluted with ultrapure water to prevent column overload during ion chromatography analysis. Dissolution and seeding experiments followed the same procedure, except that reactions were initiated by adding 1 M HCl or by additionally introducing defined amounts of seed crystals at the start of the experiment.

Modeling Methodology

The following section describes the procedure to fit the equilibrium and kinetic data that is presented during the conference.

Chemical Equilibrium

Modeling of the chemical equilibrium is performed via the equilibrium constant $K_j(T)$. For this, reactions j are defined via the law of mass action (c.f. equation 9).

$$K_{j}(T) = \frac{\prod_{n} a_{n}^{V_{n,j}}}{\prod_{m} a_{m}^{V_{m,j}}}$$
(9)

Herein, m are all substrates of the reactions, whereas n are the products. The activities are calculated from the component's molality b_i and activity coefficient y_i on the molality scale of the component i in solution. The reactions considered within this work are displayed in Table 3.

The reaction's temperature dependency of the chemical equilibrium constant is correlated via the van't Hoff equation using the reaction enthalpy in combination with Ulich's approximation. Table 3 lists the standard enthalpies of reaction as well as the equilibrium constants at 25 °C.

Table 3: Equilibrium constants and standard enthalpies of reaction for reaction j.

Reaction j	log ₁₀ (<i>K</i> _j (25 °C)	$\Delta_{ m r} H_{ m j}^0(T)$ / kJ·mol ⁻¹	Reference
$H_2O(I) \rightleftharpoons H^+(aq) + OH^-(aq)$	-14.001	55.800	[53]
CO_3^{2-} (aq) + $2H^+$ (aq) $\rightleftharpoons CO_2$ (aq) + H_2O (I)	16.767	-24.010	[54]
CO_3^{2-} (aq) + H ⁺ (aq) \rightleftharpoons HCO ₃ ⁻ (aq)	10.339	-14.889	[54]
SO_4^{2-} (aq) + H ⁺ (aq) \rightleftharpoons HSO ₄ ⁻ (aq)	1.979	20.543	[55]
Mg^{2+} (aq) + H_2O (I) \rightleftharpoons $MgOH^+$ (aq) + H^+ (aq)	-11.440	64.513	[56]

Phase Equilibria

The gas-liquid equilibrium between water and CO₂ is modeled according to Henry's Law on the molality scale:

$$H_{\text{CO}_2}^{\text{b}} b_{\text{CO}_2}^{(\text{aq})} \gamma_{\text{CO}_2}^{(\text{aq})} = p_{\text{CO}_2}^{(\text{aq})} \tag{10}$$

Here, $H^b_{CO_2}$ is Henry's Law constant of ${\rm CO_2}$ in pure water on the molality scale, taken from Rumpf and Maurer as 2.98 MPa·kg·mol⁻¹.^[57] The gas phase is treated as an infinite reservoir due to its volume being much larger than that of the aqueous electrolyte solution. For closed systems without exchange with the gas atmosphere, only reaction and solid-liquid equilibria are considered, while gas-liquid equilibria are excluded. This is particularly relevant for electrolyte solutions flowing through electrochemical reactors, where the dissolved inorganic carbon (DIC) originates from the previously saturated solution. In experiments where the solution is continuously exposed to the atmosphere, kinetic effects must be considered, as equilibrium is not established instantaneously.

The aqueous electrolyte solution serves as the base unit, while the gas and solid phases may or may not be present, depending on the reaction and environmental/spatial conditions. For the solid phase, this is especially important for sparingly soluble carbonaceous minerals M, which can form upon supersaturation. One or more such minerals may precipitate.

The condition for mineral formation can be expressed as:

$$K_{AP.M} \ge K_{SP.M}$$
 (11)

Here, $K_{SP,M}$ is the solubility product, and $K_{AP,M}$ is the activity product of the mineral M, defined as:

$$K_{AP,M} = \prod_{n} (b_n \cdot \gamma_n)^{v_n} \cdot (a_{H_2O})^{v_{H_2O}}$$
 (12)

$$K_{SP,M} = \exp\left(-\sum_{n} \frac{v_n \mu_n^0}{RT}\right)$$
 (13)

The mineral M is assumed to form from all ion species n, with v_n being the stoichiometric coefficient in the precipitation reaction and μ_n^0 the standard chemical potential of the ion. $a_{\rm H_2O}$ is the activity of water, and $v_{\rm H_2O}$ the moles of crystal water per mole of M. At a given temperature, the solubility product is constant, while the activity product reflects the solution's actual composition. Precipitation occurs when the activity product exceeds the solubility product, which indicates supersaturation. Conversely, if a mineral is present and the activity product drops below the solubility product, dissolution occurs. These processes are governed by reaction kinetics, which influence the rate and sequence of reactions. Ultimately, thermodynamic equilibrium is reached if the duration is sufficient and no metastable states intervene. At equilibrium, a reactive gas-liquid-solid equilibrium is established, as illustrated in Figure 4. This is also reflecting what is happening during mineralization pathways in surface water in nature. All solubility products used within this work are listed in Table 4.

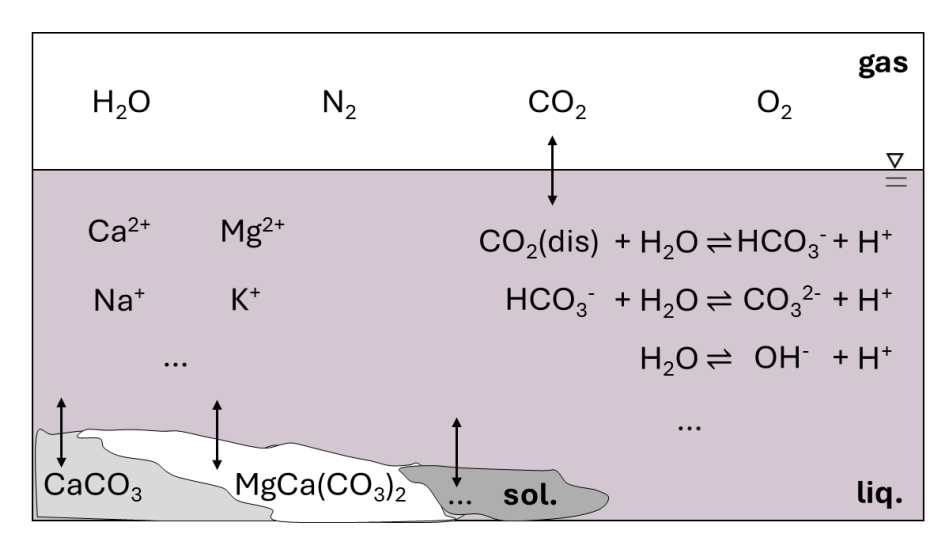


Figure 4: Reactive gas-liquid-solid equilibrium model scheme for aqueous electrolytes of natural origin.

Activity Model and Parametrization

This work employs extended Pitzer equations for the calculation of activity coefficients within the aqueous electrolyte solutions considered. The matrix notation and modeling implementation reflect the work by Keller et al.^[58] Therefore, we only provide a brief outline of the main equations used within this work.

A vector of activities can be calculated as a function of solute molalities b, their respective charge values z, and matrices containing functional values depending on interaction parameters. [60]

$$\ln(\boldsymbol{\gamma}) = \left(\ln(\boldsymbol{\gamma}_{DH}) + q'\right) \mathbf{z_2} + q^C \mathbf{z} + (2\boldsymbol{Q}(\boldsymbol{l}) + 2Z\boldsymbol{C})\boldsymbol{b} + \left(\frac{1}{2}\boldsymbol{b}^{\mathsf{t}}\mathbf{T}\boldsymbol{b}\right)^{\mathsf{t}}$$
(14)

Within this equation, t denotes transposition. The activity of water as the solvent can be calculated from the osmotic coefficient ϕ :

$$ln(a_w) = -2 \cdot W(ln \gamma_{DH}' + q^{\Phi} + Z \cdot q^C + q^L + t) - b \cdot W$$
(15)

Where M is the total number of moles of the solutes, and the molecular mass of water is W.

Main influences on the final activity originate from the interaction parameters, the temperature, and the ionic strength. The temperature dependency of parameters within the activity coefficient model used are calculated via

$$Par = A_{Par} + \frac{B_{Par}}{T/K}$$
 (16)

The ionic strength of an aqueous electrolyte solution is calculated as

$$I = \sum_{i=1}^{N} b_i z_i^2$$
 (17)

The Pitzer parameters used are given in Tables Table 5 - Table 12. Overall, all previous equations and equilibria are implemented together within a Python code using scipy's least_squares algorithm to solve for the equilibrium state.

Reaction Velocity

The dissolution and stripping of CO_2 into and from the liquid phase are described using a standard k_L a approach. The equilibrium concentration of CO_2 in the liquid phase is determined by temperature and pressure conditions, following Henry's Law, and gives the driving force for the gas mass transfer.

$$-\frac{\mathrm{d}b_{\mathrm{L}}}{\mathrm{d}t} = k_{\mathrm{L}}a \cdot (b_{\mathrm{L}} - b_{\mathrm{e}}) \tag{18}$$

The rate of a reversible chemical reaction can be expressed in terms of the extent of reaction,

$$\frac{\mathrm{d}\xi}{\mathrm{d}t} = r_{\mathrm{f}} - r_{\mathrm{b}} = k_{\mathrm{f}} \cdot \prod a_{\mathrm{subs}}^{\mathrm{V}_{\mathrm{i}}} - k_{\mathrm{b}} \cdot \prod a_{\mathrm{prod}}^{\mathrm{V}_{\mathrm{i}}}$$
(19)

Here, $\frac{d\xi}{dt}$ is the rate at which the reaction proceeds. The first term, r_f , is the forward reaction rate, and the second term, r_b , is the backward rate. The constants k_f and k_b are the rate

constants for the forward and backward reactions. The products $\prod[Subs]^{\nu_i}$ and $\prod[Prod]^{\nu_i}$ represent the activities of the reactants and products, each raised to the power of their stoichiometric coefficients.

The kinetics of precipitation and dissolution require a case-based treatment. When no solid phase is present and the solution becomes supersaturated, precipitation is initiated. Once a solid phase exists, undersaturation drives dissolution. At equilibrium, no net change occurs. The velocity can be described via a surface-controlled expression. For this, we apply the kinetic model of Koutsoukos et al. (1980), which has been applied, e.g., by Musvoto et al. [62,63]:

$$\frac{d}{dt}M_{V^{+}}A_{V^{-}} = -ks \left[\left(\left[M^{m+} \right]^{V^{+}} \left[A^{a-} \right]^{V^{-}} \right)^{\frac{1}{V}} - \left(\left[M^{m+} \right]_{0}^{V^{+}} \left[A^{a-} \right]_{0}^{V^{-}} \right)^{\frac{1}{V}} \right]^{n}$$
(20)

Here, $[M^{m+}]$ and $[A^{a-}]$ represent the activities of the crystal lattice ions in solution at time t, while $[M^{m+}]_0$ and $[A^{a-}]_0$ correspond to their activities at equilibrium. At equilibrium, the relation $[M^{m+}]_0^{V^+}[A^{a-}]_0^{V^-}=K_{\rm sp}'$ defines the apparent solubility product $K_{\rm sp}'$ of the salt. The parameter $K_{\rm sp}'$ defines the apparent precipitation rate constant, and $K_{\rm sp}'$ of the salt. The parameter $K_{\rm sp}'$ of the salt of the total number of active growth sites present on the seed material. The terms $K_{\rm sp}'$ and $K_{\rm sp}'$ refer to the stoichiometric numbers of cationic and anionic species, respectively, with $K_{\rm sp}'$ of the salt. The parameter K_{\rm

This expression can also be narrowed down and related to the supersaturation degree of the solution with respect to a certain mineral. For simplicity reasons and since previous works in literature have shown good results for such lumped expressions, we introduce the empirically determined collection parameters k and n.

$$R \propto k \cdot (\Omega - 1)^{n} \tag{21}$$

By considering homogeneous mixing, all expressions can be reduced to systems of ordinary differential equations, which can be solved using standard numerical algorithms. For this, we developed a Python code that features all the equations above in an activity-based model. The forward calculation was carried out via scipy's library scipy.integrate employing the solve_ivp module. The applied solver strategy is an LSODA algorithm from the ODEPACK library. LSODA dynamically detects stiffness and switches between the non-stiff Adams method and the stiff Backward Differentiation Formula (BDF), ensuring numerical stability and efficiency without requiring prior specification of stiffness. Where required, parameter fits were carried out using scipy's minimize module. The algorithm used is a Limited-memory Broyden–Fletcher–Goldfarb–Shanno with Box constraints (L-BFGS-B).

Results and Discussion

Excerpt of the Reactive Gas-Liquid-Solid Equilibrium Results

Mineralization experiments with SynF1 at 25 °C demonstrated that the addition of $1.5 \text{ mmol}_{\text{NaOH}} \cdot \text{kg}^{-1}$ is sufficient to induce the formation of carbonaceous minerals under equilibrium conditions (Figure 5A). Even with higher supersaturation, for example, following the addition of $3 \text{ mmol}_{\text{NaOH}} \cdot \text{kg}^{-1}$, only Ca^{2+} was consumed at equilibrium. This indicates that, in highly diluted freshwater systems, precipitation is largely restricted to calcite or other Ca^{2+} -involving minerals. By contrast, in more complex systems such as seawater, the convolution with an increasing number of ions and their higher ionic strength usually enables the formation of additional stable mineral phases. This expands the possible mineral trapping pathways.

Conversely, the addition of HCl to a calcite-containing mixture led to the expected dissolution process (Figure 5B), which was captured by the model with sufficient accuracy. Overall, the equilibrium results are consistent with model predictions, while deviations are generally within ±10% error range across most measurement points (Figure 5C). This highlights the robustness of the model (cf. subsection "Activity Model and Parametrization", Appendix), which is essential for investigating theoretical/other real-world aqueous electrolyte solutions in the context of mCDR. Optimizing electrolyte composition could significantly enhance mineral trapping efficiency, as the yield depends not only on ionic strength, temperature, and partial pressures, but also on the overall ionic composition and the interactions between ions in the electrolyte. Identifying the most suitable electrolyte is, therefore, a key step toward improving mCDR processes.

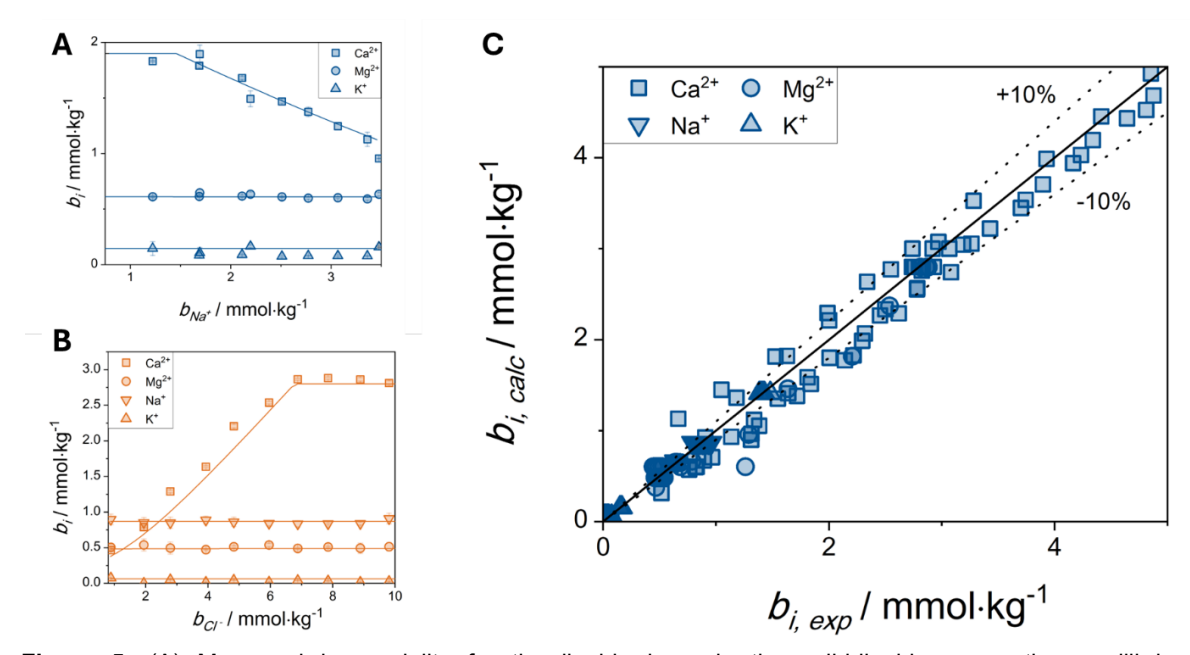


Figure 5: (A) Measured ion molality for the liquid phase in the solid-liquid-gas reactive equilibrium of homogeneously stirred SynF1 electrolytes with variation of Na⁺ quantity at 25 °C and at ambient CO₂ partial pressure. Lines: model results. (B) Ion molality in the liquid phase for variation of Cl⁻ quantity under similar conditions as in 6A. (C) Deviations between experimentally determined and calculated ion molality for Na⁺ and Cl⁻- perturbed aqueous electrolyte solutions (SynF1). Dashed lines represent ±10% deviation.

Conclusion

Mineral trapping is a promising technology for mCDR. This work demonstrates that a combined thermodynamic, kinetic, and (in future work) spatial description of the process is feasible, with good agreement between experimental observations and model predictions. However, further environmental assessments are necessary, as the discharge of both alkalinized and acidified electrolytes may impact ecosystems. In particular, the role of secondary precipitation requires closer examination. Future research should also focus on electrolyte composition, since it directly affects energy demand, process applicability, and environmental impact. Developing cost functions that integrate these factors will help evaluate the overall potential of the technology and identify opportunities for optimization. Ultimately, a rigorous process model incorporating multi-objective optimization is desirable to address this multifaceted challenge. Evaluating mineral trapping against other, more mature CDR technologies will reveal whether mineral trapping via electrochemical stimulation can be performed at scale.

Acknowledgements

D.G. was supported by the KSB Stiftung [KSB Project 1.1392.2023.1] and gratefully acknowledges their funding.

References

- [1] M. W. Jones, G. P. Peters, T. Gasser, R. M. Andrew, C. Schwingshackl, J. Gütschow, R. A. Houghton, P. Friedlingstein, J. Pongratz, C. Le Quéré, *Scientific data* **2023**, *10*, 155.
- [2] N. Rosen, A. Welter, M. Schwankl, N. Plumeré, J. Staudt, J. Burger, *Energy & fuels : an American Chemical Society journal* **2024**, *38*, 15469.
- [3] E. C. La Plante, X. Chen, S. Bustillos, A. Bouissonnie, T. Traynor, D. Jassby, L. Corsini, D. A. Simonetti, G. N. Sant, *ACS ES&T engineering* **2023**, *3*, 955.
- [4] E. C. La Plante, D. A. Simonetti, J. Wang, A. Al-Turki, X. Chen, D. Jassby, G. N. Sant, ACS Sustainable Chem. Eng. **2021**, *9*, 1073.
- [5] H. Lee, K. Calvin, D. Dasgupta, G. Krinner, A. Mukherji, P. W. Thorne, C. Trisos, J. Romero, P. Aldunce, K. Barrett et al., IPCC, 2023: Climate Change 2023: Synthesis Report. Contribution of Working Groups I, II and III to the Sixth Assessment Report of the Intergovernmental Panel on Climate Change [Core Writing Team, H. Lee and J. Romero (eds.)]. IPCC, Geneva, Switzerland, Intergovernmental Panel on Climate Change (IPCC), 2023.
- [6] W. J. RIPPLE, C. WOLF, T. M. NEWSOME, P. BARNARD, W. R. MOOMAW, 11,258 SCIENTIST SIGNATORIES FROM 153 COUNTRIES, *BioScience* **2020**, *70*, 8.
- [7] M. WiatrosMotyka, N. Fulghum, D. Jones, K. Altieri, R. Black, H. Broadbent, C. BruceLockhart, M. Ewen, M. Phil, K. Rangelova **2024**.
- [8] D. Groh, P. Chmielniak, C. W. Jones, C. Sievers, ChemSusChem 2025, e2500835.
- [9] M. Bui, C. S. Adjiman, A. Bardow, E. J. Anthony, A. Boston, S. Brown, P. S. Fennell, S. Fuss, A. Galindo, L. A. Hackett et al., *Energy Environ. Sci.* **2018**, *11*, 1062.
- [10] L. F. Vega, D. Bahamon, I. I. I. Alkhatib, ACS Sustainable Chem. Eng. 2024, 12, 5357.
- [11] R. A. Shaw, T. A. Hatton, *International Journal of Greenhouse Gas Control* **2020**, 95, 102878.
- [12] F. Zeman, K. S. Lackner, World Res. Rev. 2004, 16, 157.
- [13] S. Choi, J. H. Drese, C. W. Jones, *ChemSusChem* **2009**, 2, 796.
- [14] H. Seo, Y. Chen, E. Walter, M. Abdinejad, T. A. Hatton, *Angewandte Chemie* (*International ed. in English*) **2025**, e202505723.
- [15] H. Seo, T. A. Hatton, *Nature communications* **2023**, *14*, 313.
- [16] H. Seo, M. Rahimi, T. A. Hatton, *Journal of the American Chemical Society* **2022**, *144*, 2164.
- [17] S. Kim, M. P. Nitzsche, S. B. Rufer, J. R. Lake, K. K. Varanasi, T. A. Hatton, *Energy Environ. Sci.* **2023**, *16*, 2030.
- [18] M. Rahimi, G. Catalini, M. Puccini, T. A. Hatton, RSC advances 2020, 10, 16832.
- [19] J. L. Sarmiento, Ocean Biogeochemical Dynamics, Princeton University Press, 2006.
- [20] R. E. Zeebe, D. Wolf-Gladrow, *CO2 in seawater: equilibrium, kinetics, isotopes*, Gulf Professional Publishing, **2001**.
- [21] F. J. Dickhardt, M. P. Nitzsche, S. Rufer, T. A. Hatton, K. K. Varanasi, *Environmental science & technology* **2024**, *58*, 22953.
- [22] Canadell, J.G., P.M.S. Monteiro, M.H. Costa, L. Cotrim da Cunha, P.M. Cox, A.V. Eliseev, S. Henson, M. Ishii, S. Jaccard, C. Koven, A. Lohila, P.K. Patra, S. Piao, J. Rogelj, S. Syampungani, S. Zaehle, and K. Zickfeld, 2021: Global Carbon and other Biogeochemical Cycles and Feedbacks. In Climate Change 2021: The Physical Science Basis. Contribution of Working Group I to the Sixth Assessment Report of the Intergovernmental Panel on Climate Change [Masson-Delmotte, V., P. Zhai, A. Pirani, S.L. Connors, C. Péan, S. Berger, N. Caud, Y. Chen, L. Goldfarb, M.I. Gomis, M. Huang, K. Leitzell, E. Lonnoy, J.B.R. Matthews, T.K. Maycock, T. Waterfield, O. Yelekçi, R. Yu, and B. Zhou (eds.) (Ed.) Climate Change 2021 The Physical Science Basis, Cambridge University Press, 2023.
- [23] Simon Aram, Water geochemistry in surface and ground water systems, figshare, 2021.
- [24] F. J. Millero, R. Feistel, D. G. Wright, T. J. McDougall, *Deep Sea Research Part I:* Oceanographic Research Papers **2008**, *55*, 50.
- [25] P. M. May, E. F. May, ACS omega **2024**, 9, 46373.

- [26] F. Pawellek, F. Frauenstein, J. Veizer, *Geochimica et Cosmochimica Acta* **2002**, 66, 3839.
- [27] G. Liu, Journal of Electroanalytical Chemistry 2022, 923, 116805.
- [28] H. Liu, W. Shen, H. Jin, J. Xu, P. Xi, J. Dong, Y. Zheng, S.-Z. Qiao, *Angewandte Chemie* (International ed. in English) **2023**, *62*, e202311674.
- [29] A. Kasani, R. Maric, L. Bonville, S. Bliznakov, ChemElectroChem 2024, 11.
- [30] G. Amikam, P. Nativ, Y. Gendel, *International Journal of Hydrogen Energy* **2018**, *43*, 6504.
- [31] L. Yu, M. Ning, Y. Wang, C. Yuan, Z. Ren, Nat Rev Mater 2025.
- [32] F. Bertin, G. R. Joshi, J. Kittel, C. Sagnard, F. Ropital, M. Martinez, C. Bosch, K. Wolski, *Corrosion Science* **2024**, 227, 111778.
- [33] L. Zhao, X. Li, J. Yu, W. Zhou, Materials (Basel, Switzerland) 2023, 16.
- [34] A. Zagalskaya, M. R. Nouri, V. Alexandrov, *Current Opinion in Electrochemistry* **2023**, *41*, 101352.
- [35] N. Karo, G. Itov, O. Mayraz, C. Vogt, Chemical Engineering Journal 2024, 500, 156380.
- [36] B. Yang, J. Leonard, C. Langdon, *Marine Chemistry* **2023**, 253, 104251.
- [37] Z. Zhang, Z. Liu, F. Wang, S. Hu, ACS Sustainable Chem. Eng. 2023, 11, 9442.
- [38] M. Fuhr, S. Geilert, M. Schmidt, V. Liebetrau, C. Vogt, B. Ledwig, K. Wallmann, *Front. Clim.* **2022**, *4*.
- [39] J. Griffioen, The Science of the total environment 2017, 575, 536.
- [40] F. Montserrat, P. Renforth, J. Hartmann, M. Leermakers, P. Knops, F. J. R. Meysman, *Environmental science & technology* **2017**, *51*, 3960.
- [41] P. R. Halloran, T. G. Bell, W. J. Burt, S. N. Chu, S. Gill, C. Henderson, D. T. Ho, V. Kitidis, E. La Plante, M. Larrazabal et al., *Front. Clim.* **2025**, *7*.
- [42] N. Devi, X. Gong, D. Shoji, A. Wagner, A. Guerini, D. Zampini, J. Lopez, A. F. Rotta Loria, *Advanced Sustainable Systems* **2025**, *9*.
- [43] J. Wang, P. Zhu, H. Qin, K. Zuo, H. Zhao, Z. B. Zhang, *Energy Environ. Sci.* **2025**, *18*, 6438.
- [44] L. Wu, Y. Xu, Q. Wang, X. Zou, Z. Pan, M. K. H. Leung, L. An, *Energy Environ. Sci.* **2025**, *18*, 4596.
- [45] A. Dickinson-Cove, E. La Plante, Y. Liu, D. Simonetti, E. M. V. Hoek, G. Sant, D. Jassby, *Chemical Society reviews* **2025**, *54*, 116.
- [46] P. Aleta, A. Refaie, M. Afshari, A. Hassan, M. Rahimi, *Energy Environ. Sci.* **2023**, *16*, 4944.
- [47] X. Guan, G. Zhang, J. Li, S. C. Kim, G. Feng, Y. Li, T. Cui, A. Brest, Y. Cui, *Proceedings of the National Academy of Sciences of the United States of America* **2024**, *121*, e2410841121.
- [48] M. P. Nitzsche, M. Massen-Hane, T. A. Hatton, Ind. Eng. Chem. Res. 2025, 64, 6209.
- [49] C. A. Moras, L. T. Bach, T. Cyronak, R. Joannes-Boyau, K. G. Schulz, *Biogeosciences* **2022**, *19*, 3537.
- [50] W. G. Mook 2000.
- [51] A. G. Dickson, *Guide to best practices for ocean acidification research and data reporting* **2010**, *1*, 17.
- [52] G. Forchhammer, *Philosophical Transactions of the Royal Society of London* **1865**, 203.
- [53] F. J. Millero, Geochimica et Cosmochimica Acta 1995, 59, 661.
- [54] T. J. Lueker, A. G. Dickson, C. D. Keeling, Marine Chemistry 2000, 70, 105.
- [55] A. G. Dickson, D. J. Wesolowski, D. A. Palmer, R. E. Mesmer, *J. Phys. Chem.* **1990**, *94*, 7978.
- [56] C. Appelo, D. L. Parkhurst, V. Post, Geochimica et Cosmochimica Acta 2014, 125, 49.
- [57] B. Rumpf, G. Maurer, Ber Bunsenges Phys Chem 1993, 97, 85.
- [58] A. Keller, J. Burger, H. Hasse, M. Kohns, Desalination 2021, 503, 114866.
- [59] L. Plummer, E. Busenberg, Geochimica et Cosmochimica Acta 1982, 46, 1011.
- [60] S. A. Bea, J. Carrera, C. Ayora, F. Batlle, Computers & Geosciences 2010, 36, 526.
- [61] E. Musvoto, Water Research 2000, 34, 1857.
- [62] E. Musvoto, Water Research 2000, 34, 1868.
- [63] G. A. Ekama, M. C. Wentzel, R. E. Loewenthal, Water science and technology: a journal

- of the International Association on Water Pollution Research 2006, 53, 65.
- [64] S. W. Sötemann, P. van Rensburg, N. E. Ristow, M. C. Wentzel, R. E. Loewenthal, G. A. Ekama, *Water science and technology: a journal of the International Association on Water Pollution Research* **2006**, *54*, 109.
- [65] A. Cashmore, R. Miller, H. Jolliffe, C. J. Brown, M. Lee, M. D. Haw, J. Sefcik, *Crystal growth & design* **2023**, 23, 4779.

Appendix

A.1 Solubility Constants and Standard Reaction Enthalpies for Mineral Formation.

Table 4: Solubility constants and standard reaction enthalpies considered within this work.

Mineral M	Chemical Composition	Log ₁₀ (K _{SP,M}) @ 25°C	ΔrH ⁰ / kJ·mol ⁻¹
Anhydrite	CaSO ₄	-4.366	-15.49 ± 4.791
Antarcticite	CaCl₂ ·6 H₂O	0.077	-13.99
Aragonite	CaCO ₃	-6.258	-13.987
Arcanite	K ₂ SO ₄	-1.809	22.945
Bischofite	$MgCl_2\cdot 6H_2O$	4.436	-8.71
Bloedite	Na ₂ Mg(SO ₄) ₂ · 4 H ₂ O	-2.392	0.000
Brucite	Mg(OH) ₂	2.709	-53.245
Burkeite	Na ₆ CO ₃ (SO ₄) ₂	2.648	0.000
Calcite	CaCO ₃	-6.399	-12.716
Carnallite	KMgCl ₃ · 6H ₂ O	4.317	5.255
Chloromagne	$MgCl_2$	21.945	-158.802
site Dolomite	CaMg(CO ₃) ₂	-13.175	-42.896
Epsomite	$MgSO_4\cdot 7H_2O$	-2.027	11.687
Gaylussite	CaNa ₂ (CO ₃) ₂ · 5H ₂ O	-2.562	31.099
Ghiaraite	CaCl₂ ·4 H₂O	5.350	-11.31
Gypsum	CaSO₄ · 2H₂O	-4.572	-0.526
Halite	NaCl	1.586	3.747
Hexahydrite	$MgSO_4\cdot 6H_2O$	-1.667	-4.625
Huntite	CaMg ₃ (CO ₃) ₄ + 4H ⁺	-14.029	-124.781
Hydromagnes ite	Mg5(CO3)4(OH)2·4H2 O	0.754	-240.473
Hydrophilite	CaCl₂	11.781	-81.407
Kainite	KMgClSO ₄ ·3H ₂ O	-0.231	-12.95
Kalicinite	KHCO₃	-10.000	34.95
Kieserite	$MgSO_4 \cdot H_2O$	-0.171	0.000
Lansfordite	MgCO ₃ ·5H ₂ O	4.841	0.000
Leonhardite	MgSO ₄ ·4H ₂ O	-0.926	-24.03
Leonite	$K_2Mg(SO_4)_2 \cdot 4H_2O$	-4.024	15.29
Magnesite	MgCO ₃	-5.988	-24.16
Mercallite	KHSO ₄	-1.419	-0.59

Mirabilite	Na ₂ SO ₄ · 10 H ₂ O	-1.153	79.483
Misenite	K ₈ H ₆ (SO ₄) ₇	-10.941	0.000
Nahcolite	NaHCO₃	-6.444	23.592
Natron	Na ₂ CO ₃ ·10H ₂ O	1.067	61.795
Nesquehonite	MgCO ₃ ·3H ₂ O	-3.113	-26.76
Pentahydrite	MgSO ₄ ·5H ₂ O	-1.317	-14.187
Picromerite	$K_2Mg(SO_4)_2 \cdot 6H_2O$	-4.385	33.487
Pirssonite	Na ₂ Ca(CO ₃) ₂ ·2H ₂ O	-2.274	9.58
Polyhalite	K₂MgCa₂(SO₄)₄·2H₂ O	-13.932	0.000
Portlandite	Ca(OH) ₂	17.156	-129.309
Sinjarite	CaCl₂·2H₂O	7.950	-44.790
Sylvite	KCI	0.872	14.298
Syngenite	$K_2Ca(SO_4)_2 \cdot 2H_2O$	-7.160	-16.325
Thermonatrite	Na ₂ CO ₃ ·H ₂ O	3.051	-15.461
Thernardite	Na ₂ SO ₄	-0.132	-2.277
Trona	$Na_3H(CO_3)_2 \cdot 2H_2O$	-8.787	-18.221

A.2 Pitzer Parameters

Table 5: Model parameters for $\beta^{(0)}$.

Apar	Ca ²⁺	H⁺	K⁺	Mg ²⁺	Na⁺	Sr ²⁺
Br ⁻	0.3190	0.1960	0.0560	0.4330	0.0973	0.3310
CI-	0.3050	0.1780	0.0484	0.3520	0.0765	0.2860
CO ₃ ²⁻	0.0000	0.0000	0.0011	0.0000	0.0362	0.0000
F-	0.0000	0.0000	0.0000	0.0000	0.0000	0.0000
HCO₃ ⁻	0.4000	0.0000	-0.0107	0.3290	0.0280	0.1200
HSO₄⁻	0.2150	0.2070	-0.0003	0.4750	0.4540	0.0000
OH-	-0.1750	0.0000	0.1300	0.0000	0.0864	0.0000
SO ₄ ² -	0.2000	0.0298	0.0499	0.2210	0.0196	0.2000
B _{par}	Ca ²⁺	H⁺	K⁺	Mg ²⁺	Na⁺	Sr ²⁺
Br ⁻	-0.0005	-0.0002	0.0007	-0.0001	0.0008	-0.0003
CI-	-0.0012	-0.0003	0.0006	-0.0004	0.0090	0.0007
CO ₃ ²⁻	0.0000	0.0000	0.0011	0.0000	0.0144	0.0000
F-	0.0000	0.0000	0.0000	0.0000	0.0000	0.0000
HCO₃-	0.0000	0.0000	0.0010	0.0000	-0.0088	0.0000
HSO₄⁻	0.0000	0.0000	0.0000	0.0000	0.0000	0.0000
OH-	0.0000	0.0000	0.0000	0.0000	0.0067	0.0000
SO ₄ ²⁻	0.0000	0.0000	0.0014	-0.0043	0.0026	-0.0029

Table 6: Model parameters for $\beta^{(1)}$.

A _{par} Ca ²⁺ H ⁺	K ⁺	Mg ²⁺	Na⁺	Sr ²⁺
--	----------------	------------------	-----	------------------

Br	1.6100	0.3560	0.2210	1.7500	0.2790	1.7100
CI-	0.0000	0.0000	1.4300	0.0000	1.5100	0.0000
CO ₃ ² -	0.0000	0.0000	0.0000	0.0000	0.0000	0.0000
F-	0.0000	0.0000	0.0000	0.0000	0.0000	0.0000
HCO₃⁻	2.9800	0.0000	0.2500	0.6070	0.0440	0.0000
HSO₄⁻	2.5300	0.0000	0.3200	0.0000	0.2530	0.0000
OH-	-0.2300	0.0000	0.3200	0.0000	0.2530	0.0000
SO ₄ ² -	3.5500	0.0000	0.7790	3.3700	1.1100	3.2000
	_					- 0:
B _{par}	Ca ²⁺	H⁺	K⁺	Mg ²⁺	Na⁺	Sr ²⁺
B _{par}	0.0060	0.0004	0.0017	Mg ²⁺ 0.0038	Na ⁺ 0.0011	0.0065
Br	0.0060	0.0004	0.0017	0.0038	0.0011	0.0065
Br Cl	0.0060 -0.0154	0.0004 0.0001	0.0017 0.0011	0.0038 0.0036	0.0011 0.0001	0.0065 0.0028
Br ⁻ Cl ⁻ CO ₃ ² -	0.0060 -0.0154 0.0000	0.0004 0.0001 0.0000	0.0017 0.0011 0.0044	0.0038 0.0036 0.0000	0.0011 0.0001 0.0521	0.0065 0.0028 0.0000
Br ⁻ Cl ⁻ CO ₃ ²⁻ F ⁻	0.0060 -0.0154 0.0000 0.0000	0.0004 0.0001 0.0000 0.0000	0.0017 0.0011 0.0044 0.0000	0.0038 0.0036 0.0000 0.0000	0.0011 0.0001 0.0521 0.0000	0.0065 0.0028 0.0000 0.0000
Br ⁻ Cl ⁻ CO ₃ ²⁻ F ⁻ HCO ₃ ⁻	0.0060 -0.0154 0.0000 0.0000 0.0000	0.0004 0.0001 0.0000 0.0000 0.0000	0.0017 0.0011 0.0044 0.0000 0.0011	0.0038 0.0036 0.0000 0.0000 0.0000	0.0011 0.0001 0.0521 0.0000 0.0139	0.0065 0.0028 0.0000 0.0000 0.0000

Table 7: Model parameters for $\beta^{(2)}$.

Apar	Ca ²⁺	H⁺	K ⁺	Mg ²⁺	Na⁺	Sr ²⁺
Br ⁻	0.0000	0.0000	0.0000	0.0000	0.0000	0.0000
CI-	-1.1300	0.0000	0.0000	0.0000	0.0000	0.0000
CO ₃ ²⁻	0.0000	0.0000	0.0000	0.0000	0.0000	0.0000
F-	0.0000	0.0000	0.0000	0.0000	0.0000	0.0000
HCO₃-	0.0000	0.0000	0.0000	0.0000	8.2200	0.0000
HSO₄⁻	0.0000	0.0000	0.0000	0.0000	0.0000	0.0000
OH-	-5.7200	0.0000	0.0000	0.0000	0.0000	0.0000
SO ₄ ²⁻	-55.7000	0.0000	0.0000	-37.2000	0.0000	-54.2000
B _{par}	Ca ²⁺	H⁺	K⁺	Mg ²⁺	Na⁺	Sr ²⁺
Br ⁻	0.0000	0.0000	0.0000	0.0000	0.0000	0.0000
CI-	0.0000	0.0000	0.0000	0.0000	0.0000	0.0000
CO ₃ ²⁻	0.0000	0.0000	0.0000	0.0000	0.0000	0.0000
F-	0.0000	0.0000	0.0000	0.0000	0.0000	0.0000
HCO₃-	0.0000	0.0000	0.0000	0.0000	0.0000	0.0000
HSO₄⁻	0.0000	0.0000	0.0000	0.0000	0.0000	0.0000
OH-	0.0000	0.0000	0.0000	0.0000	0.0000	0.0000
SO ₄ ² -	-0.5160	0.0000	0.0000	0.2530	0.0000	0.0000

Table 8: Model parameters for C[♦].

Apar	Ca ²⁺	H⁺	K⁺	Mg ²⁺	Na⁺	Sr ²⁺
Br-	-0.00260	0.00827	-0.00180	0.00310	0.00116	0.00120

CI-	0.00218	0.00080	-0.00084	0.00520	0.00127	-0.00130
CO ₃ ² -	0.00000	0.00000	0.00050	0.00000	0.00520	0.00000
F-	0.00000	0.00000	0.00000	0.00000	0.00000	0.00000
HCO₃-	0.00000	0.00000	-0.00800	0.00000	0.00000	0.00000
HSO₄⁻	0.00000	0.00000	0.00000	0.00000	0.00000	0.00000
OH-	0.00000	0.00000	0.00410	0.00000	0.00440	0.00000
SO ₄ ² -	0.11400	0.04380	0.00818	0.02500	0.00570	0.00000
B _{par}	Ca ²⁺	H⁺	K ⁺	Mg ²⁺	Na⁺	Sr ²⁺
P				U		
Br	0.0000	-0.0001	-0.0001	0.0000	-0.0001	0.0000
	0.0000 -0.0004	-0.0001 0.0001	-0.0001 -0.0001			0.0000
Br				0.0000	-0.0001	
Br Cl	-0.0004	0.0001	-0.0001	0.0000 0.0000	-0.0001 0.0000	0.0000
Br ⁻ Cl ⁻ CO ₃ ²⁻	-0.0004 0.0000	0.0001 0.0000	-0.0001 0.0000	0.0000 0.0000 0.0000	-0.0001 0.0000 0.0000	0.0000 0.0000
Br Cl ⁻ CO ₃ ²⁻ F ⁻	-0.0004 0.0000 0.0000	0.0001 0.0000 0.0000	-0.0001 0.0000 0.0000	0.0000 0.0000 0.0000 0.0000	-0.0001 0.0000 0.0000 0.0000	0.0000 0.0000 0.0000
Br ⁻ Cl ⁻ CO ₃ ²⁻ F ⁻ HCO ₃ ⁻	-0.0004 0.0000 0.0000 0.0000	0.0001 0.0000 0.0000 0.0000	-0.0001 0.0000 0.0000 0.0000	0.0000 0.0000 0.0000 0.0000 0.0000	-0.0001 0.0000 0.0000 0.0000 0.0000	0.0000 0.0000 0.0000 0.0000

Table 9: Model parameters for Θ^{AA} .

Apar	Br ⁻	CI-	CO ₃ ²⁻	F-	HCO₃-	HSO₄⁻	OH-	SO ₄ ² -
Br ⁻	0.0000	0.0000	0.0000	0.0000	0.0000	0.0000	-0.0650	0.0000
CI-	0.0000	0.0000	-0.0200	-0.0164	0.0300	-0.0060	-0.0500	0.0380
CO ₃ ²⁻	0.0000	-0.0200	0.0000	0.0000	-0.0400	0.0000	0.1000	0.0200
F-	0.0000	-0.0164	0.0000	0.0000	0.0000	0.0000	0.0000	0.0000
HCO₃⁻	0.0000	0.0300	-0.0400	0.0000	0.0000	0.0000	0.0000	0.0100
HSO₄⁻	0.0000	-0.0060	0.0000	0.0000	0.0000	0.0000	0.0000	0.0000
OH-	-0.0650	-0.0500	0.1000	0.0000	0.0000	0.0000	0.0000	-0.0130
SO ₄ ²⁻	0.0000	0.0380	0.0200	0.0000	0.0100	0.0000	-0.0130	0.0000

Table 10: Model parameters for Θ^{CC} .

A _{par}	Ca ²⁺	H⁺	K⁺	Mg ²⁺	Na⁺	Sr ²⁺
Ca ²⁺	0.0000	0.0920	0.0320	-0.1840	0.0700	0.0000
H⁺	0.0920	0.0000	0.0067	0.1000	0.0368	0.0728
K⁺	0.0320	0.0067	0.0000	0.0000	0.0070	0.0000
Mg ²⁺	-0.1840	0.1000	0.0000	0.0000	0.0970	0.0000
g Na⁺	0.0700	0.0368	0.0070	0.0970	0.0000	0.0510
Sr ²⁺						
Sr ²	0.0000	0.0728	0.0000	0.0000	0.0510	0.0000

Table 11: Model parameters for λ .

Apar	CO ₂
Ca ²⁺	0.1830
H ⁺	0.0000

K ⁺	0.0510
Mg ²⁺	0.1830
Na⁺	0.0850
Sr ²⁺	0.0000
Br ⁻	0.0000
CI ⁻	-0.0050
CO ₃ ²⁻	0.0000
F-	0.0000
HCO₃⁻	0.0000
HSO₄⁻	-0.0030
OH-	0.0000
SO ₄ ² -	0.0750

Table 12: Model parameters for Ψ_{ijk} .

Species i	Species j	pecies j Species k	
Br ⁻	K ⁺	Na⁺	-0.0022
Br ⁻	K ⁺	OH⁻	-0.0140
Br ⁻	Na⁺	H⁺	-0.0120
Br ⁻	Na⁺	OH⁻	-0.0180
Ca ²⁺	CI-	H⁺	-0.0150
Ca ²⁺	CI-	K ⁺	-0.0250
Ca ²⁺	CI ⁻	Mg ²⁺	-0.0120
Ca ²⁺	CI ⁻	Na⁺	-0.0148
Ca ²⁺	CI ⁻	OH-	-0.0250
Ca ²⁺	CI ⁻	SO ₄ ²⁻	-0.1220
Ca ²⁺	K ⁺	SO ₄ ²⁻	-0.0365
Ca ²⁺	Mg ²⁺	SO ₄ ²⁻	0.0240
Ca ²⁺	Na⁺	SO ₄ ²⁻	-0.0550
CI ⁻	CO ₃ 2-	K ⁺	0.0040
CI ⁻	CO ₃ 2-	Na⁺	0.0085
CI ⁻	H⁺	K ⁺	-0.0110
CI ⁻	H⁺	Mg ²⁺	-0.0110
CI ⁻	H⁺	Na⁺	-0.0040
CI ⁻	HCO ₃ -	Mg ²⁺	-0.0960
CI ⁻	HSO ₄ -	H ⁺	0.0130
CI ⁻	HSO ₄ -	Na⁺	-0.0060
CI ⁻	K ⁺	Mg ²⁺	-0.0220
CI ⁻	K ⁺	Na⁺	-0.0015
CI ⁻	K ⁺	OH-	-0.0060
CI ⁻	K ⁺	SO ₄ ²⁻	-0.0010
CI ⁻	Mg ²⁺	MgOH⁺	0.0282
CI ⁻	Mg ²⁺	Na ⁺	-0.0120
CI ⁻	Mg ²⁺	SO ₄ 2-	-0.0080
CI ⁻	Na⁺	OH-	-0.0060

CI ⁻	Na⁺	Sr ²⁺	-0.0021
CO_3^{2-}	HCO ₃ -	K ⁺	0.0120
CO_3^{2-}	HCO ₃ -	Na⁺	0.0020
CO_3^{2-}	K ⁺	Na⁺	0.0030
CO_3^{2-}	K ⁺	OH-	-0.0100
CO_3^{2-}	K ⁺	SO ₄ 2-	-0.0090
CO_3^{2-}	Na ⁺	OH-	-0.0170
CO_3^{2-}	Na⁺	SO ₄ 2-	-0.0050
H⁺	HSO ₄ -	K ⁺	-0.0265
H⁺	HSO ₄ -	Mg ²⁺	-0.0178
H⁺	HSO ₄ -	Na⁺	-0.0129
H⁺	K ⁺	Br-	-0.0210
H⁺	K ⁺	SO ₄ 2-	0.1970
HCO ₃ -	K ⁺	Na⁺	-0.0030
HCO ₃ -	Mg ²⁺	SO ₄ ²⁻	-0.1610
HCO ₃ -	Na ⁺	SO ₄ 2-	-0.0050
HSO_4^-	K ⁺	SO ₄ 2-	-0.0677
HSO_4^-	Mg ²⁺	SO ₄ 2-	-0.0425
HSO_4^-	Na⁺	SO ₄ ²⁻	-0.0094
K ⁺	Mg ²⁺	SO ₄ ²⁻	-0.0480
K ⁺	Na⁺	SO ₄ ²⁻	-0.0100
K ⁺	OH-	SO ₄ ²⁻	-0.0500
Mg ²⁺	Na⁺	SO ₄ ²⁻	-0.0150
Na⁺	OH⁻	SO ₄ ²⁻	-0.0090

Pathways to Low Carbon Hydrogen

Axel Behrens, Jan-Peter Bohn, Nicole Schödel Linde GmbH, Linde Engineering, Pullach

Abstract

The transition to a sustainable energy future necessitates advanced solutions for reducing greenhouse gas emissions while maintaining energy reliability and scalability. Low carbon hydrogen, produced from natural gas reforming paired with carbon capture and storage (CCS) technologies, can play a key role as intermediary in this energy transition. In this presentation, we explore the processes and potential of low carbon hydrogen production from the viewpoint of an industrial gases and engineering company.

An overview of existing routes for the production of hydrogen on an industrial scale is provided, and the CO_2 reduction potential is compared. Hydrogen is primarily produced via steam methane reforming (SMR) or autothermal reforming (ATR), processes that extract hydrogen from methane while releasing carbon dioxide as a byproduct. By integration of CCS technologies majority of the CO2 can be captured , preventing its release into the atmosphere and mitigating the environmental footprint of low-carbon (blue) hydrogen production. A current Linde project is presented as an example of this type of low-carbon hydrogen production.

High activity is observed in the field of new developments based on ammonia cracking for hydrogen production on an industrial scale. This method relies on ammonia being produced from zero- or low-carbon hydrogen at renewable favored locations. The key advantage of ammonia is, that no carbon is involved. It can be produced from air nitrogen and low carbon hydrogen. Furthermore, it has a high specific hydrogen content and the transport infrastructure is available and mature. Nevertheless, challenges arise from the combination of material requirements, burner operation, emission management, and the selection of appropriate catalysts. Linde's activities in the HyPAC project are highlighted.

Renewable energy-driven water electrolysis offers a zero-carbon (green) alternative however still struggling with technology readiness and availability of affordable electric power prices. Different electrolyzer technologies are presented and linked to current projects and R&D activities.

Low carbon hydrogen serves as a transitional solution, enabling a more immediate and impactful reduction in carbon emissions at large scale while renewable energy grids and green hydrogen infrastructure are upscaling and developing. By addressing technical and economic hurdles and increasing investment in CCUS advancements, blue hydrogen can play an instrumental role in achieving net-zero emissions targets.

Decarbonization of Syngas and Hydrogen Production

Mario Marchionna Saipem SpA, Via Luigi Russolo 5, Milano, Italy

Abstract

Hydrogen is currently used as an intermediate product in the chemical (mainly ammonia and methanol) and refining industries. It is produced mostly from Natural Gas in large scale plants using Steam Methane Reforming, a very mature technology. Hydrogen produced by Natural Gas has a high carbon footprint, considering that about 6-9 tons of CO₂ are co-produced (and emitted to the atmosphere) per ton of produced hydrogen, depending on Natural Gas composition. For this reason, Hydrogen produced from fossil fuels is nowadays named as "Grey" Hydrogen. The current production of Hydrogen is responsible for about 2.5% of CO₂ emissions worldwide.

For the chemical intermediate, Hydrogen, to remain in business decarbonizing its production is a must and then become a factor in the energy transition period.

Partially decarbonized hydrogen produced from fossil fuels, through CO₂ Capture, is named "Blue" Hydrogen. A completely different path is followed to produce fully decarbonized, or "Green", Hydrogen.

Even ammonia could act as an effective indirect hydrogen carrier to be developed in the short term, especially for maritime use.

Further applications of Hydrogen can be devised in the "Hard to Abate" sector, especially regarding green steel production, and for low carbon emission fuels (biofuels and e-fuels) production. In the latter field, Saipem has elaborated its value proposition exploring opportunities to enhance SAF (Sustainable Aviation Fuels) production using its industrialized solutions "IVHY100™" and "Bluenzyme™".

Also, a few hints will be devoted to our involvement in the Puglia Green Hydrogen Valley project which will have two plants with 160 MW capacity, producing up to 260 million normal cubic meters of green hydrogen annually. The project promotes circularity by reusing wastewater and oxygen. The project will contribute to the decarbonization of nearby industrial sites and has secured EU funding approval (IPCEI). It will be operational around 2028.

Introduction

Saipem has several activities regarding energy transition and more in general to improve sustainability. Our priorities can be summarized by the following main pillars (and several mutual interconnections can be found among all the different pillars) to target the progressive decarbonization of energy and overall CO₂ emissions reduction, included the energy-intensive Hard to Abate sectors:

- 1. CO₂ Management and decarbonisation of Hard to Abate Industries: we aim to continue to produce energy and products using fossil fuels while significantly reducing their associated climate-altering emissions. This applies not only to the Oil & Gas industry but also to Hard to Abate industries (steel, cement, etc).
- 2. Offshore Renewables: we are particularly oriented towards offshore wind but also floating solar power is an option.
- 3. *Geothermal*: not only a continuous renewable source to produce electricity but also a source of zero-carbon heat for the Hard to Abate Industry and residential heating.
- 4. Offshore Nuclear: a zero-carbon energy source that can efficiently and sustainably support growing energy needs and ensure the diversification and security of energy supply.
- 5. *Hydrogen*: we see it both as a low-carbon chemical intermediate and applied to the Hard to Abate sector (especially steel); as an energy carrier (including derivatives

like ammonia and methanol) it might gradually replace natural gas in a few difficult to electrify applications.

6. Low Carbon Emissions Fuels: biofuels, synthetic hydrocarbon liquids (e-fuels) and gaseous (biogas, synthetic methane and bio-methane).

In this article, our attention will be focused on Hydrogen, taking into consideration all the connections with the other pillars (especially CO₂ Management, Renewables, Low Carbon Emission Fuels, and in perspective also Nuclear) also with the aim to understand which could be the most proper applications for "low carbon" Hydrogen.

Saipem has a very long tradition in the field of Hydrogen and Syngas-derived facilities, mostly in fertilizers and refining fields, with more than 90 plants realized to produce either Hydrogen itself or its derivatives ammonia (including urea) and methanol, Gas to Liquids, or Power through gasification of natural gas and oil residues. Practically all the most-experienced licensed technologies (steam reforming, autothermal reforming, partial oxidation, ...) to produce syn-gas have been employed and at the same time a strong experience was also matured on CO₂ Capture processes, often a key integrating part of these plants.

According to the experience recently matured [1], the aim of this paper is to understand even more which may be the most promising and realistic applications for decarbonized hydrogen.

Hydrogen today

Though hydrogen is the most abundant element in the universe, mostly it does not exist naturally on our planet, except for a few cases where the so-called "white Hydrogen" can be directly extracted from the ground [2]. Hydrogen cannot therefore be considered as an energy source, but as an energy vector that must be produced from an energy source.

Today hydrogen is used as a chemical intermediate in the production of chemicals (mainly ammonia and methanol) and in oil refining processes [3]. Fossil fuels (natural gas, but also coal and oil) are the sources for producing hydrogen, mostly via Steam Methane Reforming (SMR), a very mature technology, in production lines with capacity of 50,000-150,000 Nm³/hr of hydrogen [4]. Consequently, the production of hydrogen is associated with a high carbon footprint. About 6-9 tons of CO₂ are co-produced (and emitted to the atmosphere) per ton of produced hydrogen when Natural Gas is used as the raw material. For this reason, hydrogen produced from fossil fuels is named as "grey" hydrogen.

The production of hydrogen is responsible of about 2.5% of CO₂ emissions worldwide (almost 1 billion tons of CO₂ yearly [5]). For hydrogen remaining in business, even before becoming a positive factor in the energy transition period and later, decarbonizing its production is a must.

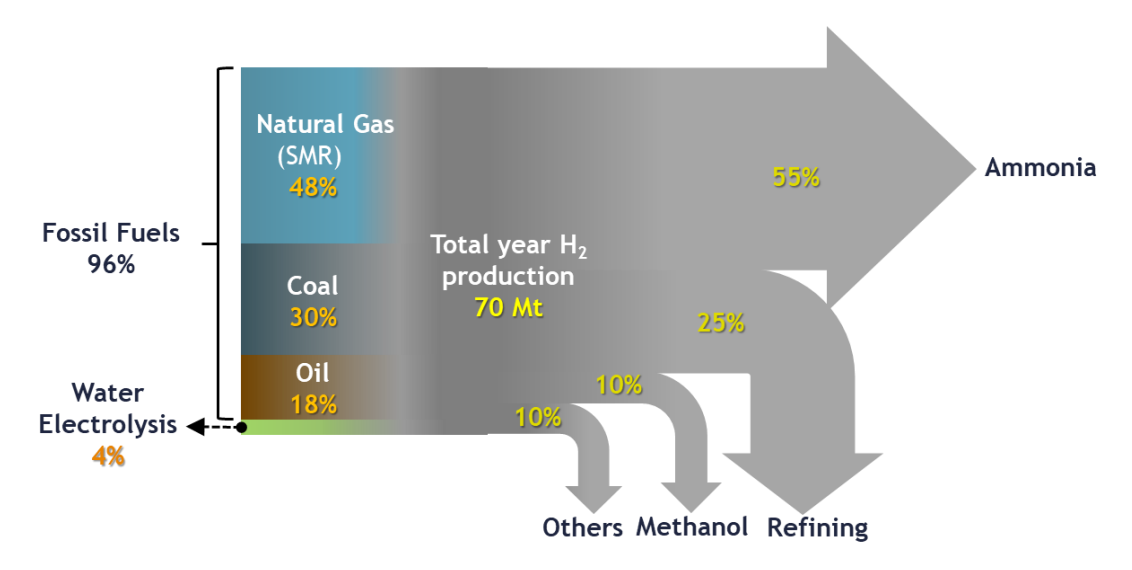


Fig. 1: Current Hydrogen Value Chain (Outlook for the energy transition September 2018; IEA 2019 The Future of Hydrogen)

As shown in Fig.1 [4], the two largest uses are bulk chemicals production such as ammonia, mostly for the fertilizer market, or methanol production, mostly an intermediate for the chemical industry, and fossil fuel processing (e.g., hydrotreating/hydrocracking).

Most hydrogen is used near the site of its production, and as it is produced, is consumed without intermediate operation of storage; furthermore, these productions besides being characterized by huge scale are also characterized by a high operational continuity (more than 8000 h/y), this means that decarbonizing any of these uses should take into account all these aspects.

Partially decarbonized hydrogen produced from fossil fuels is named "blue" hydrogen. Of course, hydrogen will be "blue" if captured CO₂ is either geologically stored or sustainably used. The deployment of blue hydrogen will therefore proceed in parallel to the development of the infrastructure needed for Carbon Capture, Storage and Utilization (CCUS).

More specifically, three main criteria have to be followed for the Blue Hydrogen option:

- Availability of affordable or cheap gas
- Existing pipeline infrastructure
- CO₂ sequestration potential (its absence could limit this option, although CO₂ reuse could be another possibility)

A few geographical areas are particularly suited for this scope: US, Canada, North Sea, Middle East, Russia, Australia, ..., where practically all the previous requirements are satisfied or easily satisfiable.

This option is well suited for retrofitting operations and displays good synergy when CO₂ is requested as a co-reactant such as in the production of urea or of methanol.

Capturing about 90% CO₂ from the steam reformer effluent at the current scale of deployment is already done today in a few petrochemical plants and refineries [6-7], particularly in urea production schemes where captured CO₂ is used to increase the production rate.

Considering blue hydrogen, the current scale of production would remain the same also in the possible extension of its use to other sectors. For instance, simple calculations show that a world scale steel mill will need about 50000 Nm³/h of hydrogen. SMR plants may be equipped with carbon capture facilities, also as a retrofit of existing units, and the required scale is commercially available and industrially referenced.

The production of blue hydrogen entails proper management of captured CO₂. CO₂ must be transported to a storage site for geological storage. An infrastructure for pipeline transportation of CO₂ is today existing only in specific areas (e.g., Texas) [8], while geological storage is in quick development is however expected in Northern Europe, where Norway, The Netherlands and UK are advancing to prepare the infrastructure for transporting CO₂ from industrial sites north of the Alpes for storage in offshore reservoirs in the North Sea, and more recently also in the Southern Europe, both in Italy (Eni's Ravenna project) and in Greece (Energean Prinos project). The development of blue hydrogen projects must go in parallel to this infrastructural development. As an alternative, captured CO₂ could be sustainably re-used. Sustainable reuse, however, means that the products obtained from CO₂ should not generate new CO₂ when used unless carbon is of biogenic origin. This is a strong limitation to all plans for CO₂ utilization, since the range of durable products obtainable from CO₂ is quite limited (plastics, construction materials) [9].

HYDROGEN CARBON FOOTPRINT



Fig. 2: Blue and Green Hydrogen

A completely different path is followed to produce fully decarbonized, or "green" hydrogen (Fig. 2). This path is already commercially available, though on a smaller scale than required for wide industrial application (mostly as a byproduct of the chloralkaline process). It is the electrolysis of water, i.e., the use of electric power (from renewable sources) to cleave the water molecule into its base element hydrogen and oxygen [10].

However, water electrolysis is much behind SMR in the maturity curve, so that substantial improvements are to be expected in the technology development. The achievement of a transformation efficiency of 80-85% [11], as well as the increase in size of the standard modules up to at least 10 MW [12], are feasible targets of ongoing activity in a perspective scenario.

Emerging technologies such as Solid Oxyde Electrolyzers (mostly based on yttrium-stabilized zirconia) will improve efficiency (up to +20%) which is essential considering the strong impact of electrolyser power consumption in the overall green hydrogen/ammonia scheme.

One peculiar feature of the electrolysis of water, often neglected, is the co-production of pure oxygen. For a hydrogen production of 100,000 Nm³/h, 50,000 Nm³/h of oxygen are co-produced. The co-production of green oxygen may improve the economics of water electrolysis plants to an extent which may be negligible today but might give a decisive push to green hydrogen development.

Decarbonized Hydrogen application to the Hard to Abate industry

In perspective, the use of "low carbon" hydrogen might not be limited only to the current use of chemical intermediate but could be advantageously extended well beside the current perimeter to "Hard to Abate" sectors, which are responsible for about 25-30% of the worldwide anthropic CO_2 emissions. While there are several alternatives for decarbonizing power production (renewables first), the situation is much more complex regarding this industry. By Hard-to-Abate we refer both to Oil & Gas industries, such as refinery and petrochemicals, and to very intensive industries such as steel, cement, paper mills, metal production (especially aluminum), ceramics, glass, waste treatment, etc.

The most advanced steel producers are targeting carbon neutrality of their production by 2050. Their selected decarbonization path involves replacement of coal in the reduction step of iron ore with green or blue hydrogen coupled to the use of an electric furnace for the melt [13].

Thus, Hydrogen may consequently contribute to about at least 30% of the decarbonization of steel production (0.8 billion tons of CO₂).

Low Carbon Ammonia and recent related projects

Ammonia is one of the most important chemicals for its use as feedstock in the fertilizer industry; it is produced in many countries and traded across the world. The current production of ammonia is energy-intensive, and it is responsible for more than 1% of the global carbon dioxide and overall Green House Gases, considering that nearly 2 tons of CO_2 are generated for each ton of ammonia. It is therefore imperative to change to a more sustainable way to produce ammonia to replace grey ammonia and provide a sustainable alternative to ensure world's food production.

Furthermore "low carbon" ammonia is expected to become a possible solution to tackle climate change also in other ways: ammonia could be also an attractive molecule for transportation of hydrogen and thus energy. Already relatively simple infrastructure for ammonia liquefaction, storage and shipping exist, making ammonia an attractive choice for H₂ transportation. In addition to the use of ammonia as hydrogen carrier, which is expected to be widely developed in the short term, the use of ammonia as direct fuel (especially for marine engines) may unlock further potential of clean ammonia market [14].

Amongst different ways to produce "low carbon" ammonia, the so-called blue ammonia, which is based on reforming natural gas coupled with carbon capture and storage, offers immediate advantages since it is based on the process schemes already adopted by the current industry and minimizes the cost especially in areas where it is possible to safely store CO₂.

Blue ammonia concept is based on the well-consolidated process scheme for production of ammonia which expands the CO_2 capture already included in the syngas purification to the full Carbon Capture Utilization and Storage (CCUS) value chain. The concept is essentially made of end-of-pipe blocks that do not affect the main process; however, minor adjustments may be required to improve the CO_2 capture rate. Despite the lack of a standard, it is generally recognized as a "blue" concept if most of the CO_2 (typically > 80%) is captured.

Leveraging decades of experience in the execution of ammonia projects, Saipem is nowadays at the forefront in the implementation of solutions that allow the development of the whole ammonia value chain; currently, Saipem is engaged in several Blue Ammonia initiatives providing solutions to achieve the highest possible carbon capture rate (up to 99%) by proper integration of the ammonia process with the utilities (especially steam and power generation) and management of the captured CO₂ [15]. These initiatives are often based on different capture technologies, selected for the specific project to meet the peculiar targets.

To facilitate the deployment of an end-to-end ammonia value chain, large infrastructures are required for the storage and transportation of ammonia as well as for its cracking, when ammonia needs to be reconverted to hydrogen. Saipem is developing innovative solutions for large ammonia terminals, such as the use of Gravity Based Structures (GBS) to overcome issues of large-scale onshore facilities, which are already under consideration by prospect clients in engineering studies and FEEDs for ammonia storage [16], cracking and pipelines.

The integration of the proprietary "Snamprogetti™ Urea Technology" in the overall ammoniaurea complex has always been a peculiar feature of Saipem. Today, Saipem is engaged in the execution of CERES Project in Western Australia, where the novel SynCOR Ammonia™ technology by Topsoe allows outstanding results in terms of energy efficiency and CO₂ emissions. While executing this project, Saipem is adopting cutting-edge solutions such as extensive modularization and integration with renewable energy; another notable project carried out by Saipem is the Barents Blue Ammonia Project [17].

As regards Green Ammonia, derived by Green Hydrogen, several case studies have been developed by Saipem for hybridization/stand-alone ammonia plant and ammonia-urea complexes for a few Clients. The capacity of the photo-voltaic (PV) plant has been optimized

through a business model in order to have the minimum value of the cost of hydrogen. The installation areas are particularly significant; for example, a PV plant of 140 MWp corresponds notably to 160 ha of soil occupied, and additional areas are to be booked for electrolysers and storage, although lower with respect to the PV plants.

Further recent Saipem projects

More generally, in this context, Saipem is able to offer solutions both for green hydrogen production, industrializing electrolysis technologies, and for blue hydrogen production (with associated CO₂ capture) targeting large-scale plants to decarbonize existing industrial complexes that already use hydrogen, such as refining, petrochemicals, fertilizers (green and blue ammonia), but also Hard to Abate industries, and more specifically steel production.

Looking at ecosystems where hydrogen demand and supply can be met, realizing synergies between production and use of hydrogen and optimizing transportation and use of renewables, in recent years Saipem's commitment and interest has also turned to those infrastructural realities called Hydrogen Valleys.

In this respect, the SPV (Special Purpose Vehicle) constituted by Edison, Sosteneo (Generali Investments) and Saipem launched the Puglia Green Hydrogen Valley (PGHyV), which represents a key step in the development of Italy's largest Hydrogen Valley, integrating PV plants, green Power Purchase Agreements, electrolysis technology, wastewater treatment and distribution to off-takers and end-users. The PGHyV aims to build two green hydrogen production plants in Italy, in Brindisi and Taranto for a total capacity of 160 MW and powered by renewable electricity provided by 260 MW dedicated photovoltaic plants as well as by the electric grid via green power purchase agreement. The two plants will produce up to 260 million cubic meters of renewable hydrogen per year and 160,000 tons of CO₂ emissions reduction, allocating hydrogen to industries in the area. As a potential example, Green Hydrogen could be used to reduce the carbon footprint of steel production through the direct reduction of iron ore as previously anticipated.

The produced green hydrogen will be transported to end users through a repurposed pure hydrogen pipeline and new connecting ancillary gas network, combining several H₂ applications into an integrated H₂ ecosystem. The project was submitted to IPCEI (Important Projects of Common European Interest) funding for the infrastructural projects, named Hy2Infra; in February 2024 IPCEI notified the SPV of the possibility of accessing a 370 million euro funding grant, among 33 projects included by the European Commission in Hy2Infra, the third IPCEI to support the development of hydrogen infrastructure in Europe. After the Directorial Decree of 11 October 2024, in January 2025 the SPV executed the formal submission, with a positive outcome in June 2025, and the Concession Decree has been issued in July for the concession of funds to start. In the meantime, Saipem assessed and scored a short list of electrolysis technology providers for the project, and the SPV has selected the technology solution that best fits the project requirements. Saipem has also been awarded for a FEED contract by the SPV to design an engineering package based on the selected electrolysis technology. The project should start to be operational in 2028.

For the PGHyV project the electrolysis plants will use wastewater from the Apulian aqueduct, avoiding the depletion of natural resources because wastewater when purified would end up into the sea. So, this usage will not subtract water from other commercial and/or residential areas. Part of the oxygen produced in the plants may be used in water purifiers to improve oxygenation of the process in which the sludge flocculation takes place, allowing a great reduction in the organic load of the output water. Additionally, the oxygen produced may also be used by industries nearby.

Furthermore, to offer ready certification plants and solutions, Saipem is developing a digital platform for the traceability and management of guarantees of origin from renewable sources to renewable hydrogen production.

Hydrogen for Low Carbon Emission Fuels

In synergy with the capture and utilization of CO_2 Saipem is also developing solutions to produce Green Hydrogen, aimed at e-fuel production, i.e. e-methane, e-methanol and e-SAF (Sustainable Aviation Fuels). In this field Saipem has been recently involved in Stockholm Exergy for the execution of a large-scale Bio-Energy CO_2 Capture project in Sweden; CO_2 is then converted with green hydrogen to e-methane.

On the biofuels side, the integration of biorefinery sections into existing facilities represents the state of the art for refineries, especially in Europe. As Saipem, we have participated, and we are continuously involved, in various conversions of existing refineries into biorefineries, such as for a few Eni refineries in Italy. This consists in both repurposing existing plants for new feedstock or adding entirely new sections to treat biogenic feedstock (e.g., Eni Venice and Eni Livorno). The technology involved, configurations, and new catalysts are at an advanced stage of development and available in the market.

Saipem possesses extensive knowledge and experience implementing these solutions effectively, allowing also the refinery to consider a lower GHG impact as part of the product has a Carbon Intensity (C.I.) below the 10 gCO₂eq/MJ respect the traditional fuels that have a C.I. close to 100 gCO₂eq/MJ. The main reason for that is due to the specific biorefinery configuration that maximizes the utilization of byproducts inside the process by minimizing the external inputs of energy coming for fossil sources. It has also to be highlighted that, in the considered scheme, the only emission from the biorefinery section consists in biogenic flue gases that have a high added value, possibly not to be lost by venting into the atmosphere.

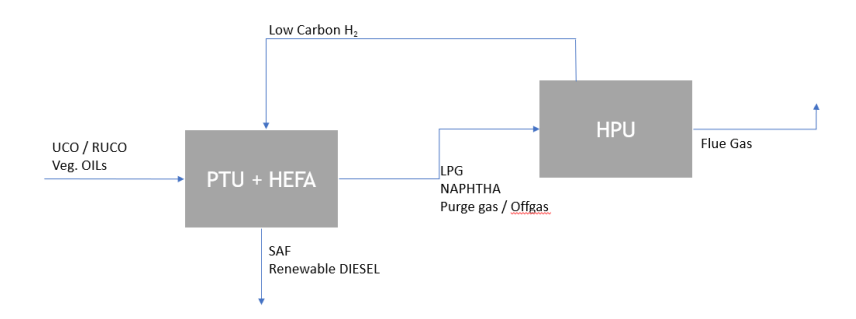


Fig. 3: Advanced scheme for a biorefinery

Saipem has also enriched its value proposition by exploring opportunities to enhance SAF production using its industrialized solutions "IVHY100™" and "Bluenzyme™".

IVHY100™ is Saipem's Green Hydrogen solution that is pre-engineered, modular, and scalable. It is designed for the creation of a 100 MW Power-to-Hydrogen industrial package using Nel alkaline technology. This approach aims to achieve reduced time-to-market and capital/operational expenditure.

BluEnzymeTM is another solution developed by Saipem engineers for carbon capture. It uses an enzyme found in the human respiratory system to capture CO_2 . The system is standardized and modular, allowing for easy installation and efficiency in capturing 200 tons per day of CO_2 in a sustainable manner. The biogenic CO_2 from the HEFA (Hydrotreated Esters and Fatty Acids) unit, and captured by BluenzymeTM on flue gas stack, can be converted with green H_2 from IVHY100TM and boost e-SAF, and other renewable fuels, production. This set-up may further maximize the conversion of carbon atoms from biomass to sustainable fuels. The rise in investment costs is offset by the increase in production of sustainable fuels that can be sold at a premium price.

Bluenzyme™ has been also selected by Ren-Gas, Finland's leading developer of green

hydrogen and e-methane projects, for it e-methane plant in Tampere, Finland.

A few final remarks on market evolution

Mixed signals are coming from the market regarding the advancement for "Low-Carbon" hydrogen projects [18].

On one side, according to the industry group Hydrogen Council, the clean hydrogen sector has reached a major milestone in its development, with more than 500 projects reaching FID representing an investment of about \$ 110 billion, with the launch of important initiatives such as in Saudi Arabia (ACWA Power in Neom) and in China, in Inner Mongolia.

On the other side, this potential has been called into question, especially over the last 12 months; major project cancellations, tinkering with government support in the US and elsewhere, and little or no meaningful progress in reducing capital and operational costs have threatened to consign hydrogen to the role of a niche transition technology, acknowledging that this nascent industry is still far from smooth. Development plans have been recently dropping both in the steel industry and in the automotive sector.

The cost issue remains very relevant, representing one of the biggest challenges: all the efforts to improve the economic attractiveness of these projects are imperative and we are playing our part to support them through our solid experience matured throughout the decades in this industry mixed with the adoption of new technologies.

References

- 1) M. Marchionna. Pure & Applied Chem. 96 (4), 465 (2024).
- 2) C. Bettenhausen. Chem. Eng. News. 22 (2025, March 17).
- 3) A. Brown. Chem. Eng. 937, (2019).
- 4) M.W. Twigg, V. Dupont. *Advances in Hydrogen Production, Storage and Distribution*, Woodhead Publishing, Cambridge (2014).
- 5) *The Future of Hydrogen,* Report prepared by the Int. Energy Agency for the G20 (2019). https://www.iea.org/reports/the-future-of-hydrogen
- 6) M. lijima, E. Takahiko, S. Daisuke. Mitsubishi Heavy Ind. Tech. Rev. 47, 37 (2010).
- 7) L. Rock, S. O'Brien, S. Tessarolo, J. Duer, V. Oropeza Bacci, B. Hirst, D. Randell, M. Helmy, J. Blackmore, C. Duong, A. Halladay, N. Smith, T. Dixit; S. Kassam, M. Yaychuk. *Energy Procedia* **114**, 5320 (2017).
- 8) CO₂ Pipeline Infrastructure, Report by International Energy Agency (2014). https://ieaghg.org/docs/General Docs/Reports/2013-18.pdf
- 9) C. Perego. La Chimica & l'Industria 1, 50 (2022).
- 10) A. Di Nardo, S. De Rinaldis, A. Di Benedetto. *Int. J. Hydrog. Energy* doi.org/10.1016/jihydene.2025.150254 (2025).
- 11) O. Schmidt, A. Gambhir, I. Staffell, A. Hawkes, J. Nelson, S. Few. *Int. J. Hydrog. Energy* 42, 30470 (2017).
- 12) M.P. Bailey, *Chem. Eng.* Mag., (2020), Apr. 15th. (https://www.chemengonline.com/asahi-kasei-starts-up-world-scale-electrolysis-system-to-generate-hydrogen-in-fukushima/)
- 13) M. Peplow, Chemical & Engineering News 22 (2021, June 14).
- 14) A. Tullo. Chemical & Engineering News 20 (2025, March 8).
- 15) A. Zambianco, M. Sala. World Hydrogen North America Houston (2025, April 1).
- 16) A. Zambianco, A. Natour, S. Corno. Nitrogen+Syngas 395, 30 (2025).
- 17) E. Haukelldsaeter Eidesen, A. Zambianco, M. Sala. Nitrogen+Syngas 364, 43 (2023).
- 18) A. Tullo. Chemical & Engineering News 11 (2025, March 10).

Experimental Investigation of Syngas Purification from Biogenic Residue Gasification

Lisa Katharina Hassel¹, Jens Martin Kaltenmorgen¹, Fabiola Panitz¹, Marc Siodlaczek¹, Philipp Eiden¹, Jochen Ströhle¹, Bernd Epple¹

¹ Institute for Energy Systems and Technology, Technical University of Darmstadt, Germany

Abstract

Fluidized bed gasification of pine forest residues represents a promising route for producing basic chemicals and synthetic fuels. The resulting raw syngas contains, in addition to the main components H₂, CO, CO₂, and CH₄, a variety of undesired impurities such as solids, nitrogen and sulfur compounds, as well as halogenated hydrogen compounds. These substances must be removed prior to further utilization to avoid catalyst deactivation, corrosion, and operational issues.

To provide a purified synthesis gas for downstream applications, the gas cleaning plant was tested at pilot scale at the Technical University of Darmstadt. The plant combines hot gas filtration, raw gas scrubbing, compression, hydrolysis, BTX removal, and amine scrubbing. A total of 156 Nm³/h of syngas are fed into the gas cleaning unit. In the raw gas scrubber, 27.02 % of H_2O , 34.92 % of NH₃, and 100 % of phenol and HCl were removed.In the subsequent condenser, up to 91.05 % of the H_2O and 99.97 % of the NH₃ were separated.The two-stage BTX washing system enabled the removal of 96.28 % of aromatic compounds, while about 55 ppm BTX remained in the syngas. The final amine scrubbing step reduced the CO_2 concentration to 2 % and lowered the hydrogen sulfide concentration to about 3 ppm. In total, 51.6 Nm³/h of cleaned syngas were produced from the raw syngas. The results demonstrate that the concept delivers an energy-rich syngas with removal of contaminants, indicating its fundamental potential for industrial application. However, further adjustments are required to completely separate the remaining BTX components as well as H_2S .

Keywords: syngas cleaning, amine scrubbing, BTX-removal, biogenic waste, gasification

1. Introduction

In the context of the energy transition, biogenic residues are gaining importance as a sustainable carbon source for the production of basic chemicals and synthetic fuels. In particular, their material utilization provides an opportunity to gradually substitute fossil raw materials in the chemical industry. Thermochemical conversion could become a key technology for the energy and material conversion of solid carbonaceous feedstocks. This process enables the transformation of solid feedstock into an energy-rich synthesis gas that serves as a versatile raw material for a wide range of industrial applications, including power and heat generation, methanol synthesis, and the production of synthetic fuels. [1]

Against this background, the gas cleaning process at TU Darmstadt is being investigated in detail in order to provide a high-purity synthesis gas from the fluidized gasification of biogenic residues, which can serve as a feedstock for methanol production and further chemical conversion processes.

The raw synthesis gas generated during gasification consists mainly of carbon monoxide (CO), carbon dioxide (CO₂), hydrogen (H₂), methane (CH₄) and water (H₂O). In addition to these main components, it also contains a variety of undesired by-products. These include fine particulates, nitrogen compounds (e.g., ammonia, hydrogen cyanide), sulfur compounds (e.g., hydrogen sulfide, COS), halogenated hydrogen compounds (e.g., HCl, HF), as well as light hydrocarbons (C₁-C₄) and volatile organic compounds (C₅-C₁₂). [2] These impurities pose significant challenges for downstream processes, as they can deactivate catalysts, cause corrosion, lead to deposits, or result in solvent degradation [3–5].

Table 1 provides an overview of the purity requirements for methanol synthesis.

Table 1: Purification requirements of synthesis gas for use in methanol synthesis [3,6–8]

Contaminant	Methanol synthesis
Particles (dust, ash)	<0.02 mg/m ³
Tars or BTX	<0.1 mg/m ³
Sulfur (COS, H ₂ S)	<1 mg/m ³
Nitrogen (NH ₃ , HCN)	<0.1 mg/m ³
Halides (HCI)	<0.1 mg/m ³

To meet these requirements, multi-stage gas cleaning is necessary, the design of which largely depends on the properties of the feedstock, the gasification process conditions, and the target applications. Gas treatment for fluidized bed gasification generally includes the following steps: particle removal, halogen removal, separation of hydrocarbons, adjustment of the CO/H₂ ratio, and sour gas removal [2]. The selection of the processes used and their sequence depend on the gasification process, the feedstock, and the downstream application. Particle separation is carried out using proven technologies such as filters or wet scrubbing processes. Halogen removal, in turn, can be implemented relatively easily through raw gas scrubbing with aqueous condensate. [2,9]

Since fluidized bed gasification produces a product gas containing a significant fraction of polycyclic aromatic hydrocarbons (PAHs), these compounds must be removed, as their condensation can lead to deposits in pipelines, catalyst deactivation, and operational problems in washing processes, such as foaming [4,10,11]. Various main processes are available for the removal of these hydrocarbons. Primary measures include catalytic and non-catalytic thermal cracking, in which the compounds are converted into lighter gases. As secondary cleaning methods, physical separation techniques such as absorption with scrubbing oils are applied, where the condensable components are absorbed and subsequently regenerated or thermally utilized [2,12].

Acid gas removal is an essential step in the processing of gasifier product gases, as these can contain significant amounts of acidic components such as CO_2 and H_2S . Even small amounts of sulphur compounds can cause major problems, because using the synthesis gas for Fischer-Tropsch synthesis or methanol synthesis requires extremely low sulfur content, otherwise the catalysts will be deactivated. Furthermore, it is imperative that part of the CO_2 is removed prior to the methanol synthesis in order to adjust the stoichiometric number (SN) to the optimum value of approximately 2. [3,4,6–8]

A wide range of technologies has been developed for the removal of acid gases, which can generally be classified into physical absorption processes, chemical scrubbing methods, and dry sorbents [13]. In industrial practice, physical absorption processes such as Rectisol® (cold methanol wash), Selexol® (polyethylene glycol), or Purisol® (N-methylpyrrolidone) have become well established [2]. These processes exploit the temperature and pressure dependent solubility of gases and achieve high separation rates even on a large industrial scale. Due to the high investment and operating costs and the complex heat integration required, Rectisol is only used in large-scale biomass gasification projects [2,14]. Another application is chemical sour gas scrubbing using amines, an established process for separating CO₂ and H₂S that is widely applied in gasification and natural gas processing plants, but requires a high energy input for solvent regeneration. [2,15,16]

In summary, gas purification is a key requirement for the utilization of raw synthesis gas, particularly in Waste-to-X applications. The aim of the investigations at TU Darmstadt is to demonstrate the entire process line. This includes the fluidized bed gasification of biogenic residues, subsequent gas cleaning, and finally methanol synthesis. Based on experiments using pine forest residues as feedstock, the aim is to illustrate that biogenic waste can be converted into high-quality synthesis gas which can serve as a basis for methanol production and further chemical conversion processes after the gas treatment.

2. Pilot Plant Setup

2.1. Configuration of the gasifier

The 1 MW_{th} pilot plant at Darmstadt Technical University is used to investigate different fluidized bed processes. The core unit is a fluidized bed reactor with an inner diameter of 400 mm and a height of 11 m, where the gasification reactions take place. The refractory lining consists of an inner layer of fireproof cement and two layers of insulating bricks, enabling autothermal operation [17,18]. Depending on the process, the thermal load ranges from 0.5 MWth to 1 MW_{th}. The produced raw syngas is partly directed to a gas cleaning facility, which allows purification of up to 200 Nm³/h. In the present study, gasification is carried out in a fluidized bed using pine forest residues. Further details on the reactor and the process are provided in Kaltenmorgen et al. (2024). [19]

2.2. Configuration of the gas treatment plant

The gas cleaning plant at the Technical University of Darmstadt was constructed in 2019 [9]. It was specifically designed for fluidized bed gasification with an integrated post-gasification zone. The gas cleaning system downstream of the fluidized bed gasifier is of modular design and comprises several cleaning stages, divided into a low-pressure section and a high-pressure section. Figure 1 presents a schematic diagram of the individual cleaning processes.

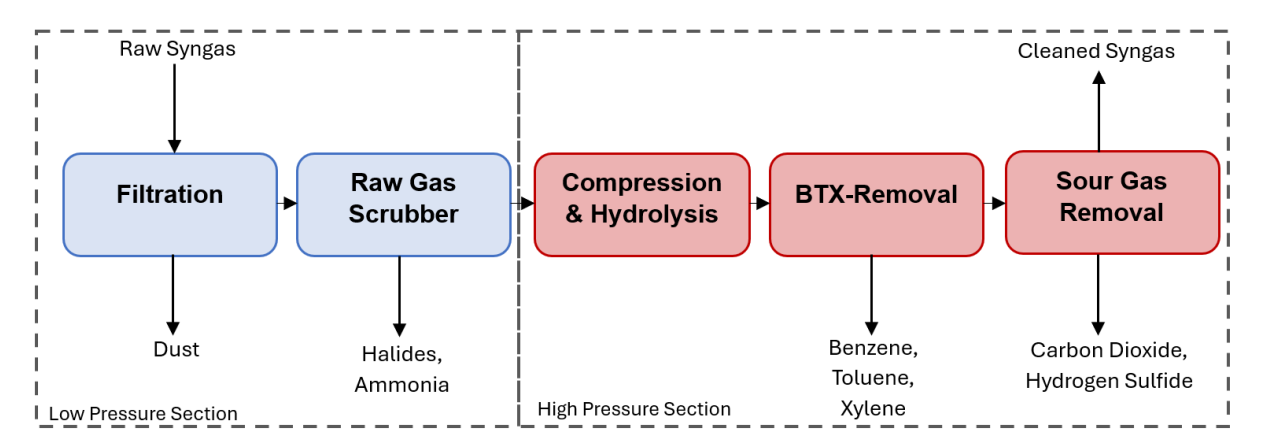


Figure 1: Overview of the gas cleaning plant at the Institute of Energy Systems and Technology, TU Darmstadt, showing the individual cleaning stages; blue: low-pressure section; red: high-pressure section.

The gas cleaning process consists of the following steps:

- Removal of solid particles by means of a hot gas filter
- Raw gas scrubbing for the removal of halides and ammonia as well as for cooling of the synthesis gas
- Compression of the synthesis gas to increase the efficiency of subsequent absorption and desorption processes
- The hydrolysis of COS and HCN to H₂S and NH₃
- Removal of ammonia, moisture, and BTX components
- Amine scrubbing for the separation of hydrogen sulfide to protect downstream synthesis processes

2.3. Removal of solid particles

To separate particles the synthesis gas at around 350 °C is fed under negative pressure into a hot gas filter supplied by TREMA with sintered metal candles developed and manufactured by GKN Powder Metallurgy. During operation, fine particles carried over from the gasifier via the cyclone deposit on the filter candles surface, providing a total filtration area of approximately 9 m². Over time, a filter cake accumulates, leading to an increased differential pressure. The filter candles are cleaned by back-pulsing with CO₂. This cleans the surface of the candle and the dust falls into the filter cone, where it is transported to the discharge container by means of a rotary valve. [9,19]

2.4. Raw gas scrubber

The synthesis gas leaving the hot gas filter is fed into the raw gas scrubber operated under slight vacuum. The hot gas enters the sump of the column through a dip tube, where it is cooled to approximately 70 °C before exiting again at the top of the column. Fresh water is continuously added at the top of the column, while recirculated water is fed into the middle section to absorb water-soluble compounds. This primarily separates H₂O, HCl and NH₃ from the gas stream.

Mass transfer in the column is achieved by a packing material (Raschig SuperRing®) and two sieve trays in the upper section, supplemented by a demister. Excess water is continuously discharged from the system to ensure stable operation. After leaving the raw gas scrubber, the synthesis gas is further cooled to 35 °C in a shell-and-tube heat exchanger, during which additional wastewater is removed from the process. [9,19]

2.5. Raw gas compression

The downstream raw gas compressor represents the interface between the low-pressure and high-pressure sections of the plant. Compressing the synthesis gas from -100 mbar(a) to around 5 bar(a) creates the basis for efficient operation of the downstream absorption and desorption processes with allowing for relatively small column diameters. The compressor is designed for a maximum flow rate of 200 Nm³/h. In the pilot tests presented here, approximately 156 Nm³/h of product gas from the fluidized bed gasification of pine forest residues was fed into the gas cleaning unit. [9]

2.6. Hydrolysis

To convert COS and HCN into NH_3 and H_2S , the synthesis gas, after compression, the synthesis gas is reheated to 210 °C in a electrical heater. In the subsequent reaction unit, COS and HCN are converted into more easily separable compounds according to Equations (1) and (2). The hydrolysis step is essential, as COS and HCN would irreversibly degrade the solvent used in the acid gas removal process.

$$COS + H_2O \iff CO_2 + H_2S \qquad (1)$$

$$HCN + H_2O \iff CO + NH_3$$
 (2)

2.7. BTX removal

After the hydrolysis reactor, the synthesis gas passes through a two-stage washing section in which BTX compounds (benzene, toluene, xylene), ammonia, and residual moisture are removed. This purification step is necessary to ensure that no solvent-reactive components enter the subsequent acid gas removal unit. The efficient separation of these substances is crucial for the long-term stability and selectivity of the amine-based process for CO2 and H2S removal. As washing medium, a process developed by Thielert et al. is used, which is based on the use of fatty acid methyl esters (FAME, biodiesel) [20,21]. Figure 2 illustrates the schematic flow diagram of the two-stage BTX scrubbing system with downstream regeneration unit. The first stage is implemented in a gas cooler, where the syngas is cooled to approximately 30 °C and contacted with a washing liquid of FAME and water. The gas cooler is equipped with a 4 m high packing (RaschigPak 250Y) and, like the subsequent absorber, is operated in the high-pressure section downstream of the syngas compressor. By lowering the temperature in the gas cooler, water vapor and nitrogen compounds are absorbed from the gas stream. In addition, the ammonia formed in the hydrolysis reactor is almost completely dissolved in the aqueous phase. A portion of this aqueous phase is continuously purged from the process, while the FAME is returned to a regeneration cycle. If required, propionic acid can be added to prevent stable emulsions. It reduces the formation of long-chain emulsifiers and breaks down existing emulsions. This enhances phase separation and prevents any impairment of the separation performance in the gas cooler. [9,19] In the second stage, the non-condensed BTX compounds are removed in the BTX absorber, which is also equipped with a 4 m packed bed (RaschigPak 250Y). The gas is contacted at 30 °C with 90 kg/h of pure FAME. The loaded FAME enriched with BTX is withdrawn at the column bottom, heated to approximately 140 °C in a wash oil heater, and subsequently regenerated in the regenerator. Stripping steam is introduced at the bottom of the column to desorb hydrocarbons. The vapors leaving at the column top are subcooled to 30 °C. In a downstream phase separator, the wastewater is separated from the two-phase overhead product. The separated BTX is utilized for further industrial applications [9].

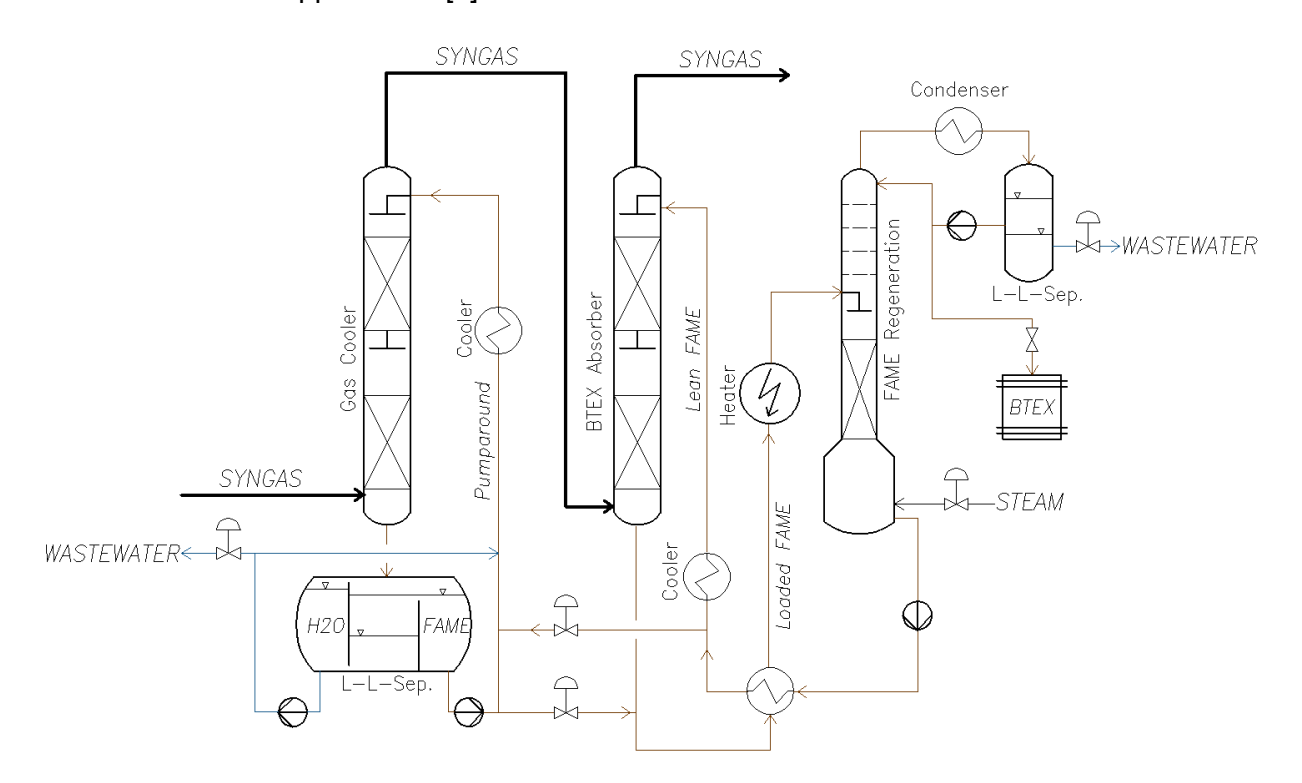


Figure 2: Flow chart of BTEX removal at the Institute for Energy Systems and Technology at TU Darmstadt. [19]

2.8. Sour gas removal

The final purification step of the gas cleaning plant is the removal of the acid gases carbon dioxide and hydrogen sulfide. This stage is implemented by means of an amine wash. Figure 3 illustrates the schematic setup of the amine scrubbing unit. The amine solution consists of 50 wt.% water, 48 wt.% MDEA (methyldiethanolamine), and 2 wt.% MEA (monoethanolamine).

The synthesis gas is introduced at the bottom of the amine absorber. The absorber is equipped with a 12 m packed section of the type RaschigPak 350X. Above this section, an additional 1 m packed bed is installed, where circulating wash water is distributed to prevent the entrainment of amine aerosols. The mass transfer between the amine solution and the synthesis gas enables the separation of carbon dioxide and hydrogen sulfide from the synthesis gas. The enriched amine is then fed into the amine desorber through a heat exchanger. In the heat exchanger, the waste heat from the stripped amine can be used to preheat the loaded amine. Before the loaded amine enters the desorber column, an antifoaming agent can also be added. The amine desorber has a total height of 14.5 m and contains a 10 m high packing. The loaded amine is fed in above this packing at a temperature of approximately 85 °C. [9] As the gases flow through the packing, the high temperatures cause the acidic gases to be removed from the amine solution. A reboiler is installed at the bottom of the desorber, which is heated with steam and evaporates part of the water contained in the amine solution. The column bottom also serves as a reservoir for the regenerated amine. This is cooled to around 45 °C by a pump through the heat exchanger, after which it passes the cooler and is returned to the absorber.

At the top of the desorber, a partial condenser cools the exiting sour gas stream to 45 $^{\circ}$ C, which separates the gaseous components. The pressure levels of the two columns are specifically selected: The amine absorber operates at the overpressure of the high-pressure section behind the synthesis gas compressor, which promotes the absorption of CO₂ and H₂S in accordance with the reaction equilibrium. [9]

In contrast, the amine desorber operates at a lower pressure of around 1.3 bar(a) to facilitate the reverse reaction and release the acidic gases from the solution.

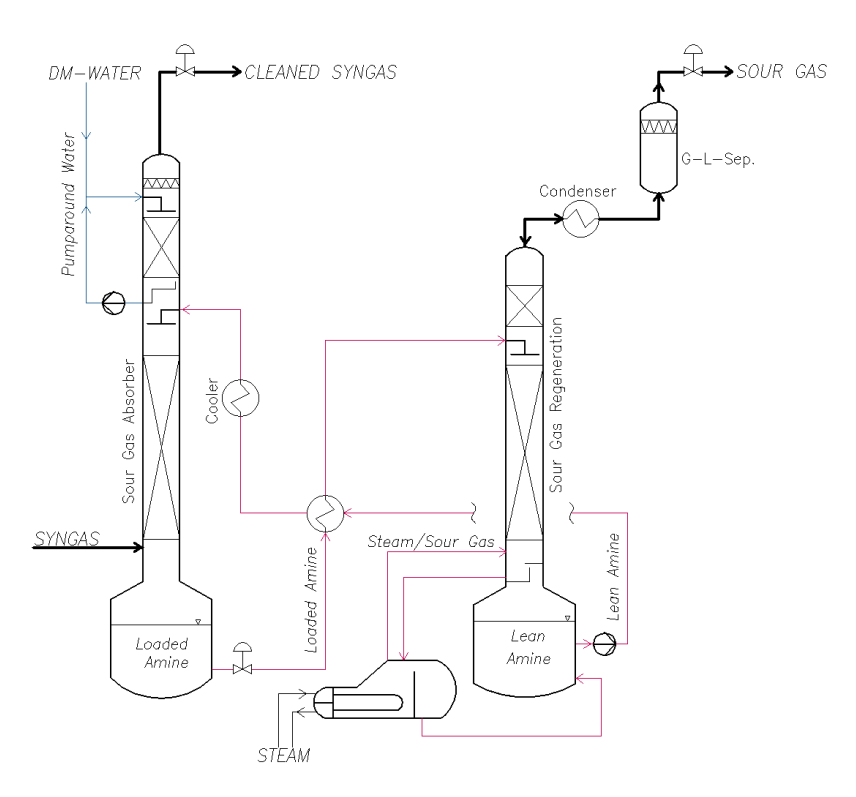


Figure 3: Flow diagram of acid gas removal at the Institute for Energy Systems and Technology at TU Darmstadt. [19]

2.9. Process Stream Analysis of the Gas Cleaning Plant

For the evaluation of the gas cleaning plant, a consistent recording of all material streams is required. Only in this way mass balances can be closed and the separation efficiencies of individual process stages be quantified. Since several partial streams cannot be measured directly, we formulate a linear system of equations that integrates the inlet and outlet streams of each process stage as well as available offline analyses. The mathematical approach comprises the system of equations \vec{M} , the solution vector of the stream compositions \vec{v} , and the boundary conditions \vec{b} . [19]

$$M \cdot \vec{v} = \vec{b} \tag{3}$$

$$\vec{v} = M^{-1} \cdot \vec{b} \tag{4}$$

The formulation of the equations, and thus the definition of the matrix entries M, is based both on the direct quantification of the material streams and on the compositional results from offline analyses. In the case of an underdetermined system of equations, additional calculations are carried out based on engineering principles (e.g., Aspen Plus). For components such as sulfur species, where no suitable measurement method was available, mass balance closure was supported by an Aspen Plus simulation using a validated plant model. [19]

3. Results and Discussion

3.1. Evaluation of the syngas cleaning plant performance

As part of the fluidized bed gasification of pine forest residues, a part of the raw synthesis gas produced was directed to the gas treatment plant for further purification. After establishing steady-state operating conditions for each treatment stage, liquid samples of the washing solutions and gas sample bags were taken at various points in the plant. The samples were analyzed using the developed data processing method, as defined by equations (3) and (4). [19] For classification of the results, Figure 4 illustrates the process path of the synthesis gas through the gas treatment plant. The analysis results of the main components (H_2 , H_2) are shown in Figure 5, and Figure 6 summarizes the separation efficiencies for relevant trace substances (H_2 S, BTX, COS, HCN, NH₃, HCl, phenol). A possible enrichment of heavy tars (H_2 Cn could not be detected with the applied method. The evaluation data were obtained from Kaltenmorgen et al. [19].

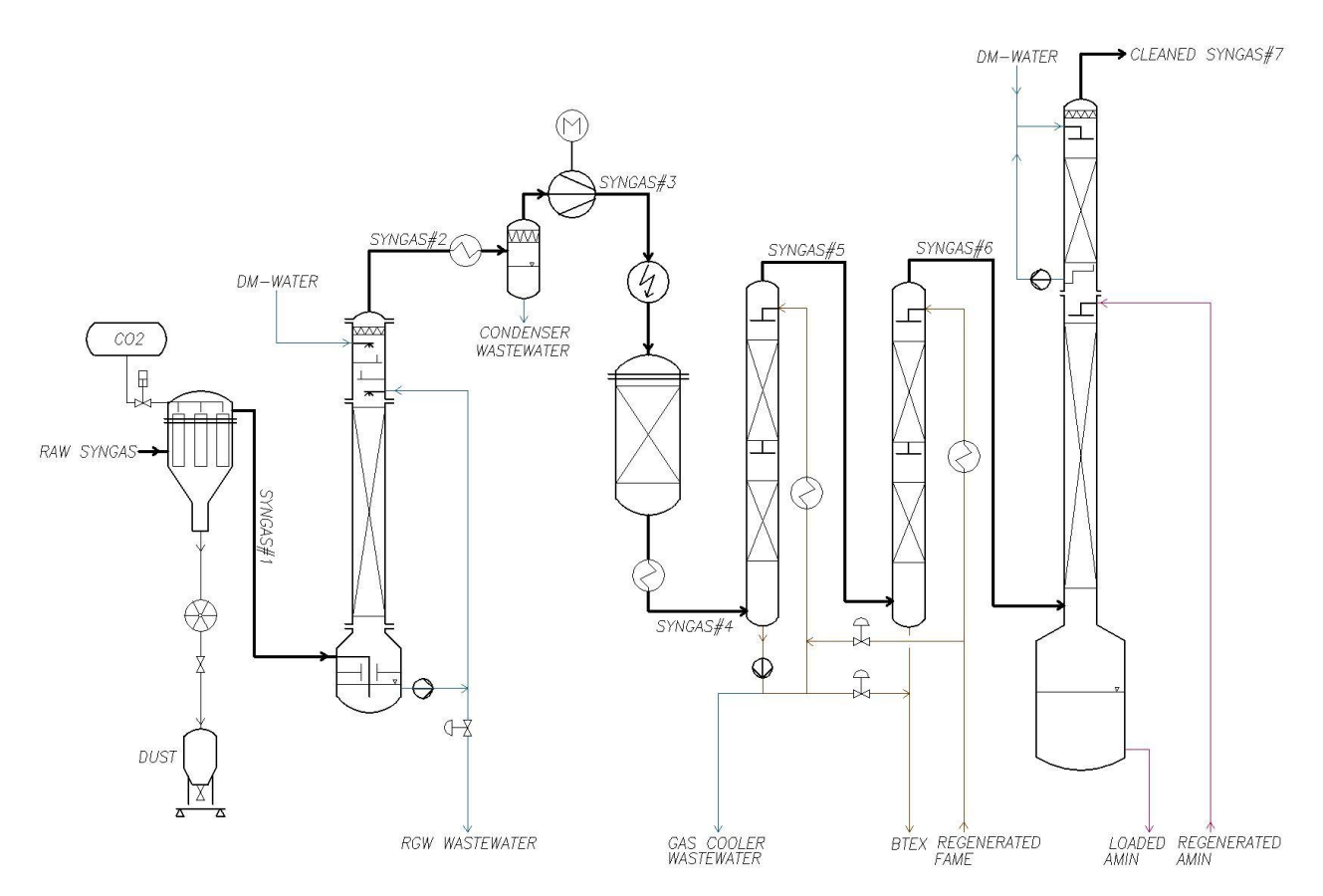


Figure 4: Basic flow diagram of the synthesis gas line in the gas cleaning plant at the Institute for Energy Systems and Technology at TU Darmstadt. [22]

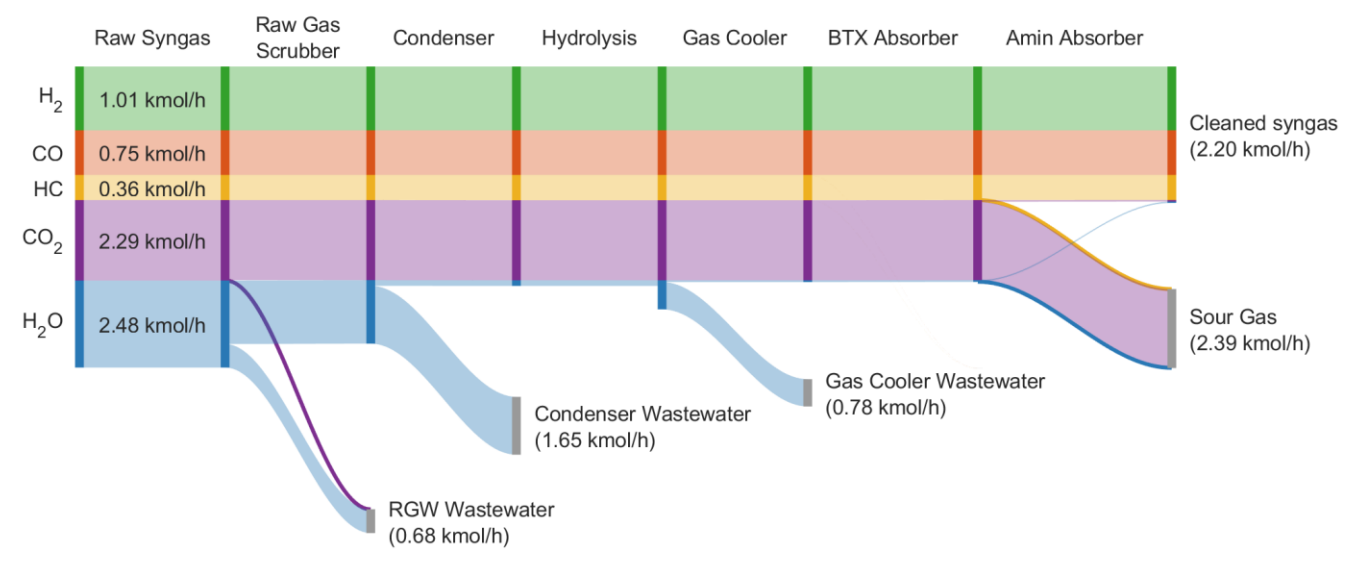


Figure 5: Visualization of molar flows and separation of main components in the gas cleaning plant.

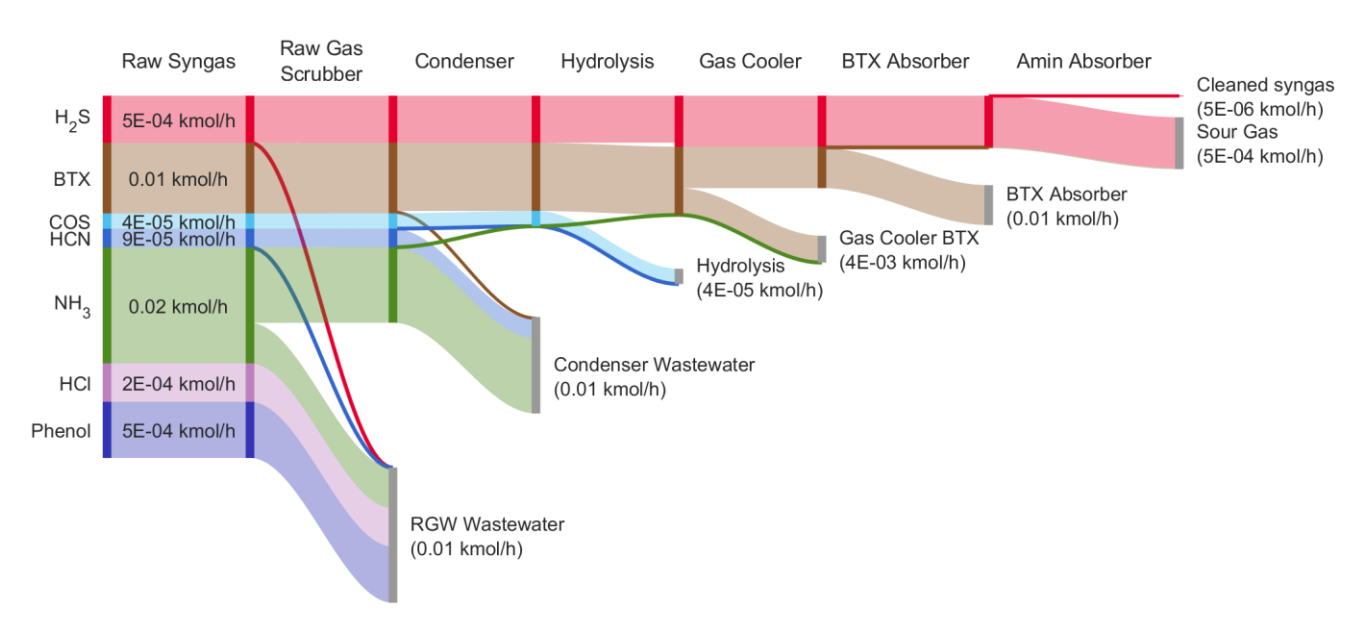


Figure 6: Visualization of molar flows and separation of trace substances in the gas cleaning plant.

The gas composition gradually changes due to the separation of different components. Separated components are mainly discharged in streams such as wastewater, BTX separation, or with the sour gas. The main components of the synthesis gas, such as H_2 , CO and hydrocarbons (HC), have very low solubility in the washing solutions used and are therefore only marginally affected during the treatment steps.

In the first purification step – the hot gas filter – all particles are removed from the gas stream. The effectiveness of the filtration was verified by liquid samples from the raw gas scrubber, which showed no solid residues. This confirmed that particle separation in the hot gas filter was almost complete. [19]

In the second stage, the raw gas scrubber, water-soluble components are removed from the gas. Specifically, water, ammonia, HCl, phenol, as well as small amounts of H_2S , HCN, and CO_2 are absorbed and separated in the washing solution. In total, 0.69 kmol/h of impurities were removed in the raw gas scrubber. During this condensation, 1.65 kmol/h H_2O and 1.2×10^{-2} kmol/h NH_3 condensed in relation to the saturated vapor pressure and were removed as wastewater. [19]

After this step the syngas were compressed to 2 bar(g) and fed into the hydrolysis reactor. In the reactor, COS and HCN are converted to H_2S and NH_3 by adding steam. This explains the observed increase in the H_2O content in step 4. Since the conversion efficiency could not be measured during the test campaign, complete conversion of COS and the remaining HCN was assumed for the evaluation. [19]

The next separation step is the BTX system, in which the synthesis gas passes through two absorption columns. Within the first column, the gas cooler, the syngas is contacted with 620 kg/h of water and 456 kg/h of FAME. During this step, part of the water contained in the syngas and the steam introduced in the hydrolysis reactor are condensed. The ammonia formed in the reactor is also removed with the wastewater stream, amounting to 0.78 kmol/h. Additionally, 4.3×10^{-3} kmol/h of BTX components are removed from the syngas in the gas cooler. In the second absorption column, the BTX absorber, the gas stream is washed with 90 kg/h of stripped FAME, resulting in the removal of an additional 6.5×10^{-3} kmol/h of BTX. The separated BTX components are not discharged as waste but collected in a BTX storage tank, making them available as feedstock for further industrial applications. After this step, about 55 ppm of BTX remained in the syngas. These residual BTX compounds subsequently dissolved in the amine system.

For an industrial-scale design, this indicates the need for further optimization, particularly by

increasing the FAME circulation rate to ensure complete removal of BTX. [19]

In the final purification stage, the amine system, hydrogen sulfide and carbon dioxide are removed from the synthesis gas using an amine solution. For this purpose, 2500 kg/h of regenerated amine solution was applied, reducing the final CO₂ concentration in the product gas to about 2 %. As no suitable measurement technique was available for determining the sulfur content, a validated Aspen Plus simulation was used to estimate the residual hydrogen sulfide concentration at around 3 ppm. In total, 2.2 kmol/h of cleaned syngas and 2.39 kmol/h of stripped sour gas left the amine system. [19]

3.2. Separation efficiencies of critical syngas impurities

While the main components hydrogen and carbon monoxide are not affected by the cleaning steps, the impurities were largely removed, although 0.56 % of the hydrocarbons were separated together with the sour gas. The separation efficiency of critical syngas impurities at each purification step can be quantified using Table 2.

With regard to the overall separation efficiency, it can be seen that 98 % of the CO_2 is removed. In addition, 98.49 % of the water contained in the raw syngas can be separated during gas treatment. H_2S is removed by 98.9 %, with about 3 ppm remaining in the cleaned syngas. [19] The 100 % removal efficiency for BTX reported in Table 2 is misleading, because about 55 ppm BTX remain in the syngas after BTX scrubbing, are carried over into the amine system, and are removed there. As a result, the removal is attributed to the wrong process step and the actual performance of the BTX stage is overrated. As already noted, further action is required at this stage to ensure that BTX components are completely removed within the BTX system itself. In total, NH₃, HCl, and phenol are completely removed in the purification steps, while the main components of the synthesis gas (CO and H_2) remain unaffected. [19]

Table 2: Com	nonent se	naration	efficiencies	at each	nurification et	en
Table 2. Colli	ponent se	paration	CHICICHOLOS	at cacii	purification st	ch.

Species	Separation efficiency [%]				Total efficiency [%]		
Unit	Raw Gas Scrubber	Condenser	Hydrolysis	Gas Cooler	BTX Absorber	Amin Absorber	Gas Cleaning Plant
from	Syngas#1	Syngas#2	Syngas#3	Syngas#4	Syngas#5	Syngas#6	Syngas#1
to	Syngas#2	Syngas#3	Syngas#4	Syngas#5	Syngas#6	Cleaned Syngas#7	Cleaned Syngas#7
H ₂	_*	_*	_*	_*	_*	_*	-*
CO	_*	-*	-*	_*	-*	_*	-*
CO ₂	0.44	-	-	-	-	98.00	98.01
HC	-	-	-	-	-	0.56	0.56
H ₂ O	27.02	91.05	-	93.89***	-	26.09	98.49
H ₂ S	0.22	-	-	-	-	98.99	98.91
COS	-	-	100.00**	-	-	-	100.00**
NH ₃	34.92	99.97	-	100.00**	-	-	100.00**
HCN	0.44	99.99	100.00**	-	-	-	100.00**
HCI	100.00	-	-	-	-	-	100.00**
BTX	-	3.39	-	39.26	96.28	100.00**	100.00**
Phenol	100.00	-	-	-	-	ı	100.00**

^{*}CO and H₂ should not be separated.

4. Conclusion

The pilot tests of the gas cleaning plant at TU Darmstadt show that raw synthesis gas from the fluidized bed gasification of biogenic residues can be purified. By combining the the process

^{**} Includes measurement uncertainties.

[&]quot;Includes the removal of the steam supplied for the hydrolysis reaction.

stages – hot gas filtration, raw gas scrubbing, compression with subsequent hydrolysis, BTX removal, and amine scrubbing – dust particles, water-soluble compounds, as well as sulfur and aromatic components can be removed, while the main constituents of the synthesis gas remain largely preserved.

The BTX system significantly reduces the concentration of aromatic hydrocarbons and enables their recovery as valuable products. Nevertheless, around 55 ppm of BTX remain after the two-stage scrubbing and are subsequently removed in the amine system. This indicates further optimization potential, particularly through improved regeneration to increase the circulation rate, as this represented the limiting factor during the campaign. [19]

In the final amine scrubbing step, the CO_2 content of the synthesis gas was reduced to approximately 2 %. Furthermore, Aspen Plus simulations indicated a final H_2S concentration of 3 ppm [19]. This demonstrates that, for industrial applications, an additional caustic scrubber would be required to reliably remove these residual amounts [23]. Overall, removal efficiencies of more than 98 % for CO_2 and nearly complete elimination of sulfur and halogen compounds were achieved [4]. The main components of the syngas remained unaffected, ensuring that its energy content was preserved.

Acknowledgment

The authors gratefully acknowledge the funding of the German Federal Ministry for Economic Affairs and Energy (BMWE) under grant agreement No. 03EE5044A (VERENA: Gasification processes with integrated excess electricity integration for flexible power generation and production of synthetic fuels from residuals).

References

- [1] P. Leuter, S. Fendt, H. Spliethoff, 2024. Requirements on synthesis gas from gasification for material and energy utilization: a mini review. Front. Energy Res. 12, 1382377. https://doi.org/10.3389/fenrg.2024.1382377.
- [2] J. Hrbek, C. Pfeifer, P. Blanco-Sanchez et al., Gas Cleaning from Gasification for Production of Biofuels and Biochemicalsm, IEA Bioenergy: Task 33, 2025.
- [3] M. Tijmensen, Exploration of the possibilities for production of Fischer Tropsch liquids and power via biomass gasification, Biomass and Bioenergy 23 (2002) 129–152. https://doi.org/10.1016/S0961-9534(02)00037-5.
- [4] P. Woolcock, R. Brown, A review of cleaning technologies for biomass-derived syngas, Biomass and Bioenergy 52 (2013) 54–84. https://doi.org/10.1016/j.biombioe.2013.02.036.
- [5] N. Abdoulmoumine, S. Adhikari, A. Kulkarni, S. Chattanathan, A review on biomass gasification syngas cleanup, Applied Energy 155 (2015) 294–307. https://doi.org/10.1016/j.apenergy.2015.05.095.
- [6] H. Leibold, A. Hornung, H. Seifert, HTHP syngas cleaning concept of two stage biomass gasification for FT synthesis, Powder Technology 180 (2008) 265–270. https://doi.org/10.1016/j.powtec.2007.05.012.
- [7] C. Hamelinck, C. Elinck, Faaij A., H. Denuil, H. Boerrigter, Production of FT transportation fuels from biomass; technical options, process analysis and optimisation, and development potential, Energy 29 (2004) 1743–1771. https://doi.org/10.1016/j.energy.2004.01.002.
- [8] H. Boerrigter, H. den Uil, H. Calis, Green Diesel from Biomass via Fischer-Tropsch synthesis, Pyrolysis and Gasification of Biomass and Waste, Strasbourg-France, (30 September 2002).
- [9] C. Heinze, Konzeption einer Pilotanlage auf Grundlage einer technoökonomischen Bewertung von flexiblen Polygenerationsprozessketten, 2022.

- [10] M. Valderrama Rios, A. González, E. Lora, et al., Reduction of tar generated during biomass gasification: A review, Biomass and Bioenergy 108 (2018) 345–370. https://doi.org/10.1016/j.biombioe.2017.12.002.
- [11] A. Paethanom, S. Nakahara, M. Kobayashi, P. Prawisudha, K. Yoshikawa, Performance of tar removal by absorption and adsorption for biomass gasification, Fuel Processing Technology 104 (2012) 144–154. https://doi.org/10.1016/j.fuproc.2012.05.006.
- [12] M. Asadullah, Biomass gasification gas cleaning for downstream applications: A comparative critical review, Renewable and Sustainable Energy Reviews 40 (2014) 118–132. https://doi.org/10.1016/j.rser.2014.07.132.
- [13] A. Kohl, R.B. Nielsen, Physical Solvents for Acid Gas Removal– Gas Purification, in: pp. 1187–1237.
- [14] A.L. Kohl and R.B. Nielsen (Ed.), Gas Purification, Elsevier, 1997.
- [15] N. Ramachandran, A. Aboudheir, R. Idem, P. Tontiwachwuthikul, Kinetics of the Absorption of CO 2 into Mixed Aqueous Loaded Solutions of Monoethanolamine and Methyldiethanolamine, Ind. Eng. Chem. Res. 45 (2006) 2608–2616. https://doi.org/10.1021/ie0505716.
- [16] J. Wenhao, Lin, Y. Sun, C. Sun, Y. Zhu, Comparative Review for Enhancing CO2 Capture Efficiency with Mixed Amine Systems and Catalysts, Molecules 29 (2024). https://doi.org/10.3390/molecules29194618.
- [17] P. Herdel, D. Krause, J. Peters, B. Kolmorgen, J. Ströhle, B. Epple, Experimental investigations in a demonstration plant for fluidized bed gasification of multiple feedstock's in 0.5 MW th scale, Fuel 205 (2017) 286–296. https://doi.org/10.1016/j.fuel.2017.05.058.
- [18] F. Panitz, J. Kaltenmorgen, M. Siodlaczek, J. Ströhle, B. Epple, Fluidized bed gasification of plastic waste and residual biomass an overview of HTW® and Chemical looping technology development, INFUB-14, Algarve, Portugal, 2024.
- [19] J.M. Kaltenmorgen, M. Siodlaczek, F.Panitz, P. Eiden, J. Ströhle, B. Epple, Valorizing biogenic waste: A comprehensive analysis of steam/oxygen fluidized bed gasification of pine forest residue including syngas cleaning (2025). https://doi.org/10.2139/ssrn.5200238.
- [20] H. Thielert, G.Wozny and D. Richter, Verfahren zur Entfernung von aromatischen Kohlenwasserstoffen aus Kokereigas durch Absorption, EP 2162511 B1 2010.
- [21] H. Thielert, D. Richter, Verfahren zur Entfernung von aromatischen Verfahren zur Entfernung von aromatischen Kohlenwasserstoffen aus Kokereigas mit Biodiesel als Waschflüssigkeit und Vorrichtung zur Durchführung des Verfahrens, WO 2014/023526 A1.
- [22] J.M. Kaltenmorgen, F. Panitz, M. Siodlaczek, J. Ströhle, B. Epple, Demonstration der stofflichen Nutzung von Biomasse und Abfällen durch Wirbelschichtvergasung und nachgeschalteter Methanolsynthese im Pilotmaßstab, Jahrestreffen der DECHEMA Fachsektion Energie, Chemie und Klima, 2024.
- [23] E. Üresin, H.I. Saraç, A. Sarıoğlan, S. Ay, F. Akgün, An experimental study for H2S and CO2 removal via caustic scrubbing system, Process Safety and Environmental Protection 94 (2015) 196–202. https://doi.org/10.1016/j.psep.2014.06.013.

Novel Joule-heated Reactor based on Radial Current and Flow for the Intensification of Endothermic Catalytic Processes

L. Cozzarolo¹, F. Romanelli¹, C. Ferroni¹, M. Ambrosetti¹, B. Mello Gabbrielleschi², M. Bracconi¹, M. Maestri¹, G. Groppi¹, A. Beretta¹, B. Williams² and E. Tronconi^{1*}

- ¹ Laboratory of Catalysis and Catalytic Processes, Politecnico di Milano, Milan (Italy)
- ² Air Liquide Forschung und Entwicklung GmbH, Frankfurt (Germany)

Abstract

Electrification of Steam Methane Reforming (eSMR) is a promising route towards the decarbonization of H₂ production. In this work we address a major topical challenge of SMR, i.e., tuning the local heat supply to the varying heat demand of the endothermic reaction. To this scope, we propose a novel eSMR reactor configuration based on centrifugal gas flow across an open-cell foam directly Joule-heated by radial electric current and packed with catalyst particles (EMERALD concept) [1]. Comparative simulations were carried out for EMERALD packed foam reactors, employing the hybrid heterogeneous approach outlined in [2]. According to a hierarchical approach, the 3D CFD simulations were used to derive correlations and parameters for 1D and 2D porous media models [3].

Figure 1 shows simulation results for a Joule heated SiSiC foam packed with Rh-based catalyst particles (dp = 1 mm), operated at inlet temperature =773 K, outlet pressure =7 bar, fed with $H_2O:CH_4$ = 2.5:1, GHSV =20 Nl/h/gcat, reactor volume =21.4 L, with power input =234 kW. The EMERALD configuration essentially eliminates the cold spot in the reactor entry region thanks to a specific power input (solid black line) which is maximum at the entrance of the catalytic bed and decreases with $1/r^2$ (at constant electrical resistivity), thus closely matching the profile of reaction heat demand.

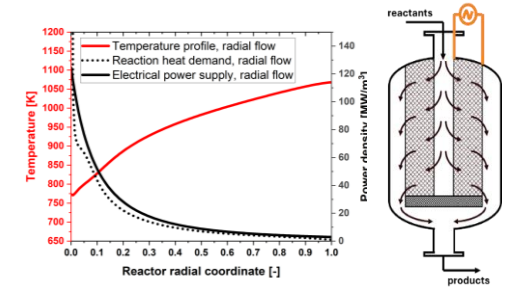


Figure 1. Simulation results for eSMR in the EMERALD reactor.

We will report on the experimental investigation of a lab-scale prototype currently ongoing at Politecnico's facilities (Fig. 2).

Acknowledgments. The authors acknowledge Air Liquide for their support of this research.

References

- [1] Patent Application IT102023000017721, August 2023.
- [2] Ferri, G.; Ambrosetti, M.; Beretta, A.; Groppi, G.; Tronconi, E. Catal. Today, 2024, 426, 114386.
- [3] Micale, D.; Ferroni, C.; Uglietti, R.; Bracconi, M.; Maestri, M.; *Chem. Ing. Tech.* 2022, 94, 634-651.

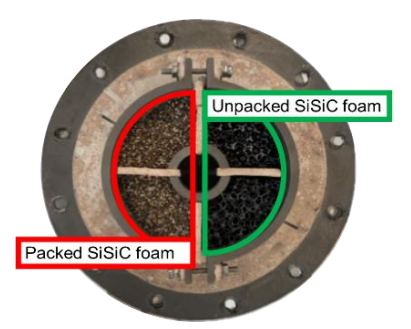


Figure 2. Lab-scale EMERALD reactor.

Potential of Dimethylether as a large-scale chemical hydrogen carrier

Andreas Peschel^{1,2}

¹ Forschungszentrum Jülich GmbH, Institute for a Sustainable Hydrogen Economy (INW), Jülich, Germany, ² RWTH Aachen University, Aachener Verfahrenstechnik, Process and Plant Engineering for Chemical Hydrogen Storage, Aachen, Germany

Abstract

A recent study by Schühle et al.[1] investigated the potential of DME as an energy carrier for intercontinental energy import in comparison to ammonia and methanol. The simple liquefaction of DME enables a high volumetric energy or hydrogen density, which, according to the study, manifests itself in advantages in transport and storage.

In this concept, DME is synthesized from CO₂ and H₂ at a location with high availability of renewable power. In addition to DME, this process also produces water, which can be purified and returned to the electrolysis process, thereby reducing the fresh water requirement by up to 50% compared to the direct transport of hydrogen or ammonia synthesis. In regions where renewable energies are only available to a limited extent, reducing the demand for fresh water for energy exports can significantly increase local acceptance. Due to the great similarity between the physical properties of DME and LPG, the existing LPG infrastructure can be used for shipping to Europe or Germany without major modifications [2]. At the import location, the DME can be used directly or reformed back to H₂ and CO₂ by adding water. The technology required for this is very similar to classic natural gas reforming, but further research and development is needed to adapt the reformer technology to DME.

The main advantage of this concept is, that CO₂ is captured at the location of used and back-transport to the location of DME synthesis. This heavily reduces the need for eligible carbon at the location of synthesis, thereby reducing costs and enabling upscaling of the concept. In this talk the overall concept of the DME/CO₂ cycle as well as the technical concept for DME reforming and medium scale power production both with integrated carbon capture will be presented and development needs will be addressed.

[1] Schühle, P., Stöber, R., Semmel, M., Schaadt, A., Szolak, R., Thill, S., Alders, M., Hebling, C., Wasserscheid, P., & Salem, O. (2023). Dimethyl ether/CO2 – a hitherto underestimated H2 storage cycle. Energy Environ. Sci., 16(7), 3002–3013. https://doi.org/10.1039/D3EE00228D

[2] Japan Science and Technology Agency, 2024, https://sj.jst.go.jp/news/202401/n0115-02k.html

Acknowledgment

The author acknowledges the funding by the German Federal Ministry of Research, Technology and Space (BMFTR) and the Ministry of Economic Affairs, Industry, Climate Action and Energy of the State of North Rhine-Westphalia through the project HC-H2.

Catalysts for Hydrogen Storage based on Liquid Organic Hydrogen Carriers

Barbara Bong, Chalachew Mebrahtu, Regina Palkovits*

Institute for a Sustainable Hydrogen Economy, Forschungszentrum Jülich GmbH, Jülich, Germany; Institute of Technical and Macromolecular Chemistry, RWTH Aachen University, Aachen, Germany

Abstract

Green hydrogen is a highly attractive energy carrier to establish a sustainable and stable energy system. For this purpose, safe and easy H₂ storage and transportation methods are required. One suitable method is chemical hydrogen storage by liquid organic hydrogen carriers (LOHCs), like the attractive LOHC system based on benzyltoluene (BT). This work focuses on the development and optimization of catalysts suitable for both hydrogenation and dehydrogenation of LOHCs. Moreover, catalyst stability over repeated loading or unloading of the LOHC is evaluated and potential optimization approaches are identified. Additionally, strategies to tackle current challenges were investigated. We present approaches to avoid the undesired side product formation and the need for high temperatures during dehydrogenation.

Introduction

Establishing a sustainable hydrogen economy (i.e., from production to storage and transportation) can decisively contribute to a successful transition of the energy system from fossil to renewables. Hence, a safe and easy technology to reversibly store and transport hydrogen is required. One promising approach is using liquid organic hydrogen carriers (LOHCs), where hydrogen is bonded to the hydrogen-lean compound (LOHC-) in a catalytic hydrogenation, forming the hydrogen-rich LOHC+, which can be stored or transported via the existing infrastructure. As soon as H₂ is required, it is released through catalytic dehydrogenation, and the LOHC can be reused. Yet, attractive LOHC systems are provided by established heat transfer oils like benzyltoluene (BT). However, alternative LOHC compounds can also be obtained via plastic recycling or from biomass.² Suitable catalysts are required for both hydrogenation and dehydrogenation steps to enable selective implementation of the desired reaction with high productivity while preventing the formation of undesired side products.3 Even though benzyltoluene (H0-BT) and perhydro benzyltoluene (H12-BT) as LOHC systems already offer great potential, in-depth understanding of the catalytic loading and unloading of the HX-BT system is still required, considering partially hydrogenated species as well. For this purpose, details on thermochemical properties of the different HX-BT species are crucial and can be applied to further establish LOHC applications. 4-6 Besides, energy efficiency of the LOHC process must be considered. For the overall process, energy efficiency is primarily determined by the endothermic dehydrogenation of H12-BT; the high reaction temperatures required for the dehydrogenation step inherently reduce the energy efficiency. Furthermore, the formation of side products must be avoided, as they can change the desired properties of the LOHC phase or lead to catalyst deactivation.8-10 In general. undesired side reactions can be suppressed upon using optimized catalysts. In addition to the high selectivity and productivity, the catalysts must also exhibit high stability over multiple hydrogen loading and release cycles. Moreover, the process can be simplified when the same catalyst is used for both hydrogenation and dehydrogenation, enabling dynamic switching between loading and unloading simply by adjusting the reaction conditions while using the same reactor.3, 11, 12 So far, the commercially available catalyst S-Pt/Al₂O₃ is considered a state-of-the-art catalyst for BT or similar LOHC systems. However, hydrogen release from H12-BT over the established catalyst results in the formation of undesired fluorene species.⁴ Thus, in this work, catalyst optimization to prevent the formation of fluorene species has been studied. Accordingly, titania-supported catalysts were prepared and investigated for the hydrogen loading and release in the BT-based LOHC system. The catalytic performance of the prepared catalysts was compared with the commercial catalyst as a benchmark. Moreover,

catalyst recycling, potential deactivation mechanisms, and regeneration strategies were also investigated. Promising catalysts were further studied in the LOHC process, including optimization of the reaction conditions to increase the energy efficiency of the process, partial hydrogenation, and consecutive hydrogen release. Additionally, chemical equilibrium calculations were applied to gain further information on loading and unloading of the LOHC system. Therefore, the experimental data obtained together with thermodynamic insights demonstrate potential for further optimization of the LOHC technology.

Experimental

S-Pt/TiO₂ and Pt/TiO₂ catalysts were synthesized by wet impregnation method, using TiO₂ support, and $H_3Pt(SO_3)_2OH$ or $Pt(NH_3)_4(NO_3)_2$ precursors as described elsewhere. The commercial benchmark catalyst S-Pt/Al₂O₃ in pellet form (EleMax D101) was provided by Clariant Produkte Deutschland and ground in a ball mill. All catalysts were reduced before usage in the reaction (at 400 °C, under pure H_2 flow for 4 h). The prepared catalysts were characterized using nitrogen physisorption, powder X-ray diffraction (XRD), H_2 temperature programmed reduction (H_2 -TPR), inductively coupled plasma optical emission spectrometry (ICP-OES), high-resolution transmission electron microscopy (HR-TEM), and thermogravimetric analysis (TGA). The preparation of the property of the property (ICP-OES) and the property (ICP-OES) are synthesized by the property of t

Hydrogenation experiments were performed in a semi-batch pressure reactor coupled to a gas burette. The substrate H0-BT and the catalyst powder were added into the reactor, the reactor was closed and afterwards flushed with hydrogen. Then, the pressure in the reactor was adjusted to the desired value. Constant feeding of hydrogen during the reaction could be applied to keep the pressure in the reactor constant. The reactor was then heated up under stirring until the desired reaction temperature was reached, and the reaction was started. Long-term hydrogenation experiments (> 12 h) were carried out in a batch autoclave. The reaction was performed similarly to the standard hydrogenation experiments, but the autoclave was only pressurized with hydrogen before starting the reaction. For dehydrogenation experiments, a round-bottom flask was used. Here, H12-BT and the catalyst powder were added to the flask, the necks were sealed and then heating and stirring were started. If required, the pressure in the flask was reduced using a pump. Samples of the reaction mixture were taken during each dehydrogenation experiment. Consecutive dehydrogenation directly after hydrogenation was performed in the same reactor that was used for hydrogenation. For each experiment, the obtained reaction mixture (liquid phase) was separated from the catalyst by filtration. Further details on the experimental procedure can be found in our previous publication.¹³

The composition of the liquid after the reaction was analyzed by gas chromatography and mass spectrometry. From the molar fraction of each species HX-BT with X hydrogen compared to H0-BT, the overall degree of hydrogenation (DOH) or degree of dehydrogenation (DOD) was calculated. To compare reactions with different amounts of the active species (platinum) and different reaction times, productivity for a given range is calculated from DOH or DOD. Positive values of productivity are obtained for the hydrogenation, while negative values are obtained for the dehydrogenation.¹³

Results and Discussion

Catalytic Hydrogen Release from Perhydro Benzyltoluene (H12-BT)

Catalytic hydrogenation and dehydrogenation of the BT-based LOHC system were performed over various potential catalysts. The initial focus was on the dehydrogenation of H12-BT, as previous studies had shown that side product formation and high energy demand are particularly relevant during hydrogen release. ^{13, 14}

Potential of the Catalyst S-Pt/TiO₂

The S-Pt/TiO₂ catalyst had been optimized for the dehydrogenation of the LOHC system

H18-DBT in previous work.^{15, 17} To further investigate the potential of this catalyst, it was applied to the dehydrogenation of other promising LOHC systems, as well as the hydrogenation of the corresponding LOHC. For this purpose, S-Pt/TiO₂ was prepared by the wet impregnation method, as reported in the literature.¹⁵ First, characterization of the catalyst was performed to confirm that the S-Pt/TiO₂ catalyst with the desired loading of 0.1 wt% S and 0.3 wt% Pt was successfully synthesized.^{13, 16} Afterwards, this catalyst was applied for the hydrogen loading and release within the favorable LOHC system HX-BT.

To evaluate the potential of the prepared catalyst in the dehydrogenation of H12-BT, its catalytic performance was compared to the commercial benchmark catalyst S-Pt/Al $_2$ O $_3$ (0.1 wt% S, 0.3 wt% Pt). Dehydrogenation experiments were performed with both catalysts under equal reaction conditions (0.10 mol% Pt relative to H12-BT, 250 °C, 400 rpm, no pressure regulation; see Figure 1).

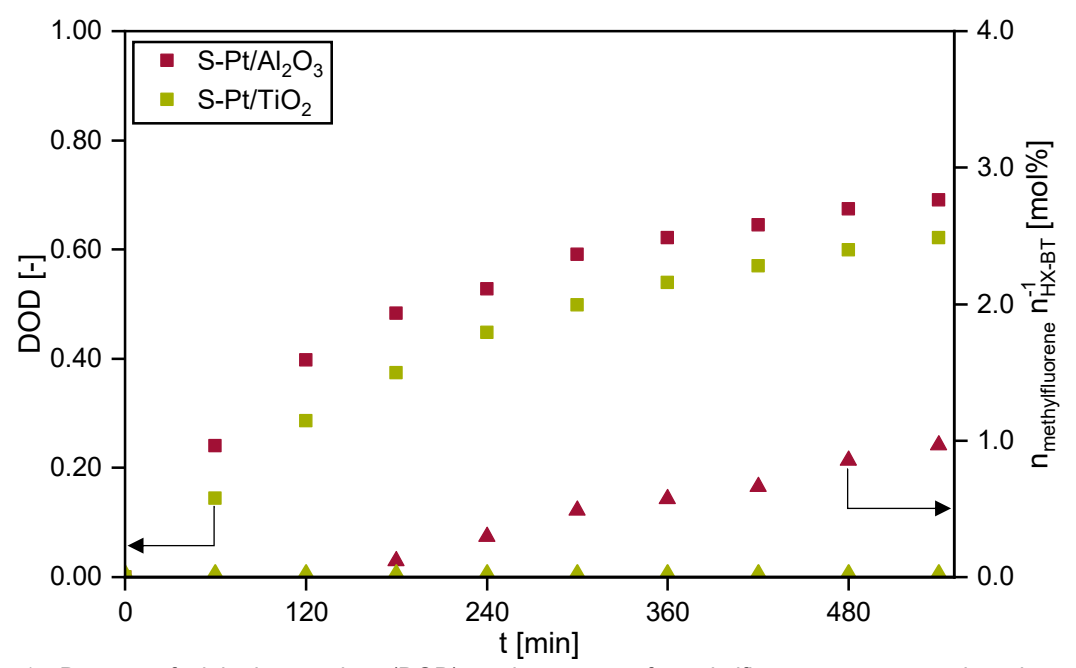


Figure 1: Degree of dehydrogenation (DOD) and amount of methylfluorene over reaction time in the dehydrogenation of H12-BT using S-Pt/Al₂O₃ or S-Pt/TiO₂ (each 0.1 wt% S, 0.3 wt% Pt) as catalyst; reaction conditions: 250 °C, 0.10 mol% Pt rel. to substrate, ambient pressure; adapted from Ref. 13 , license by CC-BY 4.0.

Compared to the S-Pt/TiO₂ catalyst, the obtained values for the degree of dehydrogenation (DOD) over the benchmark catalyst S-Pt/Al₂O₃ were consistently about 0.1 higher. Additionally, usage of S-Pt/Al₂O₃ led to a slightly higher hydrogen release productivity P_{0.24-0.53} of -0.10 g(H₂) g(Pt)⁻¹ min⁻¹ in comparison to $P_{0.14-0.50}$ of -0.09 g(H₂) g(Pt)⁻¹ min⁻¹ for S-Pt/TiO₂ (Note that negative values of productivity are obtained for the dehydrogenation reaction. Hence, a more negative value refers to higher hydrogen release per platinum mass and time). 13, 16 Therefore, the catalytic activity of the prepared catalyst S-Pt/TiO₂ was similar to the benchmark system. Additionally, the potential of the S-Pt/TiO₂ catalyst was confirmed by comparing the obtained experimental results with literature-reported results for the dehydrogenation of H12-BT using platinum catalysts. 4, 13, 18 Interestingly, a key difference between the catalysts was the formation of methylfluorene, a typical side product in the dehydrogenation of H12-BT.^{4, 13} For the dehydrogenation experiments using S-Pt/TiO₂, methylfluorene was not detected, whereas it was formed in the reaction with S-Pt/Al₂O₃. For the latter, the first detectable amount of methylfluorene (0.12 mol%) was measured after a reaction time of 180 min. After 540 min, the amount of methylfluorene increased to 0.97 mol%. Although the methylfluorene fraction is low, it is relevant as this side product negatively influences the physicochemical properties of the LOHC and may contribute to the catalyst deactivation.^{4, 9, 10} Therefore, under the studied experimental conditions, beneficial properties were found for S-Pt/TiO₂, as this catalyst offered a competitive dehydrogenation rate compared

to state-of-the-art catalyst while suppressing the formation of the undesired side product methylfluorene. 13, 16

To investigate specific catalyst structures which could promote or prevent the formation of methylfluorene, the properties of S-Pt/Al₂O₃ and S-Pt/TiO₂ were investigated using various characterization methods (details on methods see elsewhere 13, 16). The obtained results indicated differences in acidity of the different supports, morphology and dispersion of the platinum nanoparticles on the support. Furthermore, due to the reducibility of TiO₂, strong metal support interactions (SMSI) can be formed between platinum and the TiO₂ support, while this SMSI-effect does not generally occur for S-Pt/Al₂O₃. Hence, the resulting structural and electronic effects can influence the selectivity of the catalysts. 19, 20 All in all, the comparison between the prepared catalyst S-Pt/TiO₂ and the benchmark catalyst S-Pt/Al₂O₃ highlighted the potential of S-Pt/TiO₂, as it featured catalytic productivity comparable to the benchmark system which can be considered state of the art for the loading and unloading of H0-BT/H12-BT and similar LOHCs.^{3, 4, 12, 21-25} At the same time, the use of S-Pt/TiO₂ catalyst presented the advantage that the side product methylfluorene was not detected. 13, 16 Accordingly, S-Pt/TiO₂ (i.e., with 0.3 wt% Pt and 0.1 wt% S) was identified as a promising catalyst for the application of H12-BT as LOHC. For this reason, the use of S-Pt/TiO2 for the dehydrogenation and hydrogenation in the BT-based LOHC system was further investigated in our work.

Optimization of hydrogen release from H12-BT using S-Pt/TiO $_2$ focused on the reaction parameters of temperature and pressure, as the temperature required for hydrogen release is one of the key challenges for the efficient application of LOHC technology. The temperature influence on the dehydrogenation of H12-BT with S-Pt/TiO $_2$ was investigated in the range from 220 to 270 °C (see Figure 2). The temperature influence on the dehydrogenation of H12-BT with S-Pt/TiO $_2$ was investigated in the range from 220 to 270 °C (see Figure 2).

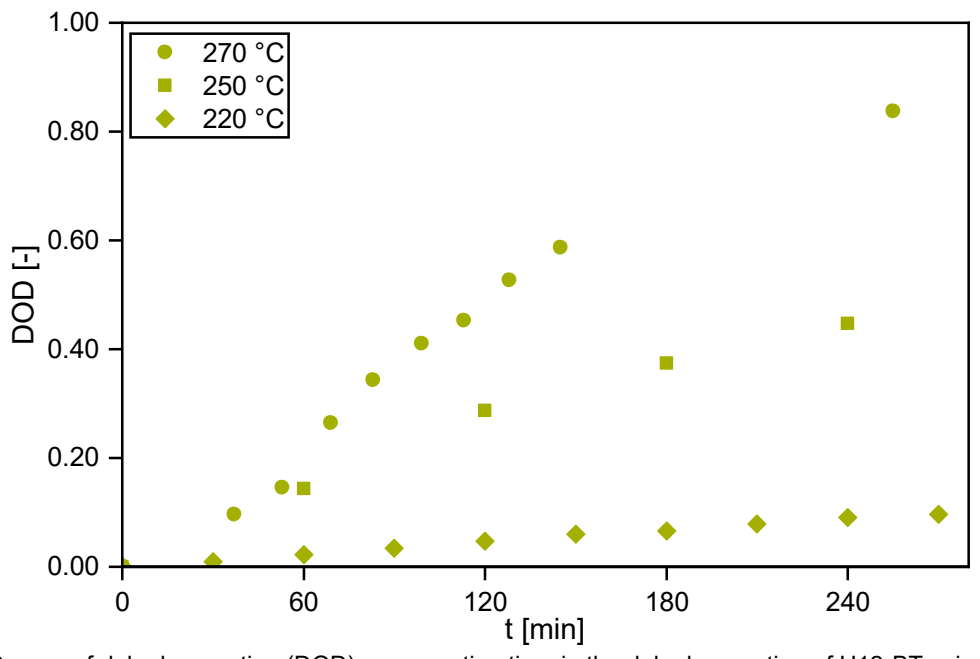


Figure 2: Degree of dehydrogenation (DOD) over reaction time in the dehydrogenation of H12-BT using S-Pt/TiO $_2$ (0.1 wt% S, 0.3 wt% Pt) as catalyst at different temperatures; reaction conditions: 0.10 mol% Pt rel. to substrate, ambient pressure; adapted from Ref. 13 , license by CC-BY 4.0.

The desired dehydrogenation reaction occurred at all temperatures investigated, ranging from 220 °C to 270 °C, as indicated by the DOD values obtained over time for the reactions at different temperatures. Additionally, the side product methylfluorene was not detected in any of the reaction mixtures obtained at the whole temperature range when S-Pt/TiO₂ has been used as a catalyst. However, the reaction temperature had a decisive influence on the reaction rate. In the experiment at 220 °C, a DOD of 0.07 was achieved after 180 min, while the DOD

reached 0.36 at 250 °C after the same time. At the highest reaction temperature of 270 °C, DOD of 0.41 was obtained after only 100 min. 13, 16 These results indicate a correlation between increasing reaction rate and increasing temperature, which is in accordance with the theoretical expectations based on kinetics and thermodynamics. 7, 28, 29 Even though the dehydrogenation rate can be significantly increased by increasing the reaction temperature, lower reaction temperatures are preferred to ensure high energy efficiency of the LOHC process and facilitate technical application.³⁰ In general, reducing the total pressure is a promising strategy to enable sufficient hydrogen release and overcome the limitation of the endothermic dehydrogenation at lower temperatures, as has already been proven for other LOHC systems.7, 31 Therefore, the potential to accelerate the reaction rate at a lower temperature of 220 °C was systematically studied by reducing the pressure. Accordingly, dehydrogenation without pressure adjustment, as discussed before, was compared to dehydrogenation reactions at reduced total pressures (i.e., 800 to 300 mbar). For all these experiments, the undesired methylfluorene formation was suppressed as it was not detected when using the S-Pt/TiO₂ catalyst. 13, 16 Moreover, the results on pressure influence showed that reduction of the total pressure, consequently the reduction in the hydrogen partial pressure in the reaction vessel, significantly accelerated the reaction rate. Overall, hydrogen release productivity increased continuously with the decrease in total pressure (see Figure 3). 13, 16 In summary, this systematic investigation of pressure influence on the dehydrogenation of H12-BT revealed a correlation between increased productivity and reduced total pressure. 13, 16 These results support the beneficial integration of the dehydrogenation unit with electrochemical hydrogen compression (EHC) for pressure reduction, thereby optimizing the overall energy balance of the LOHC process.7

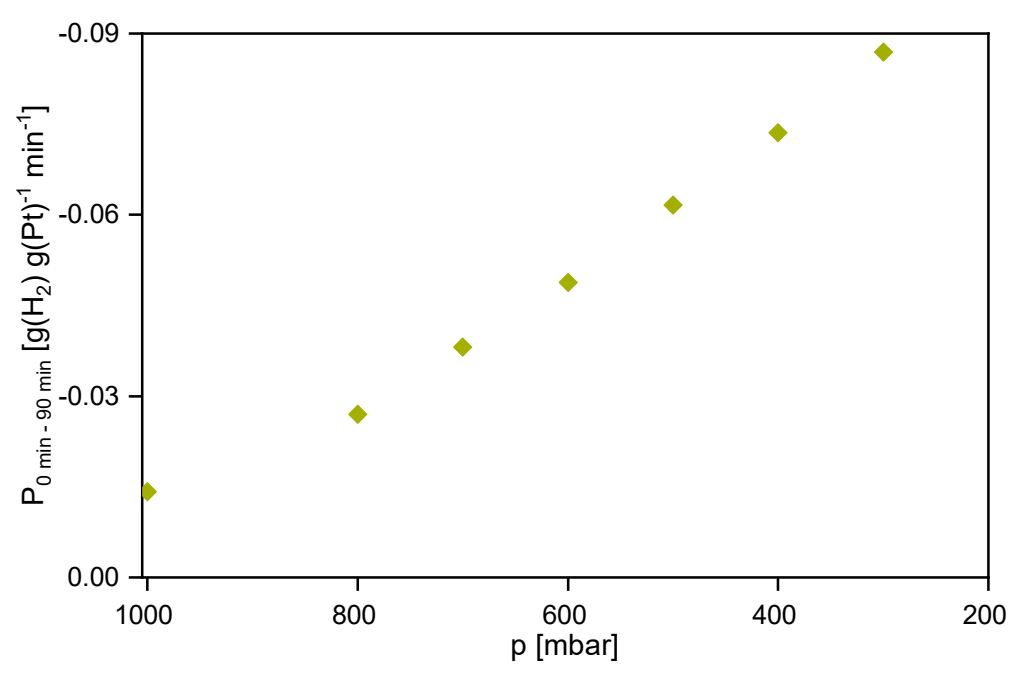


Figure 3: Correlation between initial hydrogen release productivity and total pressure in the dehydrogenation of H12-BT using S-Pt/TiO₂ (each 0.1 wt% S, 0.3 wt% Pt) as catalyst; reaction conditions: 220 °C, 0.10 mol% Pt rel. to substrate, pressure of 1000 mbar is presumed for run without pressure adjustment; adapted from Ref.¹³, license by CC-BY 4.0.

Influence of Sulfur Modification

The benchmark catalyst and the prepared titania-supported catalyst discussed earlier consist of metal species modified with sulfur on a metal oxide support. Previously, it was found that a suitable sulfur modification can increase the activity and selectivity in the dehydrogenation of H12-BT and similar LOHC systems.^{4, 15, 17} For instance, the advantage of sulfur modification has been demonstrated by using S-Pt/TiO₂ in the dehydrogenation of H18-DBT.¹⁵ To investigate the influence of sulfur modification for Pt/TiO₂ in the dehydrogenation of H12-BT,

as shown in Figure 4, its performance was compared with $S_{0.1\%}$ -Pt_{0.3%}/TiO₂ at 250 °C (9 h, 0.10 mol% Pt relative to substrate, no pressure adjustment).^{13, 16}

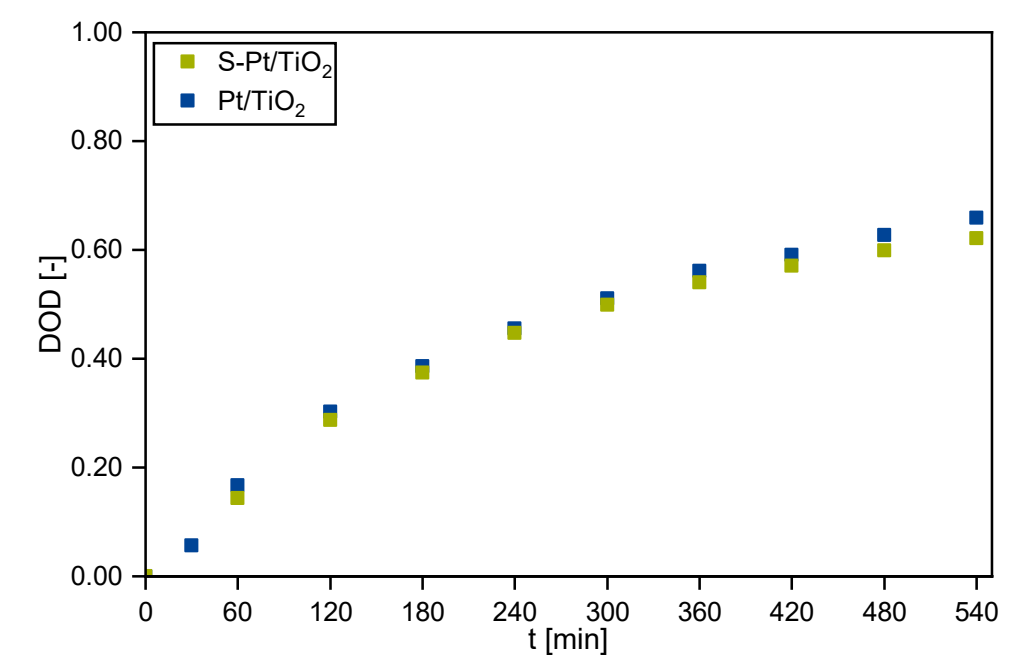


Figure 4: Degree of dehydrogenation (DOD) over reaction time in the dehydrogenation of H12-BT using Pt/TiO₂ or S-Pt/TiO₂ (0.1 wt% S, each 0.3 wt% Pt) as catalyst; reaction conditions: 250 °C, 0.10 mol% Pt rel. to substrate, ambient pressure; adapted from Ref. ¹³, license by CC-BY 4.0.

During the course of the investigated dehydrogenation reactions, the DOD values achieved using both catalysts were almost identical. Furthermore, no side products were detected in the reaction mixture. Analogous results were obtained for both catalysts in dehydrogenation experiments performed at 220 °C and a reduced pressure of 500 mbar. 13, 16 These results suggest that the used sulfur modification did not significantly influence the obtained catalytic activity and selectivity in the dehydrogenation of H12-BT. In all, in this work, no decisive influence of sulfur modification on the performance of Pt/TiO2 catalysts was found in the dehydrogenation reaction. Differences in the properties of both catalysts with and without sulfur modification can only be characterized to a limited extent, as various characterization methods cannot reliably detect influences of the used low sulfur content (further information on characterization see elsewhere 13, 16). Although sulfur modification showed no positive effect on the studied reactions, it also did not cause catalyst deactivation. In the literature, similar dehydrogenation experiments proved increased selectivity due to sulfur modification.⁴ Accordingly, the positive effect could depend on the different reaction conditions, for instance, suppression of side reactions such as C-C bond cleavages under harsher reaction conditions.4 Therefore, when selecting a catalyst for H12-BT dehydrogenation, which is to be applied under a wide range of conditions, it might be advantageous to use the sulfur-modified catalyst to ensure high activity and selectivity. 13, 16 All in all, these results demonstrate the high potential of both TiO₂-supported Pt-based catalysts for the dehydrogenation of H12-BT.

Catalyst Recycling and Regeneration

To investigate the stability of the optimized catalyst S-Pt/TiO₂ and the possibility of catalyst recycling for multiple reaction runs, the catalyst was reused after the first dehydrogenation experiment. Additionally, potential regeneration strategies were studied. When $S_{0.1\%}$ -Pt_{0.3%}/TiO₂ was reused in the dehydrogenation of H12-BT (250 °C, 9 h, 0.10 mol% Pt relative to substrate, without pressure adjustment), hydrogen release productivity decreased from -0.10 g(H₂) g(Pt)⁻¹ min⁻¹ using the fresh catalyst to -0.08 g(H₂) g(Pt)⁻¹ min⁻¹ for the recycled catalyst.^{13, 16} Similar trends were obtained during the recycling tests over Pt_{0.3%}/TiO₂ catalyst.^{13, 16} Accordingly, the reusability of these catalysts during dehydrogenation was not significantly affected by the sulfur modification. Additionally, recycling tests over the

commercial benchmark catalyst were performed and compared to the prepared catalysts. When using S_{0.1%}-Pt_{0.3%}/Al₂O₃, productivity dropped slightly from -0.12 g(H₂) g(Pt)⁻¹ min⁻¹ in the first run to -0.11 g(H₂) g(Pt)⁻¹ min⁻¹ in the second run.^{13, 16} Overall, the desired dehydrogenation of H12-BT was achieved with both fresh and recycled catalysts; however, the hydrogen release productivity declined for the recycled samples of S_{0.1%}-Pt_{0.3%}/TiO₂, Pt_{0.3%}/TiO₂, and the benchmark S_{0.1%}-Pt_{0.3%}/Al₂O₃. These results might indicate progressive deactivation of the catalysts. Deactivation of the catalysts during dehydrogenation is mainly expected due to deposition of organic species on the catalyst surface or blockage of the catalyst pore structure by reaction residues, as well as (partial) oxidation of platinum particles. 32-35 As suitable regeneration treatments for (partially) deactivated catalysts depend on the cause of deactivation, the investigation of potential regeneration strategies can also highlight deactivation mechanisms. 32-35 Therefore, to examine deactivation causes and promising regeneration procedures, various treatments of the spent catalyst were performed, and the different regenerated catalysts were reused in a second dehydrogenation run. Additionally, the properties of the fresh and recycled catalysts were compared to analyze changes in their characteristics. A reaction temperature of 220 °C was chosen to investigate whether catalyst reusage is possible under mild reaction conditions. In all the recycling experiments, the catalyst was washed after the first run, whereby easily soluble residues could be removed. 16 Potential regeneration methods were then investigated; including heat treatment (400 °C, air), re-reduction (400 °C, H₂), and heat treatment under inert gas (400 °C, N₂). Here, conditions were chosen analogous to catalyst preparation to avoid restructuring, sintering, or other negative effects caused by harsher post-reaction treatment conditions. For each recycled catalyst, hydrogen release productivity was compared to the results obtained with the fresh catalyst in the first dehydrogenation run (see Figure 5).¹⁶

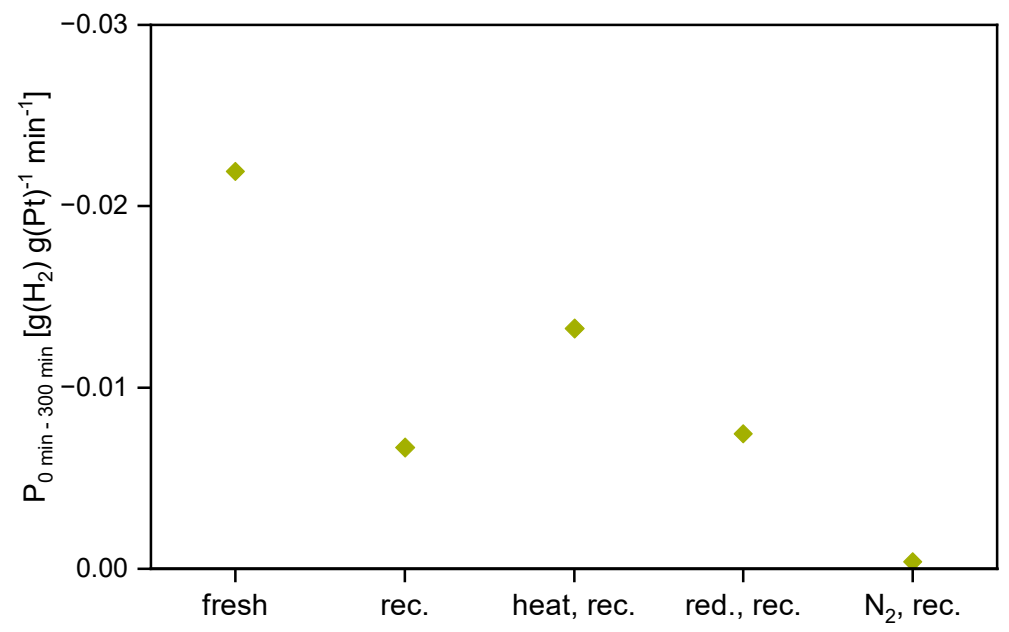


Figure 5: Productivity of the first 300 min of reaction time in the dehydrogenation of H12-BT using the fresh catalyst S-Pt/TiO₂ (0.1 wt% S, 0.3 wt% Pt) and the recycled catalysts without additional treatment (rec.), after heat treatment (heat, rec.), after reduction treatment (red., rec.), after heat treatment under nitrogen flow (N_2 , rec.); reaction conditions: 220 °C, 0.10 mol% Pt rel. to substrate, ambient pressure.

When using the different recycled catalysts, the hydrogen release productivity dropped significantly below -0.02 g(H₂) g(Pt)⁻¹ min⁻¹, compared to the productivity with the fresh catalyst. Accordingly, none of the post-reaction catalyst treatment conditions employed led to complete regeneration of the catalyst. Among the recycled catalysts, the best productivity was achieved after the heat treatment.¹⁶ These results suggest that the main deactivation cause could be related to the residues remaining on the catalyst, which can be minimized by heat treatment.^{35, 36} Although heat treatment improved productivity, complete regeneration was not achieved. This finding indicates that either a significant amount of residues was irreversibly

deposited on the catalyst or that heat treatment at 400 °C was insufficient for complete removal.35, 37 Moreover, reduction treatment of the spent catalysts did not result in any significant difference in productivity compared to the recycled catalyst without further treatment. 16 Accordingly, oxidation of the platinum species is probably not a decisive reason for the catalyst deactivation. The lowest productivity was observed for the heat-treated catalyst under nitrogen flow. 16 This indicates that the used inert gas flow did not improve the removal of residues but instead had a negative effect. In general, the conditions of this treatment could promote sintering or morphological changes in the catalyst, negatively influencing the catalytic performance.³² Additionally, the study on the different regeneration methods indicated that deactivation due to agglomeration of platinum particles is unlikely, as the heat treatment improved productivity of the recycled catalyst, although this treatment was expected to facilitate rather than reduce platinum agglomeration.³² HR-TEM analysis of the mean platinum particle size confirmed that agglomeration can be excluded as a decisive deactivation mechanism for the used catalysts. 16 Furthermore, the results for the reduction treatment of the recycled catalyst and temperature-programmed reduction (H₂-TPR) analysis indicated that deactivation was not caused by oxidation of the catalysts during dehydrogenation. To further investigate deactivation by potential residues on the catalysts, such as organic deposits and coke (precursors), thermogravimetric analysis (TGA) was employed. 16 For the spent catalysts after one dehydrogenation run without further treatment, TGA results suggested the presence of deposits that could lead to catalyst deactivation. Furthermore, the analysis showed that a large proportion of these deposits could be removed at temperatures up to 400 °C in air. 16 This is in accordance with the results of the regeneration tests, where heat treatment at 400 °C improved the catalytic activity of the recycled catalyst, as shown previously. 16 Thermal removal of the detected deposits can be used to partially reactivate the catalysts; however, the investigation showed that complete removal would only be possible at temperatures above 400 °C. 16 However, the use of higher temperatures could negatively affect the catalyst, for example, by facilitating sintering. 32 Overall, the recycling study showed that the prepared catalyst S_{0.1%}-Pt_{0.3%}/TiO₂ enabled the desired hydrogen release in a repeated reaction run, even after 5 h of reaction time at 220 °C. Nevertheless, catalyst reuse impaired productivity. Generally, deposition of residues such as organic species or coke (precursors) can play a decisive role for deactivation. 16 These results are in accordance with previous studies on catalyst deactivation in LOHC applications. Literature reports indicate that heat treatment of the catalyst could remove organic deposits from the catalyst, but complete regeneration was not possible. 17, 33, 34 Similarly, for the analyzed regeneration approaches of S_{0.1%}-Pt_{0.3%}/TiO₂, full reactivation after the first dehydrogenation run was not achieved. Nevertheless, heat treatment was identified as a promising regeneration method for the investigated catalyst. 16

Catalytic Hydrogen Loading of Benzyltoluene (H0-BT)

For the application of catalytic hydrogen loading and release of the LOHC system, it is beneficial to perform hydrogenation and dehydrogenation with the same catalyst just by adjusting the reaction conditions. Therefore, the catalysts that showed promising results for the dehydrogenation of H12-BT were studied in the hydrogenation of H0-BT. The Both prepared catalysts $S_{0.1\%}$ -Pt_{0.3\%}/TiO₂ and Pt_{0.3\%}/TiO₂ proved to be promising for the application in the BT-based LOHC systems, as they showed similar productivity to the benchmark $S_{0.1\%}$ -Pt_{0.3\%}/Al₂O₃, combined with the benefit of suppressing the undesired methylfluorene formation in the dehydrogenation of H12-BT. Thus, both catalysts were investigated in the hydrogenation of H0-BT to evaluate the suitability of these catalysts for application in the entire LOHC cycle.

Comparison of Promising Platinum Catalysts

For the hydrogenation of H0-BT, the catalytic performance of the two TiO_2 -supported catalysts, both with and without sulfur modification, was evaluated and compared with the commercial benchmark $S_{0.1\%}Pt_{0.3\%}/Al_2O_3$. Side products were not detected in any of the hydrogenation reactions investigated. This is in accordance with the literature showing that side reactions occur more often during the dehydrogenation.^{4, 5, 38, 39} Therefore, increasing activity rather than

selectivity is crucial to optimize the catalyst for hydrogenation. All three catalysts were used in the hydrogenation under the same reaction conditions (200 °C, 30 bar, 1 h), and the reached degree of hydrogenation (DOH) was compared (see Figure 6).^{14, 16}

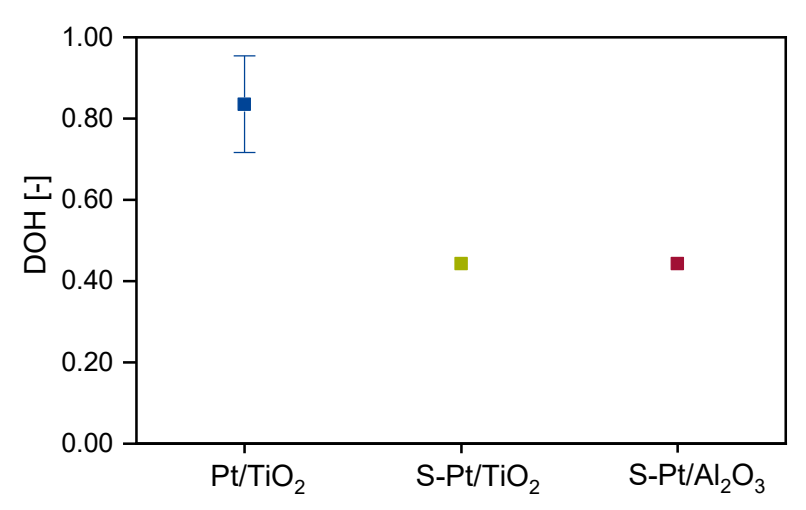


Figure 6: Degree of hydrogenation (DOH) in the hydrogenation of H0-BT using Pt/TiO_2 , S- Pt/TiO_2 or S- Pt/Al_2O_3 (0.1 wt% S, 0.3 wt% Pt) as catalyst; reaction conditions: 200 °C, 1 h, 0.02 mol% Pt rel. to substrate, 30 bar H₂.

The highest DOH of 0.84 (mean value) was achieved using Pt_{0.3%}/TiO₂, whereas both sulfurmodified catalysts reached lower values of 0.44. This corresponds to a hydrogen loading productivity P_{0 min - 60 min} of 4.33 g(H₂) g(Pt)⁻¹ min⁻¹ (mean value) for Pt_{0.3%}/TiO₂, while lower productivities were obtained with the sulfur-modified catalysts 2.24 g(H₂) g(Pt)⁻¹ min⁻¹, S-Pt/Al₂O₃: 2.25 g(H₂) g(Pt)⁻¹ min⁻¹). 13, 14, 16 Accordingly, Pt/TiO₂ was identified as the best catalyst under the investigated experimental hydrogenation conditions. Nevertheless, both S-Pt/TiO₂ and S-Pt/Al₂O₃ catalysts can also be applied for the desired hydrogenation. The catalytic performance of the prepared S-Pt/TiO₂ catalyst was found to be similar to the benchmark S-Pt/Al₂O₃, with both catalysts being suitable for hydrogenation as well as dehydrogenation in the LOHC-system H0-BT/H12-BT. Compared to the literature on hydrogenation of H0-BT using supported platinum catalysts, the S-Pt/TiO₂ catalyst outperformed other catalysts in activity under similar reaction conditions.^{4, 40} However, it is noteworthy that the obtained productivity might be influenced by the different experimental procedures used, particularly different heating processes.4, 13, 40 Overall, these results confirmed that S-Pt/TiO₂ is a promising catalyst for both hydrogenation and dehydrogenation of the BT-based LOHC system. In addition, as shown earlier, S-Pt/TiO₂ stands out due to the lower methylfluorene formation in the dehydrogenation compared to the benchmark S-Pt/Al₂O₃. Additionally, further similar hydrogenation experiments performed over both Pt_{0.3%}/TiO₂ and S_{0.1%}-Pt_{0.3%}/TiO₂ catalysts under different reaction conditions confirmed the potential of $Pt_{0.3\%}/TiO_2$ for H0-BT hydrogenation. Herein, application of the S-Pt/TiO₂ catalyst resulted again in a lower DOH compared to Pt/TiO₂. 14, 16 To better understand the negative influence of sulfur modification on hydrogenation activity, studies about optimization of the dehydrogenation catalysts can be referred. These studies showed that, for catalysts with selective sulfur poisoning, sulfur preferentially blocks low-coordinated sites of the platinum nanoparticles. 15, 17, 41 Although these low-coordinated sites can cause undesirable side reactions during the dehydrogenation, 15, 17, 41 they could be relevant for hydrogenation. Consequently, their blockage by sulfur leads to a negative effect on hydrogenation activity. Furthermore, the sulfur modification changes the electron density of platinum in the vicinity of the sulfur species, thereby facilitating the desorption of dehydrogenated species from the catalysts.41 While this effect was shown to be beneficial for dehydrogenation, it could hinder the adsorption of reactants during hydrogenation and thus slow down the hydrogenation reaction. 15, 17, 41 In summary, comparison of the catalysts proved the S_{0.1%}-Pt_{0.3%}/TiO₂ as suitable catalyst for both hydrogenation and dehydrogenation. However, in terms of hydrogenation activity, Pt_{0.3%}/TiO₂ outperformed S_{0.1%}-Pt_{0.3%}/TiO₂. Therefore, further investigation of the hydrogenation focused on Pt/TiO₂ as catalyst. 14, 16

Recycling of Pt/TiO₂

To further evaluate the potential of the Pt_{0.3%}/TiO₂ catalyst, its stability and recyclability were investigated in several hydrogenation runs. For this purpose, hydrogenation experiments (200 °C, 1 h, 0.02 mol% Pt relative to substrate, 30 bar H₂) were carried out with the freshly prepared catalyst. Then, the spent catalyst was used in a second hydrogenation run under similar conditions. Interestingly, a higher DOH value was obtained for the second reaction than in the initial run using fresh catalyst, and the DOH was increased by 19 % for the recycling compared to the first run. Similar results were obtained for experiments at a higher reaction temperature of 225 °C. ¹⁶ Moreover, no catalyst deactivation was observed during the two runs. This finding implies that modification of the catalysts occurred after the first run, which led to enhanced catalytic activity. To investigate whether this trend continues over several runs, four consecutive hydrogenation experiments were conducted over the same catalyst (225 °C, 1 h, 0.02 mol% Pt relative to substrate, 30 bar H₂). In the second and third recycling runs, the DOH decreased by about 15 % compared to the result of the first reaction, with no substantial difference between these two recycling runs. 16 Despite a slight decrease in activity occurring in the second and third runs, a DOH of more than 0.7 was still reached after four runs under the studied reaction conditions. 16 Therefore, several hydrogenation runs could be carried out using Pt/TiO₂ without the need for additional regeneration treatment.

To correlate catalytic performance and properties of the catalyst in the consecutive reaction runs, characterizations of the fresh and recycled catalysts were performed. However, no significant changes in specific surface area or total pore volume, as well as the phase of the supports, were found. 16 Besides, no Pt leaching was detected, and all the investigated catalysts contained the targeted amount of platinum. 16 Furthermore, deposition of organic residues on the used catalyst was ruled out as the cause of the observed changes, since only minor amounts of residues were detected on all samples by TGA. Moreover, no correlation between the detected organic residues and catalytic performance was found. 16 Further studies on the catalyst's reduction state indicated that the change in catalytic performance is not attributed to the degree of oxidation or reduction of platinum. 16 In contrast, during the HR-TEM analyses, an increase in mean platinum particle size of the recycled catalysts was observed compared to the fresh catalyst. While the freshly prepared Pt/TiO₂ exhibited a mean platinum particle size of 0.83 ± 0.35 nm, its size was increased to 1.28 ± 0.45 nm after two hydrogenation runs at 200 °C (each 60 min). For the catalyst used in four hydrogenation runs at 225 °C (each 30 min), the highest mean platinum particle size of 1.62 ± 0.56 nm was obtained. 16 These results suggest that agglomeration of the platinum particles occurred during hydrogenation. In general, based on previous studies, optimized platinum particle size leads to enhanced catalytic performance (higher DOH).⁴¹ To investigate whether the different particle sizes influenced the obtained DOH, hydrogenation reactions were performed using various Pt/TiO₂ samples with different platinum particle sizes. The comparison revealed no optimal platinum particle size that led to higher DOH values. Therefore, the results confirmed that platinum particle size is not the decisive factor that determines the catalytic performance.¹⁶ Moreover, as previously discussed, the SMSI effect can also occur for Pt/TiO2 under hydrogenation conditions. Thus, the catalytic performance of the studied catalysts can be influenced by TiO_x overlayers, the microstructure of platinum, and electronic effects. 15, 16, 36, 42 HR-TEM images of the recycled catalyst suggested the occurrence of TiO_x overlayers, but further research is required for explicit identification. 16 Here, it should be noted that the SMSI effect can be very dynamic. Hence, the obtained images may not necessarily reflect the state of the catalyst during or immediately after reaction. Compared to the fresh catalyst, the HR-TEM images provided further indication of changes in the platinum particles and interaction with the support due to the reuse of the catalyst. 16 These changes may depend on the reaction conditions. Additionally, TiOx overlayers can be influenced not only by conditions such as gas atmosphere and temperature, but also by the organic reaction substances. 43-46

In conclusion, the results obtained by recycling experiments confirmed the hypothesis that platinum particle size influences catalytic performance, but it is not the sole factor. The distribution of platinum species and their interactions with the supports are also expected to

play a pivotal role in the catalytic performance. Furthermore, the reusability of the catalyst Pt/TiO_2 in the hydrogenation of H0-BT was demonstrated as several hydrogenation runs were performed without pronounced catalyst deactivation. Hence, this study showed the good recyclability of $Pt_{0.3\%}/TiO_2$ in hydrogenation, in addition to its promising potential for both hydrogenation and dehydrogenation of the BT-based LOHC system.

Hydrogen Loading and Release in the HX-BT System

Investigation of Hydrogenation-Dehydrogenation Cycle

During the real application of LOHC technology, catalytic hydrogenation and dehydrogenation cycles are repeatedly carried out to enable hydrogen loading and release. To simulate this cycling, H0-BT was partially loaded with hydrogen, and afterwards, hydrogen was released from the obtained HX-BT. For this purpose, the catalyst Pt_{0.3%}/TiO₂ was applied, which was already analyzed in the dehydrogenation of H12-BT and hydrogenation of H0-BT. Both reactions were performed in the same reactor setup by adjusting the experimental conditions. First, the hydrogenation run was performed at 225 °C for 30 min. Then, subsequent dehydrogenation of the obtained HX-BT was carried out under similar conditions, changing from hydrogen pressure of 30 bar to ambient pressure (225 °C, fresh Pt_{0.3%}/TiO₂, 0.02 mol% Pt relative to substrate; hydrogenation: 30 min, 30 bar H₂; dehydrogenation: no pressure adjustment, 300 min). After each step, the obtained DOH value and the liquid phase composition were evaluated (see Figure 7).^{14, 16}

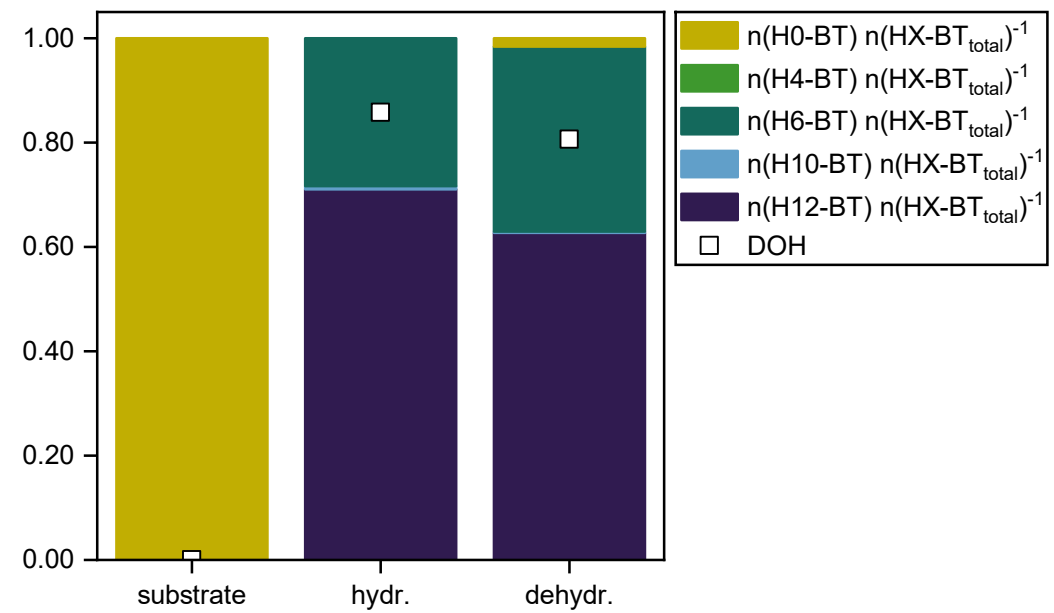


Figure 7: Course of degree of hydrogenation (DOH) and molar ratios of different HX-BT species after the hydrogenation of H0-BT (hydr.) and subsequent dehydrogenation (dehydr.) using Pt/TiO₂ (0.3 wt% Pt) as catalyst; reaction conditions: 225 °C, 1 h, 0.02 mol% Pt rel. to substrate, hydr.: 30 min, 30 bar H₂, dehydr.: 300 min, ambient pressure.

After the hydrogenation ran for 30 minutes, the substrate H0-BT was fully converted. The reaction mixture obtained consisted mainly of H12-BT (amount: 0.71), while the partially hydrogenated species H6-BT was also present (0.28). Furthermore, the mixture contained a small but measurable amount (< 0.01) of H10-BT. This composition resulted in a DOH of 0.86.^{14, 16} In the next step, the hydrogen release from this HX-BT mixture was investigated. During the dehydrogenation step, the DOH was reduced to 0.81, and non-hydrogenated H0-BT was already formed (0.02). H12-BT remained the main component of the reaction mixture, although its amount dropped to 0.63. The amount of H6-BT increased to 0.35, while a small amount of H10-BT (< 0.01) was also detected.^{14, 16} The increase of H6-BT during the dehydrogenation step indicates that the conversion of H12-BT to H6-BT was preferred over

the subsequent dehydrogenation of H6-BT to H0-BT. Nevertheless, H0-BT was formed under the reaction conditions used, albeit to a smaller extent. ^{14, 16} These findings are consistent with the course of hydrogenation as discussed earlier. In general, the first step of hydrogenation (i.e., the conversion of H0-BT to H6-BT) is energetically favored over the second step of hydrogenation from H6-BT to H12-BT, as the first step is more exothermic. ⁶ For dehydrogenation, this means that the conversion of H12-BT to H6-BT is preferred over the step from H6-BT to H0-BT. The results of the cycling experiments demonstrate that the desired hydrogen release is possible from a real partially hydrogenated HX-BT mixture using the Pt_{0.3%}/TiO₂ catalyst, though dehydrogenation is slow at the reaction temperature of 225 °C. The switch from hydrogenation to dehydrogenation was realized solely by changing pressure (30 bar H₂ to ambient pressure without hydrogen addition) using the same reactor and Pt_{0.3%}/TiO₂ catalyst. ^{14, 16} This facile transition between hydrogen loading and release can simplify the application of LOHC technology. ^{3, 11, 12}

In addition to the catalyst optimization, which was the main focus of our study, chemical equilibrium calculations are important for gaining valuable insights of LOHC loading and unloading and thus, for an according optimizing of LOHC technology. In general, such calculations define the ultimate conversion limits of both hydrogenation and dehydrogenation reactions, guide process design under optimized reaction conditions, support effective catalyst utilization, and ensure overall efficiency and safety. Accordingly, the results of the chemical equilibrium calculations performed during this study are presented in the following section.

Chemical Equilibrium of Hydrogen Loading and Release

As mentioned above, to gain further insights into the role of thermodynamics for the studied hydrogenation and dehydrogenation in the H0-BT/H12-BT system, the equilibrium composition of the LOHC phase was calculated and compared with the experimental results. ¹⁴ For the calculations, H0-BT, H6-BT, and H12-BT were considered, as other HX-BT species occur either not at all or only in negligible quantities. Furthermore, the amount of hydrogen absorbed from the gas phase into the liquid phase was taken into account. The equilibrium composition of the liquid phase obtained under hydrogen pressures of 0.3, 1.0, and 30.0 bar in the range from 25 °C to a temperature close to their respective boiling point is shown in Figure 8.

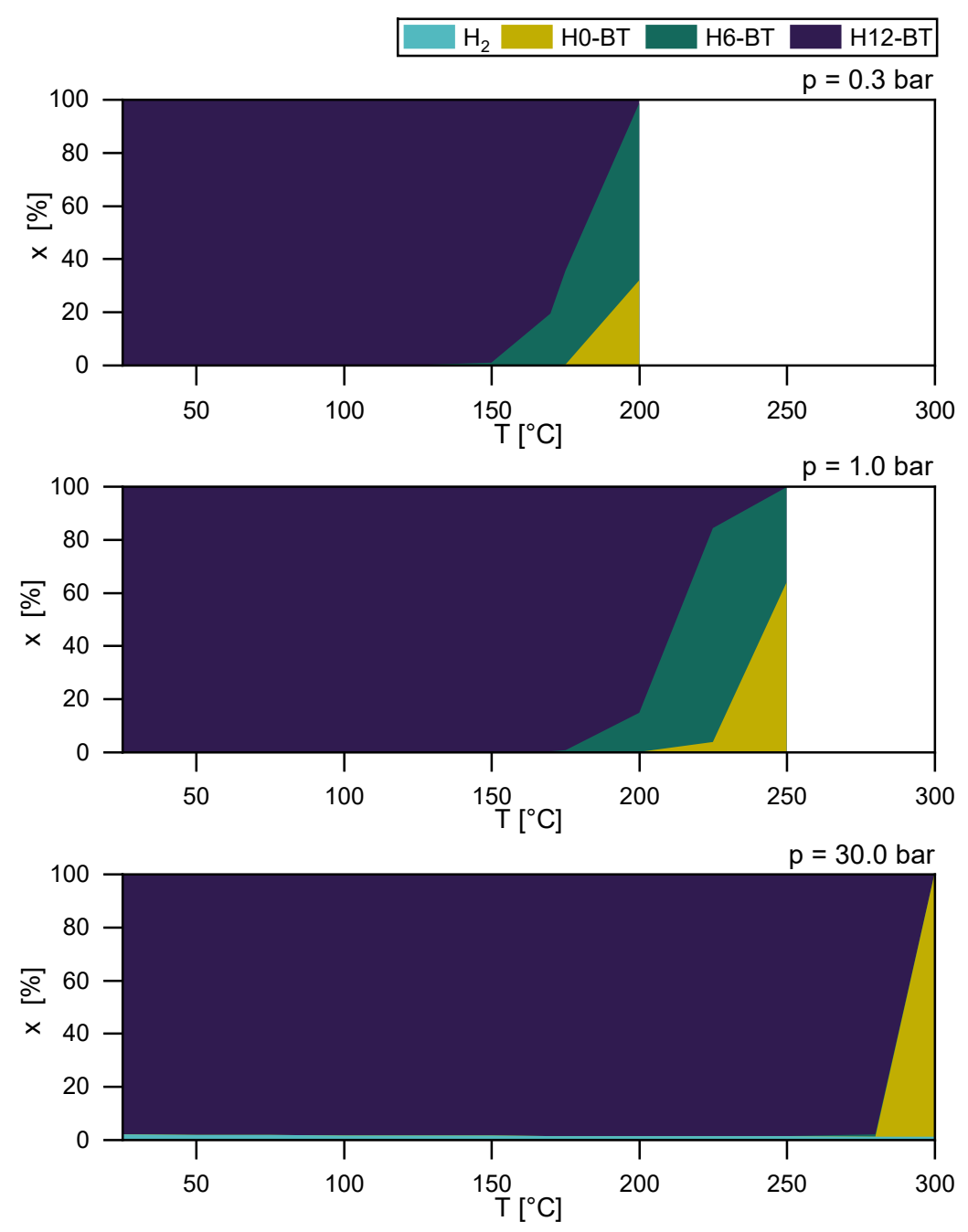


Figure 8: Calculated liquid phase composition in chemical equilibrium at pressures of 0.3, 1.0 or 30.0 bar; amount of H_2 is less than 2 % for all shown conditions; adapted from Ref.¹⁴, license by CC-BY 4.0.

From the data obtained on liquid phase composition in thermodynamic equilibrium at various pressures and temperatures, clear preferences for specific HX-BT species can be identified under specific conditions. Based on these findings, the achievable equilibrium during hydrogen loading and release of H0-BT/H12-BT as a function of reaction conditions is projected. Up to a certain temperature, depending on pressure, H12-BT is the dominant species in the reaction mixture. At low pressure (0.3 bar), relevant amounts of H6-BT are present at temperatures above 150 °C. When the temperature exceeds 175 °C, the amount of H0-BT increases significantly. A similar trend is observed at a pressure of 1.0 bar, but shifted towards higher temperatures: significant amounts of H6-BT are present at temperatures above 175 °C, while the amount of H0-BT increases only for temperatures above approximately 200 °C. Overall, for most pressures, there's a temperature window of about 30 - 60 °C in which significant amounts of partially hydrogenated H6-BT are present. While the fully hydrogenated species H12-BT dominates at low temperatures, the non-hydrogenated species H0-BT is preferred at high temperatures. At a significantly higher pressure of 30 bar, almost only H12-BT is present

up to about 280 °C, and H6-BT is found in small quantities. When the temperature increases to 300 °C, H0-BT is the dominant species in the liquid phase at equilibrium. 14

Moreover, the calculated data on equilibrium composition were compared with the experimentally obtained composition of the liquid phase. For this purpose, the reaction conditions had to be adjusted to enable reaching of thermodynamic equilibrium within a realistic reaction time. Additionally, temperature and pressure of the reaction were chosen to validate the presence of different HX-BT species in the reaction mixture as given by the calculated equilibrium composition. Hence, the hydrogenation of H0-BT was not carried out at constant pressure; instead, a defined hydrogen pressure was applied at the beginning of the experiment and not adjusted afterwards. The pressure decreased during the experiment as hydrogen was consumed by hydrogenation. To approximate equilibrium composition experimentally, a long-term reaction was carried out (2 weeks reaction time, 200 °C, 30 bar initial hydrogen pressure). During this experiment, the pressure dropped rapidly at the start of the reaction and then stabilized at around 0 bar, indicating no measurable amount of hydrogen remained in the gas phase throughout the reaction. After this long-term experiment, a DOH of 0.21 was achieved. The resulting liquid phase composition was compared with the theoretical equilibrium composition (Figure 9). Therefore, the equilibrium composition was calculated at 200 °C and a DOH of 0.21, resulting in a hydrogen pressure of 0.24 bar. 14, 16

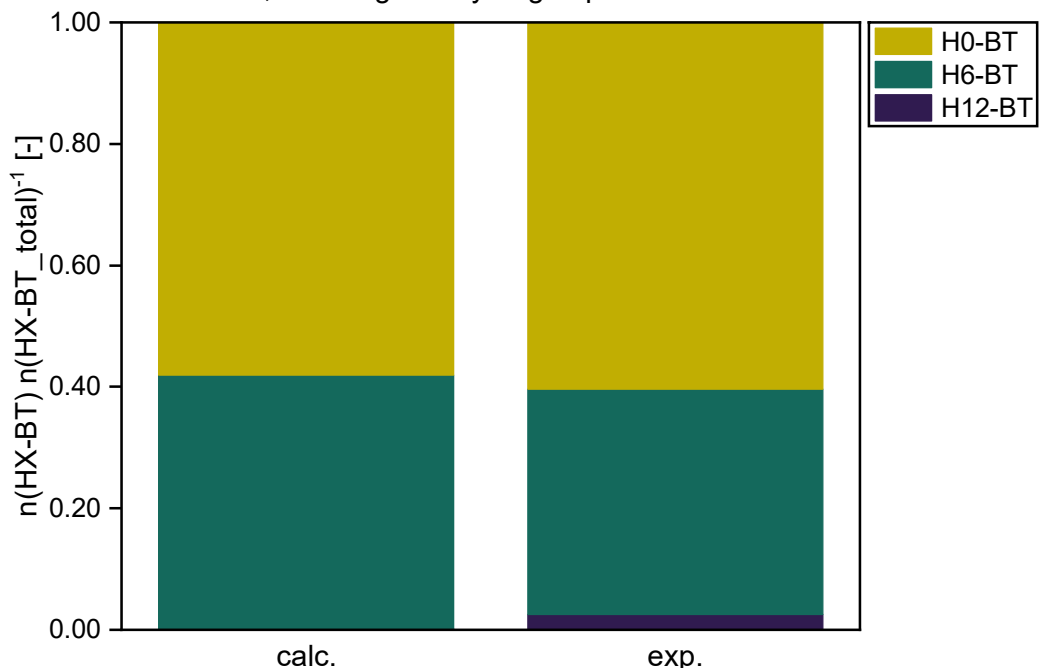


Figure 9: Liquid phase composition as calculated (200 °C, DOH = 0.21) or obtained from long-term hydrogenation experiment (200 °C, 30 bar initial H_2 pressure); calculated amount of H12-BT is less than 1 %; adapted from Ref. ¹⁴, license by CC-BY 4.0.

From the theoretical calculations, an equilibrium composition consisting of a ratio of 0.58 H0-BT and 0.42 H6-BT was obtained at 200 °C. These values are in good agreement with the experimentally obtained composition of 0.60 H0-BT and 0.37 H6-BT. Further partially hydrogenated species, such as H4-BT and H10-BT, were not detected in the reaction mixture, and thus, the previous hypothesis that these species occur only in negligible quantities, if at all, was confirmed. For the hydrogenated species H12-BT, the calculated amount was minor (< 0.01), whereas an amount of 0.03 was detected in the obtained reaction mixture. This slight deviation between the experimentally obtained and calculated amounts indicated that the formation of H12-BT was favored under real reaction conditions. Under the used reaction conditions, it could be possible that the hydrogenation of H6-BT to H12-BT proceeds significantly faster than the reverse reaction, i.e., the dehydrogenation of H12-BT to H6-BT. Hence, this would mean equilibrium was not reached in the experiment, resulting in a higher amount of H12-BT in the real reaction mixture compared to the equilibrium composition.

Furthermore, minor deviations between theoretically and experimentally obtained compositions may result from assumptions used for the calculations. Overall, the comparison illustrates that the calculated equilibrium compositions reflect the actual composition of the LOHC phase. Overall, the results demonstrate that kinetic rather than thermodynamic aspects limited the reaction. Even in the long-term experiment, thermodynamic equilibrium was not likely reached, although the obtained composition was close to the theoretical equilibrium. This suggests that equilibrium is approximated but unlikely to be fully reached under the used conditions within a realistic reaction time due to the slow reaction rate close to equilibrium. Accordingly, the reaction conditions need to be adjusted to achieve further closer values to the thermodynamic equilibrium. For this purpose, increasing the temperature could increase the reaction rate, as indicated by the investigations on the effect of temperature.^{14, 16}

Analogous to the experimental studies, the thermodynamic calculations showed that the selected temperature and pressure (both hydrogen pressure and total pressure) determine the resulting equilibrium composition. Although hydrogenation, as an exothermic reaction, is generally unfavored at higher temperatures, the calculated results illustrate the role of pressure: at 30 bar, hydrogenation is favored by the chemical equilibrium at almost all temperatures up to the boiling point of the LOHC. This was also demonstrated in experimental studies on the catalytic hydrogenation of H0-BT: using Pt_{0.3%}/TiO₂, full hydrogenation was achieved within approximately 1 h at a constant hydrogen pressure of 30 bar and temperatures above 200 °C. To promote dehydrogenation, the pressure must be significantly reduced. For example, at 1 bar, relevant amounts of H0-BT in the equilibrium composition are only achievable at temperatures above 230 °C. Accordingly, the applied pressure is crucial for optimizing the LOHC technology for both hydrogenation and dehydrogenation; by adjusting the pressure, the desired reaction can be carried out at low temperatures. These results are consistent with experimental investigations on the effects of different reaction conditions. In contrast to the formation of H0-BT during dehydrogenation, partial dehydrogenation of H12-BT to H6-BT, with the corresponding release of hydrogen, can be achieved at temperatures about 50 °C to 75 °C lower. This partial loading and unloading is also relevant for technical applications of LOHC technology. For example, in practical applications, a quantity of hydrogen may be required, corresponding to partial dehydrogenation.^{47–49} Moreover, in the technical process, partially loading the LOHC system can be advantageous to avoid harsher reaction conditions. By lowering the operating temperature and thus reducing the energy required for heating, the overall process efficiency can be increased. 21, 26, 27, 50 Both experimental results and thermodynamic analyses showed that reducing temperature, in combination with the use of lower pressures, selecting suitable catalysts, and considering partially loaded species, are key factors for an efficient and sustainable LOHC process.

Summary and Outlook

In this study, catalytic hydrogen loading and release of the LOHC-system benzyltoluene (H0-BT)/ perhydro benzyltoluene (H12-BT) using platinum on metal oxide catalysts was investigated. The results showed that the prepared catalysts consisting of platinum on titania, which had been optimized for the dehydrogenation of H18-DBT, are suitable for hydrogenation and dehydrogenation of the attractive LOHC system HX-BT and thus, present potential for the application within the whole H₂ storage cycle. Remarkably, the catalysts S_{0.1%}-Pt_{0.3%}/TiO₂ and Pt_{0.3%}/TiO₂ are characterized by high productivity in the dehydrogenation of H12-BT combined with suppression of the undesired formation of methyl fluorene, which was detected as side product when using the commercial benchmark catalyst S_{0.1%}-Pt_{0.3%}/Al₂O₃. Comparison of these catalysts in the hydrogenation of H0-BT demonstrated that S-Pt/TiO₂ is as well suited for hydrogenation as the benchmark catalyst. An even higher productivity for hydrogen loading can be reached using the Pt/TiO₂ catalyst without sulfur modification. Comparing the studied titania- and alumina-supported catalysts, the differences in side product formation during dehydrogenation might be attributed to the acidity of the support and strong metal support interactions (SMSI) influencing morphology and electronic properties of the catalyst. Further investigations, including advanced analysis techniques, can be used to investigate the

interactions for the applied catalysts and their dynamics under different conditions.

Analyses on the influence of the reaction conditions on catalytic dehydrogenation showed that both an increase in temperature and a reduction of total pressure enhances hydrogen release. Based on the conducted systematic investigation of pressure influence, further optimizations of the LOHC process can be realized. For instance, the results illustrate great potential for improving energy efficiency of the LOHC process by carrying out dehydrogenation at lower temperatures and reduced pressure. Integration with electrochemical hydrogen compression can be beneficial to reduce the pressure in the dehydrogenation unit while at the same time obtaining compressed and purified hydrogen.

Furthermore, the investigated catalysts were successfully reused in respective hydrogenation and dehydrogenation runs without drastic decline of productivity. Minor deactivation was mainly associated with deposition of organic species during dehydrogenation. As promising regeneration step, an optimized heat treatment of the spent catalyst was identified.

Following the studies on catalytic hydrogenation or dehydrogenation, the cycle of hydrogenation and consecutive dehydrogenation was carried out to simulate the use of the optimized catalyst during consecutive hydrogen loading and release as required during real application of the LOHC technology. In this case, the switch from hydrogen loading to release was enabled by adjusting the pressure while using the same reactor and $Pt_{0.3\%}/TiO_2$ catalyst, which presents an easily feasible method for the LOHC technology. In further studies, an increased number of cycles can be tested to continue these investigations.

Finally, to gain further insights into loading and unloading of the LOHC system, the experimental data was compared to calculated data on thermodynamic equilibrium of hydrogenation/dehydrogenation. Here, a good agreement between the experimentally obtained reaction mixture and the calculated equilibrium composition was found. Experimental and thermodynamic data both confirmed the potential for optimization of the catalytic hydrogenation-dehydrogenation-process by combining temperature reduction and pressure adjustment while considering partially hydrogenated states as well. These obtained results can be utilized to accordingly adapt the conditions for various applications of the LOHC technology for storage and transport of hydrogen in the most efficient and sustainable way.

Acknowledgments

The authors acknowledge the funding by the German Federal Ministry of Research, Technology and Space (BMFTR) and the Ministry of Economic Affairs, Industry, Climate Action and Energy of the State of North Rhine-Westphalia through the project HC-H2.

Associated References

- D. Teichmann, W. Arlt, P. Wasserscheid, R. Freymann, A future energy supply based on Liquid Organic Hydrogen Carriers (LOHC). *Energy Environ. Sci.* 4, 2767–2773 (2011), DOI: 10.1039/c1ee01454d.
- 2. M. Markiewicz, Y. Q. Zhang, A. Bösmann, N. Brückner, J. Thöming, P. Wasserscheid, S. Stolte, Environmental and health impact assessment of Liquid Organic Hydrogen Carrier (LOHC) systems challenges and preliminary results. *Energy Environ. Sci.* **8**, 1035–1045 (2015), DOI: 10.1039/C4EE03528C.
- 3. J. Oh, Y. Jo, T. W. Kim, H. B. Bathula, S. Yang, J. H. Baik, Y.-W. Suh, Highly efficient and robust Pt ensembles on mesoporous alumina for reversible H₂ charge and release of commercial benzyltoluene molecules. *Appl. Catal.*, *B.* **305**, 121061 (2022), DOI: 10.1016/j.apcatb.2022.121061.
- 4. T. Rüde, S. Dürr, P. Preuster, M. Wolf, P. Wasserscheid, Benzyltoluene/perhydro benzyltoluene pushing the performance limits of pure hydrocarbon liquid organic hydrogen carrier (LOHC) systems. *Sustainable Energy Fuels*. **6**, 1541–1553 (2022), DOI: 10.1039/D1SE01767E.

- 5. A. Leinweber, K. Müller, Hydrogenation of the Liquid Organic Hydrogen Carrier Compound Monobenzyl Toluene: Reaction Pathway and Kinetic Effects. *Energy Technol.* **6**, 513–520 (2018), DOI: 10.1002/ente.201700376.
- 6. S. P. Verevkin, S. V. Vostrikov, A. Leinweber, P. Wasserscheid, K. Müller, Thermochemical properties of benzyltoluenes and their hydro- and perhydro-derivatives as key components of a liquid organic hydrogen carrier system. *Fuel.* **335**, 126618 (2023), DOI: 10.1016/j.fuel.2022.126618.
- 7. S. Mrusek, P. Preuster, K. Müller, A. Bösmann, P. Wasserscheid, Pressurized hydrogen from charged liquid organic hydrogen carrier systems by electrochemical hydrogen compression. *Int. J. Hydrogen Energy.* **7**, 15624–15634 (2021), DOI: 10.1016/j.ijhydene.2021.02.021.
- 8. J. Henseler, T. Schärfe, J. Steffen, A. Görling, M. Geißelbrecht, P. Wasserscheid, Detailed analysis of coke precursor formation in catalytic perhydro benzyltoluene dehydrogenation processes. *Fuel.* **398**, 135500 (2025), DOI: 10.1016/j.fuel.2025.135500.
- 9. P. M. Modisha, D. Bessarabov, Stress tolerance assessment of dibenzyltoluene-based liquid organic hydrogen carriers. *Sustainable Energy Fuels.* **50**, 74 (2020), DOI: 10.1039/D0SE00625D.
- 10. M. Kerscher, J. H. Jander, J. Cui, P. Wasserscheid, M. H. Rausch, T. M. Koller, A. P. Fröba, Thermophysical properties of the liquid organic hydrogen carrier system based on diphenylmethane with the byproducts fluorene or perhydrofluorene. *Int. J. Hydrogen Energy.* **48**, 29651–29662 (2023), DOI: 10.1016/j.ijhydene.2023.04.103.
- 11. H. Jorschick, P. Preuster, S. Dürr, A. Seidel, K. Müller, A. Bösmann, P. Wasserscheid, Hydrogen storage using a hot pressure swing reactor. *Energy Environ. Sci.* **10**, 1652–1659 (2017), DOI: 10.1039/C7EE00476A.
- 12. L. Shi, S. Qi, J. Qu, T. Che, C. Yi, B. Yang, Integration of hydrogenation and dehydrogenation based on dibenzyltoluene as liquid organic hydrogen energy carrier. *Int. J. Hydrogen Energy.* **44**, 5345–5354 (2019), DOI: 10.1016/j.ijhydene.2018.09.083.
- 13. B. Bong, C. Mebrahtu, D. Jurado, A. Bösmann, P. Wasserscheid, R. Palkovits, Hydrogen Loading and Release Potential of the LOHC System Benzyltoluene/Perhydro Benzyltoluene over S-Pt/TiO₂ Catalyst. ACS Eng. Au. 4, 359–367 (2024), DOI: 10.1021/acsengineeringau.4c00003.
- 14. B. Bong, W. A. Kopp, T. Nevolianis, C. Mebrahtu, K. Leonhard, R. Palkovits, Reaction Equilibria in the Hydrogen Loading and Release of the LOHC System Benzyltoluene/Perhydro Benzyltoluene. *Chem. Eng. Technol.* 48, 1–12 (2025), DOI: 10.1002/ceat.12002.
- 15. X. Chen, C. H. Gierlich, S. Schötz, D. Blaumeiser, T. Bauer, J. Libuda, R. Palkovits, Hydrogen Production Based on Liquid Organic Hydrogen Carriers through Sulfur Doped Platinum Catalysts Supported on TiO₂. *ACS Sustainable Chem. Eng.* **9**, 6561–6573 (2021), DOI: 10.1021/acssuschemeng.0c09048.
- 16. B. Bong, doctoral dissertation, *Heterogene Katalysatoren für die Hydrierung von Benzyltoluol und Dehydrierung von Perhydro-Benzyltoluol zur chemischen Wasserstoffspeicherung*, RWTH Aachen University (2025).
- 17. F. Auer, D. Blaumeiser, T. Bauer, A. Bösmann, N. Szesni, J. Libuda, P. Wasserscheid, Boosting the activity of hydrogen release from liquid organic hydrogen carrier systems by sulfur-additives to Pt on alumina catalysts. *Catal. Sci. Technol.* 9, 3537–3547 (2019), DOI: 10.1039/C9CY00817A.
- 18. M. Geißelbrecht, S. Mrusek, K. Müller, P. Preuster, A. Bösmann, P. Wasserscheid, Highly efficient, low-temperature hydrogen release from perhydro-benzyltoluene using reactive distillation. *Energy Environ. Sci.* **13**, 3119–3128 (2020), DOI: 10.1039/D0EE01155J.
- 19. B.-J. Hsieh, M.-C. Tsai, C.-J. Pan, W.-N. Su, J. Rick, H.-L. Chou, J.-F. Lee, B.-J. Hwang, Tuning metal support interactions enhances the activity and durability of TiO₂-supported Pt nanocatalysts. *Electrochim. Acta.* **224**, 452–459 (2017), DOI: 10.1016/j.electacta.2016.12.020.

- 20. S. Zhang, P. N. Plessow, J. J. Willis, S. Dai, M. Xu, G. W. Graham, M. Cargnello, F. Abild-Pedersen, X. Pan, Dynamical Observation and Detailed Description of Catalysts under Strong Metal-Support Interaction. *Nano Lett.* **16**, 4528–4534 (2016), DOI: 10.1021/acs.nanolett.6b01769.
- 21. S. Biswas, K. Moreno Sader, W. H. Green, Perspective on Decarbonizing Long-Haul Trucks Using Onboard Dehydrogenation of Liquid Organic Hydrogen Carriers. *Energy Fuels*. **37**, 17003–17012 (2023), DOI: 10.1021/acs.energyfuels.3c01919.
- 22. D. Zakgeym, J. D. Hofmann, L. A. Maurer, F. Auer, K. Müller, M. Wolf, P. Wasserscheid, Better through oxygen functionality? The benzophenone/dicyclohexylmethanol LOHC-system. *Sustainable Energy Fuels*, 1213–1222 (2023), DOI: 10.1039/D2SE01750D.
- 23. I. S. Lim, Y. Jeong, Y. Kwak *et al.*, Maximizing clean hydrogen release from perhydro-benzyltoluene: Energy-efficient scale-up strategies and techno-economic analyses. *Chem. Eng. J.* **478**, 147296 (2023), DOI: 10.1016/j.cej.2023.147296.
- 24. H. Jeong, T. W. Kim, M. Kim, G. B. Han, B. Jeong, Y.-W. Suh, Mesoporous Acidic SiO₂-Al₂O₃ Support Boosts Nickel Hydrogenation Catalysis for H₂ Storage in Aromatic LOHC Compounds. *ACS Sustainable Chem. Eng.* **10**, 15550–15563 (2022), DOI: 10.1021/acssuschemeng.2c04978.
- 25. Clariant International Ltd, *EleMax® Series*, *Catalysts for storage of hydrogen from renewable sources via liquid organic hydrogen carriers (LOHC)* (available at https://www.clariant.com/de/Solutions/Products/2019/05/21/15/19/EleMax-Series).
- 26. R. Dickson, M. S. Akhtar, A. Abbas, E. D. Park, J. Liu, Global transportation of green hydrogen via liquid carriers: economic and environmental sustainability analysis, policy implications, and future directions. *Green Chem.* **24**, 8484–8493 (2022), DOI: 10.1039/D2GC02079C.
- 27. C. Wulf, P. Zapp, Assessment of system variations for hydrogen transport by liquid organic hydrogen carriers. *Int. J. Hydrogen Energy.* **43**, 11884–11895 (2018), DOI: 10.1016/j.ijhydene.2018.01.198.
- 28. K. Müller, T. Skeledzic, P. Wasserscheid, Strategies for Low-Temperature Liquid Organic Hydrogen Carrier Dehydrogenation. *Energy Fuels.* **35**, 10929–10936 (2021), DOI: 10.1021/acs.energyfuels.1c01170.
- 29. Y. Kwak, J. Kirk, S. Moon *et al.*, Hydrogen production from homocyclic liquid organic hydrogen carriers (LOHCs): Benchmarking studies and energy-economic analyses. *Energy Convers. Manage.* **239**, 114124 (2021), DOI: 10.1016/j.enconman.2021.114124.
- 30. P. M. Modisha, C. N. M. Ouma, R. Garidzirai, P. Wasserscheid, D. Bessarabov, The Prospect of Hydrogen Storage Using Liquid Organic Hydrogen Carriers. *Energy Fuels.* **33**, 2778–2796 (2019), DOI: 10.1021/acs.energyfuels.9b00296.
- 31. S. Kiermaier, D. Lehmann, A. Bösmann, P. Wasserscheid, Dehydrogenation of perhydro-N-ethylcarbazole under reduced total pressure. *Int. J. Hydrogen Energy.* **46**, 15660–15670 (2021), DOI: 10.1016/j.ijhydene.2021.02.128.
- 32. M. Amende, A. Kaftan, P. Bachmann, R. Brehmer, P. Preuster, M. Koch, P. Wasserscheid, J. Libuda, Regeneration of LOHC dehydrogenation catalysts: In-situ IR spectroscopy on single crystals, model catalysts, and real catalysts from UHV to near ambient pressure. *Appl. Surf. Sci.* **360**, 671–683 (2016), DOI: 10.1016/j.apsusc.2015.11.045.
- 33. L. Shi, Y. Zhou, S. Qi, K. J. Smith, X. Tan, J. Yan, C. Yi, Pt Catalysts Supported on H_2 and O_2 Plasma-Treated Al_2O_3 for Hydrogenation and Dehydrogenation of the Liquid Organic Hydrogen Carrier Pair Dibenzyltoluene and Perhydrodibenzyltoluene. *ACS Catal.* **10**, 10661–10671 (2020), DOI: 10.1021/acscatal.0c03091.
- 34. P. Modisha, P. Gqogqa, R. Garidzirai, C. N. Ouma, D. Bessarabov, Evaluation of catalyst activity for release of hydrogen from liquid organic hydrogen carriers. *Int. J. Hydrogen Energy.* **44**, 21926–21935 (2019), DOI: 10.1016/j.ijhydene.2019.06.212.
- 35. A. J. Martín, S. Mitchell, C. Mondelli, S. Jaydev, J. Pérez-Ramírez, Unifying views on catalyst deactivation. *Nat. Catal.* **5**, 854–866 (2022), DOI: 10.1038/s41929-022-00842-y.
- 36. G. Ertl, H. Knözinger, J. Weitkamp, Eds., *Handbook of heterogeneous catalysis* (Wiley-VCH, Weinheim, 2008).
- 37. M. Argyle, C. Bartholomew, Heterogeneous Catalyst Deactivation and Regeneration: A Review. *Catalysts.* **5**, 145–269 (2015), DOI: 10.3390/catal5010145.

- 38. M. Guisnet, P. Magnoux, Organic chemistry of coke formation. *Appl. Catal., A.* **212**, 83–96 (2001), DOI: 10.1016/S0926-860X(00)00845-0.
- 39. P. M. Modisha, J. H. Jordaan, A. Bösmann, P. Wasserscheid, D. Bessarabov, Analysis of reaction mixtures of perhydro-dibenzyltoluene using two-dimensional gas chromatography and single quadrupole gas chromatography. *Int. J. Hydrogen Energy.* **43**, 5620–5636 (2018), DOI: 10.1016/j.ijhydene.2018.02.005.
- 40. H. Jorschick, M. Geißelbrecht, M. Eßl, P. Preuster, A. Bösmann, P. Wasserscheid, Benzyltoluene/dibenzyltoluene-based mixtures as suitable liquid organic hydrogen carrier systems for low temperature applications. *Int. J. Hydrogen Energy.* **45**, 14897–14906 (2020), DOI: 10.1016/j.ijhydene.2020.03.210.
- 41. F. Auer, A. Hupfer, A. Bösmann, N. Szesni, P. Wasserscheid, Influence of the nanoparticle size on hydrogen release and side product formation in liquid organic hydrogen carrier systems with supported platinum catalysts. *Catal. Sci. Technol.* **120**, 109620 (2020), DOI: 10.1039/D0CY01173H.
- 42. K. I. Hadjiivanov, D. G. Klissurski, Surface chemistry of titania (anatase) and titania-supported catalysts. *Chem. Soc. Rev.* **25**, 61 (1996), DOI: 10.1039/CS9962500061.
- 43. M. Monai, K. Jenkinson, A. E. M. Melcherts *et al.*, Restructuring of titanium oxide overlayers over nickel nanoparticles during catalysis. *Science*. **380**, 644–651 (2023), DOI: 10.1126/science.adf6984.
- 44. H. Frey, A. Beck, X. Huang, J. A. van Bokhoven, M. G. Willinger, Dynamic interplay between metal nanoparticles and oxide support under redox conditions. *Science*. **376**, 982–987 (2022), DOI: 10.1126/science.abm3371.
- 45. A. Beck, X. Huang, L. Artiglia, M. Zabilskiy, X. Wang, P. Rzepka, D. Palagin, M.-G. Willinger, J. A. van Bokhoven, The dynamics of overlayer formation on catalyst nanoparticles and strong metal-support interaction. *Nat. Commun.* **11**, 3220 (2020), DOI: 10.1038/s41467-020-17070-2.
- 46. S. Liu, H. Qi, J. Zhou *et al.*, Encapsulation of Platinum by Titania under an Oxidative Atmosphere: Contrary to Classical Strong Metal–Support Interactions. *ACS Catal.* **11**, 6081–6090 (2021), DOI: 10.1021/acscatal.1c01347.
- 47. L. Li, P. Vellayani Aravind, T. Woudstra, M. van den Broek, Assessing the waste heat recovery potential of liquid organic hydrogen carrier chains. *Energy Convers. Manage.* **276**, 116555 (2023), DOI: 10.1016/j.enconman.2022.116555.
- 48. S. P. Verevkin, A. A. Samarov, S. V. Vostrikov, P. Wasserscheid, K. Müller, Comprehensive Thermodynamic Study of Alkyl-Cyclohexanes as Liquid Organic Hydrogen Carriers Motifs. *Hydrogen.* **4**, 42–59 (2023), DOI: 10.3390/hydrogen4010004.
- 49. D. Zakgeym, T. Engl, Y. Mahayni, K. Müller, M. Wolf, P. Wasserscheid, Development of an efficient Pt/SiO₂ catalyst for the transfer hydrogenation from perhydro-dibenzyltoluene to acetone. *Appl. Catal.*, *A*. **639**, 118644 (2022), DOI: 10.1016/j.apcata.2022.118644.
- 50. M. M. Distel, J. M. Margutti, J. Obermeier, A. Nuß, I. Baumeister, M. Hritsyshyna, A. Weiß, M. Neubert, Large-Scale H₂ Storage and Transport with Liquid Organic Hydrogen Carrier Technology: Insights into Current Project Developments and the Future Outlook. *Energy Technol.* (2024), DOI: 10.1002/ente.202301042.

Advanced Catalyst and Reactor Engineering for Efficient Hydrogen Release from Perhydro-Benzyltoluene

Elisabeth Herzinger, Hannah Park, Jennifer Weimann, Jona Berger, Ozan Kırlangıçoğlu, Jakob Biesinger, Moritz Wolf

Karlsruhe Institute of Technology (KIT), Karlsruhe/Germany

Abstract

Hydrogen storage via liquid organic hydrogen carriers (LOHCs) such as perhydrobenzyltoluene (H12-BT) is a promising route for safe, reversible, and compact hydrogen storage under ambient conditions. Recent developments in both catalyst design and reactor engineering have significantly enhanced dehydrogenation performance, a critical step for hydrogen release. In this study the performance of bimetallic platinum-rhenium (PtRe) catalysts² supported on Al_2O_3 was investigated and optimised for dehydrogenation in a continuous three phase slurry reactor. The slurry reactor represents a promising alternative to conventional fixed-bed reactor designs. Superior heat management and rapid separation of released hydrogen mitigate the dewetting effects commonly encountered in endothermic LOHC dehydrogenation processes.

Modification of the $PtRe/Al_2O_3$ catalysts focussed on the influence of support morphology, surface chemistry, and synthesis conditions. By tailoring synthesis procedures—including support calcination parameters and the order of metal precursor during sequential impregnation—and analysing the resulting catalysts by ICP-AES, XRD, CO-pulse chemisorption, NH_3 -TPD, TEM, and N_2 physisorption, observed effects on catalyst productivity and dehydrogenation activity were characterised. Additional selective sulphur poisoning resulted in improved by-product suppression. The findings provide critical insight into the optimisation of metal-support interactions and preparation methods to enhance hydrogen release kinetics and catalyst lifetime.

The slurry reactor demonstrated stable long-term operation at elevated temperatures (330 °C) and pressures (4.7 barg), with high platinum-based productivity and low by-product formation. Operation parameters, such as stirrer speed, temperature, pressure, and feed rate, were systematically varied to optimise space-time-yield and degree of dehydrogenation. Kinetic analyses based on Arrhenius parameters were conducted to deepen mechanistic understanding. Catalyst and reactor performance were benchmarked using both commercial and custom-designed platinum-based catalysts, including S-poisoned Pt/Al₂O₃ and PtRe/Al₂O₃ formulations. Ultimately, the synergy between advanced Pt-based catalysts and optimised slurry reactor design enabled a significant enhancement in hydrogen release efficiency from H12-BT.

This study highlights a holistic approach to LOHC dehydrogenation by combining rational catalyst design with innovative reactor engineering. The integration of tailored PtRe catalysts and continuous slurry reactor operation establishes a robust framework for improving the viability and scalability of hydrogen storage technologies in real-world energy systems.

- 1. E. Herzinger, M. Wolf, Chem. Ing. Tech. 2024, 96, 65.
- 2. D. Strauch, P. Weiner, B. B. Sarma, A. Körner, E. Herzinger, P. Wolf, A. Zimina, A. Hutzler, D. E. Doronkin, J.-D. Grunwaldt P. Wasserscheid, M. Wolf, *Catal. Sci. Technol.* **2024**, *7*, 1775.

Light-assisted thermal catalysis for hydrogen storage in a "methanol economy"

Matthias Rehner, Katharina Blank, Junhao Huang, Jennifer Strunk

Technical University of Munich, Chair for Industrial Chemistry and Heterogeneous Catalysis, Garching, München, Germany

Abstract

As proposed by Nobel laureate G.A. Olah, methanol is a highly versatile hydrogen carrier and platform chemical that might form the foundation of a sustainable economy [1]. The heterogeneously catalyzed methanol synthesis is an established industrial process, known already for over a century. It requires elevated pressures, and the used high-pressure synthesis gas is commonly obtained from fossil resources. Within the scope of a sustainable economy, it is desirable to convert low-pressure CO₂-rich gases, for example derived from flue gases, with hydrogen from water electrolysis. Previous works have demonstrated that an additional irradiation of a reacting thermal heterogeneous catalyst at 20 bar increased methanol yield already at lower temperature [2].

Here, we studied systematically the influence of the reaction conditions on light-assisted methanol synthesis and methanol reforming at ambient pressure on a series of doped Cu/ZnO-based catalysts. Different from the observations at 20 bars, it was hardly possible to increase the yields of methanol with light, regardless of whether only visible, only UV, or both UV and visible light was used. Slightly increased methanol yields are only achievable under very limited sets of temperature, irradiation conditions, and synthesis gas compositions.

However, two reactions were significantly enhanced by light: Firstly, when irradiating the reacting catalysts with visible light in CO_2 : H_2 atmosphere, the reverse water gas shift reaction (RWGS) was dramatically enhanced compared to the steady state in the dark, such that the CO formation rate in some cases was improved by a factor of 10. Secondly, some Cu/ZnO-based catalysts proved to be exceptionally active in methanol decomposition, achieving ~90% conversion at relatively mild conditions.

In conclusion, the results highlight two potential applications of light-assisted thermal catalysis: (i) for a first-stage conversion of CO_2 to CO for follow-up processes such as methanol synthesis or the Fischer-Tropsch process, and (ii) for rapid methanol decomposition or steam reforming under mild conditions, when methanol is used a hydrogen storage molecule.

[1] G.A. Olah, A. Goeppert, G.K.S. Prakash, *Beyond Oil and Gas: The Methanol Economy*, 3. Edition, Wiley-VCH, Weinheim, 2018.

[2] B. Xie, R.J. Wong, T.H. Tian, M. Higham, E.K. Gibson, D. Decarolis, J. Callison, K.-F. Aguey-Zinsou, M. Bowker, R.A. Catlow, J. Scott, R. Amal, *Nature Commun.* **11** (2020) 1615.

CO₂ methanation as a strategy for green H₂ storage and distribution: experimental optimisation and process design

M. Tommasi¹, A. Gramegna^{1,2}, S. Romegialli^{1,2}, G. Ramis³, <u>I. Rossetti^{1,2}</u>

- ¹ Chemical Plants and Industrial Chemistry Group, Dip. Chimica, Università degli Studi di Milano and CNR-SCITEC, Milan, Italy.
- ² INSTM Unit Milano-Università, Dip. Chimica, Università degli Studi di Milano, Milan, Italy
- ³ Dip. DICCA, Università degli Studi di Genova and INSTM Unit-Genova, Genoa, Italy

Abstract

The aim of this work was to synthesise, characterise and test catalysts for CO₂ methanation with the final aim of deigning a CO₂ methanation plant offering a strategy for green H₂ storage and distribution.

Ni-based catalysts were prepared with different composition. The supports were Al_2O_3 , SiO_2 , ZSM5, CeO_2 , TiO_2 , ZrO_2 and MgO, with different Ni loadings (6%, 16%, 25%, 36%, 45% and 94%). The samples were synthesised using various procedures. Comparisons were also made on the same support from different manufacturers and with different specifications.

The catalysts were characterised using different techniques. BET, XRD, FT-IR, SEM EDS, DRS, XRD, Raman and *operando* DRIFTS. All the catalysts were first screened in an ambient pressure continuous plant and the products were analysed with an on-line GC. For each catalyst, CO₂ conversion and CH₄ selectivity were assessed over a temperature range from 200 to 550°C. The most promising samples were also tested at higher pressure and under widely variable reaction conditions.

The experiments confirmed the superior activity and selectivity of CeO₂ over the other supports tested, in particular achieving 86% conversion and 100% methane selectivity at 345°C ambient pressure.

The results allowed the sizing of a pilot and a commercial scale plant through Aspen Plus process simulator.

GR and IR are grateful to NextGenerationEU and to the Italian ministry MASE (ex MITE bando A) through the PNRR, Missione 2 Componente 2 investimento 3.5 measure funding the project "Stoccaggio e distribuzione di idrogeno attraverso una strategia "power-to-gas/gas-to-power" con cattura ed utilizzo completi del carbonio - Hydrogen storage and distribution through power-to-gas strategy, with full carbon capture and utilization".

The authors gratefully acknowledge the financial contribution of Tasks 8.2.3 and 8.4.1 of the Agritech National Research Center, funded from the European Union NextGenerationEU - PNRR – Missione 4 Componente 2, Investimento 1.4 – D.D. 1032 17/06/2022, CN00000022.

IR acknowledges Università degli Studi di Milano for support through the grant PSR 2021 - GSA - Linea 6 "One Health Action Hub: University Task Force for the resilience of territorial ecosystems".

A chemical and engineering analysis of the conversion of biomass to lactic acid using POMs under nitrogen atmosphere

Elisabeth Hundt ¹, Jan-Dominik Krueger ¹, Andreas Pawlig ¹, Leon Schidowski ¹, Ira Wirth ¹, Maximilian J. Poller ¹, Dorothea Voß ¹, Jakob Albert ¹

¹ Institute of Technical and Macromolecular Chemistry, University of Hamburg, Hamburg/Germany

Abstract

The rising growth of the world's population is leading to a greater need to utilise waste and to use sustainable processes. These processes serve to meet the increasing demand for platform chemicals such as lactic acid or formic acid, which are required to manufacture a wide range of products.

The BioValCat (Enhanced <u>Bio</u>mass <u>Val</u>orisation by Engineering of Polyoxometalate <u>Cat</u>alysts) project investigates the conversion of biomass by selective homogeneous catalysis into various platform chemicals, while avoiding the formation of unwanted by-products such as humins or carbon dioxide (Figure 1). Part of this project is the selective production of lactic acid under anaerobic conditions.

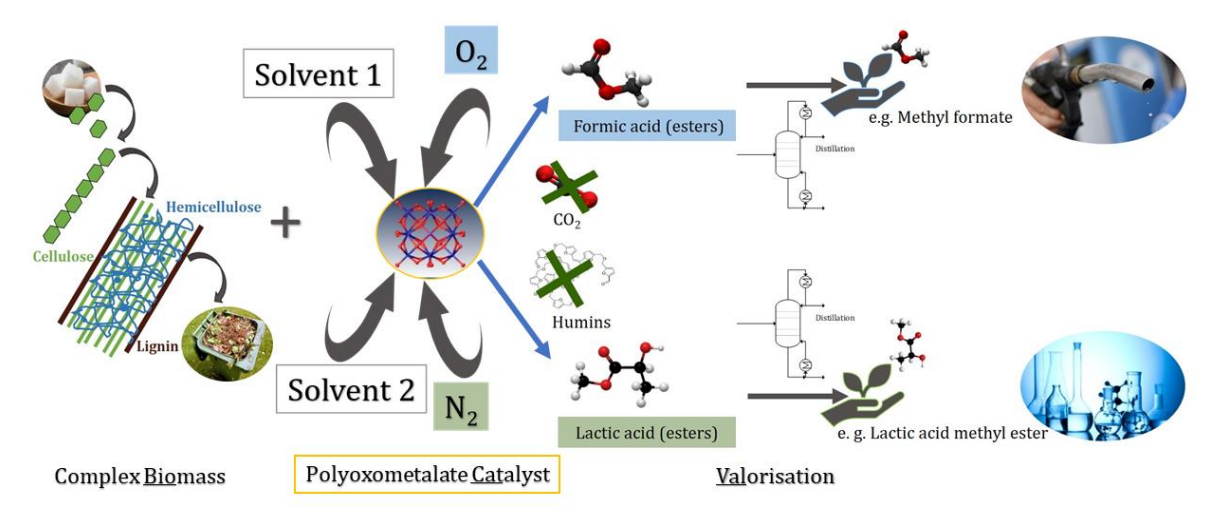


Figure 1: Conversion of different biomass to platform chemicals.

To this end, biomass is converted to lactic acid under anaerobic reaction conditions by polyoxometalate catalysts. Polyoxometalates (POMs), which are anionic molecular clusters of transition metals and oxo-ligands, are used as homogeneous catalysts. These POM catalysts are characterised by their high Brønsted acidity and redox activity. The process efficiency can be influenced by various reaction parameters like gas atmosphere, temperature, solvent or type of POM catalyst.

Our aim is to gain a deeper understanding of the influences of these factors on the reaction performance, such as humins.

Transforming wet biomass waste into sustainable methanol: Concept study of a competitive and mild process route

Phillip Nathrath¹, Fabian Kroll², David Karmann², Vera Haagen², Dennis Weber³, Tanja Franken³, Michael Geißelbrecht², Patrick Schühle^{1*}

- ¹ Friedrich-Alexander-Universität Erlangen-Nürnberg, Erlangen/Germany
- ² Forschungszentrum Jülich GmbH, Helmholtz Institute Erlangen-Nürnberg for Renewable Energy, Erlangen/Germany
- ³ Technical University Darmstadt, Darmstadt/Germany

Abstract

Methanol is a versatile chemical feedstock and a promising clean fuel alternative with vast market potential expected to grow in the future. To significantly reduce climate impact, efficient and economic methanol production from non-fossil feedstocks is urgently required. Biomass waste, especially agricultural, forestry, or industrial residues, presents significant potential as a feedstock. In our research, we developed a novel process route that could be a game changer for biomass-to-methanol conversion, as it operates under mild process conditions (pressures below 10 bar and temperatures around 200 °C) and reduces the need for prior biomass drying and intensive product purification. This route could complement future methanol synthesis or even outperform sustainable alternatives based on harsh gasification and expensive power-to-X technologies. The proposed concept can be divided in three steps: 1) Oxidation of wet biomass waste to formic acid, 2) Esterification of formic acid to methyl formate and 3) Hydrogenolysis of methyl formate to Methanol.

In this study, the previously unexplored pathway was simulated in Aspen Plus assessing possible operating scenarios and achievable methanol prices. Depending on the assumptions applied competitive methanol production costs between 0.69 and 2.31 € kg⁻¹ are feasible. While the first steps of biomass oxidation reassembles an already established process, that is demonstrated to deliver formic acid in the lower ton scale[1], the hydrogenolysis of methyl formate was investigated experimentally to support the simulation with valuable first hand data. Long-term stable continuous formation of methanol is demonstrated in high selectivity (>95 %) by applying novel inexpensive copper-based spinel catalysts. [2] Following the simulation results the novel concept yields a superior single-pass carbon efficiency of >80% compared to biomass gasification routes or even fossil methanol production. By integrating biomass valorisation with hydrogen and oxygen from water electrolysis, the need for fossil-based reactants is completely eliminated. Furthermore, a fully decentralized and autonomous system can be achieved expanding the application field of this technology. Since biomass typically accumulates in decentralized locations, the new process can be implemented close to these sources, minimizing feed transport distances and further reducing greenhouse gas emissions. Although still in the early stages of development, the new process opens up possibilities for the future, such as enabling agricultural cooperatives to locally produce methanol and use it as a drop-in fuel for their own consumption.

[1] OxFA GmbH, https://www.oxfa.eu/en/, accessed on 30.04.25

^[2] Haagen et al., Green Chem. 2023, 25 (6), 2338–2348.

NET-Fuels – Integrating negative emission technologies in biofuels production

M. Meiller¹, C. Groves¹, F. Lehner¹, C. Kick¹, R. Daschner¹, B. Kocacenk¹, A. Apfelbacher¹ N. Hagemann², D. Chiari³, A. Contin³, D. Marazza³, M. Proniewicz⁴, K. Petela⁴, A. Szlek ⁴ M. Vega-Paredes⁵, D. Molognoni⁵, E. Borràs

¹Fraunhofer-Institut für Umwelt-, Sicherheits- und Energietechnik, UMSICHT, Sulzbach-Rosenberg

²Ithaka Institute, Goldbach

³Alma Mater Studiorum – Università di Bologna, Ravenna Campus

⁴Silesian University of Technology, Gliwice

⁵ Leitat, Terrassa

Abstract

NET-Fuels is a pioneering EU-funded research and innovation project that demonstrates a complete lab-scale process chain for climate-positive fuel production. The system integrates multiple technologies - each of which can also operate independently in diverse contexts - to produce valuable outputs such as bio-oil, hydrogen, synthetic methane, and certified biochar starting with biogenic residues. At the core of NET-Fuels is the modular combination of Thermocatalytic Reforming (TCR®), non-oxidative use of biochar to achieve Biochar Carbon Storage (BCS), and oxyfuel combustion. Fraunhofer UMSICHT is responsible for developing and testing the pyrolysis and oxyfuel subsystems, converting biogenic residues into syngas, stable biochar, and oil. Hydrogen is separated from the syngas via Vacuum Pressure Swing Adsorption (VPSA), while the remaining tail gas is used in oxyfuel combustion to recover energy and capture CO₂ with a purity of 97%. The oxygen required for combustion is supplied by Leitat's Bioelectrochemical Methanation (BEM) system, which simultaneously produces synthetic methane from the captured CO2 - closing the carbon loop. The TCR®-oil can be upgraded to fully equivalent substitutes for gasoline and diesel—compliant with European standards EN228 and EN590, which has been established in previous research projects. The technical process integration is ongoing; thus, the paper shows preliminary results.

Introduction

The EU-funded NET-Fuels project develops a novel, integrated approach to renewable syngas and hydrogen production, while simultaneously enabling negative emissions through advanced carbon management strategies. By combining biomass pyrolysis (TCR®), nonoxidative use of biochar for biochar carbon storage, and Bioenergy with Carbon Capture and Storage or Utilization (BECCS, BECCU) via oxyfuel combustion, the project addresses both energy transition and climate mitigation goals and aims to take pyrogenic carbon capture and storage (PyCCS[1]) to the next stage. Within this framework, Fraunhofer UMSICHT focuses on the development and optimization of the pyrolysis and oxyfuel subsystems. Biogenic residues are thermochemically converted via Thermocatalytic Reforming (TCR®) into a volatile gas phase, solid biochar and TCR®-oil. The biochar, containing stable carbon compounds, is either sequestered or valorised in long-term applications, leading to certified carbon removal. The volatile fraction is upgraded by thermal treatment within the TCR®-unit to high-quality syngas, from which hydrogen is extracted using Vacuum Pressure Swing Adsorption (VPSA). The remaining tail gas is utilized in the oxyfuel process, ensuring efficient energy recovery and CO₂ capture. The thermally stable oil is used in refineries. A central innovation of NET-Fuels is the integration of oxyfuel combustion to utilize syngas and generate a concentrated CO₂ stream suitable for capture and storage. The oxygen required for this process is provided by Leitat's Bioelectrochemical Methanation (BEM) system, which produces oxygen as a byproduct while converting captured CO₂ into synthetic methane. This coupling not only enhances overall system carbon efficiency but also creates a circular carbon economy by linking carbon capture (biochar) with utilization (synthetic methane). The modular and

decentralized design of the NET-Fuels system allows for flexible deployment both in rural and industrial regions. The project thus contributes to the development of regional value chains and supports the implementation of the European Green Deal and hydrogen strategy. This publication will showcase NET-Fuels approach to system integration, process development, and environmental assessment, while highlighting the broader impact of NET-Fuels as a platform technology for a climate-positive energy future. Although full system integration is still underway, preliminary results already highlight the potential of NET-Fuels as a flexible, decentralized platform for regional deployment.

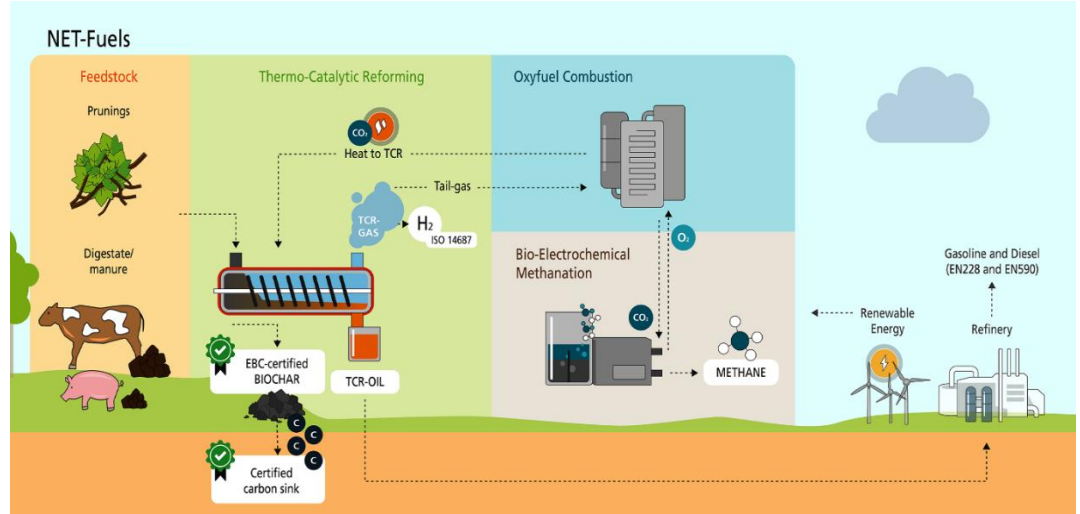


Figure 1: NET-Fuels in a nutshell. TCR® = thermo-catalytic reforming (pyrolysis technology). EBC = European Biochar Certificate [2].

TCR® Process and TCR®-Oil as potential drop-in fuel in refineries

Thermo-Catalytic Reforming (TCR®) is a pyrolysis-based process developed by Fraunhofer UMSICHT to convert waste into biofuels and chemicals. It combines intermediate pyrolysis at moderate temperatures with high-temperature catalytic reforming, producing syngas and organic vapors with enhanced properties.

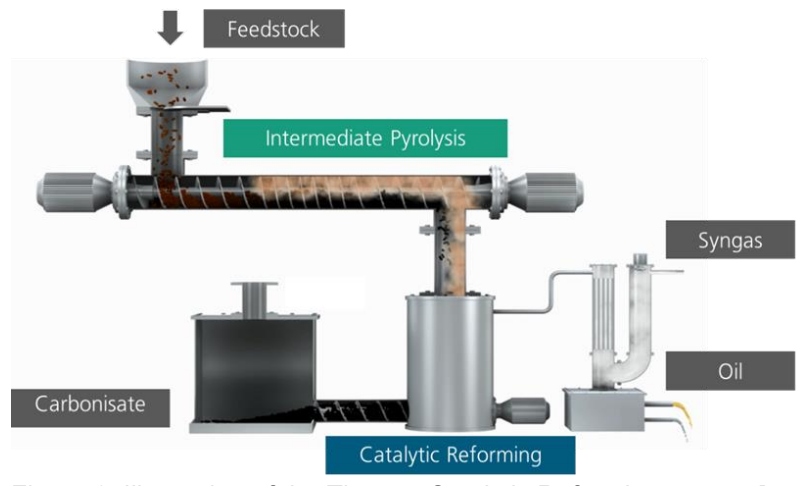


Figure 2: Illustration of the Thermo-Catalytic Reforming reactor [own illustration]

The intermediate pyrolysis step is operated at 400-500 °C in an auger reactor with a residence time between 5 and 15 minutes of the solid material. Biomass is converted to biochar and collected in the reforming reactor (moving bed reactor). Finally, the reforming treatment is performed using biochar as a moving bed reactor through which the intermediate pyrolysis

vapors flow, thus creating a catalytic effect in all products and improving their physicochemical properties [3, 4]. The temperature of the post reformer is between 500 and 700°C. The higher post reformer temperature forms a higher yield of syngas. The upgraded vapors are then condensed and make three different products, which are a bio-oil fraction (6-12 wt%), an aqueous phase (18-26 wt%), and syngas fraction (19-45 wt%).

The unique selling point of the TCR® approach is the quality of the generated conversion products. The main compounds of syngas are hydrogen (up to 45 vol%) and then carbon dioxide (35 vol% maximum), carbon monoxide (25 vol% maximum), methane and some other hydrocarbons. In the chapters **Gas cleaning** and **Oxyfuel combustion** the further utilization of the syngas is discussed. The biochar from TCR® can be conform with the EU fertilizing product regulation (EU 2019/1009, depending on feedstock selection) with the expected requirements for carbon removal certification according to EU 2024/3012. In chapter **Biochar quality and certification** more details about biochar quality and utilization in the context of NET-Fuels is discussed.

Especially the produced **biooil** exhibits certain properties that were previously unknown in this form from the slow to intermediate pyrolysis of biomass. Bio-oils derived from the Thermo-Catalytic Reforming (TCR®) exhibit chemical and physical properties that significantly differ from conventional petroleum-derived crude oils. These differences are primarily associated with higher oxygen contents and high viscosity. Consequently, an upgrading step is crucial to transform raw bio-oils. Among the available upgrading technologies, catalytic hydrotreatment is a well-established method in fossil oil refineries [5]. This process enables the removal of heteroatoms, the stabilization of reactive components, and the conversion of oxygenates into hydrocarbons with fuel-like properties.[6]

The catalytic hydrogenation of bio-oils represents a decisive technological step to achieve specifications comparable to established fuel standards such as EN 228 (gasoline) and EN 590 (diesel). In practice, the hydrotreatment approach has proven its particularly effectiveness. In an initial stabilization stage under moderate conditions, the most reactive oxygenated species are selectively converted, thus suppressing undesirable side reactions such as coking and polymerization. A subsequent deep hydrodeoxygenation stage, typically operated under higher pressures and temperatures, facilitates the comprehensive removal of residual oxygen, nitrogen, and sulfur while simultaneously saturating unsaturated bonds. Experimental investigations with TCR®-derived oils have demonstrated that fractions can be obtained whose distillation profiles and calorific values fall within the specification ranges of conventional gasoline and diesel products. [7]



Figure 3: Visual comparison of raw bio-oil, hydrotreated oil and upgraded fuel fractions

These results underscore the potential of hydrotreated bio-oils not merely as blending components but as genuine drop-in fuels, capable of substituting fossil-derived refinery streams without requiring substantial modifications to the existing infrastructure. [7] In summary, the upgrading of TCR® oils through catalytic hydrotreatment and distillation provides a robust route to the production of norm-compliant fuels. Consequently, the technology holds strong potential to contribute to the decarbonization of the transportation fuel sector.

Biochar quality & certification

In the context of NET-Fuels, negative emissions are generated by the non-oxidative use of the produced biochar. NET-Fuels focuses on the use of biogenic residues from forestry and agriculture, and in turn the use of biochar is researched in these industries, i.e. as a soil amendment and a carrier material for fertilizers. As a prerequisite of any type of biochar application, product safety and compliance with the application-specific regulations must be ensured. In an additional step, carbon sink certificate (also referred to as carbon removal certificate) can only be granted, if the quality of the biochar fulfils an accepted standard and the non-oxidative use of biochar is confirmed.

Biochar product regulation, quality assurance and certification

A prerequisite for any use of biochar in soil is compliance with the relevant legal framework, whereby there are parallel national and EU regulations. Examples of national regulations include the Fertilizer Ordinance (Düngemittelverordnung) in Germany, which only permits biochar from wood with at least 80% C, or the Danish Ordinance on the use of waste for agricultural purposes (Bekendt-gørelse om anvendelse af affald til jordbrugsformål, BEK nr 1001, 27/06/2018) that allows pyrolysis as a treatment for digestate, manure and other defined secondary biomass prior to soil application. At the EU-level, the EU 2019/1009 ordinance allows the use of a broad range of biogenic residues in fertilizing products. On top, the European Biochar Certificate (EBC, REF) [8] is as system for third-party certified quality assurance in biochar production that was established in 2014 and is a generally accepted industry standard for biochar production with distinct certification classes for use in animal feed, soils, and materials. Key aspects of EBC include to sustainable biochar production with regard to feedstock provision and efficient use of energy generated by biochar production as well as the regular sampling [9] and analysis of biochar to provide representative data on elemental composition and pollutant content [10]. NET-Fuels biochars have been produced from digestate, hops extraction residue, vine pruning residues, and forest wood analyzed according to EBC Guidelines (Table 1).

The parameters of the biochar samples are within the expected range for the respective feedstock. Molar ratio of hydrogen to organic carbon is well below 0.4 (<0.7 is the threshold according to EBC and EU 2019/1009, 0.4 is the threshold for highest persistence class in carbon sink certification REF). This demonstrates the stability and the reliability of the TCR® process and enables carbon sink certification.

Of all samples, digestate biochar has the lowest carbon and the highest ash content, as anaerobic digestion has already enriched mineral matter in the feedstock. It also has the highest content of potentially toxic elements (PTE, commonly referred to as "heavy metals"). This aligns with a review paper on manure and digestate biochar, which suggests co-pyrolysis of digestate with other biomass to reduce the biochar's ash content [11]. The exceedances of the limit values for copper and zinc content would currently prevent EBC certification for agricultural use (certification class EBC-Agro). Since these two elements are considered PTE but also represent essential nutrients, NET-Fuels partner ITHKAKA proposes an adjustment of these limit values.

The EU Fertilizer Products Regulation does not specify any PTE limits for biochar as a feedstock for fertilizer production; these only apply to the final product (e.g. biochar-compost mixture, biochar with mineral fertilizers, pure biochar), so that the increased Zn and Cu contents do not per se prevent marketing under EU regulations. Greenhouse trials have already been set up to compare the agronomic impact and to prove nutrient release by biochar (potassium, phosphorous).

Carbon sink certification

The goal of carbon sink certification, also referred to as carbon removal certification aims at precise quantification and third party verification of the amount of atmospheric carbon (CO2-equivalents) stored in the biochar. Currently, there are several voluntary biochar C-sink standards are available (EBC, Global Artisan C-Sink, Verra VM0044, Puro.earth [12, 13, 14,

15]) available and operational, suitable for various production scales and markets. At the same time, the Europeans Carbon Removal Certification Framework (CRCF) is approaching operational readiness, with the EU 2024/3012 already being implemented and methodologies for biochar certification expected to be amended soon—paving the way for formal recognition and future issuance of EU-certified biochar carbon units. Therefore, certified removals—including biochar—as of today cannot be used within the ETS for compliance purposes. They can only contribute to Member States' climate objectives or Nationally Determined Contributions (NDCs). However, it is likely that CRCF—including biochar will be merged into the EU ETS in the near future. The Commission is mandated to evaluate integration by 2026, and both experts and industry stakeholders are advocating for a phased, well-regulated inclusion of CRCF-certified permanent removals into the ETS.

Biochar C-sink certification works by tracking the biomass (ensuring its sustainability), quantifying the carbon locked in biochar and proxies for its persistence like molar H/C ratio and others [16], data verification through independent auditors, and issuing certificates that can be traded as carbon removal credits.

Regarding biomass, only eligible biomass can be used where no competition with food production or deforestation appears. The emissions related to the whole production chain of the biochar (calculated via LCA) must be compensated with C-sinks prior to issuing the certificate to ensure net carbon removal.

Table 1: Properties of TCR® biochars Quantified following the analytical guidelines of the European Biochar Certificate. Limit values are shown for the EBC-Agro certification class. Limit exceedances are highlighted in yellow.

		Limit values	Digestate	Hops extraction residue	Vine pruning	Calamity wood
Bulk density < 3 mm			734	570	515	574
Water holding capacity (WHC) <	2 mm	†	15.6			68
2 1 11						
Ash content (550°C)	Mass%	1	48	26.4	18.7	1.7
Total carbon	Mass%	1	47.7	63.5	75.8	92.7
Total inorganic carbon	Mass%		0.3	1	1.2	0.2
Organic carbon	Mass%		47.4		74.6	92.5
Hydrogen	Mass%		0.9	1.8	1.1	2.4
Total nitrogen	Mass%		1.54	3.81	1.07	0.35
Sulphur (S)	Mass%		0.52		0.15	< 0.03
Oxygen	Mass%		2.6	•	5.6	3.2
- 19						
H/Corg ratio (molar)		0.7	0.22	0.34	0.17	0.31
O/C ratio (molar)		1	0.041	0.095	0.055	0.026
pH in CaCl2			9.6	+	•	8.3
Salt content	g/kg		14.9		•	0.8
	197779	1	1.4.0	20.0	20.1	0.0
Conductivity at 1.2 t pressure	mS/cm	†	53	0.02	98	< 0.01
Conductivity at 2 t pressure	mS/cm	†	68			0.01
Conductivity at 3 t pressure	mS/cm	†	79			0.01
Conductivity at 4 t pressure	mS/cm	†	96			0.02
Conductivity at 5 t pressure	mS/cm	+	110		190	0.02
Conductivity at 5 t pressure	Поуст	+	110	0.04	190	0.02
Determination from microway	o proceuro digo	tion according to D	IN 22022-1: 2014-07	,		
Arsenic (As)	mg/kg	13			1	< 0.8
Lead (Pb)	mg/kg	120	4.3			< 2
Cadmium (Cd)	mg/kg	1.5	<u> </u>			< 0.2
Copper (Cu)		100	237	173	46	6
Nickel (Ni)	mg/kg	50			-	< 1
	mg/kg	1		< 0.07	< 0.07	< 0.07
Mercury (Hg)	mg/kg	400		112	184	
Zinc (Zn)	mg/kg					30
Chromium (Cr)	mg/kg	90		8		2
Boron (B)	mg/kg	+	71	64		33
Manganese (Mn)	mg/kg	-	903	-		490
Silver (Ag)	mg/kg	-	< 5	< 5	< 5	< 5
	1		<u> </u>	1		
Elements from borate digestic	1	C according to DIN !				
Calcium as CaO	Mass% of ash		13.4		22.5	27.7
Iron as Fe2O3	Mass% of ash		5.9		4.9	1.4
Potassium as K2O	Mass% of ash		9.7	31.9	16.2	14.3
Magnesium as MgO	Mass% of ash		7.4	-		6.3
Sodium as Na2O	Mass% of ash		1.6			1.1
Phosphorus as P2O5	Mass% of ash		20.5		-	4.6
Sulfur as SO3	Mass% of ash		1.6		4.3	1.4
Silicon as SiO2	Mass% of ash		22.3	7.3	22.2	9.8
Organic pollutants in tolue	ene extract ac	cording to DIN EN	16181:2019-08	(extraction meth	od 2)	
Total 8 EFSA PAHs excl. BG		1	(n. b.) 1)	< 0.1	< 0.1	< 0.1
Total 16 EPA PAHs excluding	BG	6 ±2.4	1.9	0.5	2.9	0.5
Polychlorinated dibenzodioxis	⊥ ns/furans (17 PC	│ DD/F) using GC-HRM	IS			
I-TEQ (NATO/CCMS) inc.LOC		20		0.936	0,939	0.921
		1	5.505	0.350	0,535	V.32.1
Polychlorinated biphenyls	(7 PCR) using	GC-HDMS				
Total 6 DIN-PCB incl. BG	μg/kg TS	200	3.75	0.478	0.48	0.499
	Ira''a 'V	1	100	14	101.0	0

This confirms that the used TCR® process is suitable to produce clean and certifiable biochar to generate negative emissions via Biochar Carbon Removal.

Gas Cleaning strategy

The Thermo-Catalytic Reforming (TCR®) process is inherently fuel-flexible, allowing for the conversion of a wide range of biomass feedstocks. However, this flexibility introduces complexity: the composition of the input fuel directly influences the syngas quality, including the concentration of valuable components like hydrogen and the presence of undesirable pollutants. Within the NET-Fuels project, the overarching goal is the valorization of hydrogenrich syngas and the integration of CO_2 capture via oxyfuel combustion. Achieving this requires a robust and adaptable gas cleaning strategy. A central challenge lies in the efficient removal of nitrogen- and sulfur-containing species, particularly ammonia (NH $_3$) and hydrogen sulfide (H $_2S$), as well as their precursors. These compounds can impair downstream processes and must be eliminated to meet purity requirements. Furthermore, the cleaned syngas must be

suitable for pressurization and subsequent separation via Vacuum Pressure Swing Adsorption (VPSA). This imposes stringent demands on the gas cleaning system in terms of both performance and integration.

The following chapter describes the gas cleaning strategy.

After the pyrolysis gas production, there is first a course treatment of the pyrolysis gas by quenching and subsequent particulate and tar removal by means of electrostatic precipitation, as is standard for coke oven gas [17]

Hydrogen (H2) is separated from the gas by Vacuum Pressure Swing Adsorption (VPSA) with activated carbon and zeolite layered beds. To obtain the gas quality for storage and then separate H2 in the VPSA, further gas processing is required to mitigate corrosion and adsorbent poisoning by the reactive species hydrogen sulfide (H2S) and ammonia (NH3). Whilst H2S does not necessarily result in corrosion of carbon steel due to a protective iron sulfide film [18], it will poison the adsorption beds of the VPSA. The quantities of these elements which are present in the feedstock vary, requiring a treatment strategy which allows for large variance in the H2S and NH3 concentrations present in the pyrolysis gas stream.

The current state of the art removal using activated carbon is not possible due to the requirement of additional oxygen (O2) to react with the H2S and convert it into elemental sulfur [19]. O2 cannot be added because the pyrolysis process has a large variance in both gas flow and gas composition, excluding the possibility of sufficiently precise O2 dosage to the gas stream.

The gas treatment of pyrolysis gas first removes pollutants by scrubbing with a biological washing medium designed for biogas treatment [20]. This differs from the closer related treatment of tail gases from refineries and similar processes, where NH3 and H2S are most commonly scrubbed with water (H2O). The sour water would then be stripped with steam (H2O) or an inert gas after hydrocarbon separation [18]. An unwanted consequence would be the removal of a large proportion of the CO2 in the pyrolysis gas due to its profuse absorption in the high flow rates associated with water scrubbing. Additionally, the advantage of the biological process used instead is its operation at room temperature and pressure, producing ammonium sulfate salts as a byproduct. Therefore, the novel technological development is the use of the robust biological process to treat pyrolysis gas. The process also ensures chemical H2S and NH3 removal in the case of failure of the biological removal.

The washing medium circulates between the counterflow gas scrubber and the bioreactor. On the flow from the bioreactor to the gas scrubber, the medium is constituted of H2O, solute iron, henceforth referred to as the most soluble ferric species amorphous ferrihydrite (Fe(OH)3(aq)), aqueous sulfuric acid (H2SO4(aq)), the circulating biology, ammonium sulfate ((NH4)2SO4(aq)) salt, minimal quantities of solute air from the aeration process, and other constituents remaining after the regeneration process. The washing medium is acidic, with an acidic pH between 1.5 and 3.

NH3 binds with H2SO4(aq) via chemisorption as with commercial fume scrubbers, directly producing (NH4)2SO4(aq). The scrubber design adapts conventional air purifying technology to clean syngas. The assumptions made in the design are that the process is analogous to removing NH3 in air with a dilute H2SO4(aq) washing solution, which is a gas-film controlled system. This is considered a valid assumption because syngas has a similar density to air. The process design can be further simplified in the case of constantly varying gas composition by assuming the NH3 quantity in the gas is diluted, giving a constant NH3 transfer rate. This allows a simplified calculation to be used to estimate the scrubbing efficiency [21]. The reaction is sufficiently prompt that almost complete removal of NH3 from the gas flow occurs. The other species to be removed from the pyrolysis gas stream, H2S, becomes solute in the washing medium via diffusion and is subsequently carried in the washing medium to the bioreactor. In the bioreactor, solute iron, referred to as the most soluble ferric species amorphous ferribydrite. (Fe(OH)3(aq)) binds with dissolved hydrogen sulfate. (H2S) and oxygen (O2)

ferrihydrite (Fe(OH)3(aq)), binds with dissolved hydrogen sulfate (H2S) and oxygen (O2) provided by the aerator in the bioreactor. The subsequent products are iron sulfide (FeS), sulfuric acid (H2SO4), and water. The iron sulfide is then converted by the acidophilic bacteria over several steps into H2SO4(aq) and amorphous ferrihydrite (Fe(OH)3(aq)), amongst others. This reduces the required dosage of H2SO4, which is subsequently pumped into the gas

scrubber to neutralize NH3 in a new cycle.

The downstream fixed bed reactors serve three functions; primarily to remove any H2S in the pyrolysis gas stream when none could be absorbed in the washing medium; secondly to remove the remaining fraction of H2S which remains after most is absorbed in the washing medium; and thirdly to remove any H2SO4 slip from the gas washing medium into the pyrolysis gas stream.

The fixed bed reactors use a simple process, common in the last century to treat biogas. H2S in the gas stream reacts with iron hydroxide (FeO(OH)), which has a moderate loading and breakthrough time for oxidized iron [22], but is comparatively cheap material, which is economical for single use. Another advantage is the reaction occurs at room temperature and pressure. Heat effects within the pellets do not need to be considered, because the local temperature change when penetrating the porous structure is negligible. The possible sulfur loading without oxygen or alkaline gas is estimated to be 10% weight/weight before regeneration [23]. The loaded material can be oxidized by flooding and aeration, before disposal either as household waste or contemplatable further use as an iron and sulfur source in the bioreactor. Any minute quantities of H2SO4 in the gas are absorbed by the binding agent calcium carbonate (CaCO3), which holds the FeO(OH) pellets in the fixed bed reactors in their stable form. This then forms solid calcium sulfate (CaSO4), H2O and CO2.

The main advantages of the process are that no new chemicals are introduced into the pyrolysis gas, only a minimal proportion of CO2 is lost, all side products are potentially useful, and all processes occur at ambient conditions in a robust, stable and scalable process.

These cleaning steps will allow the gas to be compressed and to use VPSA to provide H2.

Carbon Capture with Oxyfuel Combustion

Oxyfuel combustion is a promising approach to apply carbon capture while simultaneously providing process heat at a high temperature level. In this process, pure oxygen is used instead of ambient air to combust the fuel. Due to the absence of atmospheric nitrogen, the flue gas is idealized to consist solely of the combustion products CO_2 and H_2O . Simple separation of the water vapor through condensation leads to a flue gas stream with a very high CO_2 content [24], which can then be captured more efficiently [25] or can be utilized directly. If a biogenic fuel such as pyrolysis gas is utilized in this combustion process to provide thermal energy, and the captured CO_2 is utilized, this process can be classified as Bioenergy with Carbon Capture and Utilization (BECCU). NET-Fuels focusses on the combustion of TCR® syngas or rather the tailgas stream with reduced H2 concentrations after VPSA.

Until now, it has been criticized that the high energy input of $875-1200 \text{ kJ/(kg }O_2)$ at the desired purity of 95-99.5 vol.%[26], required to provide the necessary oxygen through air separation significantly reduces the overall efficiency of oxyfuel processes[27, 28]. However, due to the growing global electrolysis capacity for producing green hydrogen [29] and the associated potential for utilizing surplus oxygen, a by-product of electrolysis, the oxyfuel process is increasingly attracting attention in the development of CO_2 capture technologies [30]. In NET-Fuels O2 is a by-product from the bioelectrochemical methanation (BEM).

Figure 4 illustrates the schematic layout of the pilot plant located at the Fraunhofer UMSICHT technical center in Sulzbach-Rosenberg (Bavaria, Germany), which is organized as follows: The fuel (TCR® gas or biogas) is supplied to a 50 kW burner, where it is introduced into the combustion chamber together with the oxidizer – a mixture of recirculated flue gas and pure oxygen (gas quality 3.5). The combustion reaction occurs there at atmospheric pressure. The flue gas subsequently exits the combustion chamber through the recuperative burner, whereby the oxidizer is preheated. In a first step, the flue gas is cooled in a high-temperature heat exchanger. In the second step, the cooled flue gas is directed into the condenser, where it is sub-cooled to 20 °C to facilitate the separation of a significant portion of the water vapor present in the flue gas. The condensate is discharged via a siphon to prevent ambient air from entering the plant. A part of the dry flue gas ($CO_2 > 95$ vol.%) is recirculated and oxygen is added upstream of the burner to form the oxidizer. The remaining portion is removed via an

exhaust fan, which regulates the combustion chamber pressure. To moderate the temperature within the combustion chamber, liquid water is injected through three nozzle lances using a dosing pump. The flue gas composition is measured (FTIR Fourier Transform Infrared Spectroscopy) in the dry flue gas after the condenser. Air may be utilized as an oxidizer to bring the system up to operating temperature. After the exhaust fan, a part of the flue gas is further dried with zeolite and is then compressed into gas cylinders to store it for downstream utilization processes, e.g. bioelectrochemical methanation.

In the NET-Fuels process chain, the tail gas from Vacuum Pressure Swing Adsorption (VPSA) is intended to be utilized for oxyfuel combustion to enable efficient CO_2 capture. However, since the VPSA unit is not yet operational, current experimental setups rely on a direct connection to the TCR® reactor, using raw TCR® syngas as a substitute to evaluate combustion behavior and carbon capture potential.

In Figure 5, the CO₂ content in the flue gas of the Oxyfuel system during combustion of TCR® gas from wood pyrolysis is shown. The Oxyfuel system and the TCR® unit are directly coupled without any additional process gas treatment. Initially, the combustion chamber is heated up with natural gas and air. Under these operating conditions, the CO₂ concentration in the flue gas is typically around 10 vol.%. Once the combustion chamber has reached operating temperature, the natural gas supply is stopped and pyrolysis gas from the TCR® unit is introduced into the combustion chamber. As a result, the CO₂ content in the flue gas increases slightly due to the marginally higher carbon content of TCR® gas compared to natural gas. Subsequently, the supply of pure oxygen is initiated and the air supply gradually shut off, while the valve in the recirculation gas line is opened. It can be observed that this causes the CO₂ concentration in the flue gas to rise rapidly. Once the air supply is fully closed, the system requires some time to purge the remaining nitrogen from the air. During this phase, the CO₂ concentration increases slowly and approaches its steady-state level, which is ≥ 97 vol.%. At this operating point, the H₂O content is approximately 2 vol.%. The CO emissions depend on the residual oxygen content. In near-stoichiometric operation with 0.01-0.5 vol.% residual oxygen in the flue gas, the CO emissions range from 2787 - 28 ppm. The NO_x emissions are in the order of 35 ppm.

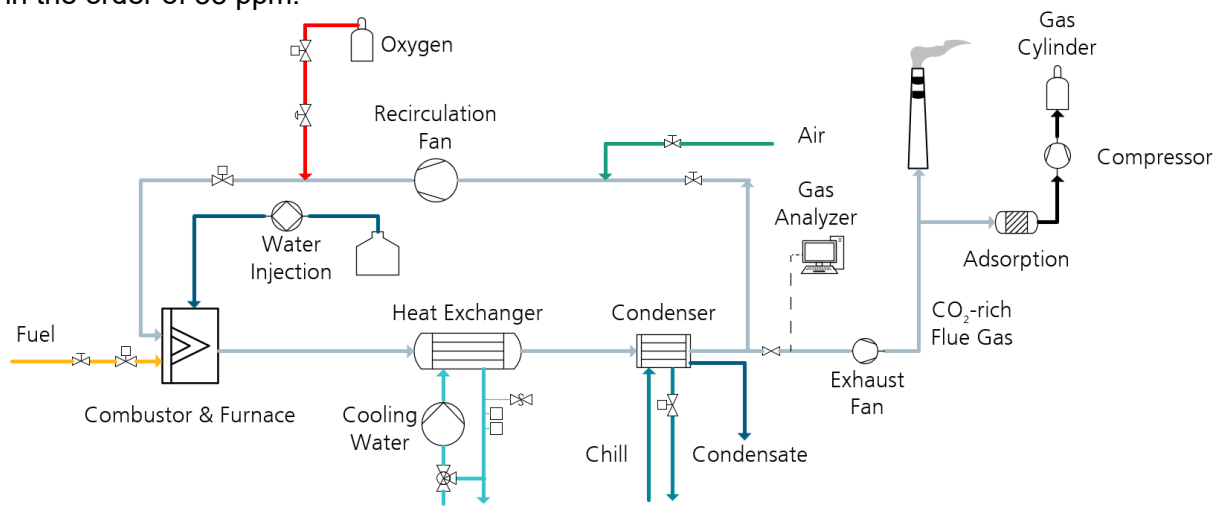


Figure 4: Schematic representation of the pilot plant designed for the oxyfuel combustion of gaseous fuels at Fraunhofer UMSICHT

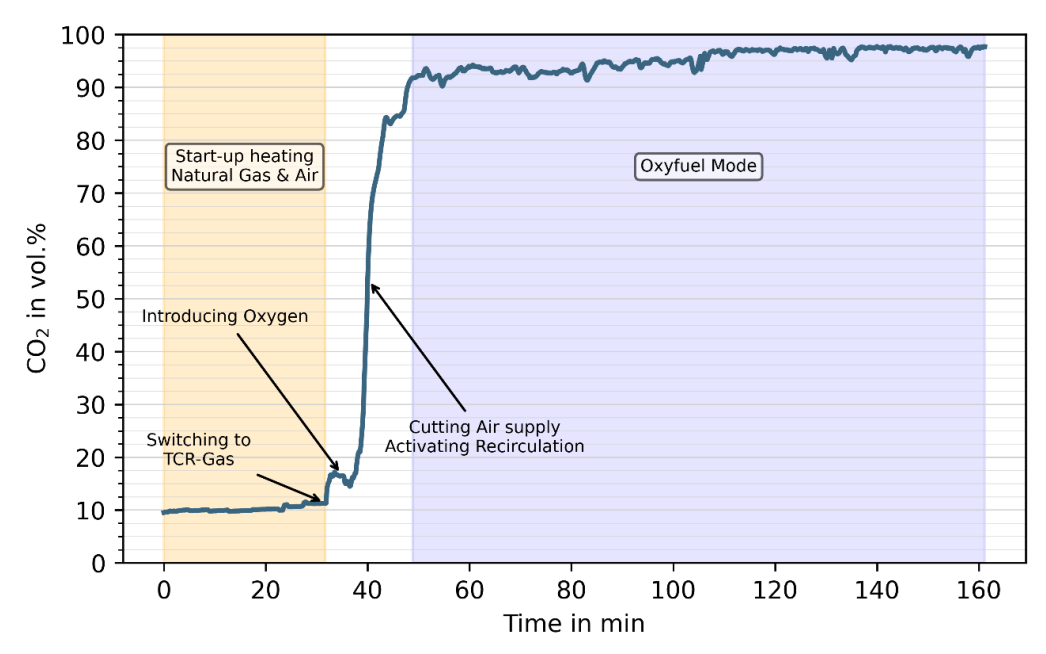


Figure 5: CO₂ content in the flue gas over time measured downstream of the condenser during direct coupling of the Oxyfuel system with a TCR® unit.

Bioelectrochemical methanation

Bioelectrochemical methanation (BEM) is an emerging power-to-gas technology that also serves for carbon capture and utilization (CCU), converting CO₂ to synthetic methane [31]. A BEM cell typically consists of two electrodes, an anode and a cathode, inserted into two adjacent chambers of a bioelectrochemical cell, separated by a cationic exchange membrane (CEM) and connected by an external electrical circuit, through which additional electrical energy is injected, at low voltage. The water splitting reaction at the anode generates oxygen, protons and electrons. Electrons flow through the external electrical circuit to reach the cathode, while protons and other cations migrate through the membrane to maintain the charge balance within the cell [32]. At the cathode, the electromethanogenesis process takes place. The electrode surface is colonized by an electro-active biofilm that catalyses hydrogen (H₂) production. Then, a hydrogenotrophic microbial community uses the produced H₂ to convert an injected flux of CO₂ into synthetic methane [33]. To enable future pilot-scale demonstrations, laboratory-scale studies are still needed to understand fundamental processes, evaluate and optimize electrode and membrane materials, and optimize operational strategies under controlled conditions

This study represents the first coupling of an optimized laboratory-scale BEM with a thermochemical reforming and oxyfuel process chain. The usage of a real combustion gas as carbon feedstock, allows to demonstrate BEM tolerance to gas impurities and variable CO₂ concentration. The next step of the project will involve the operation of a pilot scale BEM plant, with a treatment capacity of 50 L-CO₂ d⁻¹, and its integration with the TCR®/VPSA/Oxycombustion plant, validating the overall system at TRL 5.

The laboratory-scale BEM system (Figure 1) consisted of three double-chambered cells (100 cm² cross section, 200 mL chamber volume), assembled in a single stack and hydraulically operated in parallel. The cathodes of the three cells consisted of stainless-steel wool (~10 g, 100 cm²), while the anodes were made by titanium mesh coated with IrO₂ mixed metal oxides. Anode and cathode chambers of each cell were separated by a 100 cm² CEM. Each cell operated individually in galvanostatic mode, at a current density of 12 A m⁻² provided by a power supply. At the cathode side, the CO₂-rich gas was injected into the bulk catholyte solution through a porous diffuser. Its flow-rate was regulated by a mass flow controller at 10 mL min⁻¹ to maintain stable dissolved CO₂ levels, ensuring no substrate limitation while preventing excess CO₂ outflow that could reduce synthetic methane quality. The anolyte was

recirculated through a 2 L external buffer tank, where produced oxygen was separated and quantified at atmospheric pressure. The catholyte was recirculated through a 14 L liquid–gas separation column, maintained at 35 °C by a thermostatic bath, at an overpressure of 180–200 mbar and continuously monitored for dissolved CO₂ and synthetic methane production, using online sensors and gas chromatography.

Before testing the BEM system with the real off gas coming from the oxyfuel reactor, pure CO_2 was injected for 27 days, maintaining a dissolved CO_2 concentration in the catholyte of 300 mg L⁻¹, corresponding to ~20% of its theoretical solubility. The real off-gas contained impurities (3% air), with the remainder volume being CO_2 .

A summary of the results obtained with the two gases in shown in Table 1. When fed with pure CO_2 , the BEM system achieved a higher quality synthetic methane (72 ± 4% CH_4), compared to exhaust gas conditions (61 ± 4% CH_4). The CO_2 concentration in the outlet was slightly lower with pure CO_2 (8 ± 3%) than with exhaust gas (10 ± 8%). Hydrogen accumulation was more pronounced with exhaust gas (18 ± 13% vs. 8 ± 5%), suggesting its reduced consumption by methanogens. This was likely because the presence of oxygen in the detected air could negatively affect BEM performance, as oxygen is highly detrimental to methanogenic microorganisms [34]. Oxygen levels were also higher with exhaust gas (5 ± 4% vs. 3 ± 2%), consistent with the presence of air impurities in the feed.

Table 3: Comparison of BEM performance using pure CO₂ versus oxyfuel exhaust gas.

	CH ₄ (%)	CO ₂ (%)	H ₂ (%)	O ₂ (%)	N ₂ (%)	Carbon conversion efficiency (%)	synthetic methane production (L CH ₄ L _{cat} ⁻¹ day-1)	Coulombic efficiency (%)
Pure CO ₂	72 ± 4	8 ± 3	8 ± 5	3 ± 2	8 ± 2	71 ± 2	1.14 ± 0.05	69 ± 3
Oxyfuel exhaust gas (with air)	61 ± 4	10 ± 8	18 ±13	5 ± 4	8 ± 1	58 ± 4	1.01 ± 0.04	62 ± 2

In terms of performance indicators, carbon conversion efficiency decreased from 71 \pm 2% with pure CO₂ to 58 \pm 4% with exhaust gas. Similarly, both specific synthetic methane production (1.14 \pm 0.05 vs. 1.01 \pm 0.04 L CH₄ L_{cat}⁻¹ day⁻¹) and Coulombic efficiency (69 \pm 3% vs. 62 \pm 2%) were negatively affected by the presence of oxygen in the exhaust gas.

The average specific production rates and cathodic Coulombic efficiencies achieved with synthetic CO_2 are within the upper range of values previously reported in the BEM literature, for laboratory-scale operated BEM systems [35]. Remarkably, comparable performances were obtained here using real oxyfuel exhaust gas containing air impurities. Demonstrating stable operation under such realistic conditions is highly relevant, as it validates the applicability of BEM beyond idealized laboratory setups with pure CO_2 and underscores its potential for the future pilot-scale integration.

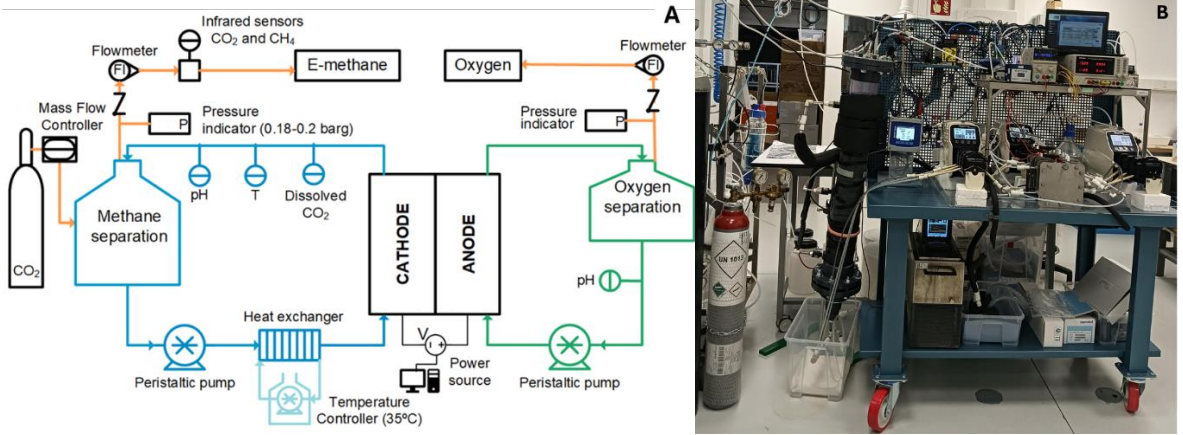


Figure 6: Laboratory system schematics (only one BEM cell is shown for simplicity) (**A**); Photograph of the laboratory set-up (**B**)

Preliminary Assessment of Carbon Negativity

NET-Fuels aims at generating carbon-negative advanced fuels (synthetic methane, green hydrogen and liquid biofuel) with maximum biomass utilization efficiency from a wide range of low-quality and low-cost feedstocks, such as the secondary biomass resources enlisted in Part A of Annex IX of the RED (the Renewable Energy Directive). This includes (a) lignocellulosic residues not requiring drying and pre-treatments and (b) feedstock requiring drying and densification in addition to mechanical pre-treatments. The former group includes nut shells, husks, cobs cleaned of kernels and other fruit shells. Group "b" includes algae, biowaste, straw, animal manure and sewage sludge, bagasse, grape marc, wine lee together with all biomass fraction of wastes and residues from forestry and forest-based industries, other non-food cellulosic material and lignocellulosic material. A wide range of biomass fractions of industrial waste not fit for use in the food or feed chain (including material from retail and wholesale) and the agri-food and fish and aquaculture industry.

In Europe, groups "a" and "b" together range from 200 to 350 million tons (dry weight). The use of this source of secondary biomass avoids land competition with food production and potential threats to biodiversity.

NET-Fuels considers three different selected biogenic residues will be treated:

- 1. Digestate. Digestate obtained from the anaerobic digestion of manure and maize silage is an important agricultural residual material with great potential.
- 2. Calamity wood. The effects of climate change on forest stands are becoming apparent in Central Europe. Damage caused by drought, bark beetle infestation and storms has resulted in large quantities of calamity wood accumulating.
- 3. Pruning. Offcuts from vineyards and orchards regularly accumulate in large quantities, especially in Southern Europe.

The preliminary carbon balance of the process is determined by the carbon removed (captured and stored) and the CO₂-eq emissions due to the external energy (heat and power) needed by the system.

The carbon-negative value of the generated fuels (CR_{Fuels}) is the carbon balance of the process for a reference carbon removal value (CR_{Ref} , expressed in mass unit of CO₂-eq) divided by the energy in the generated fuels (E_{Fuels} , expressed in energy units). A positive value indicates a removal, while a negative one an emission.

$$CR_{Fuels} = \frac{CR_{Ref}}{E_{Fuels}}$$
 [1]

The data used for the calculations is based on past test results for the feedstocks the TCR® process, and chemical reaction notations for the Bio-Electrochemical Methanation (BEM) process, supplemented by values from literature and estimation calculations. A lignocellulosic feedstock containing 50% water is used. The total carbon removal of the process (CR_{Ref}) is determined by the difference of the carbon nominally stored in the biochar which is fixed to 1000 g of CO_2 (reference value) and the CO_2 -eq emissions due to the use of external energy (heat and power) required by the product system to generate the reference value (GHG_0)

$$CR_{Ref} = CR_0 - GHG_0 = 1000 - GHG_0$$
 [2]

The following values refer to the processing of calamity wood. To remove 1 kg of CO_2 equivalent from the atmosphere (the reference value), 0.27 kg of carbon must be stored, according to the molar ratio of the molecules. The tested biochar has a carbon content of 76.8%, as a consequence, 0.35 kg of biochar must be generated and stored in a permanent sink. For the following calculations a biomass-to-biochar conversion rate of 28.9% and a water content of 50% of water in the primary feedstock have been considered; the primary feedstock is dried to a water content of around 10% to be processed in the TCR®. This results in a dry

mass of 1.20 kg starting from a total mass of the primary feedstock of 2.20 kg. Based on the preliminary results, the pelletizing process requires a power demand of 0.13 kWh on account of the corresponding reference value. This preliminary assessment uses recovered heat from the oxyfuel process, which covers the drying energy demand. Energy for chipping is not included.

TCR® allows for the production of oil, biochar and syngas, requiring an electric energy demand of 0.04 kWh. Hydrogen is recovered from the TCR®-gas via a VPSA with an efficiency of 85% based on past experimental data, with an electrical demand of 0.42 kWh. The remaining gas is combusted with oxygen in the oxy-combustion unit to generate thermal energy for drying and for the TCR® process. Oxyfuel technology requires approximately 0.40 kg O₂. The oxygen supply is provided by the BEM. BEM represents the most energy intensive process, with an electrical demand of around 5.62 kWh.

If an electricity carbon intensity of 161 g CO_2 eq/kWh is assumed, the total emissions of NET-Fuels system would be covered by the biochar carbon removal. The mean EU carbon intensity is around 230 g CO_2 eq/kWh¹ and would only allow in the future to produce negative emission fuels through NET-Fuels. Nevertheless, producing carbon negative fuels is already possible today in countries such as Austria, Finland and France. For instance, if we consider the Austrian electricity carbon intensity, which is 103 g CO_2 eq/kWh the NET-Fuels process case, would emit:

$$GHG_{productsystem}(E_{Power}) = 640gCO_{2eq}$$
 [3]

When applying [2] a value higher than ~360 g CO₂-eq of carbon removal, a negative emission is obtained. Taking the reference value into consideration, 0.21 kg of CH₄ is produced corresponding to an output of 2.9 kWh together with 0.49kWh of TCR® oil and approximately 0.33 kWh of H₂, totaling 3.7 kWh, this pool being the (advanced) "Fuels" generated by the product system. This leads to a preliminary value of ~95 g CO₂-eq removed per kWh_{Fuels} (~25 g CO₂-eq /MJ_{Fuels}), i.e. the "carbon intensity" of the advanced fuels is negative.

By 2030, with an EU estimated electricity carbon intensity of 120 g CO2eq/kWh, the emissions would be about 745 g of CO2eq, with a negative carbon intensity of the produced biofuels of 255 g CO_2 -eq/kWh_{Fuels} (~20 g CO2eq/MJ).

Depending on the feedstock condition, the heat recovery from the oxy-combustion, the inclusion of the energy for chipping the material, the electricity carbon intensity, the actual amount of carbon permanently stored in a sink and other considerations of the basis of a preliminary Life Cycle Analysis, the NET-Fuels solution would generate synthetic methane and advanced biofuels having a carbon negative value of around 20- gCO2eq per MJ of produced biofuel from the point of harvest (farm) to energy end use (wheel) when the electricity carbon intensity is around 120 g CO2eq/kWh.

-

 $^{1 \\ {\}tt https://www.eea.europa.eu/ims/greenhouse-gas-emission-intensity-of-1} \\$

Summary and Conclusion

The NET-Fuels project demonstrates a modular and climate-positive process chain for the production of advanced renewable fuels and carbon removal. Central to this system is the Thermo-Catalytic Reforming (TCR®) technology, which converts biogenic residues into three valuable products: biochar, syngas, and bio-oil.

Bio-oil:

TCR®-derived bio-oils exhibit unique properties, including high oxygen content and viscosity, distinguishing them from conventional crude oils. Catalytic hydrotreatment has proven effective in upgrading these oils to meet fuel standards (EN 228, EN 590). Stabilization and deep hydrodeoxygenation stages enable the removal of heteroatoms and the production of drop-in fuels suitable for direct use in existing refinery infrastructure. Experimental results confirm that upgraded TCR® oils can match the distillation profiles and calorific values of fossil-derived fuels.

Biochar: The solid residue from TCR® is a highly stable carbon-rich material. It may serve as a certified carbon sink when used in long-term applications such as soil amendment. Biochar samples from various feedstocks (digestate, pollard willow wood, olive stones, olive pressing residue) have been analyzed for elemental composition and contaminants. The low H/C_{org} ratio and minimal organic pollutants confirm the suitability of TCR® biochar for use in soil. Most samples meet the criteria for certification under frameworks like EBC, with the exception of digestate

Syngas: The volatile fraction from TCR® contains up to 45 vol% hydrogen, along with CO, CO_2 , CH_4 , and other hydrocarbons. This syngas is cleaned, and VPSA is used to extract hydrogen, while the tail gas is directed to oxyfuel combustion for energy recovery and CO_2 capture. The fuel-flexible nature of TCR® introduces variability in syngas composition, necessitating advanced gas cleaning strategies. A robust combination of cleaning steps to remove NH_3 and H_2S , ensuring compatibility with VPSA and minimizing corrosion and adsorbent poisoning.

Bioelectrochemical Methanation (BEM) and Results

The BEM subsystem plays a dual role in carbon capture and utilization. It converts CO₂ into synthetic methane using biological processes, and provides oxygen as a by-product. Laboratory-scale tests have demonstrated stable operation under both ideal and realistic conditions

When fed with pure CO_2 , the BEM system achieved a CH_4 concentration of $72 \pm 4\%$, Carbon conversion efficiency of $71 \pm 2\%$ and a coulombic efficiency of $69 \pm 3\%$. When fed with oxyfuel exhaust gas (containing air impurities) the results were slightly worse.

These results validate the robustness of BEM under real-world conditions and its potential for pilot-scale integration. The presence of oxygen slightly reduces performance, but the system remains effective in converting CO₂ into synthetic methane.

Carbon Negativity and Outlook

Preliminary life cycle assessments indicate that NET-Fuels can produce carbon-negative fuels with a carbon intensity of approximately –20 g CO₂eq/MJ, depending on feedstock, energy sources, and system configuration. The integration of recovered heat, renewable electricity, and certified carbon sinks positions NET-Fuels as a scalable solution for climate mitigation.

In conclusion, NET-Fuels offers a comprehensive and flexible platform for renewable fuel production and carbon removal. Its integration of thermochemical, biological, and electrochemical technologies supports the European Green Deal and hydrogen strategy, paving the way for a sustainable and climate-positive energy future.

Acknowledgements Co-funded by the European Union Co-funded by the European Union

References

- [1] Schmidt, H.-P., Anca-Couce, A., Hagemann, N., Werner, C., Gerten, D., Lucht, W., & Kammann, C. (2019). Pyrogenic carbon capture and storage. Global Change Biology Bioenergy, 11(4), 573-591. doi:http://doi.org/10.1111/gcbb.12553
- EBC. (2012-2025). 'European Biochar Certificate Guidelines for a Sustainable Production of Biochar.' [2] Carbon Standards Internation-al (CSI), Frick, Switzerland. (http://carbon-standards.com/ebc). Version 10.5E from 14th August 2025.
- Hornung A., Jahangiri H., Ouadi M., Kick C., Deinert L., Meyer B., Grunwald J., Daschner R., [3] Apfelbacher A., Meiller M., Eder S.: Thermo-Catalytic Reforming (TCR®)-An important link between waste management and renewable fuels as part of the energy transition, Applications in Energy and Combustion Science 12 (2022) 100088
- Neumann J., Meyer J., Ouadi M., Apfelbacher A., Binder S., Hornung A.: The conversion of anaerobic [4] digestion waste into biofuels via a novel Thermo-Catalytic Reforming process. Waste Manage 2016:47:141-8. https://doi.org/10.1016/i.wasman.2015.07.001.
- Hsu CS and Robinson PR, Practical Advances in PetroleumProcessing. Springer Science & Business [5] Media Inc., New York(2006)
- [6] Schmitt, N., Apfelbacher, A., Jäger, N., Daschner, R., Stenzel, F., & Hornung, A. (2019). Thermochemical conversion of biomass and upgrading to biofuel: The Thermo-Catalytic Reforming process-A review. Biofuels, Bioproducts and Biorefining, 13(3), 822-837.
- Grunwald J. Entwicklung, Auslegung und Aufbau eines kontinuierlich betriebenen Hochdruck-[7] Hochtemperatur-Reaktorsystems zur Herstellung von Benzin-und Dieselkaftstoff durch die Hydrierung von TCR®-Öl aus biogenen Reststoffen. Karl Maria Laufen Buchhandlung und Verlag (2023)
- EBC. (2012-2025). 'European Biochar Certificate Guidelines for aSustainable Production of Biochar.' [8] Carbon Standards Internation-al (CSI), Frick, Switzerland. (http://carbon-standards.com/ebc). Version 10.5E from 14th August 2025.
- [9] Bucheli, T. D., Bachmann, H. J., Blum, F., Buerge, D., Giger, R., Hilber, I., Keita, J., Leifeld, J., & Schmidt, H.-P. (2014). On the heterogeneity of biochar and consequences for its representative sampling. Journal of Analytical and Applied Pyrolysis, 107, 25-30. doi:https://doi.org/10.1016/j.jaap.2014.01.020
- [10] Hagemann, N., Schmidt, H.-P., Bucheli, T. D., Grafmüller, J., Vosswinkel, S., Herdegen, V., Meredith, W., Uguna, C. N., & Snape, C. E. (2025). Proxies for use in biochar decay models: Hydropyrolysis, electric conductivity, and H/Corg molar ratio. Plos One, 20(9), e0330206. doi:10.1371/journal.pone.0330206
- https://zenodo.org/records/8436814)
- [12] Etter, H., Vera, A., Aggarwal, C., Delaney, M., & Manley, S. (2021). Methodology for biochar utilization in soil and non-soil applications. Available from: https://verra.org/wpcontent/uploads/imported/methodologies/210803 VCS-Biochar-Methodology-v1.0-.pdf [last accessed: Mar 29, 2025].
- Puro.earth. (2022). Puro standard- Biochar methodology, (Edition 2022 Version 2). Available from: [13] https://fs.hubspotusercontent00.net/hubfs/7518557/Supplier%20Documents/Puro.earth%20Biochar%20 Methodology.pdf. [last accessed: Mar 29, 2025].
- [14] Hagemann, N. (2024). Description of the certification process for biochar-based carbon sinks. Ithaka Insitute, Arbaz, Switzerland, 2024. https://doi.org/10.5281/zenodo.10580112
- EBC. (2020). Certification of the carbon sink potential of biochar, Ithaka Institute, Arbaz, Switzerland. [15]
- (http://european-biochar.org). Version 2.1E of 1st February 2021. Hagemann, N., Schmidt, H.-P., Bucheli, T. D., Grafmüller, J., Vosswinkel, S., Herdegen, V., Meredith, [16] W., Uguna, C. N., & Snape, C. E. (2025). Proxies for use in biochar decay models: Hydropyrolysis, electric conductivity, and H/Corg molar ratio. Plos One, 20(9), e0330206. doi:10.1371/journal.pone.0330206
- [17] Svoboda, K. P.; Diemer, P. E. (1990): Catalytic decomposition of ammonia from coke-oven gas. In Iron and Steel Engineer; (USA) 67:12. Available online at https://www.osti.gov/etdeweb/biblio/6035453.
- Kohl, Arthur L.; Nielsen, Richard B. (1997): Gas purification. 5. ed. Houston, Tex.: Gulf Publ. Co. [18] Available online at http://www.loc.gov/catdir/description/els032/96052470.html.
- Awe, Olumide Wesley; Zhao, Yaqian; Nzihou, Ange; Minh, Doan Pham; Lyczko, Nathalie (2017): A [19] Review of Biogas Utilisation, Purification and Upgrading Technologies. In Waste and Biomass Valorization 8 (2), pp. 267-283. DOI: 10.1007/s12649-016-9826-4.
- [20] MicroPro (2025): H2S-removal from biogas. MicroPro GmbH. Gommern, Germany. Available online at https://www.micropro.de/english/processes-products_h2s-removal.htm, checked on 7/22/2025.
- Strigle, Ralph F. (1994): Packed tower design and applications. Random and structured packings. 2., [21] [rev.] ed. Houston: Gulf Publ.
- [22] Raabe, Toni; Mehne, Marcel; Rasser, Heidi; Krause, Hartmut; Kureti, Sven (2019): Study on iron-based adsorbents for alternating removal of H2S and O2 from natural gas and biogas. In Chemical Engineering Journal 371, pp. 738-749. DOI: 10.1016/j.cej.2019.04.103.
- [23] Wang, De Ming (2008): Breakthrough Behavior of H2S Removal with an Iron Oxide Based CG-4 Adsorbent in a Fixed-Bed Reactor. Degree of Master of Science. Department of Chemical Engineering, Saskatoon, Canada. University of Saskatchewan. Available online at

- https://harvest.usask.ca/server/api/core/bitstreams/a6eed3fa-15ef-4029-a5f1-
- [24] C.Y. Liu, G. Chen, N. Sipöcz, M. Assadi, X.S. Bai, Characteristics of oxy-fuel combustion in gas turbines, Applied Energy 89 (2012) 387–394. https://doi.org/10.1016/j.apenergy.2011.08.004.
- [25] S. Talei, D. Fozer, P.S. Varbanov, A. Szanyi, P. Mizsey, Oxyfuel Combustion Makes Carbon Capture More Efficient, ACS omega 9 (2024) 3250–3261. https://doi.org/10.1021/acsomega.3c05034.
- Y. Hu, H. Li, J. Yan, Integration of Evaporative Gas Turbine with Oxy-Fuel Combustion for Carbon Dioxide Capture, International Journal of Green Energy 7 (2010) 615–631. https://doi.org/10.1080/15435075.2010.529405.
- [27] Z. Abubakar, E.M.A. Mokheimer, M.M. Kamal, A review on combustion instabilities in energy generating devices utilizing oxyfuel combustion, Intl J of Energy Research 45 (2021) 17461–17479. https://doi.org/10.1002/er.7010.
- [28] K. Goto, K. Yogo, T. Higashii, A review of efficiency penalty in a coal-fired power plant with post-combustion CO2 capture, Applied Energy 111 (2013) 710–720. https://doi.org/10.1016/j.apenergy.2013.05.020.
- [29] M. Wappler, D. Unguder, X. Lu, H. Ohlmeyer, H. Teschke, W. Lueke, Building the green hydrogen market Current state and outlook on green hydrogen demand and electrolyzer manufacturing, International Journal of Hydrogen Energy 47 (2022) 33551–33570. https://doi.org/10.1016/j.ijhydene.2022.07.253.
- [30] F. Schorn, D. Lohse, R.C. Samsun, R. Peters, D. Stolten, The biogas-oxyfuel process as a carbon source for power-to-fuel synthesis: Enhancing availability while reducing separation effort, Journal of CO2 Utilization 45 (2021) 101410. https://doi.org/10.1016/j.jcou.2020.101410.
- [31] Vega-Paredes, M. et al. (2025) 'Stabilising methane production in a series-stack of bioelectrochemical systems', Journal of Power Sources, 656, p. 238119. Available at: https://doi.org/10.1016/j.jpowsour.2025.238119.
- [32] Van Eerten-Jansen, M.C.A.A. et al. (2012) 'Microbial electrolysis cells for production of methane from CO2: long-term performance and perspectives: A methane-producing MEC to increase land use efficiency', International Journal of Energy Research, 36(6), pp. 809–819. Available at: https://doi.org/10.1002/er.1954.
- [33] Deutzmann, J.S., Kracke, F. and Spormann, A.M. (2023) 'Microbial electromethanogenesis powered by curtailed renewable electricity', Cell Reports Physical Science, 4(8), p. 101515. Available at: https://doi.org/10.1016/j.xcrp.2023.101515.
- [34] Cristiani, L. et al. (2024) 'Impact of extended starvation conditions on bioelectrocatalytic activity of a methane-producing microbial electrolysis cell', Bioresource Technology, 413, p. 131491. Available at: https://doi.org/10.1016/j.biortech.2024.131491.
- [35] Horváth-Gönczi, N.N. et al. (2023) 'Bioelectrochemical Systems (BES) for Biomethane Production—Review', Fermentation, 9(7), p. 610. Available at: https://doi.org/10.3390/fermentation9070610.

The role of hydrogen and syngas for coupling energy transformation and circular economy

<u>F. Scheiff</u>, T. Kolb, S. Bajohr, F. Graf, S. Fleck, U. Santo, T. Jakobs, M. Haas, W. Köppel Karlsruher Institut für Technologie (KIT), Engler-Bunte-Institut (EBI)

Abstract

Hydrogen is a key element for the energy transition, as well as for the path towards a circular carbon economy. Both transformation processes face individual challenges, such as clean energy demand, import technologies and transport infrastructure in case of hydrogen. Circular carbon economy has to address feedstock varieties, technology development needs and specific customer demand for sustainable hydrocarbon products. However, hydrogen as energy carrier and feedstock will be an important contact point between energy transition and future circular economy. This presentation will give an overview of the different perspectives on this interplay.

In case of hydrogen, supply and distribution are key questions. According to the German National Hydrogen Strategy up to 70% of the German hydrogen demand have to be covered by import of hydrogen or its derivatives in short to mid-term. Different hydrogen import options, such as liquid hydrogen, ammonia, methane or methanol will be evaluated in terms of energy efficiency and infrastructural demand. Additionally, Germany has to build up a hydrogen gas grid infrastructure, which will be embedded in the European hydrogen backbone. Current hydrogen grid plans will be evaluated with hydraulic grid models.

In case of circular carbon economy, the presentation will focus on the role of syngas production via entrained flow gasification. Biogenic or anthropogenic (mainly mixed plastic waste) sources may offer an entry into circular carbon value chains with existing gasifier assets. However, the switch from conventional fossil gasifier feedstocks to biogenic or plastic-based pyrolysis oils poses significant thermochemical challenges on the conversion process. Thus, feedstock switch requires detailed understanding of the underlying physical and thermochemical processes, such as atomization, flame stabilization, fuel conversion, slagging and heat release.

This presentation will shed a light on the German's gas industry view on hydrogen and the work of the DVGW (Deutscher Verein des Gas- und Wasserfaches e.V.) research center at the Engler-Bunte-Institut in Karlsruhe. And it will give insights into the multiscale work at the gasification department in the Institute for Technical Chemistry (ITC) as part of the Helmholtz research program.

Excellent T Control in Compact Fischer-Tropsch Reactor with AI Packed POCS

Martino Panzeri, Carlo Giorgio Visconti, Gianpiero Groppi, Enrico Tronconi Laboratory of Catalysis and Catalytic Processes, Politecnico di Milano, Milan, Italy

Abstract

In recent years the interest in the conversion of CO, CO_2 , hydrogen, and biomass into valuable products has grown significantly, driven by the need to reduce greenhouse gas emissions and produce green fuels. Among the viable pathways, Fischer–Tropsch synthesis (FTS) stands out due to its versatility in generating suitable fuels. The FTS process, however, presents several challenges: it is highly exothermic ($\Delta H^{\circ}_{n} = -165 \text{ kJ/mol CO}$), kinetically controlled, and strongly influenced by temperature in terms of product selectivity. To efficiently utilize distributed feedstocks (i.e. carbon oxides and hydrogen), miniaturization and redesign of conventional reactor technologies become essential. A promising approach involves integrating thermally conductive structured internals into cooled tubular reactors [1]. Such internals, based on periodic open cellular structures (POCS), offer a controlled geometry and can be packed with catalyst pellets, enabling a large catalyst inventory and enhanced heat management [2]. In

fact, thanks to the open design offered by 3D printing techniques, adoption of conductive internals boosts the heat removal from the reactor core toward the external coolant. Aluminium POCS with a skin [2,3] recently emerged as strong candidates for such applications, combining mechanical integrity with excellent thermal

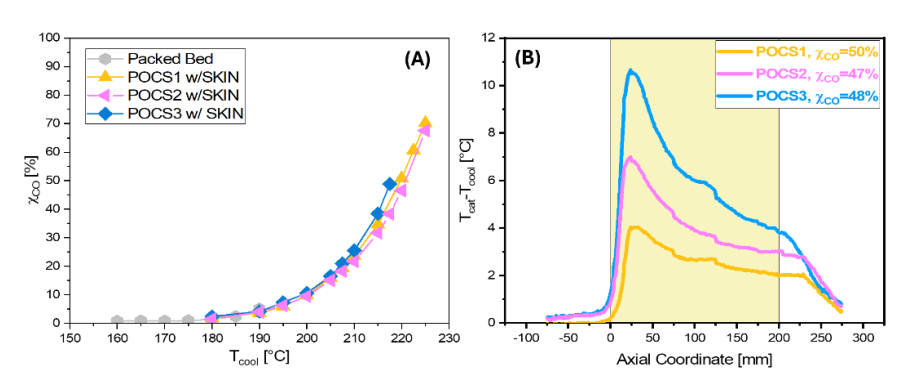


Fig. 1. (A) CO conversion in packed bed reactor and with Al packed POCS, (B) axial T-profiles in FTS reactor loaded with different Al packed POCS

performance. In this study we assess the effect of POCS geometry (porosity, cell density, clearance with tube wall) on the operation of a compact pilot-scale FTS reactor. We show that tailored designs allow single-pass CO conversions exceeding 70% (Fig. 1A), heat duties around 1 MW/m³, and C_5^+ productivities up to 0.35 kg/kg_{cat}/h. The appropriate design of the conductive structured internals impacts the axial temperature profiles, with reduced gradients as the overall heat transfer coefficient grows to 1.3 kW/m²/K, Fig. 1B.

- 1. F. Kapteijn, J. Moulijn, *Cat. Today* **2022**, 383, 5-14
- 2. L. Fratalocchi, G. Groppi, C.G. Visconti, L. Lietti, E. Tronconi, Cat. Today 2022, 383, 15-20.
- 3. C.G. Visconti, M. Panzeri, G. Groppi, E. Tronconi, Chem. Eng. Journal 2024, 481, 148469.
- 4. M. Bracconi, M. Ambrosetti, M. Maestri, G. Groppi, E. Tronconi, CEPPI 2020, 158, 108169.

Shaping of a methanol catalyst: Parameter study of the tableting of CuO/ZnO/ZrO₂

F. Neumann, M. Herfet, S. Grewe, L. Warmuth, T.A. Zevaco, T.N. Otto, M. Zimmermann, S. Pitter, M. Wolf Institute of Catalysis Research and Technology (IKFT), Karlsruhe Institute of Technology (KIT), Eggenstein-Leopoldshafen, Germany.

Abstract

Methanol is a crucial base chemical and has additional potential as a chemical hydrogen carrier. While today, it is mainly produced from fossil fuel-generated synthesis gas, green hydrogen and CO₂ could be used in future. Cu/ZnO/ZrO₂ (CZZ) has been identified as a promising catalyst. While the focus in catalysis research in academia is mainly on the synthesis and catalytic performance of powdered catalysts, application in industrial reactors requires a scalable synthesis and shaping of the catalyst into bodies. Here, additional properties, such as pressure drop and mechanical stability, also become important. Although the scale-up into technical bodies is crucial in catalyst development, it is mainly driven by industry and partly governed by empirical knowledge, leading to a lack of in-depth understanding in the open literature. [3,4]

Herein, a scientific approach towards catalyst shaping using a highly instrumented tableting machine is presented. The effect of various tableting parameters as well as the addition of the lubricant graphite on the tableting behaviour and mechanical stability of a co-precipitated CuO/ZnO/ZrO₂ catalyst were investigated. Selected catalyst tablets were thoroughly characterized and tested for methanol synthesis.

The tableting behaviour and mechanical stability of the catalyst were mostly insensitive towards the tableting parameters, such as the compaction profile, except for the compaction pressure. Here, increasing pressures led to an increased stability up to moderate pressures. Afterwards the stability plateaued and showed a lower reliability. Variation of the content of the lubricant graphite revealed a trade-off between a facilitated tableting process and high mechanical stability. Detailed characterization of tablets of varying density revealed a loss of porosity and shift of the pore size distribution. Additionally, a change of the reduction behaviour was observed. A lower reduction rate of the tablets, likely induced by mass transport limitations, is expected to facilitate the formation of Cu₂O during temperature-programmed reduction. The effect of mass transport limitations was also clearly observed during pulsed N₂O titration. Reduction led to size reduction and had a negative effect on the mechanical stability. However, most of the tablets remained stable during the reduction and during more than 1000 h time on stream in the methanol synthesis. Tablet density showed the expected effect on catalytic performance, which additionally showed a significant dependence on the reaction conditions.

References

- [1] S. Navarro-Jaén et al. Nat. Rev. Chem. 2021, 5, 564-579.
- [2] S. Wild et al., React. Chem. Eng. 2021, 6, 868-887.
- [3] S. Mitchell, N.-L. Michels, J. Pérez-Ramírez, Chem. Soc. Rev. 2013, 42, 6094-6112.
- [4] J.T. García-Sánchez, V.G. Baldovino-Medrano, Ind. Eng. Chem. Res. 2023, 62, 7769-7838.

Towards Sustainable Ethene Production: Modified Fischer-Tropsch Synthesis from CO₂ and H₂

K. Laichter, A. Chowdhury, V. Hagen, T. Liese, M. Doeker, F. Buschsieweke,

- J. Hannes, F. Heck, H.-J. Woelk, I. J. Graef, T. E. Müller^{1,*}
- ¹ Carbon Sources and Conversion, Ruhr-Universität Bochum
- ² RUBOKAT GmbH, Bochum
- ³ RWE Power AG, Essen
- ⁴ Heraeus Precious Metals GmbH & Co. KG, Hanau

Abstract

Ethene is a central base chemical at the foundation of numerous petrochemical value chains. However, its conventional production via steam cracking involves high fossil energy consumption and substantial CO_2 emissions. This study addressed this challenge by investigating a modified Fischer-Tropsch synthesis (mFTS) process for the direct conversion of CO_2 and 'green' hydrogen into ethene and light alkenes (C_2 - C_6). Unlike classic FTS, which predominantly yields long-chain hydrocarbons, this approach emphasizes tailored catalyst and process design to selectively generate light alkenes.

Evaluating Ru- and bimetallic Ru/Fe-based catalysts for their performance revealed that the incorporation of a basic component is critical for enhancing alkene selectivity. Experimental studies in a laboratory-scale tubular reactor highlighted the influence of temperature, residence time, and feed composition on conversion and selectivity. Reaction conditions were optimized to maximize alkene yield, supported by detailed kinetic analyses, including determination of activation energies and rate constants. Aspen Plus™ simulations incorporating reactor kinetics provided the foundation for scenario analysis and virtual scale-up. To guide future process design, life cycle assessments were conducted and environmental impacts evaluated, with a focus on global warming potential. Although current process configurations are less ecologically favorable than steam cracking, the analysis shows that, under idealized conditions using renewable hydrogen and CO₂ from direct air capture, a *cradle-to-gate* carbon-negative ethene process is achievable.

Embedding mFTS into a broader carbon capture and utilization infrastructure supports the development of closed carbon cycles, from renewable syngas production to downstream separation and integration with olefin polymerization. This system-level approach highlights the strategic integration of reaction engineering, separation technologies, and renewable energy systems. These findings contribute to the design of integrated value chains for circular carbon utilization in the process industry. Furthermore, the simulation framework developed in parallel enhances process understanding by linking experimental data with predictive digital twins, offering a scalable pathway from laboratory-scale insights to industrial implementation. This integrated approach strengthens the role of ethene as a sustainable carbon vector in a future net-zero economy.

Introduction

The chemical industry is one of the most important sectors of the German economy and, at around 12.5%, contributes significantly to national greenhouse gas (GHG) emissions. ¹ Ethene is an important raw material: around 4.8 million tons are produced in Germany every year, most of which is processed into polyethylene and numerous other intermediate products. However, the production of alkenes is associated with substantial GHG emissions. Each ton of ethene currently causes 1.21 tons of CO₂ emissions (ecoinvent, EU).² For propene, the figure is 1.24 tons of CO₂ per ton of product, and for mixed butenes, 1.28 tons of CO₂ per ton. At the end of the value chain, the products manufactured from these raw materials are mostly thermally recycled, ultimately leading to a predominantly linear process chain (Fig. 1).



Fig. 1: Current linear value chain of carbon-containing chemical products.

Ethene and other light alkenes are conventionally produced by steam cracking, an energyintensive process associated with high emissions that alone accounts for around 3.5% of industrial GHG emissions in Germany. Alternative routes, methanol-to-olefins (MTO) and modified Fischer-Tropsch synthesis (mFTS), have so far faced technological limitations: The MTO process chain is multi-stage and includes equilibrium-limited steps, leading to high recycle streams. In contrast, mFTS is constrained by the insufficient selectivity of currently available catalysts.3

Against this backdrop, the goal of this study 4 was to develop new catalyst formulations and to identify a process window that enables higher selectivities and yields for the conversion of CO₂ to ethene and other light alkenes up to hexene (C_2-C_6) . Using multifunctional catalysts based on highly active noble metals, the process was tested in continuous operation, and the reaction conditions were optimized. In addition, an ecological assessment was carried out to estimate the environmental benefits of the Fig. 2: Targeted closed carbon loop for technology.



ethene and other light alkenes (C2-C6) 5

A key element of the concept is transition from a linear value chain to a closed carbon cycle (Fig. 2 6): At the end of their lifetime, carbon-containing products are sorted; recyclable fractions are reused, while mixed or heavily contaminated plastic fractions are subjected to pyrolysis or gasification.⁷ This generates synthesis gas consisting of carbon dioxide (CO₂), carbon monoxide (CO) and hydrogen (H₂), which can serve as feedstock for mFTS. Biogenic residues can likewise be converted into synthesis gas through pyrolysis or gasification and tapped as a renewable carbon source. In combination with green hydrogen from sustainable sources,8 this approach enables the establishment of a closed carbon cycle. Against the backdrop of the global search for climate-neutral production processes and the declining availability of fossil raw materials, the study addresses one of the key challenges faced by industry: the transformation from linear to circular carbon utilization.

Experimental

Catalysts were supplied by Heraeus Noble Metals and are designated according to the scheme Na content / Ru content / Fe content / support material (Table 1). Supports included silica SiO₂, alumina Al_2O_3 , and SiO_2 - Al_2O_3 mixed oxides. Powder and pelletized forms were tested. Basic characterization included BET surface area, pH, water content, and packing volume. Selected catalysts were further analyzed by SEM/EDX for morphology and elemental distribution, and by ICP for composition before and after the reaction.

Table 1: Catalyst formulations with composition and basic characterization.

Designation		Nominal composition				Basic characterization				
	Na⁺	Ru	Fe	Cupport	H ₂ O	BET	рН	PV		
	[wt.%]	[wt.%]	[wt.%]	Support	[wt.%]	[m ^{2.} g ⁻¹]	[-]	[ml·g ⁻¹]		
0.5/5/-/SiO ₂	0.50	5	_	SiO ₂	n.d.	235	9.1	4.55		
0.2/8/-/SiO ₂	0.19	8.15	_	SiO ₂	n.d.	235	9.1	4.55		
0.5/5/-/SiO ₂ -Al ₂ O ₃	0.5	5		SiO ₂ -Al ₂ O ₃		235	7.9	2.16		
-/5/-/Al ₂ O ₃	_	5	_	Al ₂ O ₃	4	155	4.6	1.34		
-/5/0.5/Al ₂ O ₃	_	5	0.5	Al ₂ O ₃	4	135	8.1	1.21		
0.3/5/0.5/Al ₂ O ₃	0.3	5	0.5	Al ₂ O ₃	5.46	135	9.5	1.26		
1/5/0.5/Al ₂ O ₃	1	5	0.5	Al ₂ O ₃	6.07	130	10.30	1.27		
2/5/0.5/Al ₂ O ₃	2	5	0.5	Al ₂ O ₃	3.14	125	11.4	1.23		
3/5/0.5/Al ₂ O ₃	3	5	0.5	Al ₂ O ₃	3	125	10.9	1.03		
3/5/0.5/pellets	3	5	0.5	Al ₂ O ₃ -pellets	n.d.	125	10.1	0.3		

Al₂O₃, aluminum oxide; SiO₂, silicon oxide; BET, specific surface area according to Stephen Brunauer, Paul Hugh Emmett, and Edward Teller; PV, packing volume (bulk density)

Catalytic performance was first screened by temperature-programmed methods (TPSR, TPX) developed at Rubokat GmbH. Measurements were carried out with linear heating ramps (10 $\text{K}\cdot\text{min}^{-1}$, room temperature to 400 °C) in CO/H_2 or CO_2/H_2 mixtures, with online mass spectrometry for product analysis.

Selected formulations were subsequently tested under continuous operation (Table 2). Experiments were conducted in a tubular fixed-bed reactor at 10–20 bar with feed gases CO/H_2 and CO_2/H_2 at varying ratios (typically H_2/CO_x = 2:1 to 3:1) and gas hourly space velocities (GHSV) between 1,200 and 6,000 ml_N g_{Cat}^{-1} h⁻¹. The temperature range investigated was 250–360 °C. Long-term tests up to 24 h were carried out to assess stability and identify deactivation. Product compositions were analyzed by gas chromatography (GC), quantifying hydrogen, carbon monoxide, carbon dioxide, and alkenes and alkanes up to C₆. Nitrogen or argon was used as internal standards.

Table 2: Selected experimental series for catalyst evaluation in the conversion of CO₂/CO/H₂-mixtures to alkenes; catalysts are designated according to the scheme Na content / Ru content / Fe content / support material; the contents is given in wt.%.

	Facus	Carbon	GHSV	р	Т	H ₂ :CO _x -Ratio
Catalyst	Focus	source	[ml _N g _{Cat} -1 h-1]	[bar]	[°C]	[mol:mol]
-/5/-/Al ₂ O ₃	T-dependence	CO ₂	6,000	65	330-410	3
-/5/-/Al ₂ O ₃	T-dependence	CO	6,000	10	140-200	2
-/5/-/Al ₂ O ₃	Residence time	CO	4,000 - 12,000	10	200	2
-/5/-/Al ₂ O ₃	Partial pressure	CO	6,000	10-40	200	2
-/5/0.5/Al ₂ O ₃	T-dependence	CO	1.200	10	250-350	2/1
-/5/0.5/Al ₂ O ₃	Partial pressure	СО	1.200	10	250	5/1, 3/1, 2/1, 1/1, 1/2
0.3/5/0.5/Al ₂ O ₃	T-dependence	CO	3000	20	290-330	2
1/5/0.5/Al ₂ O ₃	T-dependence	CO	3000	20	290-330	2
2/5/0.5/Al ₂ O ₃	T-dependence	CO	3000	20	290-330	2
3/5/0.5/Al ₂ O ₃	T-dependence	СО	3000	20	290-330	2
3/5/0.5/Al ₂ O ₃	Partial pressure	CO	3000	20	300	2/1, 3/1

A simulation model of the RWGS–mFTS process chain was developed in Aspen Plus® (Fig. 3), incorporating experimental product distributions and heat-integration effects. This model formed the basis for a subsequent life cycle assessment (LCA), which compared current (German electricity grid, industrial CO_2) and future (wind power, DAC) scenarios.

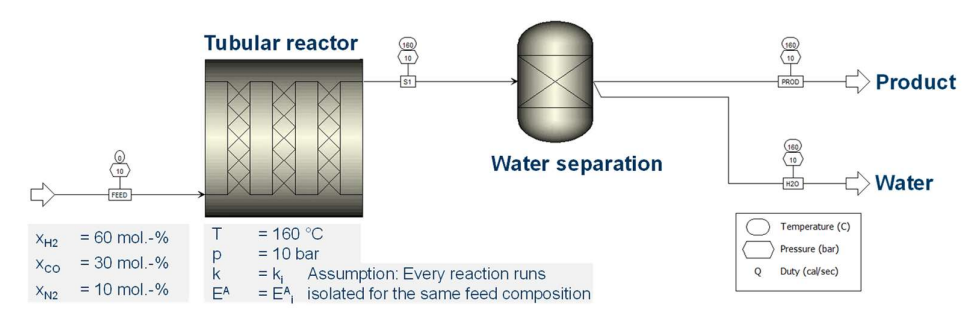


Fig. 3: Aspen Plus® process model of the RWGS-mFTS chain for ethene production.

Results and Discussion

Targeting the development of a GHG-neutral technology for the sustainable production of light alkenes, a process sequence was chosen that starts with CO_2 or synthesis gas from sustainable sources and, through gas conditioning followed by mFTS on highly active noble metal catalysts, opens a new route to produce ethene and other light alkenes (C_2 - C_6). The approach involved the use of innovative multifunctional catalysts based on ruthenium as the noble metal component, in combination with iron as dopant metal and sodium additives as promoters.

The international research landscape is currently focused primarily on Fe-based systems. Numerous studies have demonstrated their high activity in RWGS and FTS, but they are typically limited by the ASF distribution-related limitation of olefin selectivity. In addition, theoretical reviews summarize recent advances in iron oxides, carbides, and the role of alkali metals such as Na and K, which improve CO_2 adsorption and olefin release. In addition, CO_2 hydrogenation to C_2 products is positioned as a field of future interest, with particular emphasis on the high barriers to C–C coupling and the need for bifunctional catalyst concepts.

Ruthenium was chosen as the noble metal component, 11 owing to its high intrinsic activity in CO activation and C–C coupling. While there are only few previous studies on Ru-based systems, it has been shown that bimetallic systems such as Ru/Ni nanoparticles in ionic liquids exhibit significant synergy for RWGS and FTS. 12

Two reaction pathways were examined in more detail: (i) a two-stage reaction sequence with conversion of CO_2/H_2 via the reverse water gas shift (RWGS) reaction to CO/H_2 , with water separation as needed, followed by conversion of the synthesis gas to ethene and light alkenes; and (ii) direct conversion of CO_2/H_2 mixtures under Fischer-Tropsch-analogous conditions. Depending on the choice of the catalyst, the two reaction pathways may have occurred in parallel.

Catalyst Selection and Catalyst Design

In exploratory hydrogenation experiments, monometallic Ru catalysts showed very high activity with CO as feed but were essentially inactive for the conversion of CO₂ to alkenes. Therefore, the investigations were extended to bimetallic Ru/Fe catalysts, enabling the use of

 ${\rm CO_2}$ as feed or co-feed via an integrated RWGS function. Through stepwise catalyst modification and the use of alkali promoters (Na compounds), the selectivity was progressively shifted towards light alkenes (ethene, propene and other lower alkenes). Support materials investigated included silicon oxide (${\rm SiO_2}$), aluminum oxide (${\rm Al_2O_3}$), and ${\rm SiO_2}$ - ${\rm Al_2O_3}$ mixed oxides, tested in powder form. Different catalysts, varying in the choice of the support material, preparation method, metal component (Ru, Ru/Fe, Fe), and promoter were prepared and tested. The catalytic performance was first evaluated in rapid tests using ${\rm CO_2/CO}$ feeds; selected systems were subsequently tested under high-pressure conditions in continuous operation.

The morphology of all catalysts was evaluated. As an example, scanning electron microscopy (SEM) images of the $3/5/0.5/\text{Al}_2\text{O}_3$ catalyst doped with 3 wt.% Na is shown in Fig. 4. The sample exhibited a spherical core-shell structure with particle sizes between 10 and 40 μm and a homogeneous element distribution. SEM-EDX analyses performed after the reaction confirmed unchanged Na, Ru, and Fe contents compared to the initial state, indicating high stability and durability of the catalysts under reaction conditions.

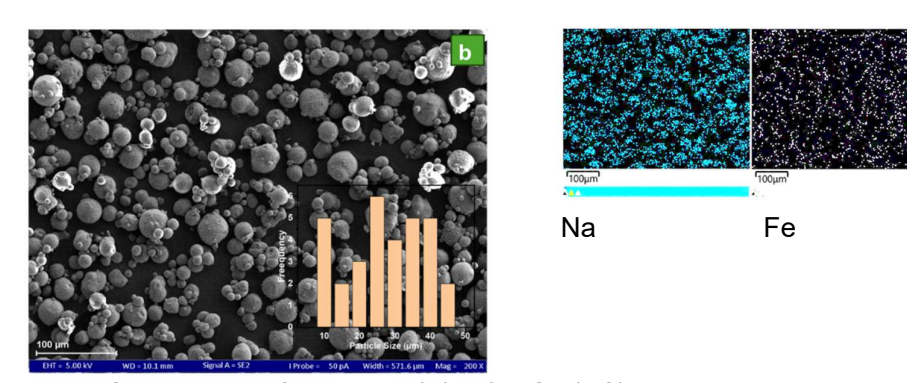


Fig. 4: SEM image of catalyst $3/5/0.5/Al_2O_3$ (left), particle size distribution (inset) and EDX element maps (right); scale bar: 100 μ m.

Ru

Rapid Testing

A rapid test method was used to assess the potential of catalyst samples for the synthesis of ethene and light alkenes from synthesis gas. Two suitable temperature-programmed methods were identified and an analytical method based on online mass spectrometry was simplified to such an extent that it could be operated stably and provided all the essential information for evaluating the catalysts in terms of activity and selectivity.

Temperature-programmed reaction (TPX) provides results that are close to the measurement conditions of technical reaction control and consider, for example, the influence of the partial pressures of the reactants. Here, TPX was carried out with a linear heating ramp of 10 K·min⁻¹ from room temperature to 400 °C in a mixture of H₂: CO of 5:1. This method yielded important insights into the interactions of various by- and coupling products on the reaction kinetics. The influence of methanol, as a representative of oxygenates, and water, as a by-product of the selective reaction step, was investigated.

Temperature-programmed surface reaction (TPSR) uses a pre-coating of the catalyst surface with a reactive component, followed by subsequent linear heating of the sample in the presence of at least one other reactive component, to shed light on the reactions taking place on the catalyst surface. This method was applied to determine the appropriate reaction parameters (including temperature) and enhance the general understanding of the reaction mechanism, including the identification of the carbon source in Ru-catalyzed ethene synthesis).

The TPSR measurement on $-/5/-/Al_2O_3$ (Fig. 5) showed that CH₄ as well as C₂- and C₃-hydrocarbons are formed from adsorbed CO on the surface in contact with H₂ from the gas phase. This also occurs in the presence of mixtures of CO and CO₂. Unreacted CO_x can be circulated, and a suitable CO content restored by means of the RWGS reaction. As can be seen from Table 3, CO₂ was practically unreactive.

Table 3: TPSR results: Desorption maxima and desorbed quantities with –/5/–/Al₂O₃ after pretreatment with CO, CO₂, or a CO/CO₂ mixture for experimental verification of the formation of CH₄, C₂-, and C₃-species.

Desorbed species	Desorption	Desorbed quantity after pretreatment with							
	maximum		со		CO/CO ₂				
	[°C]	[a.u.]	[%]	[a.u.]	[%]	[a.u.]	[%]		
C ₂ H ₄	159 - 162	1.09	0.87	1.59	1.10	0.017	0.05		
C ₂ H ₆	164 - 170	0.52	0.42	0.76	0.53	0	0		
C ₃ H ₆	150 - 151	0.05	0.04	0.09	0.06	0	0		
C ₃ H ₈	153 - 157	0.23	0.18	0.27	0.19	0	0		
CH ₄	182 - 183	123.16	98.49	141.90	98.12	33.07	99.94		
Total	_	125.05		144.61		33.09			

Another important finding from the TPSR measurement was that the selective reaction to the target product C_2H_4 takes place on the Ru catalyst at low temperatures (< 200 °C). This is probably the first time that it has been shown that the formation temperatures of C_1 -, C_2 -, and C_3 -hydrocarbons on the catalyst are different. This is a key finding for understanding the selectivity of the reaction. Mechanistically, this highly interesting observation is consistent with the idea that electron-deficient compounds such as carbocations are present at the carbon in the reactive transition state.

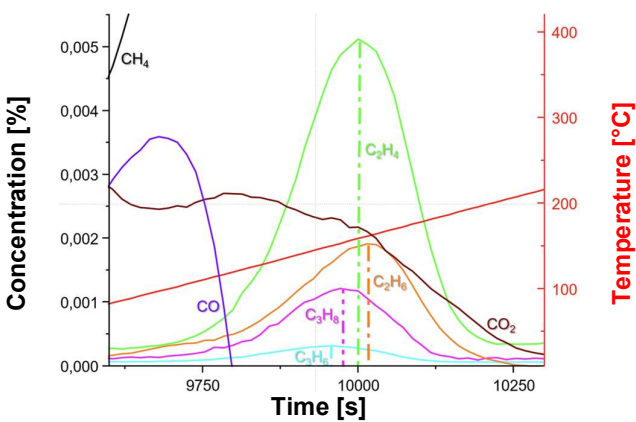


Fig. 5: TPSR of $-/5/-/Al_2O_3$ catalyst pretreated with CO/H₂ at 30°C, showing CH₄, C₂-, and C₃-hydrocarbon formation from adsorbed CO.

The TPX measurements were compared with stationary data (Table 4). The left column shows the reference case with a CO/H_2 feed (1:5). In this experiment, the formation of all products decreased significantly within a relatively short period of time, indicating catalyst deactivation. This effect was much more pronounced when CO was replaced by methanol as the carbon source (middle column). Although methanol also reacts to form ethene, it more strongly promotes the formation of other products such as dimethyl ether. The strong deactivation observed with methanol in the feed suggests that methanol contributes significantly to catalyst coking.

Table 4: TPX results: Desorbed quantities and temperature of desorption maxima (TP_{max}) with $-/5/-/Al_2O_3$ under different feeds after 1 h *time-on-stream* at 215 °C for experimental verification of the role of intermediately formed methanol. DME = dimethyl ether.

	CO:H ₂ = 1:5		CH₃OH:	H ₂ = 1:5	CO:H ₂ = 1:5 + 1% H ₂ O		
Species	Conc.	TP _{max}	Conc.	TP _{max}	Conc.	TP _{max}	
	[ppm]	[°C]	[ppm]	[°C]	[ppm]		
C ₂ H ₄	133	201	75	210	127	158	
C ₃ H ₆ ⁺	292	480	49	272	346	311	
CH₃OH	126	1223	-		152	158	
DME	10	119	1170	4140	13	11	

If methanol and other oxygenates contribute to deactivation, the key to prevention is either to avoid the methanol formation by catalyst modification or to suppress its re-adsorption. The latter was achieved by adding a small amount of water (1%) to the feed gas. This strategy exploits the similar adsorption properties of water and methanol in terms of competitive adsorption. Both molecules compete for active sites that enable protolytic cleavage of adsorbates. For thermodynamic reasons, the protolysis of water is much easier than that of methanol and other alcohols. Therefore, even a small amount of water can effectively block alcohol adsorption.

The data in the right-hand column exemplify that the concept of competitive adsorption works well to suppress deactivation: all carbon-containing products have much smaller concentration differences between the TPX maxima and the stationary values after one hour. Long-term measurements confirmed that the positive effect of water addition almost completely suppressing deactivation also persists over extended periods (24 h).

Temperature Control

The TPSR results showed that the reaction temperature has a decisive influence on the selectivity of light hydrocarbons. In real reactors, however, temperature gradients can develop within the catalyst bed. Investigations in the study demonstrated that design measures such as improved isothermicity and preheating of the reactor feed can reduce these gradients and significantly increase selectivity. Figure 6 compares product distributions in the non-optimized reactor (left) and in the reactor with improved isothermicity (right), both at the same target temperature. Improved isothermicity led to a distinctly different distribution, with higher yields of alkenes and lower methane formation. The results suggest that future studies should systematically explore isothermal operation and control of reaction exothermicity.

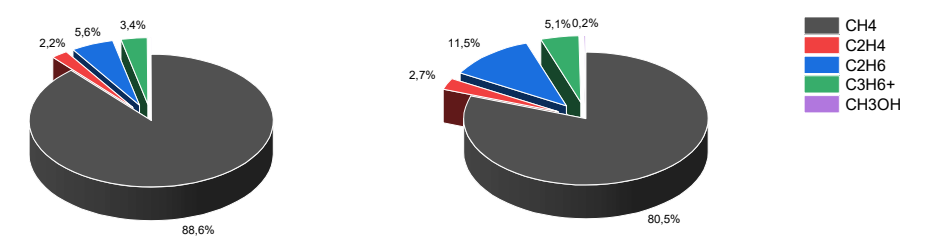


Fig. 6: Effect of reactor isothermicity on product distribution: non-optimized (left) *vs.* optimized profile (right).

Contribution of Rapid Testing

In addition to its analytical value for deepening our understanding of global kinetics, the TPX method has also been successfully used as a screening method. Since this method delivers

results very quickly (usually a sample result within 24 hours), the influence of different *in* situ pretreatment temperatures was also investigated. An influence of the pretreatment temperature (between 400 and 700 °C) was observed. Surprisingly, in the most active sample $(-/5/-/Al_2O_3)$, an increase in product formation of approximately 20% was observed when the temperature was increased from 400 to 600 °C. Other samples (e.g., many Na-doped samples) reacted to temperatures higher than 400 °C with a loss of activity. The latter is of great importance for practical reaction control to avoid temperature peaks.

Fig. 7 shows the systematic progress made in optimizing ethene yield (through insights gained regarding reaction control) on the catalyst $-/5/-/Al_2O_3$ which was achieved through a clever combination of transient temperature-programmed methods (TPSR and TPX) as well as other transient methods (switching experiments) and stationary measurements. All measurements show results from the rapid test apparatus at atmospheric pressure. Here, the reaction temperature was first optimized, then deactivation was controlled by adding water, and finally the catalyst pretreatment was optimized. Finally, the catalyst loading (gas hourly space velocity, GHSV) was optimized.

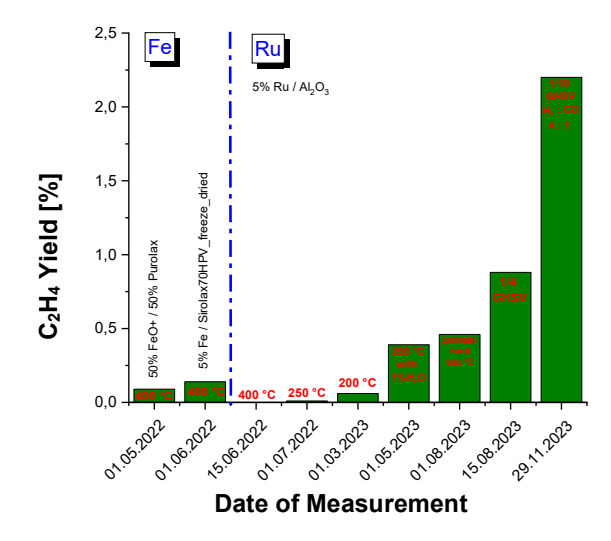


Fig. 7: Stepwise improvement in C_2H_4 yield on $-/5/-/Al_2O_3$ catalyst using TPX/TPSR rapid tests and stationary experiments.

Structure-Property Relationships

Systematic investigations into structure-property relationships were conducted to better understand the catalyst samples intended for scale-up and to narrow down the relevant operating parameter range for their use.

The two samples listed in Table 5 were given special consideration for this purpose. The catalyst $-/5/-/Al_2O_3$ proved to be the most active catalyst in terms of C_2H_4 formation observed to date in temperature-programmed measurements (TPX). The catalyst $3/5/0.5/Al_2O_3$ was the most efficient Na-doped catalyst to date and is characterized by a significantly higher selectivity than $-/5/-/Al_2O_3$. This applies not only to ethene formation (C_2H_4) but also to the formation of higher products (C_3H_6+). The latter indicates the influence of the iron component, which will be investigated further. The tests were carried out under standardized conditions with CO/H_2 (5:1) as the reaction gas and a linear heating ramp. C_3H_6+ denotes the sum of the detected C_3 species and higher olefins (e.g., propene, butene), measured as integral signal intensity in the mass spectrometer. The values are the peak maxima during the temperature ramp.

Table 5: Hydrocarbon formation in TPX rapid tests for selected catalysts in dependence of pretreatment temperature (*in situ* under H₂/He) and elemental composition of the catalysts measured by ICP.

Catalyst	Pre-treatment	Signal	intensity	(max.)	Composition		
	temperature	C ₂ H ₄	C ₂ H ₆	C ₃ H ₆ +	Na	Ru	Fe
	[°C]	[ppm]	[ppm]	[ppm]	[%]	[%]	[%]
-/5/-/Al ₂ O ₃	600	149	289	307	0.024	3.86	0.024
3/5/0.5/Al ₂ O ₃	400	87	54	93	3.26	3.76	0.46

The apparent activation energies (E_a) for the hydrogenation of CO in mFTS were determined experimentally (Fig. 8). The evaluation was based on a series of experiments in the temperature range from 280 to 330 °C at constant pressure and GHSV. The Arrhenius plot yielded an apparent activation energy of 63.8 kJ·mol⁻¹ for CO conversion, a value that lies within the typical range of heterogeneous catalytic reactions and indicates a kinetically controlled mechanism. The observed temperature dependence reflects the activation energy of the RWGS reaction with subsequent C–C coupling. Comparable literature values (60–80 kJ·mol⁻¹) support the plausibility of the data obtained. For the formation of alkenes and alkanes of different chain lengths, the activation energy is comparable within the error limits, indicating a common rate-determining reaction step. It is striking that the activation energies for the iron-doped catalyst are lower than for the non-doped reference catalyst, indicating the beneficial influence of iron on the reaction kinetics. Overall, the results demonstrate good reactivity of the catalyst combination investigated in the technically relevant temperature range.

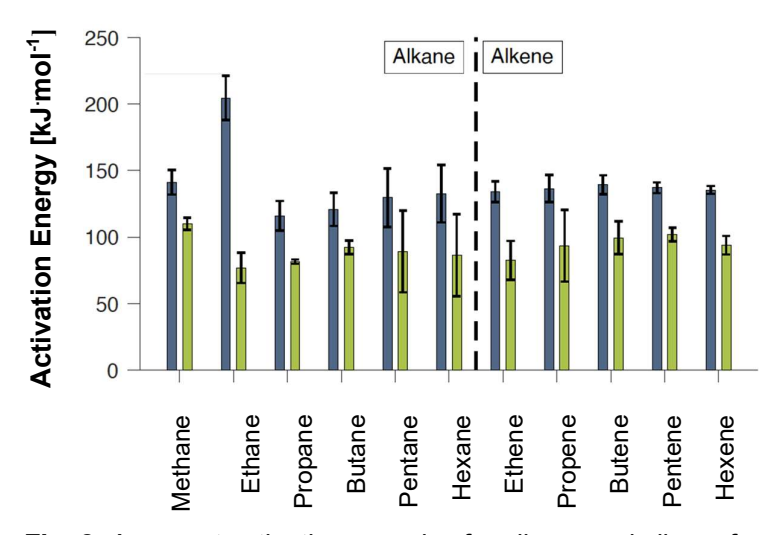


Fig. 8: Apparent activation energies for alkene and alkane formation in CO hydrogenation over Ru catalysts (95% confidence intervals).

Optimization of Alkali Doping in High-Pressure Experiments

Detailed evaluations of kinetic measurements for the scale-up candidate $3/5/0.5/Al_2O_3$ showed that it is not sufficient to effectively prevent hydrogenation of alkenes. Particularly at high conversions, over-hydrogenation to ethane markedly limits the achievable yield. Figure 9 summarizes the consistent trend observed in the ethene/ethane ratio across various experiment series. Regardless of pressure, temperature, or residence time, a satisfactory ratio could only be achieved at low CO conversions. This highlights a clear need for further optimization of alkali doping to reduce over-hydrogenation. Since total C_2 -hydrocarbon yields $(C_2H_4 + C_2H_6)$ of almost 10% were achieved, addressing this limitation will be a decisive factor in enabling economically viable operation in the future.

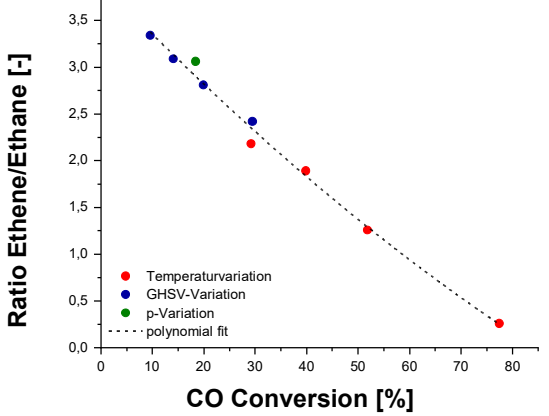


Fig. 9: Ethene/ethane ratio as a function of CO conversion from different experimental series.

Influence of Sodium as a Promoter

Next, the influence of basic sodium compounds as a promoter was explored. A series of catalytic tests were carried out at a constant space velocity (GHSV) of 3000 ml_N·g_{Cat}⁻¹·h⁻¹ and a pressure of 20 bar. Figure 10 shows the temperature dependence of CO conversion for the investigated catalyst series.

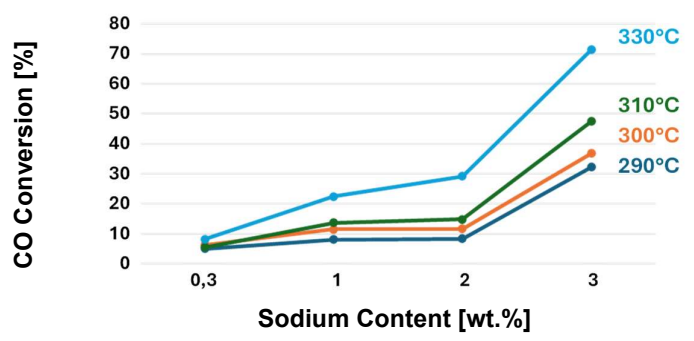


Fig. 10: Influence of sodium content and temperature on CO conversion over Ru/Fe/Al₂O₃ catalysts.

At 290°C, increasing the sodium content from 0.3% to 3% led to a significant increase in CO conversion from around 5% to 32%, underscoring the positive promoting effect of sodium even at moderate temperatures. At 330°C, the catalyst with 3% sodium achieved a CO conversion of around 72%, significantly outperforming all other compositions. These results illustrate the synergistic relation between sodium content and optimal temperature selection.

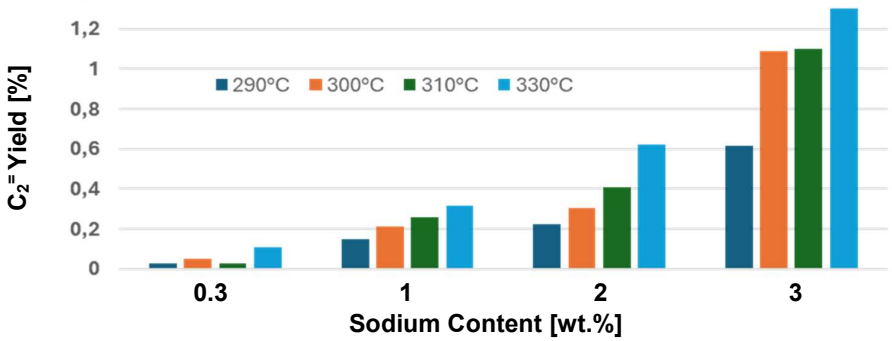


Fig. 11: Influence of sodium content and temperature on ethene yields over Ru/Fe/Al₂O₃.

Analysis of product distribution illustrates the influence of sodium content on selectivity toward alkenes and on the chain length of the products formed (Fig. 11). At a Na content of 0.3%, the formation of C_2 – C_6 alkenes was severely limited, while addition of just 1% Na significantly improved selectivity. The highest yield of C_2 – C_6 alkenes was observed at 3 wt.% Na and 300°C, accompanied by an improved ratio of alkenes to alkanes. Even at a higher temperature of 330 °C, the formation of alkenes remained high, but the selectivity decreased slightly, indicating secondary reactions or incipient sintering of the catalyst.

Ethene selectivity and yield were greatly increased by sodium doping and the selected temperature (Fig. 12). The highest selectivity was obtained at 300°C with the 3/5/0.5/Al₂O₃ catalyst, while the highest yield was observed at 330°C.

The catalyst $3/5/0.5/Al_2O_3$ was identified as the most efficient formulation in terms of CO conversion, selectivity, and yield. Long-term stability tests at 300° C showed a stable CO conversion of 31.3% over several hours of operation.

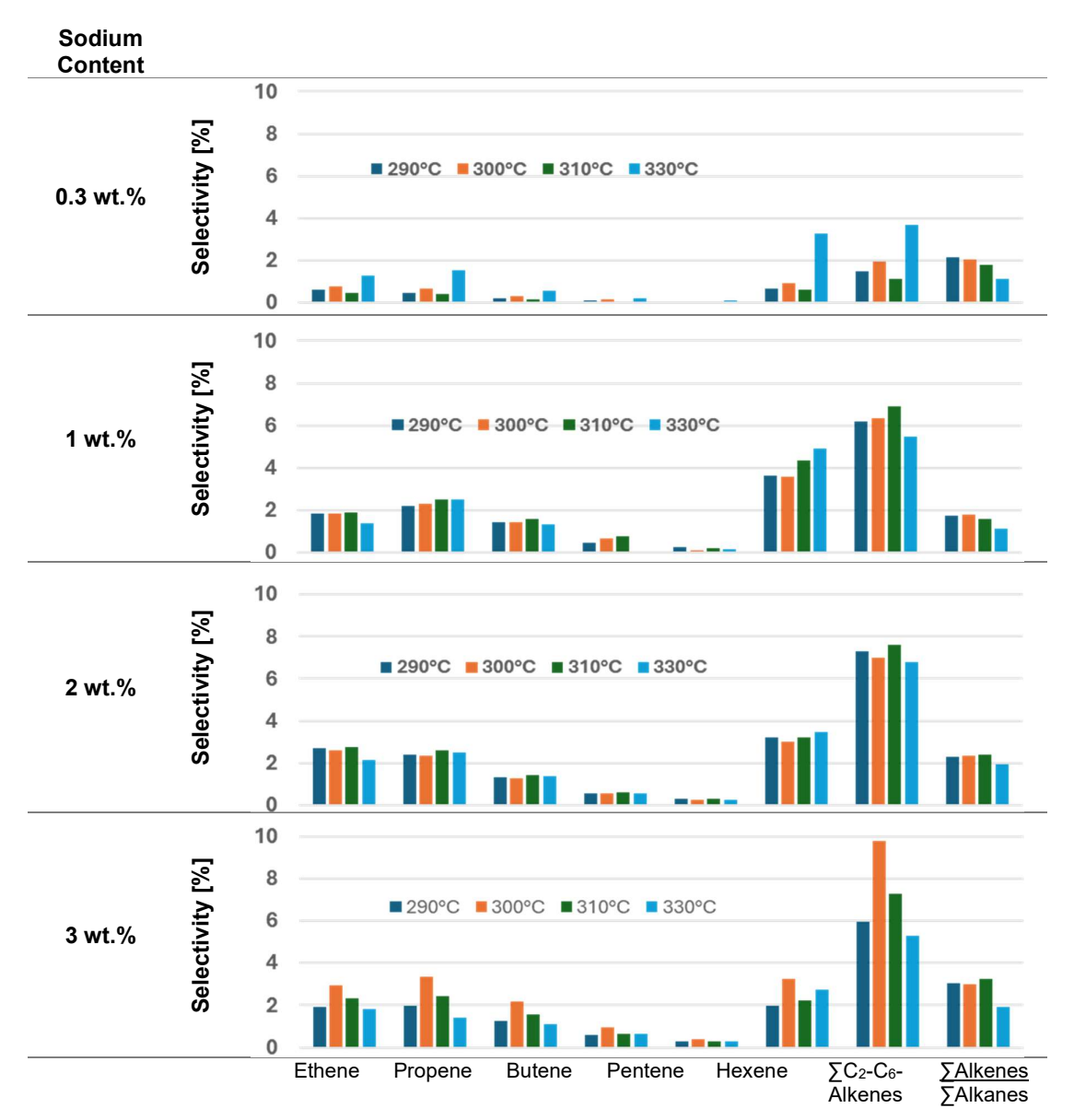


Fig. 12: Influence of sodium content and temperature on the alkene chain length distribution over Ru/Fe/Al₂O₃.

Influence of the Support Material

Last, but not least, the influence of the support was explored. SiO₂-supported catalysts have been described in the literature as promising for the synthesis of alkenes from synthesis gas (CO + H₂).¹³ In our experiments, the reported high activity and selectivity were confirmed; however, pronounced formation of higher-molecular-weight waxes was also observed. To counteract this effect, a mixed oxide-supported catalyst was prepared (0.5/5/–/SiO₂-Al₂O₃). In a long-term test under constant conditions (260 °C, H₂: 140 ml_N min⁻¹, CO: 70 ml_N min⁻¹, N₂: 6 ml_N min⁻¹), significant wax formation occurred. The results indicate that aluminum oxide represents the most robust support material, owing to its low tendency toward wax formation.

Furthermore, the performance of the shaped catalyst was investigated in comparison to powder samples, with the aim of further narrowing down the optimal operating conditions. First, the shaped body was tested in the temperature range from 290 to 330 °C after activation at 450 °C at 20 bar. In the subsequent test, activation was carried out at 400 °C. At a reaction temperature of 300 °C, the H_2 /CO ratio was systematically varied in the range from 3:1 to 2:1, followed by a gradual reduction of the space velocity (GHSV) from 3000 to 1200 ml_N g⁻¹ h⁻¹. The same measurement program was applied with the powder catalyst to ensure direct comparability. Building on the findings, the optimal operating range ("sweet spot") was specifically approached. It was noted that the shaped catalyst performed better than the powder catalyst at a higher hydrogen concentration.

Sodium-doped Bimetallic Ru/Fe-Catalysts

For the catalyst 3/5/0.5/Al₂O₃, a comparison was made between the rapid test results and stationary measurements under high pressure (20 bar). This clearly confirms the trend observed in the rapid testing regarding the Na content. For the comparative presentation (Fig. 13), the highest C₂H₄ concentrations observed during the tests were equated to be able to assess the trend. The positive effects of sodium doping on alkene selectivity was confirmed under high-pressure operating conditions. The comparison shows that the positive influence of Na is slightly more pronounced in the stationary high-pressure measurements than in the rapid testing at atmospheric pressure.

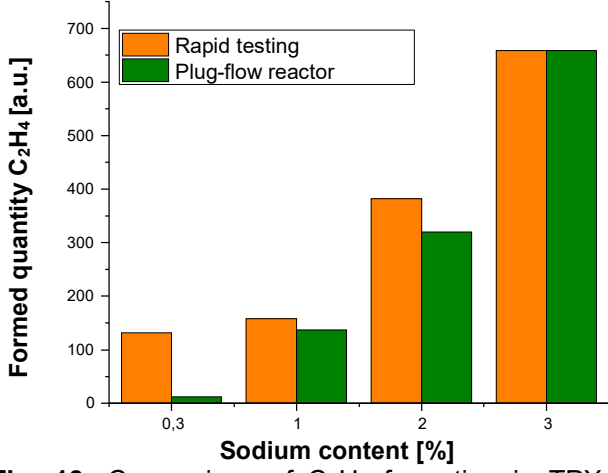


Fig. 13: Comparison of C_2H_4 formation in TPX rapid tests and stationary high-pressure experiments for sodium-doped Ru/Fe/Al₂O₃ catalysts (0.3/5/0.5/Al₂O₃, 1/5/0.5/Al₂O₃, 2/5/0.5/Al₂O₃, 3/5/0.5/Al₂O₃).

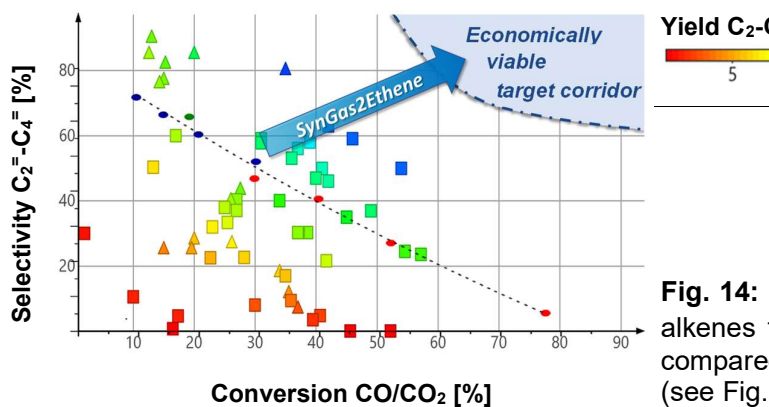
State of the Art, Process Simulation, and Life Cycle Assessment

According to the current state of the art, ethene together with other light alkenes is mainly produced by steam cracking. This process requires temperatures of 750–900 °C, is highly

energy-intensive, and causes substantial CO₂ emissions due to the necessary heat supply and complex cryogenic separation operations.

Two alternative routes to produce alkenes from synthesis gas have been investigated. In MTO, CO_2/H_2 is first converted in multiple stages to methanol and dimethyl ether before the target products are formed *via* a rearrangement to alkenes. This route is equilibrium-limited and requires high recycle flows. The second option is mFTS, in which CO/H_2 or CO_2/H_2 mixtures are converted directly to alkenes, typically after an upstream RWGS step. Both processes have shown limited selectivity and yields to date: while MTO is constrained by its multi-stage character, the maximum ethene yield of mFTS remains below 40%. Accordingly, the technology readiness level (TRL) is about 7 for MTO and 3–4 for mFTS.

The results of this study show that Ru/Fe-based catalysts in combination with alkali additives can achieve an ethene/ethane ratio of up to 3.5, corresponding to an ethene selectivity of about 78%. The results therefore exceed the typical limitations of mFTS and define a new target corridor for the selective production of C_2 alkenes (see Fig. 14).



Yield C₂-C₄ [%]
5 10 15 20 25

Fig. 14: Selectivity and yield of C_2 - C_4 alkenes for MTO (\triangle) and mFTS (\square) compared with results from this study (see Fig. 9, dashed line)

A process simulation of the modified Fischer-Tropsch synthesis (mFTS) was created in Aspen Plus®, covering the complete chain from CO₂ and H₂ supply ¹⁴ through the RWGS reaction and the mFTS stage to product separation. Experimental product distributions were implemented; heat-integration effects were included in the model. The simulation shows that electricity demand is dominated by electrolysis, while the exothermicity of the reaction provides sufficient heat to cover external requirements (e.g., for *direct air capture*, DAC). The model forms the basis for the subsequent life cycle assessment and supports the evaluation of the process chain in terms of energy efficiency, CO₂ intensity, and scalability.

The LCA (Fig. 15) evaluates the global warming potential (GWP100, *cradle-to-gate*) for 1 kg of ethene produced *via* mFTS under two scenarios: (i) a current reference case with electricity from the German grid and CO₂ from industrial sources, and (ii) a future scenario with wind power and CO₂ from *direct air capture* (DAC).

In the reference scenario, the high electricity demand of electrolysis (here: proton exchange membrane electrolysis, PEMEL) leads to $100.7~\rm kg~CO_2$ equivalent per kilogram of ethene, with hydrogen production as the dominant source of GHG emissions. Process heat utilization and the crediting of co-products (other hydrocarbons, waste heat) partially reduce the footprint. In the future scenario, the GWP drops to $-2.5~\rm kg~CO_2$ equivalent per kilogram ethene, illustrating the potential for $\rm CO_2$ -neutral or even slightly $\rm CO_2$ -negative production in a *cradle-to-gate* perspective.

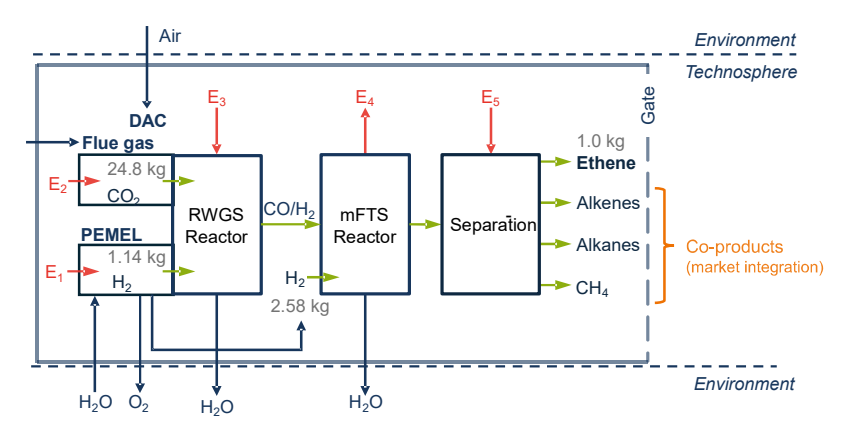


Fig. 15: Life-cycle model (GWP100, *cradle-to-gate*) for ethene production *via* mFTS under current and future scenarios.

Note: The laboratory-scale data obtained within the study are not directly comparable to industrial benchmarks due to differences in scale, energy integration, and system boundaries. The comparison to steam cracking therefore serves as an orientation, while the relevant perspective is the transition from today's fossil-based benchmark toward renewable and circular future scenarios.

The analysis demonstrates that the environmental footprint of mFTS is determined primarily by the energy source for hydrogen production,⁸ and the origin of the CO₂. This conclusion aligns with our earlier work on the role of CO₂ and H₂ supply chains.¹⁵ Due to the spatial distribution of renewable energy sources, renewable hydrogen has to be supplied over long distances that is often covered by pipelines.¹⁶ Under idealized conditions with high selectivity for ethene, the GWP can be reduced to as low as -2.5 kg CO₂ equivalent per kg ethene (*cradle-to-gate*). This clearly underscores the transformative potential of this technology for sustainable alkene production (Fig. 16).

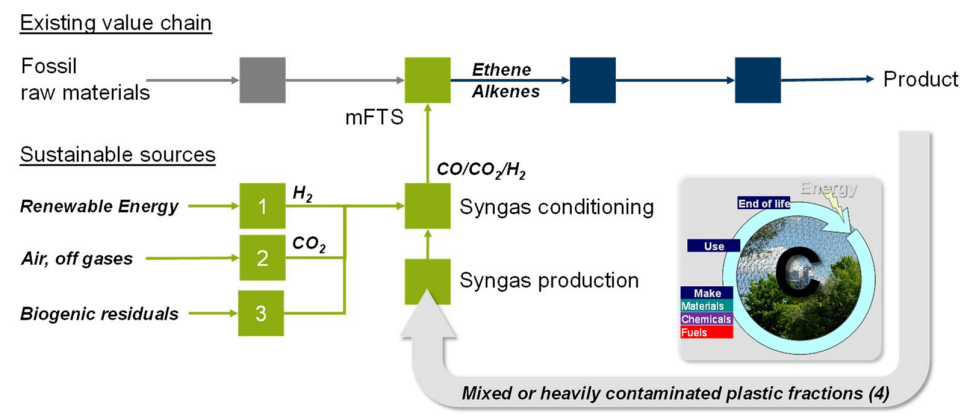


Fig. 16: Chemical industry value chain with process steps (squares) and associated material and energy flows (arrows), showing integration of hydrogen production by water electrolysis (1) and sustainable raw material sources (2-4) *via* syngas and mFTS (green).

Conclusions

Can ethene, a key petrochemical traditionally produced by fossil-based steam cracking, be made greenhouse-gas-neutral from CO_2 and renewable H_2 ? To address this question, two complementary process routes were investigated: (a) a two-stage pathway *via* reverse watergas shift to CO/H_2 followed by a modified Fischer–Tropsch synthesis to light alkenes, and (b) single-stage direct conversion of CO_2/H_2 under FTS-analogous conditions. Catalyst

development centered on ruthenium-based systems with high intrinsic catalytic activity. Multifunctionality was introduced by iron doping, while alkali promotion tuned selectivity. Rapid temperature-programmed testing methods enabled high-throughput screening and provided first structure—property insights. The most promising catalysts were validated in a continuously operated lab reactor with attention to operando temperature control. In parallel, process simulation and life-cycle assessment benchmarked both routes against steam cracking and evaluated their integration into closed carbon cycles. The overarching goal was to establish a new process window for sustainable ethene production as a building block in the transformation of the basic materials industry towards climate neutrality.

Innovative temperature-programmed methods, temperature-programmed surface reaction (TPSR) and temperature-programmed reaction (TPX), were developed and implemented as rapid catalyst screening tools. These transient methods allowed for systematic testing of catalyst libraries within hours, in contrast to the much longer times required for conventional steady-state experiments. TPSR enabled mechanistic insight by probing surface reactions of pre-adsorbed species under controlled heating in reactive atmospheres, thereby distinguishing carbon sources and identifying the formation pathways of C_1 – C_3 -hydrocarbons. TPX, by mimicking near-technical conditions with controlled heating ramps, provided quantitative trends in activity, selectivity, and deactivation behavior under relevant syngas feeds. Together, these methods yielded first structure–property relationships, for example, clarifying the role of sodium promotion in shifting selectivity toward light alkenes and identifying conditions under which methanol formation accelerates catalyst deactivation. The approach thus not only accelerated the identification of promising formulations but also provided guidance for rational catalyst optimization in subsequent continuous reactor tests.

Ruthenium-based catalysts exhibited the anticipated high catalytic activity but utilized only CO as a carbon source, whereas iron-based catalysts could also activate CO_2 . This motivated the design of bimetallic Ru/Fe systems, combining both functions. For single-stage CO_2/H_2 conversion, the presence of an iron component proved essential. Work on the catalytic conversion of CO and CO_2 with H_2 to light alkenes in a continuously operated reactor aimed to optimize selectivity and activity through promoter addition and structural variation of the catalysts. Key features identified include:

- Bimetallic catalysts tuned with an alkali-metal component proved particularly promising.
 A formulation with 3 wt.% Na, 5 wt.% Ru, 0.5 wt.% Fe on Al₂O₃ achieved high CO conversion up to 82% with good selectivity toward ethene and other light alkenes.
- Alloying of the metallic ruthenium component with iron significantly improved both activity and selectivity, especially under CO₂ feeds.
- Sodium promotion increased alkene formation at moderate temperatures (250–330°C) but also led to enhanced methane formation and accelerated catalyst deactivation at higher temperatures.
- SiO₂-supported catalysts, as reported in the literature, showed high activity and selectivity but suffered from excessive formation of higher molecular weight waxes, making Al₂O₃ the more robust support.

The catalytic performance proved highly temperature-sensitive, with only a narrow window favoring alkene formation. Both monometallic Ru and Na/Ru/Fe/Al $_2$ O $_3$ catalysts showed that formation of alkenes increased with temperature up to a threshold, beyond which methanation became predominant. The identified narrow temperature window underlines the need for precise thermal control in technical operation. Continuous reactor studies established optimal conditions in the range of 250–330 °C at 10 bar, with a feed composition of H $_2$ /CO = 2/1 and a gas hourly space velocity of 1200 ml $_N$ gCat $^{-1}$ h $^{-1}$, providing the best compromise between activity and selectivity.

The ecological assessment emphasized both the challenges and the long-term potential of the concept. When assessed under today's boundary conditions, laboratory-scale operation, industrial CO₂ sources, and electricity from the German grid, the specific carbon footprint of ethene remains significantly higher than that of conventional steam cracking, which typically emits around 1.2 kg CO₂ equivalent per kilogram of ethene. In contrast, an idealized *cradle-to-gate* scenario based on renewable electricity (wind power) and CO₂ from direct air capture points to the possibility of a CO₂-negative balance of up to –2.5 kg CO₂ equivalent per kilogram of ethene. Since the products can be recycled back into syngas at the end of their lifetime, the process offers a pathway toward fully climate-neutral olefin value chains.

This study has demonstrated that the direct production of ethene from CO_2 is feasible, scalable, and compatible with closed-loop carbon utilization. The results achieved in the study contribute to establishing Ru/Fe-based catalysts as a promising alternative to the dominant Fe catalysts. The combination of catalyst innovation, rapid testing methodologies, and system-level analysis provides a blueprint for future process development. The results highlight that light alkenes (C_2 - C_6) from CO_2 -containing streams can make a meaningful contribution to the climate-neutral production of base chemicals. Beyond the scientific advances achieved, establishing a sustainable olefin platform in Germany and Europe that integrates catalyst design, process development, and ecological assessment will be essential. Looking ahead, research must address long-term catalyst stability, optimized promoter strategies, and pilot-scale validation, with the broader goal of embedding such processes into international net-zero value chains and strengthening the role of ethene as a sustainable carbon vector in a future circular economy.

Abbreviations

ASF - Anderson-Schulz-Flory (distribution)

CCU - Carbon Capture and Utilization

CSC - Carbon Sources and Conversion (chair at RUB)

DAC - Direct Air Capture

EDX - Energy-Dispersive X-ray Spectroscopy

GHG - Greenhouse Gas

GHSV - Gas Hourly Space Velocity

GWP100 - Global Warming Potential, 100-year horizon

ICP - Inductively Coupled Plasma (analysis)

LCA – Life Cycle Assessment

MTO - Methanol-to-Olefins

mFTS - modified Fischer-Tropsch synthesis

PEMEL - Proton Exchange Membrane Electrolysis

RWGS - Reverse Water-Gas Shift

SEM - Scanning Electron Microscopy

TPX – Temperature-Programmed Reaction

TPSR – Temperature-Programmed Surface Reaction

TRL – Technology Readiness Level

Acknowledgements

The financial support of the Bundesministerium für Forschung, Technologie und Raumfahrt (BMFTR) for the study Syngas2Ethene (grant number 01LJ2107A) is gratefully acknowledged. Additional funding from the State of North Rhine-Westphalia (grant number IRR-2018-1), RWE Power AG, and the Faculty of Mechanical Engineering, Ruhr-Universität Bochum, as part of the endowed chair Carbon Sources and Conversion (CSC), is also gratefully acknowledged. T.E.M. further thanks Prof. M. Dröscher for valuable scientific discussions on energy and raw material supply for the chemical industry and on production pathways for base chemicals.

References

_

- ³ J. Liu, J. Feng, Y. Gao, Y. Han, C. Xu, Recent advances hydrogenation of carbon dioxide to light olefins and liquid fuels via modified Fischer–Tropsch pathway, *ACS Omega* 9, 256102 (2024).
- For further information concerning the BMFTR-funded project Syngas2Ethene, see https://www.fona.de/de/massnahmen/foerdermassnahmen/KlimPro/SynGas2Ethene.php, Heraeus Noble Metals: Gemeinsames Forschungsprojekt zur nachhaltigen Herstellung von Ethen, https://www.ls-csc.ruhr-uni-bochum.de/csc/projekte/syngas2ethene.html.de
- ⁵ RWE Power AG, VERENA Gasification processes with integrated surplus electricity integration, Niederaußem multifuel gasifier pilot plant, Niederaußem Innovation Center, 2021.
- ⁶ Heraeus Noble Metals, Joint research project on the sustainable production of ethene, 2019.
- ⁷ T. E. Müller, Green Approaches to Polyurethane Sourcing and Carbon Management, in A. Buettner, E. Weidner, Springer Handbook of Circular Plastics Economy, 2025, 213-234.
- ⁸ M. Hermesmann, T. E. Müller, Green, turquoise, blue, or grey? Environmentally friendly hydrogen production in transforming energy systems, PECS 90, 100996 (2022).
- ⁹ H. Tang, T. Qiu, Y. Wang, X. Liu, A brief review of recent theoretical advances in Febased catalysts for CO₂ hydrogenation, *Molecules* 29, 1194 (2024).
- R.-P. Ye, J. Ding, W. Gong, M. D. Argyle, Q. Zhong, Y. Wang, C. K. Russell, Z. Xu, A. G. Russell, Q. Li, M. Fan, Y.-G. Yao, CO₂ hydrogenation to high-value products via heterogeneous catalysis, *Nat. Commun.* 10, 5698 (2019).
- ¹¹ T. E. Müller, Catalysis with Ruthenium for Sustainable Carbon Cycles in Y.-F. Chang, Ruthenium Materials Properties, Device Characterizations, and Advanced Applications, 2023. https://doi.org/10.5772/intechopen.112101
- M. I. Qadir, F. Bernardi, J. D. Scholten, D. L. Baptista, J. Dupont, Synergistic CO₂ hydrogenation over bimetallic Ru/Ni nanoparticles in ionic liquids, *Appl. Catal. B* 252, 10 (2019).
- ¹³ H. Yu, Y. Han, J. Xu, Y. Yang, Z. Tian, Z. Ren, W. Ding, J. Lin, Direct production of olefins from syngas with ultrahigh selectivity, *Nat. Commun.* 13, 5967 (2022).
- M. Hermesmann, C. Tsiklios, T. E. Müller, The environmental impact of renewable hydrogen supply chains: Local vs. remote production and long-distance hydrogen transport, *Applied Energy*, 351, 121920 (2023).
- T. E. Müller, Supply Chains for Hydrogen and Carbon Dioxide for Sustainable Production of Base Chemicals, in Á. Bányai, Supply Chain Perspectives and Applications, 2023. https://doi.org/10.5772/intechopen.114031
- C. Tsiklios, M. Hermesmann, P. Stumm, T. E. Müller, Comparative analysis of hydrogen vs. methane pipeline transport systems with integrated methane pyrolysis for low-carbon hydrogen supply, *Applied Energy*, 383, 125276 (2025). https://doi.org/10.1016/j.apenergy.2025.125276

¹ R. Geres, A. Kohn, S. Lenz, F. Ausfelder, A. M. Bazzanella, A. Möller, Roadmap Chemistry 2050, VCI, 2019.

ecoinvent Association (2022): ecoinvent 3.9.1 Database. Zurich, Switzerland. https://ecoinvent.org

Enzyme-Inspired Gel Materials: Tuneable Gels for Hydroformylation

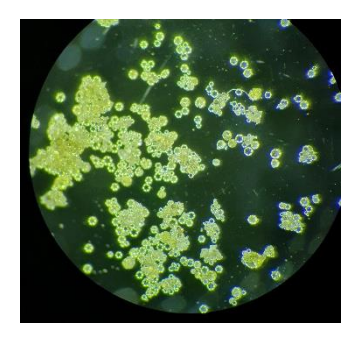
Peter McNeice¹, Walter Leitner^{1,2}, Andreas J. Vorholt¹

Abstract

In nature, many reactions are performed by multiple enzymes, and therefore multiple active sites working in tandem.¹ Gel materials consist of a solid matrix with a liquid phase dispersed throughout it. The solid matrix can be polymer, molecular, or colloidal, while the liquid phase can be organic (organogel), aqueous (hydrogel) or ionic liquid (ionic liquid gel). Both components can be selected to form a designer material. Furthermore, metal catalysts can be entrapped within gels, which can enhance their activity and facilitate their reuse.^{2,3}

We present the synthesis of novel gels, with entrapped metal catalysts (See Figure). We vary the solid and liquid phases, as well as the entrapped metal catalyst, building functionality into each component of the material. This allows the active site of the gels, along with their morphology, to be tailored for a specific reaction, or multiple reactions, thereby mimicking enzymatic processes. The gels show promising activity for hydroformylation reactions.





Examples of different catalyst gels prepared in this work.

¹ Max Planck Institute for Chemical Energy Conversion

² RWTH Aachen University

¹ Zhang, X.; Li, G.; Chen, G.; Wu, D.; W. Y.; James, T. D. Enzyme Mimics for Engineered Biomimetic Cascade Nanoreactors: Mechanism, Applications, and Prospects. *Adv. Funct. Mater.* **2021**, *31*, 2106139.

² Craythorne, S. J.; Anderson, K.; Lorenzini, F.; McCausland, C.; Smith, E. F.; Licence, P.; Marr, A. C.; Marr, P. C. The Co-Entrapment of a Homogeneous Catalyst and an Ionic Liquid by a Sol–gel Method: Recyclable Ionogel Hydrogenation Catalysts. *Chem. Eur. J.* **2009**, *15*, 7094-7100.

³ McNeice, P.; Reid, A.; Imam, H. T.; McDonagh, C.; Walby, J.; Collins, T. J.; Marr, A. C.; Marr, P. C. Designing Materials for Aqueous Catalysis: Ionic Liquid Gel and Silica Sphere Entrapped Iron-TAML Catalysts for Oxidative Degradation of Dyes. *Environ. Sci. Technol.* **2020**, *54*, 14026-14035.

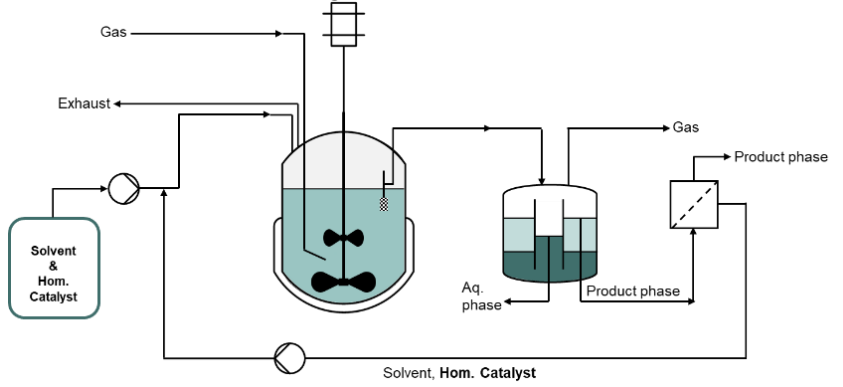
From Syngas to Alcohol E-fuels -Scale up from lab to miniplant

Hannah Stieber¹, Stephan Popp¹, Walter Leitner^{1,2}, Gonzalo Prieto³, Andreas J. Vorholt¹

- 1 Max Planck Institute for Chemical Energy Conversion, Mülheim a.d. Ruhr, Germany
- 2 Institute of Technical and Macromolecular Chemistry, RWTH Aachen University, Aachen, Germany
- 3 ITQ Institute for Chemical Technology (CSIC-UPV), Valencia, Spain

The European Green Deal aims for a climate-neutral economy by reducing greenhouse gas emissions to zero^[1]. As transport is a major emitter, replacing fossil fuels in this sector is crucial^[2]. While electrification suits private vehicles, alternatives like e-fuels are needed for heavy transport and shipping. E-fuels, made from renewable electricity and resources, are CO₂-neutral and compatible with existing combustion engines^[3].

The EU project E-TANDEM aims to realise an efficient and direct production of a new, higher oxygenate, diesel-like e-fuel for marine and heavy-duty transport. This involves the use of CO₂ as the only carbon source and renewable electricity as the only energy. The fuel is produced in a hybrid catalytic process, starting with the high pressure electrocatalytic syngas production from CO₂ and water, coupled with a tandem catalytic e-syngas conversion. The presented work focusses on this second step, the tandem reaction in which the olefin-selective Fischer-Tropsch reaction is coupled with the olefin-reducing hydroformylation to produce long-chain alcohols from the produced e-syngas. These alcohols can either be used directly as fuel or further processed.^[4] After proving the tandem reaction works in batch mode, the new e-fuel concept will now be tested in a continuous operation in a miniplant as a step toward industrial application^[5]. A key aspect is the recycling of the homogenous catalyst. Due to the high energy efficiency, the use of membranes is targeted. The concept of the miniplant is shown below.



Literature:

- [1] Europäische Kommission: Der europäische Grüne Deal, 2019.
- [2] Eurpäisches Parlament, CO₂-Emissionen von PkW, www.europarl.europa.eu, 2019.
- [3] A. Ramirez, M. Sarathy, J.Gascon, Trends in Chemistry, 2020.
- [4] E-Tandem Website, https://e-tandem.eu/, 2022.
- [5] K. Jeske, T. Rösler+, M. Belleflamme, T. Rodenas, N. Fischer, M. Claeys, W. Leitner, A.J. Vorholt, G. Prieto, Angew. Chem. Int. Ed. 2022, 61.



Funded by the European Union under grant number 101083700.

Upstream and Feedstock Requirements for Cost-Competitive Green Methanol Production

M. Checinski, R. Krähnert, H. Mehmke, J. von der Ohe C1 Green Chemicals AG

Abstract

Price is the most significant factor influencing changes in the chemical market. This is particularly true in the commodity market, where the price of raw materials is a key factor. For the majority of commodities, such as methanol, hydrocarbons, and aldehydes, the synthesis gas cost factor is the most relevant. The capital expenditure (CAPEX) may play a dominant role in the case of small plants, given the smaller scale of decentral sustainable feedstock volumes.

A willingness to pay a premium of up to twice the cost of fossil fuels for green hydrogen or green syngas-based products can be observed. Given the circumstances that only a limited number of commercial projects on relevant scales are currently operational, and many where canceled within the last years, there are some significant barriers to overcome. Regulatory pressure on sectors such as aviation and shipping has led to an artificial increase in the willingness to pay. To ensure the long-term viability of the green hydrogen and green syngas markets, it is essential to comprehensively address the technical, economic, and distribution-related challenges.

Different feedstocks require different purification processes, which in turn affects the process design and the economics of the plant. It is essential to consider the whole process from the raw material composition, impurity grade, and availability to the technical specification of the final product.

Given the pivotal role that hydrogen and, in particular, synthesis gas play in the transformation of the chemical industry, it is essential to address the key factors hindering the large-scale production of green chemicals surviving a FID (final investment decision). These factors will be discussed in that presentation.

Catalyst study for selective catalytic oxidation of residual ammonia for purification of green hydrogen from ammonia cracking

A. Sack^{1,2,3}, A. Gradel¹, H.-P. Schmid⁴, J. Wünning⁴, T. Plessing¹, A. Jess^{2,3}
¹Institute for hydrogen and energy technology, University of Applied Sciences Hof
²Chair of Chemical Engineering, University of Bayreuth
³Center of Energy Technology, University of Bayreuth
⁴WS GmbH, Renningen

Abstract

The Federal Government of Germany assigns hydrogen in its national hydrogen strategy a "[...] central role in the further development and completion of the energy transition" [1] while acknowledging that "[...] the greater part of demand will have to be covered permanently by imports of hydrogen and its derivatives." [2] Green ammonia as a hydrogen carrier will play a significant role and the Federal Ministry for Economic Affairs and Climate Action recently signed the first delivery contract for green ammonia starting 2027. [3]

To use the hydrogen after importing, the ammonia must be cracked. Due to the thermodynamic equilibrium of the reaction, the resulting product gas contains a residual amount of ammonia that must be removed for further gas separation and usage. For the operation parameters of the used industrial ammonia cracker in this project (T: $750\,^{\circ}\text{C} - 850\,^{\circ}\text{C}$, p: 10 bar) the resulting product gas contains between 850 and 1500 ppm residual ammonia. One possible technology for the purification of the product gas is selective catalytic oxidation of the residual ammonia in a second reactor after the cracker.

In this study different catalysts were used in ammonia oxidation experiments to determine their usability and performance for the proposed process. Two sets of experiments for ammonia oxidation in nitrogen and cracking gas atmosphere were undertaken to be able to compare the catalysts in the three target dimensions: maximum conversion of ammonia, maximum selectivity to nitrogen and least catalytic effects on hydrogen oxidation. While the experimental results in nitrogen fit well with literature, the results in cracking gas (75 Vol.-% H_2 , 25 Vol.-% N_2 , 1500 ppm NH_3) with stochiometric oxygen addition shows no ammonia conversion independent of reaction temperature (200 °C - 350 °C). A third study with a variation of the added oxygen amount showed promising ammonia conversion results for further use.

References

- [1] Bundesministerium für Wirtschaft und Klimaschutz (BMWK), "Die Nationale Wasserstoffstrategie", BMWi, Berlin, 2020
- [2] Bundesministerium für Wirtschaft und Klimaschutz (BMWK), "Fortschreibung der Nationalen Wasserstoffstrategie", BMWK, Berlin, 2023
- [3] Bundesministerium für Wirtschaft und Klimaschutz, "Wichtiger Schritt für globalen Deutschland 2027 Wasserstoffhochlauf importiert ab mit H2Global grüne großen [Online] Wasserstoffprodukte im Umfang", 11.07.2024. Available: https://www.bmwk.de/Redaktion/DE/Pressemitteilungen/2024/07/20240711-h2global.html.

Elevating the C₂ to C₄ Chemistry

Maurice Belleflamme¹, Frederike S. Heinen^{1,2}, Stefan Mersmann¹, Andreas J. Vorholt¹

¹ Max Planck Institute for Chemical Energy Conversion, Mülheim an der Ruhr

Abstract

In current times, implementing bio-based materials into the chemical value chain is both highly desired and necessary to reduce the greenhouse gas emissions and the carbon footprint of the sector. In this context, using bio-mass derived ethanol has received a lot of attention. Besides its direct application as a fuel additive, ethanol is increasingly recognized as a promising building block for bulk chemicals such as 1-butanol, acetic acid, and 1,3-butadiene, also from an economic perspective.

In the upgrading sequence of ethanol to value-added chemicals, the first step typically involves the dehydrogenation of ethanol to acetaldehyde. With the emerging potential of the hydrogen economy, this route might even become economically advantageous over the state-of-the-art *Wacker-Hoechst* process. Starting from ethanol derived acetaldehyde, *Guerbet* or aldol pathways follow. Despite the availability of tailor-made homogeneous catalysts, *Guerbet* reactions struggle to achieve high yields towards the respective C₄ compound. The selective aldol condensation of acetaldehyde to crotonaldehyde is equally challenging.

To overcome these challenges, we have developed an efficient, mild, selective and scalable process to convert acetaldehyde, into acetoin, using N-heterocyclic carbenes as catalyst. Acetoin, a valuable flavouring compound that is usually prepared via fermentation from various biomass sources, can be upgraded into valuable C_4 chemicals like butenes, butanediol, and dioxolanes. These value-added compounds can be used in sectors such as chemicals, pharmaceuticals, and materials.

Utilizing a chemo catalytic, solvent-free approach, we have achieved complete elimination of the need for water, enzymes, and cofactors which currently contribute to the high cost of bio-based acetoin and limit its widespread industrial use. Instead, we employ a recyclable, metal-free solid catalyst that converts acetaldehyde, which is readily available from the established bioethanol infrastructure, into acetoin in a highly selective and efficient manner. This innovation not only simplifies the acetoin purification process but also significantly reduces waste water treatment and purification costs.

In summary, we are addressing a significant gap in the current chemical production landscape by potentially making the large-scale production of acetoin both economically viable and environmentally responsible, starting from bio-ethanol derived acetaldehyde as C_2 building block. This development paves the way for its integration into a diverse array of sustainable chemical value chains, ranging from fuels and solvents to polymers and plastics.

² Institut für Technische und Makromolekulare Chemie, RWTH Aachen University, Aachen

Power2ValueChemicals: Evaluating the Suitability of CO₂-Derived CO for the Chemical Industry

Lisa Steinwachs¹, Alexander Bauer², Eva Jodat², Rüdiger Eichel², Remigiusz Pastusiak³, Elfride Simon³, Marc Kristen⁴, Robert Franke⁴, Andreas Vorholt¹

¹Max-Planck-Institut für Chemische Energiekonversion, 45470 Mülheim a.d. Ruhr

Abstract

Carbon monoxide is an essential building block in the chemical industry and is used on a large Scale. Since carbon-containing raw materials like coal, natural gas, and petroleum are to be completely eliminated from production chains as part of the defossilation of the chemical industry, new production routes are needed to provide CO in sufficient quantities as a climate-neutral feedstock. One way to achieve this while keeping the carbon cycle closed is the coelectrolysis of carbon dioxide to CO using sustainably produced electricity [1].

As part of the Power2ValueChemicals project, the Forschungszentrum Jülich plans the installation and continuous operation of a low-temperature CO2-to-CO electrolyzer developed by Siemens Energy in various operating modes. In the second part of the project, the continuous conversion of the electrolysis gas through a homogeneously catalyzed methoxycarbonylation reaction will be carried out to evaluate the economic and ecological potential of the electrolysis gas for the chemical industry. For this purpose, a mini-plant will be planned and built at the Max Planck Institute for Chemical Energy Conversion.

To ensure the continuous operation of the process, an efficient method for catalyst recycling is required. Since homogeneous catalysts are dissolved in the reaction medium, their separation and reuse pose a significant challenge for process efficiency and sustainability. Therefore, various commercially available membranes were investigated regarding their catalyst retention performance. Based on these findings, a process was designed, and a corresponding miniplant was constructed to enable the continuous operation of the reaction using the selected membrane system for efficient catalyst recycling.

Literature

[1] S. Foit, I. C. Vinke, L. G. J. de Haart, R. A. Eichel, Power-to-Syngas: An Enabling Technology for the Transition of the Energy System?, Angewandte Chemie, 2017

²Forschungszentrum Jülich IEK-9, Jülich

³Siemens Energy Global GmbH & Co KG, München

⁴Evonik Oxeno GmbH & Co. KG, Marl

Microwave-Assisted Catalytic Polymer Cracking into Hydrogen at Low Temperatures Using Ionic Liquids and Nanoparticles

K. Bürner, M. Haumann Friedrich-Alexander-Universität Chemische Reaktionstechnik

Abstract

The conversion of polymers into valuable products, including, hydrogen (H₂) and carbon, at low temperatures represents a promising approach to achieving economic feasibility in industry. This EU-funded project examines a new catalytic concept designed to enhance the efficiency of polymer cracking, with the objective of producing a high-yield H2 stream at temperatures below 300°C. Our approach is a novel catalytic concept that involves the dissolution of polymers in new high-temperature-stable ionic liquids (ILs), which should enhance the catalytic activity of the nanoparticle catalysts. The use of microwave radiation as an alternative heating method allows for rapid and uniform energy transfer to the system, which may result in lower reaction temperatures and reduced energy costs. It is anticipated that this catalytic system will yield high-purity hydrogen at lower temperatures than in conventional processes. Furthermore, the utilisation of ILs should facilitate easy catalyst recovery and reduce coking. This study proposes a novel catalytic concept that integrates the use of hightemperature-stable ILs and microwave-heated catalysts, potentially creating a more efficient and sustainable approach to polymer cracking. This approach could pave the way for the design of tailored ILs and the development of microwave-compatible catalysts that significantly enhance performance and cost-efficiency in clean hydrogen production.

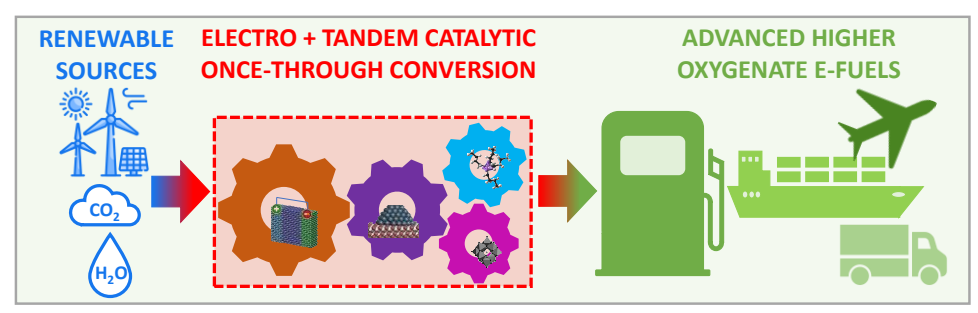
Tandem Fischer-Tropsch Synthesis and Reductive Hydroformylation under Mild Conditions for Optimized Higher Oxygenate E-Fuels

Stephan Popp¹, Hannah Stieber¹, Walter Leitner^{1,2}, Gonzalo Prieto³, Andreas J. Vorholt¹

- ¹ Max Planck Institute for Chemical Energy Conversion, Mülheim a.d. Ruhr, Germany
- ² Institute of Technical and Macromolecular Chemistry, RWTH Aachen University, Aachen, Germany
- ³ ITQ Institute for Chemical Technology (CSIC-UPV), Valencia, Spain

Abstract

The EU project E-TANDEM aims to unlock an efficient and direct production of a new higher-oxygenate diesel-like e-fuel for the marine and heavy-duty transport sector in a once-through hybrid catalytic conversion process^[1]. Using renewable electricity and resources, the production of e-fuels offers a CO2-neutral option for the energy-intensive transport sector^[2]. The process combines syngas production via co-electrolysis using CO2 and water with a tandem catalytic e-syngas conversion cou-pling the Fischer-Tropsch reaction and the reductive hydroformylation reaction to pro-duce long-chain alcohols. These alcohols can be used directly as fuel or further pro-cessed into ethers^[3]. The concept of the E-TANDEM project is shown in the figure below.



While the heterogeneous catalyzed Fischer–Tropsch and the homogeneous catalyzed hydroformylation were already successfully integrated in a tandem reaction, both the scale and the reaction conditions are not feasible for technical implementation yet. Therefore, our research is focused on operating a continuous miniplant to demonstrate the aimed reaction and the downstream processes including product separation and catalyst recycling on a larger scale. Catalyst engineering and optimization of the reaction conditions are crucial approaches to address challenges related to the technical feasibility of high pressures and undesired side product formation. This supports the potential for a synergistic collaboration between homogeneous and heterogeneous metal catalysts, ensuring efficient and selective tandem reactions.

Literature:

- [1] A. Ramirez, M. Sarathy, J. Gascon, Trends in Chemistry, 2020.
- [2] E-Tandem Website, https://e-tandem.eu/, 2025.
- [3] K. Jeske, T. Rösler+, M. Belleflamme, T. Rodenas, N. Fischer, M. Claeys, W. Leitner, A.J. Vorholt, G. Prieto, Angew. Chem. Int. Ed. 2022, 61.

Development and Enhancement of Iron-Based Catalysts to Boost the Conversion of CO₂ to Liquid Hydrocarbons

Florian Mai, Andreas Jess

Chair of Chemical Process Engineering, Faculty of Engineering, University of Bayreuth, Bayreuth, Germany

Abstract

Background and motivation.

A significant challenge in mitigating climate change is the sustainable production of liquid fuels from renewable resources. Conventional power-to-liquid (PTL) plants utilize a two-stage process: initially, CO_2 (separated from flue gases and potentially from air) and renewable H_2 are converted into CO via the reverse-water-gas-shift reaction (RWGS), followed by Fischer-Tropsch synthesis (FTS) to produce hydrocarbons. This research aims to develop iron-sintered catalysts that can perform both reactions in a single step and reactor, respectively, thereby enhancing the efficiency of the overall process. The study examines the effects of CU, CU, and CU representation on Fe-based catalysts, evaluating their activity, selectivity, and stability under various CU conversion levels.

Results and discussion.

The properties of different promoters (Cu, Zn and K) were studied by varying the temperature (210-300°C), the CO $_2$ /CO reactant ratio and the CO $_2$ conversion. All studies have identified that the FeCuZnK catalyst exhibits lowest methane selectivity and the highest selectivities to the desired long chain hydrocarbons (C $_{5+}$) and olefins. By varying the CO $_2$ /CO feed concentration, FeCuZnK was shown to be the only catalyst that is able to convert CO $_2$ in the presence of CO (up to 30 mol-%). Furthermore, FeCuZnK has been shown to suppress the direct methanation of CO $_2$. The CO $_2$ conversion profile as a function of temperature also indicates that potassium presumably inhibits the oxidation of iron carbides to iron oxides, thereby enabling higher CO $_2$ conversions which can be seen in Figure 1.

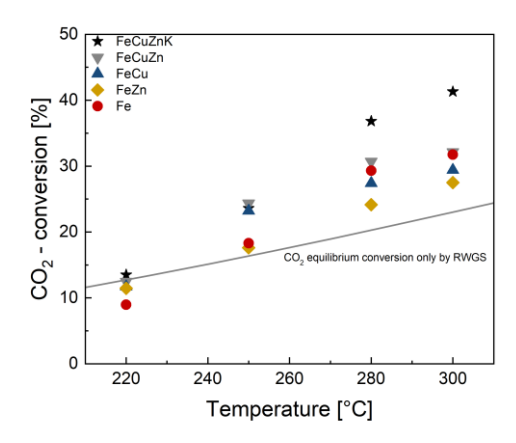


Figure 1: Achieved CO₂ conversion of each catalyst at different temperatures.

WasteWood2Fuel – Development of a technology for the decentralised synthesis of liquid fuels from solid biogenic residues

S. Kolb, C. Kern, A. Jess Chair of Chemical Engineering, University of Bayreuth

Abstract

In the context of global energy transition, synthetic fuels derived from renewable carbon sources are seen as indispensable for defossilizing sectors such as aviation, maritime transport, and heavy-duty logistics, where direct electrification is not feasible. The WasteWood2Fuel project addresses this need by developing a decentralized, modular process chain for the conversion of biogenic waste wood into synthetic fuels. The technological approach combines oxygen-enriched fixed-bed gasification, advanced gas cleaning, and downstream catalytic synthesis of methanol and Fischer–Tropsch (FT) hydrocarbons. The focus is on scalable process modules that enable regional value creation using locally available biomass and renewable electricity.

Within this project, the Chair of Chemical Engineering (CVT) at the University of Bayreuth focuses on the Fischer–Tropsch synthesis step. An oil-cooled single-tube fixed-bed reactor (30 mm ID and 1000 mm bed length) has been designed and manufactured to provide realistic thermal boundary conditions and representative flow regimes. Several catalysts are investigated experimentally with respect to CO conversion, hydrocarbon selectivity (CH $_4$ vs. C $_2$ ⁺), and temperature profile formation under varying syngas compositions and space velocities.

Complementary to the experimental campaign, a detailed reactor model has been developed. It includes coupled heat and mass balances, accounts for pressure drop as well as axial variation of molar flow due to reaction stoichiometry. The model also incorporates the dependency of radial heat conductivity and wall heat transfer coefficients on local gas velocities. These aspects have been shown to significantly impact the accuracy of predictive simulations, as demonstrated in recent work by Jess and Kern [1,2].

Validation of the model is in preparation using data from the single-tube reactor, with the goal of transferring insights to the design of market-appropriate size modules. In the long term, such systems could play a key role in securing renewable fuel supply chains for sectors with no alternative to chemical energy carriers.

References

- [1] Jess, A.; Kern, C. Significance of Pressure Drop, Changing Molar Flow, and Formation of Steam in the Accurate Modeling of a Multi-Tubular Fischer–Tropsch Reactor, Processes, 2023, 11, 3281.
- [2] Kern, C.; Jess, A. Improvement of a Multi-Tubular Fischer–Tropsch Reactor with Gas Recycle by Appropriate Combination of Axial Activity Distribution and Gas Velocity, Catal. Sci. Technol., 2023, 13, 2212–2222.

Homogenous catalyst recovery by nanofiltration for the production of a potential hydrogen carrier such as formic acid from biomass

Leon Schidowski 1, Dorothea Voß 1, Maximilian Poller 1, Jakob Albert 1

¹ Institute of Technical and Macromolecular Chemistry, Universität Hamburg, Hamburg, Germany

Abstract

Hydrogen is seen as a promising energy carrier of the future that has the potential to reduce dependence on fossil fuels and make a significant contribution to the decarbonization of global energy systems. To increase the efficiency of this concept hydrogen carrier are needed. One potential hydrogen carrier is formic acid (FA). Various integration options of FA have already been investigated like hydrogen fuel cells or direct FA fuel cells.

FA is conventionally produced by carbonylation of syngas-based methanol but can be produced sustainably from biomass via the OxFA-Process. The OxFA-process employs homogeneous polyoxometalate catalysts (POMs) to selectively oxidize biomass to FA. Using biomass as a source for hydrogen could combine utilizing waste streams with the energy system. The OxFA process could therefore be used as an alternative pathway for a future hydrogen economy.

POMs are bifunctional polynuclear metal-oxo-anion cluster characterized by a high proton mobility combined with fast multi-electron transfer and tunable redox potential. Furthermore, POMs are soluble in water, which is the most important green solvent, and exhibit resistance to hydrolytic and oxidative degradation. However, employing POMs as homogeneous catalysts, e.g. to produce FA, comes with the challenge to separate the desired products from the homogeneous POM catalyst in aqueous solution. Efficient catalyst recycling is an essential aspect for cost effective and sustainable implementation of chemical processes. Therefore, we explored the potential of nanofiltration membranes to recover the homogeneous POM catalyst. This technology is particularly promising because of their relative sustainability advantage over thermal separation processes due to their unique properties such as increased selectivity towards polyvalent ions. To establish an efficient downstream process for the recovery of the homogenous catalyst a laboratory-scale membrane system was designed, constructed and tested. Several membranes, such as polymer membranes or ceramic membranes were investigated for the recovery of different POM catalysts. In addition, the separation performance of various system components was determined by varying different process parameters.

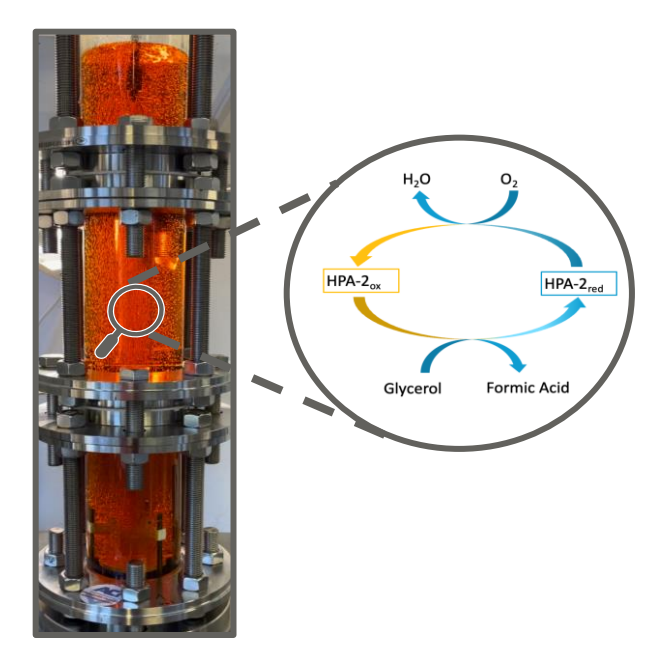
Advanced biphasic selective glycerol oxidation in a jet loop reactor using polyoxometalates

Ira Christina Wirth, Daniel Niehaus, <u>Dorothea Voß</u>, Jakob Albert Institute of Technical and Macromolecular Chemistry, University of Hamburg, Hamburg

Abstract

The selective oxidation of glycerol to formic acid is investigated using an innovative jet loop reactor (JLR) and compared with a traditional stirred tank reactor, to highlight the potential economic advantages of the JLR system. The product distribution (with formic acid being the main product) of both reactor setups is compared, with the JLR anticipated to achieve a significantly higher space-time yield.

By utilizing glycerol, a renewable by-product of biodiesel production, a promising approach for generating green formic acid from sustainable resources is introduced. Comprehensive studies on the kinetics of selective glycerol oxidation in the JLR will be shown, with an emphasis on assessing gas-liquid mass transfer characteristics, including the determination of the mass transfer coefficient and specific energy dissipation rates. The Hatta number will be determined to assess potential mass transfer limitations and the reactor's efficiency. Kinetic analyses will focus on determining reaction orders for both oxygen and glycerol. The anticipated activation energy for the reaction will be compared with typical values seen in catalyzed systems. Overall, the research aims to establish a robust foundation for sustainable formic acid production and identify key parameters necessary for scaling the process from laboratory to pilot plant settings.



Carbon-Encapsulated Magnetic Nanoparticles for Magnetocatalytic CO₂ Hydrogenation to CO

Junhui Hu, Walter Leitner, Alexis Bordet MPI für Chemische Energiekonversion Mülheim an der Ruhr

Abstract

The reverse water-gas shift (rWGS) reaction, which converts CO₂ and H₂ into CO and H₂O, offers a sustainable route to synthesis gas for low-carbon fuel production, such as Fischer-Tropsch synthesis. However, this transformation is equilibrium-limited and requires mild pressures and high temperatures (typically above 600-700 °C) to limit the formation of methane. The development of rWGS catalysts with high activity and CO-selectivity at low temperatures is highly desired, but remains challenging. In the past years, our group has shown that magnetocatalysis (i.e. the activation of magnetically susceptible catalysts via the application of an alternating current magnetic field ACMF) can enable challenging transformations under particularly mild conditions. [2.3] Herein, we hypothesize that the strong temperature gradients generated by the direct and localized ACMF-mediated heating of magnetic catalysts (i.e. hot catalyst in a cold environment) will result in substantial benefits for the conversion of CO₂ to CO, for example by allowing the quick condensation of the H₂O coproduct, thereby shifting the position of the thermodynamic equilibrium. Therefore, carboncoated iron carbide nanoparticles (ICNCs) were immobilized as magnetically-susceptible heating agents on a Cu/Al₂O₃ spinel catalyst to produce a ICNCs@Cu/Al₂O₃ multifunctional catalytic system. Under ACMF (80 mT, 350 kHz) and H₂/CO₂ (5 bar, 3/2 ratio), localized hot spots generated by ICNCs selectively activated the Cu/Al₂O₃ surface at high temperature (~ 300 °C) while maintaining a low bulk reaction temperature (~150 °C) and low pressure (~5bar). This resulted in performances (47 % CO₂ conversion, 90% CO selectivity) superior to what was observed under conventional heating at 150 °C (no reaction) or 300 °C (11.7 % conversion, 99% CO selectivity). Most interestingly, these performances lay substantially above the typical thermodynamic equilibrium given for these reaction conditions, presumably due to the condensation of H2O. This multifunctional system shows significant potential for lowtemperature rWGS reactions, paving the way for sustainable fuel and chemical synthesis. In addition, this is an important demonstration of the potential thermodynamic benefits that the localized activation by magnetocatalysis can bring.

References:

- [1] Sudipta De, A. D., Adrian Ramirez, and Jorge Gascon. Advances in the Design of Heterogeneous Catalysts and Thermocatalytic Processes for CO₂ Utilization. ACS Catal. 2020, 10, 14147–14185.
- [2] Lin, S.-H.; Hetaba, W.; Chaudret, B.; Leitner, W.; Bordet, A. Copper-Decorated Iron Carbide Nanoparticles Heated by Magnetic Induction as Adaptive Multifunctional Catalysts for the Selective Hydrodeoxygenation of Aldehydes. Adv. Energy Mater. 2022, 12 (42), 2201783.
- [3] Bordet, A.; Lacroix, L.; Fazzini, P.; Carrey, J.; Soulantica, K.; Chaudret, B. Magnetically Induced Continuous CO 2 Hydrogenation Using Composite Iron Carbide Nanoparticles of Exceptionally High Heating Power. Angew. Chem. 2016, 128 (51), 16126–16130.

Improving Reactivity in Biphasic Hydroformylation of Long-Chain Olefins

Frederike S. Heinen^{1,2}, Andreas J. Vorholt¹

Abstract

Homogeneous catalysis is gaining importance in industrial processes and complements traditional heterogeneous catalysis approaches.[1] A prominent example Ruhrchemie/Rhône-Poulenc hydroformylation process, which uses two immiscible phases: An organic phase containing the substrate and an aqueous phase containing a water-soluble rhodium catalyst complex.[2] This biphasic system allows efficient catalyst recycling without complex purification steps. While initially applied to short-chain alkenes, recent advances have shown that even long-chain, poorly water-soluble alkenes such as 1-octene can be hydroformylated under intensified mixing conditions. Evidence suggests that the reaction occurs predominantly at the interface between the two liquid phases, emphasizing the importance of understanding and controlling the interfacial dynamics in such systems. [3-5]

A high-pressure mini-plant with real-time optical imaging was used to study interfacial phenomena during the hydroformylation of 1-octene to nonanal. Image analysis revealed that nonanal formation at 40 mol% increased the interfacial area by up to 322%, but its amphiphilic nature led to accumulation at the interface, reducing its effectiveness. [3] To counteract this, β-cyclodextrins (CDs) were tested as additives. Due to their hydrophilic outer surface and hydrophobic cavity, CDs enhance solubility and stabilize hydrophobic substrates such as 1-octene through inclusion complex formation. [6, 7] At the interface, CDs promote the interaction between the olefin and the water-soluble catalyst and release the product after the reaction. [8] Although the chemical role of CDs in hydroformylation has been thoroughly documented, our investigations were the first to reveal their influence on liquid-liquid interfacial dynamics. [9] In addition to cyclodextrins, many other additives offer interesting possibilities for improving the reaction rates of hydroformylation of long-chain olefins via interface modifications. [10]

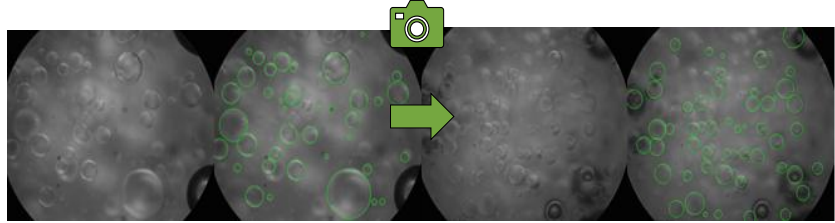


Figure 1 Sample images at the beginning (left) and the end of the hydroformylation of 1-octene and their analysis (right).

- M. Baerns, A. Behr, A. Brehm, J. Gmehling, K.-O. Hinrichsen, H. Hofmann, U. Onken, R. Palkovits, A. Renken, *Technische chemie*, John Wiley & Sons, 2013.
 A. Behr, D. W. Agar, J. Jörissen, A. J. Vorholt, *Einführung in die technische Chemie*, Vol. 120, Springer, 2010.
 M. Schrimpf, P. A. Graefe, A. Holl, A. J. Vorholt, W. Leitner, *Acs Catal* 2022, 7850-7861
 M. Schrimpf, P. A. Graefe, A. E. Kaczyna, A. J. Vorholt, W. Leitner, *Ind Eng Chem Res* 2022, 61, 2701-2713
 H. Warmeling, R. Koske, A. J. Vorholt, *Chemical Engineering & Technology* 2017, 40, 186-195
 G. Wenz, *Angewandte Chemie International Edition in English* 1994, 33, 803-822
 J. Szejtli, *Chem. Rev.* 1998, 98, 1743-1753,
 F.-X. Legrand, M. Sauthier, C. Flahaut, J. Hachani, C. Elfakir, S. Fourmentin, S. Tilloy, E. Monflier, *Journal of Molecular Catalysis A: Chemical* 2009, 303, 72
 K. E. Nalse, F. S. Heinen, N. Pawlowsky, M. Schrimpf, E. Monflier, S. Tilloy, W. Leitner, A. J. Vorholt, *Chemical Engineering Journal* 2024, 497
 F. S. Heinen, J. T. Vossen, A. J. Vorholt, *ClT*, 2025, 97, 5, 378-394

- [1] [2] [3] [4] [5] [6] [7] [8] [9] [10]

¹ Max Planck Institute for Chemical Energy Conversion, Mülheim an der Ruhr

² Institut für Technische Chemie und Makromolekulare Chemie (ITMC), RWTH Aachen University, Aachen, Germany

Continuous Reductive Hydroformylation in a Segmented Slug Flow Reactor Using a Single Catalyst Enabled by CO-Degassing

Arno Windisch, Peter Pey, Dieter Vogt and Thomas Seidensticker Laboratory of Industrial Chemistry, TU Dortmund

Higher alcohols are widely used as components for surfactants, lubricants, solvents, and plasticizers and are typically produced via heterogeneous hydrogenation of aldehydes. However, this often requires harsh reaction conditions. A more sustainable approach would be a tandem reaction, where both hydroformylation and aldehyde reduction occur under similar homogeneous conditions, reducing environmental impact.

Rhodium catalysts, known for their reducing properties in hydroaminomethylation, have the potential to efficiently catalyze this tandem process. However, carbon monoxide (CO) strongly inhibits aldehyde reduction, even at low concentrations. To overcome this challenge, existing tandem systems typically employ multiple catalysts, use significantly different reaction conditions for each step, or incorporate highly reactive monodentate alkylphosphine ligands, which in turn result in the formation of undesired branched alcohols.

We hypothesize that efficient CO removal after hydroformylation could enable conventional hydroformylation catalysts to facilitate reductive hydroformylation under otherwise similar conditions for both steps. To investigate this, we developed a continuous flow system. First, we studied CO inhibition and identified a suitable tube-in-tube capillary degassing technique. This setup was then integrated into a continuous flow reactor, where 1-octene undergoes hydroformylation, followed by the removal of residual syngas. Subsequently, hydrogen is introduced, enabling the hydrogenation of nonanal to nonanol under otherwise identical reaction conditions (Figure 1).

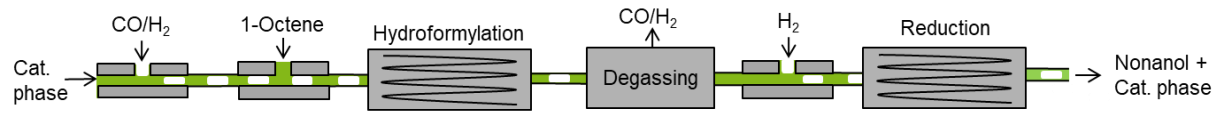


Figure 1: Schematic illustration of the continuous flow set-up.

In our feasibility study, the first-ever continuous reductive hydroformylation system with integrated CO degassing demonstrated a fourfold increase in alcohol formation compared to reactions without CO removal. The system also achieved higher product linearities and yields of up to 80%, outperforming many methods reported in the literature - even without optimization.

We expect that with further optimization and a more comprehensive kinetic and catalytic understanding, this approach could pave the way for a more efficient and sustainable alcohol synthesis process.

Synthesis of suitable catalysts to produce synthesis gas through dry reforming of methane for green kerosene

M. Bachstädter, A. Jess

Chair of Chemical Engineering, Center of Energy Technology (ZET) University of Bayreuth

Abstract

To the pivotal challenges of the 21st century belongs the problem of global warming, mainly caused by the CO₂-emissions. To face this challenge, the Federal Government of Germany has currently (2021) released a Power-to-Liquid-Roadmap. According to the current research, an electrical solution of the transport, e.g. for the transport by air, is impossible. The solution is a partly use of sustainable liquid fuels. A contribution of the development of such fuels has just started in 2023 under the project name 'PlasmaFly' [1].

Coordinated by the University of Stuttgart, several project partners, Overspeed, Infraserv Höchst, LINDSCHULTE, and the University of Bayreuth, are involved, to work on a solution for the development of sustainable kerosene out of biogas [1]. The task of Bayreuth (Chair of Chem. Eng.) focusses on the synthesis of catalysts and their characterization for the dry reforming of methane.

This endothermic reaction enables the conversion of methane and CO₂ to synthesis gas. While several noble metals allow a high reaction rate and stable performance, they are too expensive for commercial use. Promising alternatives are metals like nickel or cobalt, with the disadvantage of deactivation from carbon deposition [2].

Currently, the University of Bayreuth works on a solution for a catalyst with high performance and low deactivation rate. The process is running at high temperatures of about 800 °C and atmospheric pressure. Specific amounts of water shall help to reduce the expected amount of carbon deposition on the catalysts.

So far, first characterizations of different catalysts are showing good results for conversion rate, yield, and selectivity. The decision for a suitable catalyst is still open, but the results show a tendency to nickel-catalysts, especially because of the low reaction rate for cobalt. The final decision will be done soon, so hopefully, there will promising results until the conference.

References

- [1] NOW GmbH, Nationale Organisation Wasserstoff- und Brennstoffzellentechnologie, "PlasmaFly", BMDV, Berlin, 2023.
- [2] Budiman W. A. et al., Dry Reforming of Methane Over Cobalt Catalysts: A Literature Review of Catalyst Development. Catal. Surv. Asia, 2012, 183-197.

Development of catalyst recycling strategies for the hydroformylation of olefins using methanol as a syngas source

Jonas T. Groteguth¹, Sebastian Stahl¹, Jan Mädicke^{1,2}, Walter Leitner^{1,2}, Andreas J. Vorholt¹ Max Planck Institute for Chemical Energy Conversion, Mülheim a.d. Ruhr, Germany ² Institute of Technical and Macromolecular Chemistry, RWTH Aachen University, Aachen, Germany

Abstract

Hydroformylation of olefins is the most important homogeneously catalyzed process on an industrial scale, with a production volume exceeding 12 million tonnes per year. The resulting aldehydes can be subsequently converted into alcohols, opening up a wide range of applications.^[1] Traditionally, hydroformylation is carried out using synthesis gas; however, our group recently introduced a novel approach using methanol as a source of synthesis gas, which we termed the *methanolation* reaction.^[2]

The methanolation process is performed as an orthogonal tandem reaction using two different types of catalysts. The first catalyst, a Mn/Pincer complex, splits methanol *in situ* into synthesis gas. The second catalyst, a Rh/P complex, catalyzes the hydroformylation reaction. Additionally, the Mn/Pincer complex catalyzes the reduction of the resulting aldehyde to the corresponding alcohol, enabling the conversion of olefins into alcohols using methanol in a 100% atom-efficient manner.^[2]

In our previous work, we achieved an alcohol yield of 80% using 1-octene as substrate, with a linear-to-branched ratio of 93:7 and a turnover number exceeding 17,000 based on rhodium, all while maintaining a total pressure below 10 bar and a partial pressure of synthesis gas in the range of 1–2 bar. Furthermore, we successfully scaled up the reaction from a 5 mL laboratory scale to a 250 mL miniplant scale. [2]

Our upcoming research focuses on the development of catalyst recycling strategies to enable the transition from a batch process to a continuous process at miniplant scale. Various techniques will be considered and tested experimentally.

Literature

[1] S. Tao, D. Yang, M. Wang, G. Sun, G. Xiong, W. Gao, Y. Zhang, Y. Pan, *iScience* **2023**, 26, 106183.

[2] S. Stahl, J. T. Vossen, S. Popp, W. Leitner, A. J. Vorholt, *Angew. Chem. Int. Ed.* **2025**, 64, e202418984.

Polyoxometalates and strongly non-ideal solvent mixtures (SNISMs) towards boosting acid-catalysed esterification reactions

L. Prawitt¹, P. Figiel², C. Held², M. Poller¹, J. Albert¹

Institute for Technical and Macromolecular Chemistry, University of Hamburg, Hamburg, Germany

²Department of Biochemical and Chemical Engineering, TU Dortmund, Dortmund, Germany

Abstract

The ester substance class provides a wide variety of applications. Esters are not only used as flavouring additives but fatty acid methyl esters (FAME) won by vegetable oils and methanol (from syngas) are also used as biodiesel, which makes them ideal products of biomass valorisation. Esterification reactions are limited by their thermodynamic equilibrium. Therefore, it is one of the goals of this research work to exceed equilibrium yields calculated by classical means using the assumption that concentration and activity of all reacting components are equal.

Process economics depend strongly on the solvent and on the solvent/catalyst combination. Finding sustainable non-toxic solvents that allow high activity of the catalyst even at low temperatures is a growing field of research. Because single-component solvents usually only allow optimization of one important parameter (activity of substrates, products, catalyst or phase behaviour) this research project explores strongly non-ideal solvent mixtures (SNISMs). The focus lies on acid-catalysed esterification reactions of short-chain alcohols and carboxylic acids like formic acid, acetic acid or lactic acid at temperatures between 298 K and 323 K. With the use of tailor-made SNISMs it is possible to tune the thermodynamic activity of the catalyst and of the reacting agents. Ideally the SNISM also allows separation and recycling of the catalyst to approach more sustainable processes. Our catalysts of choice are heteropoly acids (HPAs), which are inorganic metal-oxide clusters with high Brønsted acidity. Thermodynamic modelling using ePC-SAFT advanced is used for the screening of suitable SNISMs and has successfully been applied to esterification reactions before without any catalyst. [2]

Reaction progress and kinetics were investigated using ¹H-NMR spectroscopy and Karl Fischer titration. Catalyst characterisation was performed with IR spectroscopy, thermogravimetric analysis and inductively coupled plasma optical emission spectroscopy for the pure catalyst and NMR spectroscopy (³¹P and ²⁹Si) as well as Raman spectroscopy in (reaction) solution.

Equilibrium yields and kinetics will be discussed for different alcohol-acid combinations, HPAs (Keggin and Wells-Dawson types) and varying reaction parameters (T, molar ratio of starting materials, c_{cat}). Furthermore, this experimental data will be compared to predictions calculated using ePC-SAFT modelling. Phase behaviour of reaction solutions is investigated as well as the acidity of the HPA catalysts.

Funded by the German Research Foundation (DFG) under the funding code 525252957. **References**

- [1] Raabe, J.-C. et al. ChemSusChem 2023, 16, 2013-2015.
- [2] Pabsch, D. et al. Chem. Eng. Sci. 2022, 263, 118046.

Photocatalytic processes for energy storage

S.N. Degerli¹, M. Tommasi², A. Gramegna^{1,2}, I. Rossetti^{1,2}, G. Ramis³

- ¹ INSTM Unit Milano-Università, Dip. Chimica, Università degli Studi di Milano, Milan, Italy
- ² Chemical Plants and Industrial Chemistry Group, Dip. Chimica, Università degli Studi di Milano and CNR-SCITEC, Milan, Italy.
- ³ Dip. DICCA, Università degli Studi di Genova and INSTM Unit-Genova, Genoa, Italy

Abstract

Solar energy is intermittent and fluctuating, imposing the use of energy storage to accomplish continuous exploitation. Two fundamental uphill reactions are considered: solar conversion of CO₂ to solar fuels and H₂ production by photoreforming of carbohydrates, i.e. water splitting assisted by organic molecules acting as hole scavengers (HS).

The screening of heterogeneous photocatalysts has been carried out for both reactions considering surface decoration of TiO₂ P25, in detail:

- a. 0,1% mol noble metal loaded catalyst (0,1% mol Me/P25).
- b. 1,0% wt Au_xPt_y/P25.
- c. CuO/P25 catalysts with various co-catalysts loading.
- d. 1,0% wt CuO based P25 catalysts co-loaded with metal nanoparticles (Pt and Au).

Photoreforming for H₂ production has been carried out with model carbohydrate solutions and on simulated process liquors from pulp industry. The highest H₂ productivity and glucose conversion were obtained with 0.1% mol Pt/P25, reaching a value of 4.2 mol kg_{cat}-1·h-1 and 13 % respectively. 25 to 50% lower values were obtained when reforming more complex molecules in mixture, such as liquors from pulp industry.

Photoreduction of CO₂ has been carried out at high pressure and high temperature achieving a productivity of formic acid overperforming most literature results, i.e. ca. 60 mol kg_{cat}⁻¹·h⁻¹.

The authors gratefully acknowledge the financial contribution of Fondazione Cariplo through the grant 2021-0855 – "SCORE - Solar Energy for Circular CO₂ Photoconversion and Chemicals Regeneration", funded in the frame of the Circular Economy call 2021 and of MUR funding the project RIN2022PNRR "P20227LB45 - SCORE2 - Solar-driven COnveRsion of CO2 with HP-HT photorEactor" within PIANO NAZIONALE DI RIPRESA E RESILIENZA (PNRR).

CO₂ Assisted Primary Amine Isolation and Catalyst Recycling in the Homogeneously Catalyzed Nitrile Hydrogenation and Alcohol Amination

B. Rienhoff, N. Oppenberg, F. Zolthoff, D. Vogt, T. Seidensticker TU Dortmund University, Laboratory of Industrial Chemistry, Germany

Abstract

Primary amines are of significant value as intermediates in the chemical industry. On an industrial scale, they are produced through nitrile hydrogenation with molecular hydrogen or by the conversion of alcohols with ammonia. These processes frequently yield secondary and tertiary amine side products, which necessitate energy-intensive rectification processes for separation.

Homogeneous catalysis presents a promising alternative for selective primary amine synthesis. However, it introduces challenges related to catalyst recovery during downstream processing. To address this issue, we developed a novel approach that leverages the reaction of primary amines with CO_2 to form ammonium carbamate species (Figure 1). This reversible and wastefree salt formation enables the selective crystallization of the target product from non-polar reaction solutions, followed by solid-liquid separation via filtration. The free amine is recovered from the carbamate salt through thermal CO_2 removal, while the homogeneous catalyst remains dissolved in the filtrate for direct reuse in subsequent reaction cycles.

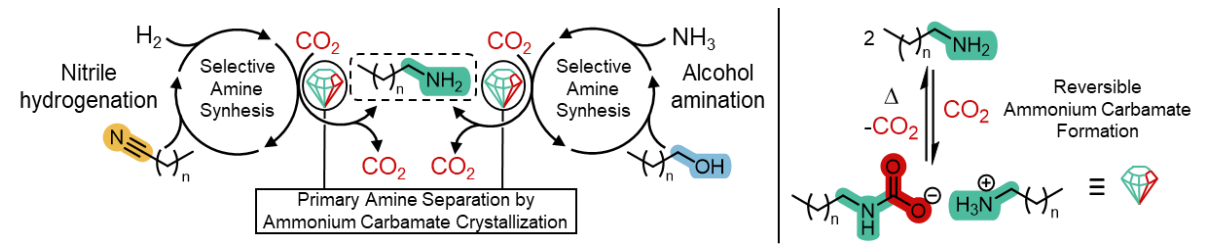


Figure 1: Illustration of the primary amine product isolation and catalyst recycling in the homogeneously catalyzed nitrile hydrogenation and alcohol amination by ammonium carbamate crystallization.

This strategy successfully achieved efficient product isolation with minimal catalyst losses in homogeneously catalyzed nitrile hydrogenation and alcohol amination reactions. Catalyst recycling was demonstrated exceeding five successive cycles for both systems, thereby emphasizing the robustness of this method. Furthermore, due to the distinctive ammonium carbamate solubilities of primary, secondary and tertiary amine species this method demonstrates additional potential in the purification of primary amines from amine mixtures.

Challenges of catalyst development for the load-flexible and integrated production of molecular hydrogen carriers from CO₂ and water

Tobias Duyster¹, Jens Artz¹, Chalachew Mebrahtu^{1, 2}, Regina Palkovits^{1, 2}

¹Forschungszentrum Jülich GmbH, Institut für nachhaltige Wasserstoffwirtschaft, Jülich, Germany

²Institute for Technical and Macromolecular Chemistry, RWTH Aachen University, Aachen, Germany

Abstract

In the context of the energy transition, molecules such as methane, methanol, dimethyl ether and ammonia are ascribed a special role as energy carriers and basic chemicals. They can also serve as hydrogen carriers, provided they are subjected to reforming or cracking prior to utilization of hydrogen. To achieve sustainable and CO2-neutral production, the utilization of renewable energy, water as a hydrogen source and CO₂ from sustainable resources (e.g. biomass or direct air capture) is preferred. However, the intermittent nature of renewable energy and dynamic material flows (e.g. waste gases, biogenic resources) poses various challenges to the overall process. Conventional chemical processes operate continuously, whereas integrating fluctuating renewable energy requires either costly storage of energy and hydrogen or load-flexible hydrogen production (e.g. via electrolysis) and chemical synthesis. Additionally, waste and recycling streams as sustainable inputs often contain impurities, which either require costly pre-treatment or robust processing technology. This in turn places high demands on the individual components of the respective technology - including the catalysts. A main challenge for catalysts in this field is their susceptibility to the byproduct water, as it may shift the equilibrium to the reactant side via the undesired water-gas shift reaction, while also causing irreversible catalyst deactivation due to water-induced sintering of the active phase. Thus, hydrothermal stability is essential. In addition, catalysts should withstand drastic changes of harsh reaction conditions, requiring both high thermal and mechanical stability especially when they are shaped into certain dimensions providing high selectivity to desired products via pellet-diffusion and controlled contact times.

Hence, this contribution addresses these challenges and provides insights into how advanced catalyst development can overcome them. In recent work, we demonstrated the importance of impurities in the gas feed and the influence of catalyst preparation for the hydrogenation of CO₂ to methane and higher alcohols.^[1,2] By integrating co-electrolysis with direct methanation, we also developed a novel concept for the production of synthetic methane from CO₂ and water.^[4] Furthermore, for the production of higher alcohols, the significant influence of promoters was demonstrated^[5], highlighting the importance of catalyst development on various levels, from nano- to meso- and microscopic scales.

- [1] J. Ren, F. Zeng, C. Mebrahtu, R. Palkovits, J. Catal. 2022, 405, 385.
- [2] J. Ren, C. Mebrahtu, L.v. Koppen, F. Martinovic, J.P. Hofmann, E. J. M. Hensen, R. Palkovits, *Chem Eng. J.* **2021**, *426*, 131760.
- [3] C. Mebrahtu, M. Nohl, L. Dittrich, S. R. Foit, L.G.J. de Haart, R.-A. Eichel, R. Palkovits, *ChemSusChem.* **2021**, *14* (*11*), 2295.
- [4] X. Xi, F. Zeng, H. Zhang, X. Wu, J. Ren, T. Bisswanger, C. Stampfer, J. P. Hofmann, R. Palkovits, H. Heeres, *ACS Sustain. Chem. Eng.* **2021**, 9, 18, 6235.

Sustainable Hydrogen Generation via Continuous Dehydrogenation of Biomass-derived Formic Acid

Tamara Hein¹, Dr. Patrick Schühle¹
¹Institute of Chemical Reaction Engineering, Friedrich-Alexander-Universität Erlangen-Nürnberg, Erlangen, Germany

Abstract

Hydrogen generation from biomass waste offers a sustainable alternative to fossil-based energy and complements intermittent solar and wind power. Today's technologies for biomass-derived H₂ production, e.g. gasification, require harsh reaction conditions. An efficient alternative involves the conversion of wet biological waste to aqueous formic acid (e.g. so called OxFA process), followed by its dehydrogenation. Temperatures below 150 °C are sufficient to release hydrogen and carbon dioxide, enabling decentralized applications^[1]. Heterogeneous Pd-based catalysts show high activity for formic acid (FA) dehydrogenation, but poisoning by the side-product carbon monoxide causes catalyst deactivation^[2].

In this study, Pd/C catalysts were evaluated in continuous aqueous formic acid dehydrogenation under different process conditions. In the gas-phase reaction, a mean formic acid conversion of 52 % and productivity of 2.8 g_{H2} g_{Pd}^{-1} min⁻¹ were achieved at 150 °C (see Fig. 1). Despite the formation of CO in an average concentration of 1269 ppm, the catalyst shows stable activity over 24 h. Catalyst deactivation was not observed, even at temperatures ranging from 130 °C to 175 °C. Thus, gas-phase reaction conditions enable stable formic acid dehydrogenation, providing a promising basis for biogenic hydrogen generation at a technical scale. Further catalyst systems will be developed, including phosphides and Pd supported on carbon nitride. The aim is to achieve higher H₂ release rates and improve

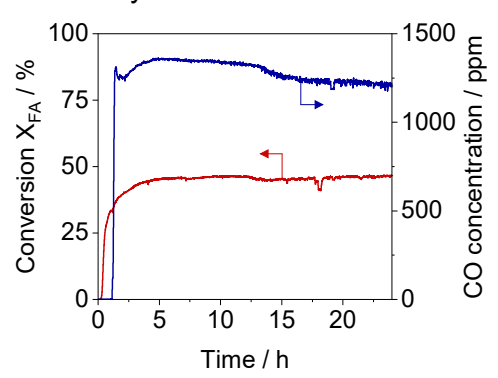


Fig. 1: Formic acid conversion and CO concentration versus time in continuous dehydrogenation. Reaction conditions: 0.1 g Pd/C (1 wt.% Pd), 150 °C, 7500 g_{FA} g_{Pd}^{-1} h⁻¹, 25 wt.% FA.

selectivity for dehydrogenation to minimize product purification for fuel cell applications.

For the process efficiency, the liquid-phase reaction is advantageous due to lower temperatures. But Pd/C showed significant deactivation in formic acid dehydrogenation at 50 °C. Therefore, alternative and modified catalyst systems will be investigated with a focus on enhanced CO tolerance. In addition, process parameters will be adjusted, including temperatures above 100 °C and pressures exceeding vapor pressure. The objective is to identify reaction conditions that suppress deactivation and enable stable formic acid dehydrogenation for sustainable hydrogen generation.

[1] Preuster, P.; Albert, J. *Energy Tech* **2018**, 6 (3), 501–509.

[2] Kosider, A. et al. Catal. Sci. Technol. 2021, 11 (12), 4259-4271.

Production of Syngas via Dehydration of Biogenic Aqueous Formic Acid coupled with the Water-Gas Shift Reaction

Emanuel Hoffmann¹, Dr. Patrick Schuehle¹

¹Institute of Chemical Reaction Engineering (CRT) at Friedrich-Alexander University (FAU) Erlangen Nuremberg

Abstract

Biomass-derived formic acid (FA) represents a promising intermediate for sustainable and renewable syngas production. Starting with the OxFA-process, which enables the partial oxidation of wet biomass into aqueous FA under mild conditions, efficient biomass utilization derived from a broad range of bio-based waste products is feasible. FA can serve as a versatile storage molecule for hydrogen (H₂) and carbon monoxide (CO), making it a promising renewable syngas source. The conversion of FA to CO occurs via dehydration using acidic catalysts, while H₂production is achieved with a second step through water-gas shift (WGS) reaction [1-2]. Figure 1 illustrates the overall concept for producing syngas from waste biomass.

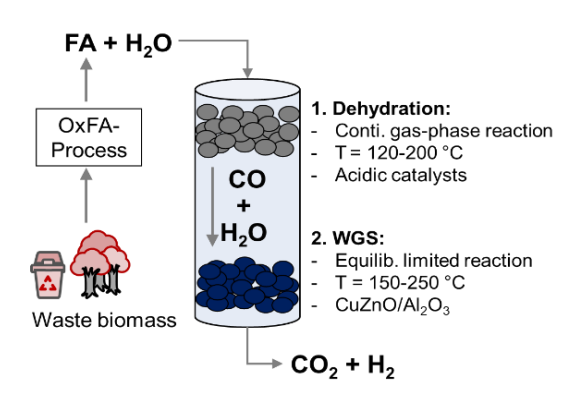


Figure 1: Illustration of the process concept of biomass valorization for syngas production via formic acid.

The presented work investigates the catalytic two-step process route for continuous syngas production from FA on a technical relevant scale by using a fixed bed reactor. In the first step, aqueous FA is dehydrated over Brønsted-acidic heterogeneous catalysts under gas-phase conditions. Experimental measurement for the dehydration already shown FA conversions up to 60 %. The high catalytic activity can mainly be attributed to the strong acidity of these materials. In addition, CO-selectivity above 98 % were achieved using catalysts such as ZSM-5 zeolites or TiO₂. In initial long-term experiments, deactivation was observed, which is likely caused by coke formation.

In the subsequent step, the conversion of formic acid via dehydration will be coupled with the water-gas shift (WGS) reaction. To this end, various catalyst systems will be investigated, focusing on high activity and catalyst stability. In order to achieve significant activity at temperatures below 200 °C, ultra-low temperature WGS catalysts based on the Supported lonic Liquid Phase (SILP) concept will be tested $^{[3]}$. By adjusting the process parameters, it is aimed to generate biomass-derived synthesis gas with variable H_2/CO ratios.

^[1]P. Preuster et al., Energy Technology, 2018, 6, 501–509.

^[2] W. Supronowicz et al., Green Chemistry, 2015, 17, 2904–2911.

[3] P. Wolf et al., Green Chem., 2019, 21, 5008–5018.

Shaping Methanol Synthesis from CO₂: Phase Transitions, Residence Time, and Reactor Design

A. Böhmeke, 1 K. Laichter, 1 G. Nell, 2 T. E. Müller 1*

¹ Carbon Sources and Conversion, Ruhr-Universität Bochum

Abstract

Methanol synthesis from CO_2 and 'green' hydrogen is a promising strategy to reduce fossil carbon dependency and establish circular carbon flows. This study investigates the influence of phase transitions and hydrodynamics on methanol formation using a ternary $CO_2/H_2/N_2$ (24/66/10 mol%) feed gas in two reactor configurations: a plug flow tubular reactor (PFTR) and a continuously stirred tank reactor (CSTR, Berty type). The work is structured in three parts: (1) phase equilibria studies using a high-pressure view cell, (2) residence time distribution analysis *via* tracer experiments, and (3) catalytic methanol synthesis over a commercial $Cu/ZnO/Al_2O_3$ catalyst at elevated pressures.

Although the system exceeded the critical pressure of pure CO₂, phase equilibrium measurements up to 95 bar showed that the ternary gas mixture remained subcritical under the investigated conditions. Nonetheless, near-critical effects may enhance methanol formation at industrially relevant temperatures. Residence time distribution experiments confirmed the expected backmixing in the Berty reactor, resulting in improved reactant—catalyst contact and smoother temperature profiles.

Catalytic testing with a commercial $\text{Cu/ZnO/Al}_2\text{O}_3$ catalyst demonstrated that the Berty reactor achieved up to 36% methanol selectivity and 38% CO_2 conversion at 280 °C and 2400 rpm. By contrast, the PFTR yielded significantly lower methanol output under similar conditions, highlighting mass transport limitations and underscoring the role of reactor design and flow dynamics.

Looking ahead, methanol has the potential to serve as a flexible hydrogen carrier and carbonneutral fuel. Its compatibility with existing infrastructure and versatility as a precursor for alkenes and aromatics establish it as a cornerstone of future Power-to-X (PtX) strategies. These findings underscore methanol's central role in connecting renewable hydrogen production with the defossilization of chemical manufacturing.

² Parr Instrument GmbH, Frankfurt

Towards Sustainable Ethene: Techno-Environmental Assessment of a Modified Fischer-Tropsch Pathway from CO₂ and H₂

M. Hebenbrock, ¹ V. Hagen, ² T. E. Müller ^{1,*}

- ¹ Carbon Sources and Conversion, Ruhr-Universität Bochum
- ² Rubokat GmbH, Bochum

Abstract

Ethene is an important base chemical of the petrochemical industry, yet its conventional production *via* steam cracking is highly carbon intensive.

To provide a sustainable alternative, the SynGas2Ethene project explored an alternative route based on a modified Fischer-Tropsch synthesis (mFTS) based on renewable syngas generated from CO_2 and green hydrogen. The pathway aims to establish a more sustainable and circular value chain for light alkenes. In this subproject, the carbon footprint of mFTS-based ethene production was benchmarked against state-of-the-art technologies.

Data were obtained from mini-plant experiments using Ru- and Ru/Fe-based catalysts in a laboratory scale tubular reactor, exploring a range of process conditions. The focus was on quantifying conversion, product selectivities, and apparent activation energies across relevant temperature and pressure windows. A mechanistically guided kinetic model was implemented in Aspen Plus and validated against experimental data. Deviations between model and experiment were below 6% in high-yield regimes. under low-yield conditions, segmented regression and non-linear fitting methods markedly improved model accuracy.

To assess environmental performance, a cradle-to-gate life cycle assessment (LCA) was carried out. Under current technological conditions, assuming industrial grid electricity and conventionally sourced CO_2 , the Global Warming Potential (GWP) of the mFTS-based ethene production was estimated at +1.2 kg CO_2 -eq. per kg ethene. In a future scenario relying on renewable electricity and closed-loop CO_2 recycling, the GWP shifts to -7.4 kg CO_2 -eq./kg ethene in an idealized cradle-to-gate estimation. This substantial difference underscores the importance of energy source defossilization and carbon circularity.

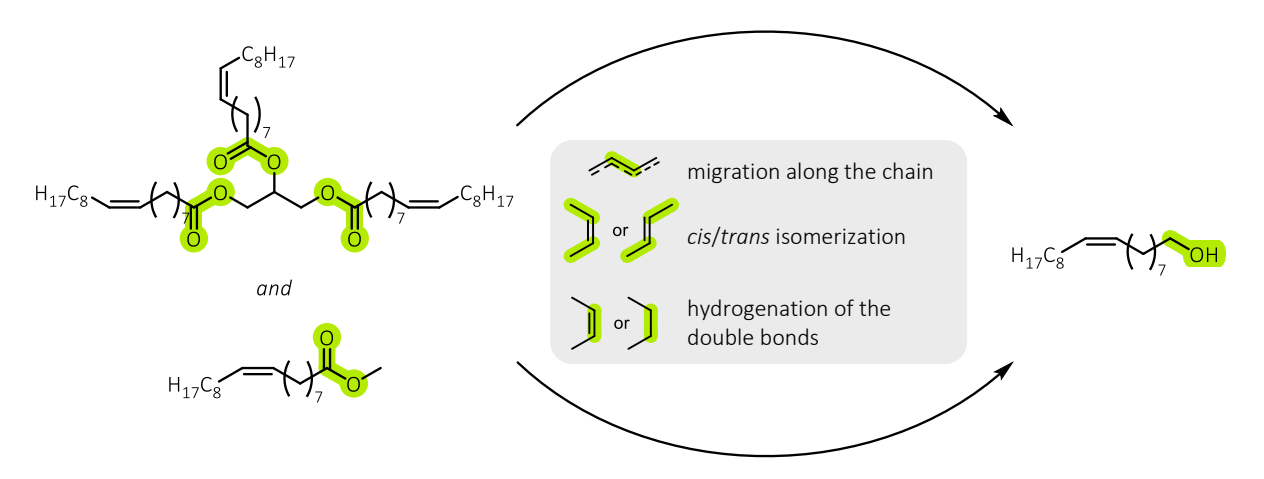
The results highlight the potential of mFTS to support a transition to carbon-negative alkene production, provided that infrastructure for renewable inputs is in place.

Selective Hydrogenation of Renewable Raw Materials Using Commercial Catalyst Systems

<u>D. Pietschmann</u>, J. Bernstein, D. Vogt, T. Seidensticker Laboratory of Industrial Chemistry/Department of Biochemical and Chemical Engineering, TU Dortmund University, Dortmund, Germany

Abstract

The selective hydrogenation of fatty acid methyl esters to unsaturated fatty alcohols is a key process in the chemical industry. Unsaturated fatty alcohols are essential raw materials for the production of environmentally friendly surfactants, cosmetics and bio-based polymers. Selective hydrogenation of C=O bonds without hydrogenating, migrating, or isomerizing the C=C double bonds requires the employment of specifically designed catalyst systems.



Scheme 1. General reaction scheme and challenges of the catalytic hydrogenation of methyl oleate and trioleate with molecular hydrogen to oleyl alcohol.

The heterogeneously catalyzed hydrogenation of fatty acid methyl esters is a process that is carried out in industrial settings using zinc chromite catalysts under relatively harsh conditions. The comparatively low activity of such catalysts requires temperatures from 200 to 300 °C and hydrogen pressures of up to 300 bar. The scientific literature offers only a limited description of homogenous transition metal complexes that can be used for the selective hydrogenation of methyl oleate to oleyl alcohol. These catalyst systems are predominantly based on transition metals such as manganese and ruthenium, while osmium complexes are rarely considered. A significant disadvantage of these systems is that the complexes are often not commercially available, and their synthesis is time-consuming and resource-intensive.

Given that commercially available oleyl alcohol exhibits an industrial purity level of only 50–85%, the objective of our investigations was to identify a homogeneous catalytic approach with commercially available catalysts that would yield a final product purity level exceeding 90%, employing HOSOME (high-oleic sunflower oil methyl ester) as the initial substrate.

Carbon Capture and Hydrogen Plants - Overcoming Challenges and Optimizing Integration

Annette Wincierz Siemens AG, Karlsruhe, Germany

Abstract

Carbon capture technology and the hydrogen economy have become essential for achieving the ambitious sustainability goals of governments and industries. This article addresses the various challenges these sectors face today, emphasizing the critical need to tackle these issues to ensure economic and sustainable operations. Key barriers and challenges related to both industries are identified, along with strategies to overcome them.

We uncover the key points to consider when designing, simulating, automating and operating these types of plants to ensure their optimal performance.

Additionally, we highlight the importance of integrating and optimizing the operations of various plants within the entire ecosystem, such as carbon capture, hydrogen production, and other power-to-X technologies. By examining these integration strategies, we provide a comprehensive roadmap for enhancing efficiency and effectiveness in the sector.

Keywords: Carbon capture, green hydrogen production, digital twins, process optimization, system integration, sustainability

1. Introduction

The global drive toward climate neutrality is accelerating the development and deployment of transformative technologies aimed at decarbonizing key sectors. Green hydrogen, produced using renewable energy, offers versatile applications across industry, transportation, and energy systems. Carbon Capture, Utilisation and Storage (CCUS) enables the removal of CO_2 from hard-to-abate industrial processes, the atmosphere, or biogenic sources. When combined, green hydrogen and captured CO_2 can be converted into sustainable synthetic fuels and chemicals, fostering synergies that support circular carbon economies and enhance overall system sustainability.

Although both technologies have made significant progress in recent years, their large-scale implementation continues to face economic, technical, and regulatory barriers. Studies point to high capital expenditures, energy demands, and challenges in system integration as major obstacles (Capgemini-Siemens, 2024; Laws & Szeliga, 2025). In addition, fluctuating renewable energy supply and the absence of harmonized certification frameworks further complicate deployment.

Despite increasing interest and investment, many green hydrogen and CCUS projects still lack comprehensive lifecycle approaches that cover design, simulation, automation, and optimization. This gap underscores the need for integrated engineering strategies and digital solutions that can enhance system performance, reduce costs, and ensure compliance with regulatory standards.

This work provides a technically detailed and application-oriented analysis of hydrogen and CCUS systems, guided by the following key questions:

- How can process design and system architecture be optimized to balance availability and investment?
- What role do digital twins and simulation tools play in improving operational efficiency and scalability?
- How can automation and performance optimization contribute to reducing lifecycle costs?
- What integration strategies enable synergies between green hydrogen, CCUS, and Power-to-X technologies?

The analysis draws on current research, demonstrator projects, and industry best practices, with a particular focus on Siemens' integrated engineering and automation solutions.

2. Process Overview of Green Hydrogen Production and Carbon Capture, Utilization, and Storage (CCUS) Systems

Green hydrogen production and carbon capture, utilization, and storage (CCUS) are two essential technologies for achieving industrial decarbonization. The following process overview highlights the key subsystems, components, and operational principles of each system, emphasizing the importance of balancing technical reliability with economic efficiency.

2.1 Green Hydrogen Production System

A green hydrogen production system consists of the following five main subsystems, which work together to convert renewable energy into clean hydrogen with minimal environmental impact:

- 1. Electricity Supply and Conversion: The process begins with the electricity supply, ideally sourced from renewables such as wind or solar. This energy is distributed and converted from alternating current (AC) to direct current (DC) to power the electrolyzers.
- 2. Water Supply and Pre-Treatment: High-purity water is required for electrolysis. The water undergoes filtration, softening, and deionization to meet the strict quality standards required by electrolyzers.
- 3. Electrolysis and Hydrogen Production: In the core subsystem, electrolyzers (e.g., PEM, alkaline, or solid oxide) split water molecules into hydrogen and oxygen using DC electricity. This stage requires precise thermal management and control systems to ensure efficiency, durability and safety.
- 4. Hydrogen Purification and Compression: The produced hydrogen is purified to meet quality standards and then compressed for storage or transport. This involves purification units (such as pressure swing adsorption), dryers, and compressors.
- 5. Storage and Distribution: Compressed hydrogen is stored in high-pressure tanks. It is then prepared for distribution via pipelines or transport vehicles, or directed to enduse applications such as mobility or industry.

Ultimately, the successful deployment of green hydrogen systems depends on the seamless integration of technical components, operational reliability, and economic feasibility.

2.2 Carbon Capture, Utilization, and Storage (CCUS) System

A typical Carbon Capture, Utilization, and Storage (CCUS) system consists of several interconnected subsystems designed to capture carbon dioxide from industrial sources or the atmosphere, utilize it in value-added processes, or store it securely. Like green hydrogen systems, CCUS requires a careful balance between system availability and capital investment to ensure long-term financial and environmental viability.

The process begins with the CO_2 source and pre-treatment, where CO_2 -rich gas streams are prepared for capture. These sources include power plants, cement or steel factories, and direct air capture units. Pre-treatment involves filtering particulates, adjusting temperature and pressure, and ensuring the gas stream is suitable for efficient CO_2 separation.

Next is the CO_2 capture subsystem, which uses technologies such as chemical absorption (e.g., amines), physical absorption, membrane separation, adsorption, or cryogenic methods. This stage is energy-intensive and must be optimized for high capture rates and minimal solvent degradation or loss.

If utilization is part of the system, the captured CO_2 can be directed to the utilization subsystem, where it serves as a feedstock for synthetic fuels, chemicals, or building materials. This adds economic value but requires integration with downstream processes and market demand for CO_2 -derived products.

The compression and transport subsystem prepares CO₂ for delivery to storage or utilization sites. CO₂ is compressed to high pressures and transported via pipelines or tankers. This stage demands robust infrastructure and materials resistant to corrosion and high pressure.

Finally, the storage subsystem ensures long-term containment of CO₂, typically in deep geological formations such as saline aquifers or depleted oil and gas fields. Monitoring systems track pressure, seismic activity, and potential leakage to ensure regulatory compliance and environmental safety.

Reliable operation and cost-effectiveness are both essential for the success of CCUS systems. Integration with existing infrastructure, modular design, and supportive policies like carbon pricing help make these systems economically and environmentally sustainable.

3. Current Challenges in Carbon Capture and Green Hydrogen Production

The development and implementation of carbon capture and hydrogen production technologies face economic, technical, and regulatory challenges that must be addressed to enable widespread use and long-term sustainability.

3.1 Economic Challenges

The economic viability of both carbon capture and hydrogen production remains a significant barrier to widespread adoption. The Levelized Cost of Hydrogen (LCOH) is still higher than fossil-based alternatives, making it difficult to compete in the market without government subsidies or incentives.

Electricity costs represent the largest component of the LCOH for electrolysis-based hydrogen production, accounting for approximately 40-60% of the total cost. Additionally, capital expenditure (CAPEX) for electrolysis equipment, system components, and balance of plant contribute significantly to the overall cost structure (Capgemini-Siemens, 2024).

For carbon capture technologies, the main economic challenges include high investment

costs, energy intensity, and the costs of CO_2 transportation and storage. High investment costs are one of the primary obstacles to implementing carbon capture, particularly in industries like cement production. Moreover, the cost of carbon capture can vary significantly depending on the technology used, the concentration of CO_2 in the emission stream, and the intended application of the captured CO_2 .

3.2 Technical and Operational Challenges

Hydrogen production and carbon capture facilities face a range of technical and operational challenges that affect performance, cost-efficiency, and scalability. A key issue is system integration: components such as compressors, pumps, heat exchangers, and electrolyzers must work together reliably. Poor coordination can lead to inefficiencies, higher costs, and safety risks (Capgemini-Siemens, 2024).

The use of intermittent renewable energy sources like solar and wind introduces variability in hydrogen production, which can cause operational instability and increase energy costs (Laws & Szeliga, 2025). Equipment sizing and design are also critical—incorrect specifications may result in excessive investment and higher maintenance needs (Capgemini-Siemens, 2024).

Carbon capture processes are particularly energy-intensive. This impacts operating costs and overall feasibility. Material durability and chemical resistance are important for long-term reliability. Dynamic operating conditions require advanced control systems to maintain efficiency.

Data management represents a critical operational challenge for both hydrogen production and carbon capture facilities. These systems generate large volumes of real-time and historical data across various subsystems, which must be effectively integrated to enable reliable monitoring, control, and optimization. Maintaining process stability requires careful management of parameters such as water balance, energy input, and reaction rates.

3.3 Regulatory and Certification Challenges

Hydrogen production and carbon capture facilities must comply with evolving regulatory frameworks and certification requirements.

For example, in the EU, hydrogen can qualify as a renewable fuel of non-biological origin (RFNBO) only if it meets three key three criteria: additionality (the use of newly built renewable energy sources), temporal correlation (alignment between the time of renewable electricity generation and its use), and geographic correlation (proximity between the renewable source and the electrolyzer) (Capgemini-Siemens, 2024).

Furthermore, the EU's Carbon Border Adjustment Mechanism (CBAM) targets carbon-intensive imports, initially focusing on products like cement, iron and steel, aluminum, fertilizers, electricity, and hydrogen. CBAM requires importers to report on imports during the transitional phase (2023-2025), with full implementation scheduled for January 2026. Under the EU's Carbon Border Adjustment Mechanism (CBAM), hydrogen importers are required to calculate and report the carbon intensity of imported hydrogen using a standardized EU methodology. Importers must register with national authorities, purchase CBAM certificates based on the average weekly price of EU Emissions Trading System (ETS) allowances and annually declare embedded emissions. Corresponding certificates must be surrendered to cover these emissions. If a carbon price was paid in the country of origin, the equivalent amount may be deducted upon verification. (Capgemini-Siemens, 2024).

Also, Carbon Capture, Storage, and Utilization (CCSU) faces several regulatory challenges.

A major issue is the lack of internationally harmonized standards, which complicates cross-border projects. In addition, long-term legal responsibility for stored CO₂, especially in the event of leakage, is often unclear. The permitting process is complex and requires approvals across multiple sectors. Moreover, strict monitoring, reporting, and verification (MRV) requirements must be met to ensure the safety and permanence of storage. Certifying suitable storage sites is technically demanding and costly.

Without clear policy incentives and public acceptance, the economic viability of CCSU remains a significant challenge. (BNP Paribas, 2025)

Ensuring compliance with these regulations while maintaining economic viability presents a significant challenge for project developers and operators.

4. Digital Twins: A Transformative Approach for Carbon Capture and Hydrogen Plants

Digital Twins offer a foundational approach to lifecycle optimization in process plants by providing a consistent digital representation of the physical facility. In the process industry, this concept encompasses various specialized digital models, each addressing specific phases and aspects of the plant lifecycle, from early design stages to continuous operation and optimization.

In the process design phase, Process & Energy Twins enable the simulation of chemical and physical processes using steady-state and dynamic models. These simulations support efficiency analysis, cost estimation, sensitivity studies, and the identification of process limitations. They also facilitate informed decision-making during the conceptual phase and allow for the virtual validation of proposed process improvements.

During engineering and documentation, Plant Twins deliver integrated plant engineering solutions, including process flow diagrams (PFDs), piping and instrumentation diagrams (P&IDs), electrical and control schematics, hardware configurations, and as-built documentation. This integration ensures consistent engineering workflows and supports effective maintenance and operational planning.

For automation development, Automation Twins enable the virtual testing of control systems, including safety functions and sequence logic. They also support virtual commissioning and operator training under simulated conditions.

In the operational phase, Digital Twins are used for continuous monitoring and performance optimization. They apply advanced techniques such as soft sensing to estimate variables that cannot be measured directly, track equipment health and key performance indicators (KPIs), integrate energy management, and support predictive maintenance. Additionally, they assist in forecasting and scheduling production activities and enable real-time optimization to improve efficiency and reduce operational costs.

4.1 Integrated Engineering for Hydrogen and Carbon Capture Plants

Integrated engineering enables a consistent, data-centric workflow across all project phases, from process design to automation and operation. This approach improves efficiency, reduces errors, and ensures data consistency throughout the lifecycle of hydrogen and carbon capture facilities.

Usually, the first process phase begins with the definition of essential process and material data, design parameters, and block flow diagrams are collected. Process Simulation tools such as gPROMS are often used at this stage to validate and optimize initial design

concepts. These inputs feed into a central engineering environment, typically platforms like COMOS, which supports process design (P&ID), electrical and instrumentation engineering (EI&C), and automation development (PAA). Changes in one phase are automatically reflected across others, ensuring data consistency.

COMOS acts as a centralized, object-oriented data platform that provides standardized, consistent transfer of plant data to the Distributed Control System (DCS). This approach minimizes errors, accelerates engineering processes, and ensures high data quality and operational efficiency throughout the entire plant lifecycle.

Engineering data is directly linked to automation systems such as SIMATIC PCS 7, allowing fast and reliable generation of operator interfaces. Additional tools like SIMIT for simulation extend the integrated workflow: SIMIT utilizes the consistent data foundation to enable realistic simulations, system testing, and operator training.

This integrated setup reduces rework, shortens construction time, and supports the creation of digital twins. It enables continuous optimization of plant performance and reliability. Studies show potential CAPEX savings of up to 15% when applied early in the project lifecycle (Capgemini-Siemens, 2024; Laws & Szeliga, 2025).

A schematic overview of this integrated engineering approach is illustrated in Figure 1, showing the data flow from process data input through engineering, simulation, and automation to optimized operation.

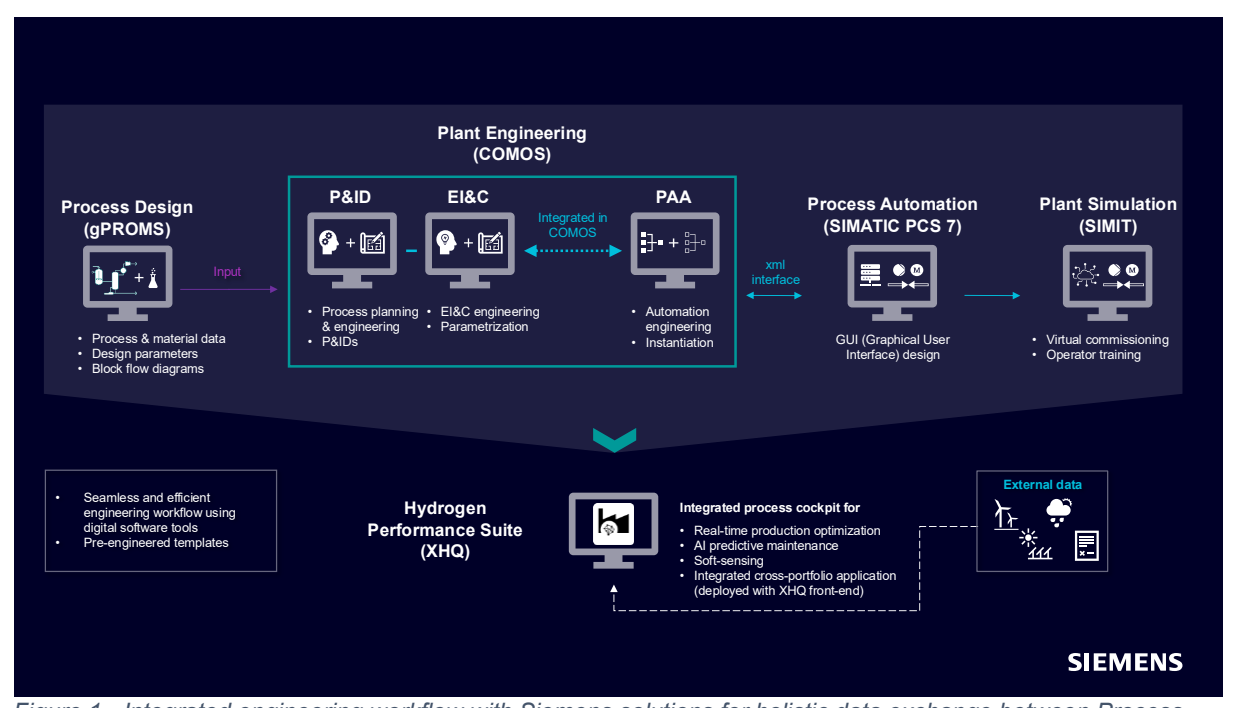


Figure 1 - Integrated engineering workflow with Siemens solutions for holistic data exchange between Process Design, Plant Engineering, Process Automation, Simulation and Process Performance Suite

4.1 Understanding Digital Twins for Carbon Capture and Hydrogen Production

A digital twin is "a virtual representation of the current and future physical reality of a product, a production process, or a plant having multiple critical assets, including their behavior and health status." Digital twins bring together data from all lifecycle phases and from all functions and levels, helping to understand, manage, and predict the performance of the corresponding process or plant (Capgemini-Siemens, 2024).

For green hydrogen plants, digital twins typically include high-fidelity process models describing key system units, from energy input to hydrogen production, purification, compression, storage, and export. These models integrate real-time plant data from critical units and flows, as well as external data such as energy supplies, tariffs, and demand profiles (Laws & Szeliga, 2025).

In the field of Carbon Capture, Storage, and Utilization (CCSU), Digital Twins provide a structured and data-driven approach to optimize process systems across their entire lifecycle by integrating detailed virtual representations of physical assets and operations. In CCSU systems, Digital Twins provide a data-driven foundation for optimizing each stage of the carbon management process. From the initial capture of CO_2 , whether via post-combustion, pre-combustion, or oxy-fuel technologies, digital models enable precise simulation and performance evaluation under varying operational conditions. During transport and storage, Digital Twins support integrity monitoring of pipelines and reservoirs, ensuring safety, regulatory compliance, and long-term reliability. In the utilization phase, where CO_2 is converted into valuable products (e.g., fuels, chemicals, or building materials), digital twins assist in process design, reaction modeling, and economic assessment.

By integrating real-time data and predictive analytics across these stages, Digital Twins enhance system transparency, reduce uncertainties, and support informed decision-making, ultimately contributing to the scalability and sustainability of CCSU technologies.

4.2 Benefits of Digital Twins in Carbon Capture and Hydrogen Production

The application of Digital Twins in carbon capture and hydrogen production processes offers several functional advantages across design, operation, and maintenance stages:

1. Design and Engineering Support

Digital Twins enable the simulation of plant operations under realistic conditions, allowing engineers to fine-tune process designs, identify potential inefficiencies early on stage, and evaluate alternative configurations. This contributes to reduced commissioning time and cost, which is particularly relevant for the economic feasibility of hydrogen and carbon capture systems.

2. Operational Optimization

Real-time data integration allows Digital Twins to support continuous monitoring and adjustment of operational parameters. In large-scale hydrogen production facilities, such as a 100 MW electrolyzer operating 8,000 hours annually, even minor improvements can significantly reduce yearly energy costs (e.g., by more than €500,000 per percentage point of optimization enabled by the Digital Twin) [Capgemini-Siemens, 2024].

In carbon capture operations, real-time data integration enables continuous monitoring and adjustment of process parameters, contributing to improved operational efficiency.

3. Dynamic Real-time Optimization

Digital Twins assist in optimizing production schedules and storage strategies to meet demand-side requirements while minimizing the levelized cost of hydrogen. Demonstrator projects have shown potential cost reductions exceeding 10%, indicating the relevance of such tools for economic optimization [Laws & Szeliga, 2025].

4. Predictive Maintenance

By continuously monitoring equipment performance and identifying anomalies, digital twins can help prevent over 80% of potential shutdowns, reducing downtime and maintenance costs [Capgemini-Siemens, 2024].

5. **Soft-Sensing Functionality**

Digital twins provide 'soft-sensing' capabilities, calculating key process variables using calibrated process models when direct measurements are not available or reliable [Laws & Szeliga, 2025].

6. Asset Replication and Scalability

Digital twins facilitate faster construction by ensuring consistency and continuity from the "as required" to the "as designed" and the final "as built" state. This is particularly important for green hydrogen production, where many identical package units are used to scale up plant capacities [Capgemini-Siemens, 2024].

5. Designing and Simulating Carbon Capture and Hydrogen Plants

The design and simulation of carbon capture and hydrogen production facilities involve complex interdisciplinary considerations. These systems must be planned to ensure technical feasibility, regulatory compliance, and economic viability across all lifecycle stages. Digital tools, including Digital Twins, play a central role in supporting design decisions, evaluating system behavior under varying conditions, and optimizing performance before physical implementation.

5.1 Key Considerations for Plant Design

The design of carbon capture and hydrogen production plants requires careful attention to several interrelated factors. One of the primary considerations for hydrogen plants is the energy and water supply/consumption strategy, which must ensure reliable access to resources while accounting for potential intermittency, particularly in renewable energy-based systems [Capgemini-Siemens, 2024].

Regulatory requirements also play a critical role, as facilities must comply with environmental standards, emissions thresholds, and safety regulations. These constraints influence technology selection, process configuration, and operational limits.

Equipment selection is another essential aspect. In hydrogen production, the choice between alkaline and proton exchange membrane (PEM) electrolyzers affects efficiency, cost, and system integration. For carbon capture, available technologies include absorption, adsorption, oxyfuel combustion, and membrane separation, each with distinct advantages and limitations depending on the application context [Siemens, 2025].

The system capacity and storage configuration must be designed to accommodate fluctuations in production and demand. This includes sizing of hydrogen storage tanks, and buffer systems to ensure operational flexibility and reliability [Capgemini-Siemens, 2024].

Furthermore, the integration with existing infrastructure, such as energy grids, industrial networks, and transportation systems is crucial for enabling seamless deployment and minimizing additional investment costs.

A typical green hydrogen production system consists of five interconnected subsystems, ranging from energy input to hydrogen purification and storage. Each subsystem involves specific components such as compressors, pumps, heat exchangers, and electrolyzers. Achieving a balance between system availability and capital investment is essential for ensuring long-term financial performance [Cappemini-Siemens, 2024].

Carbon capture, utilization, and storage (CCUS) systems are designed to remove CO₂ from industrial or atmospheric sources, process it for utilization, or compress it for secure geological storage. This requires careful integration of subsystems to balance operational reliability with capital investment. Efficient design and lifecycle optimization are essential to achieving both environmental impact and economic viability [IEA CCUS Handbook, 2022].

5.2 Simulation Tools and Techniques

Digital simulation tools are increasingly integrated into engineering workflows, especially in the design, optimization, and operational planning of facilities for carbon capture and hydrogen production. These tools are used throughout the entire project lifecycle, including conceptual design, detailed engineering, commissioning, and operator training. Their use improves process understanding, enhances planning reliability, and helps reduce technical and operational risks.

A key category of simulation tools is process simulation software, such as gPROMS and Siemens' Process Performance Suite. These platforms allow engineers to model and analyze complex systems, supporting the development of energy-efficient and cost-effective solutions through detailed evaluation of process behavior and performance.

Another important technique is virtual commissioning, which uses tools like Siemens' SIMIT to simulate control systems and operating procedures before they are implemented in the real plant. This approach shortens commissioning time and helps identify potential issues early, reducing risks during startup.

Training simulations, developed by companies such as Siemens and Capgemini, also play a crucial role in preparing plant personnel. By simulating plant operations before startup, these tools ensure that operators are well-prepared to manage systems effectively from day one (Capgemini-Siemens, 2024).

The use of simulation technologies has also shown clear economic benefits. Operational costs (OPEX) can be reduced by 5% to 15%, while capital costs (CAPEX) may decrease by 10% to 15% (Capgemini-Siemens, 2024). These savings highlight the strategic importance of simulation tools in achieving sustainable, reliable, and cost-efficient engineering solutions.

6. Automation and Performance Optimization as Drivers of Production Efficiency

As carbon capture and hydrogen production technologies continue to evolve, the role of automation becomes increasingly critical. Efficient automation systems are essential for ensuring safe, reliable, and optimized operation of these facilities.

6.1 Automation System Architecture

Effective automation is essential for the reliable and efficient operation of carbon capture and hydrogen production facilities. The automation system governs critical parameters such as voltage, current, temperature, and pressure, and supports safety systems, data logging, analysis, simulation, and optimization.

Automation architectures for hydrogen plants typically fall into three categories:

- Fully Integrated DCS Architecture: Based on systems like Simatic PCS 7 or PCS neo, this approach integrates complex package units (e.g., electrolyzers) into a centralized Distributed Control System (DCS). A single controller can manage multiple units via remote I/O, enabling high availability with minimal additional cost.
- 2. Standalone Fieldbus Architecture: Each package unit, such as an electrolyzer, is equipped with its own controller and automation system. While this offers flexibility for OEMs, it limits integration for operators in terms of safety, diagnostics, and centralized updates (Capgemini-Siemens, 2024). The orchestration of these standalone units can be managed either through a Distributed Control System (DCS) or a Supervisory Control and Data Acquisition (SCADA) system, depending on the complexity and scale of the plant.
- 3. Hybrid Architecture: Combines standalone PLCs for specific units (e.g., electrolyzers

or compressors) with a DCS for the balance of plant. Integration is facilitated via Modular Type Package (MTP) standards. Siemens' hybrid solutions leverage compatibility across engineering tools like TIA Portal and PCS 7/PCS neo, enabling seamless integration of hardware components, cybersecurity, and operator training.

The choice of automation architecture for hydrogen plants depends on several factors, like for example electrolyzer stack size, number of installed electrolyzers or plant complexity.

In the context of carbon capture, automation system architecture plays a similarly critical role. For large-scale industrial carbon capture facilities, such as those integrated into cement or chemical plants, a Distributed Control System (DCS) is typically the preferred solution. These environments demand high availability, robust safety integration, and long-term lifecycle support, all of which are core strengths of DCS platforms like Simatic PCS 7 or PCS neo.

In contrast, smaller-scale carbon capture applications, such as Direct Air Capture (DAC) units, often benefit from the flexibility and cost-efficiency of SCADA-based systems. SCADA solutions provide sufficient control capabilities for less complex setups, while enabling remote monitoring, data logging, and secure fleet management. The choice between DCS and SCADA should be guided by the scale, complexity, and integration needs of the specific carbon capture application.

6.2 Performance Optimization Systems

Performance optimization systems are designed to address the operational and maintenance challenges inherent in hydrogen production facilities. An example is the Hydrogen Performance Suite from Siemens, which exemplifies how advanced digital technologies can be leveraged to enhance efficiency, reliability, and sustainability in hydrogen production. By integrating insights derived from digital twins, simulation models, and process automation systems, as visualized in Figure 2, the suite enables a comprehensive and data-driven approach to performance optimization.



Figure 2 - Digital Hydrogen Plant for Monitoring, Performance Analysis, and Production Optimization via the Hydrogen Performance Suite

The Hydrogen Performance Suite offers real-time monitoring capabilities, ensuring precise data acquisition and continuous oversight of production processes. This functionality is essential for maintaining operational control, promptly identifying anomalies, and mitigating inefficiencies and safety risks. As Capgemini-Siemens (2024) emphasizes, "Managing multiple production units requires efficient integration to minimize downtime and maintenance

costs."

By simulating and monitoring key process parameters the suite supports production optimization. It enables real-time decision-making that balances technical performance with economic indicators, thereby improving overall productivity and cost-effectiveness.

The suite incorporates predictive maintenance functionalities. Through integration with predictive analytics systems, it helps prevent unplanned downtimes and extends the operational lifespan of critical equipment (Cappemini-Siemens, 2024).

A comparable solution with similar capabilities offers the Process Performance Suite for carbon capture facilities. It enables advanced monitoring and optimization of carbon capture operations, contributing to improved efficiency and reliability in decarbonization efforts).

Figure 3 presents the system architecture of the Siemens Hydrogen Performance Suite, which enables seamless integration between Operational Technology (OT) and Information Technology (IT) for the management of hydrogen and Power-to-X plants. It shows how the physical plant is represented through digital twins at various levels, providing a comprehensive online platform for real-time optimization, performance monitoring, and predictive maintenance.

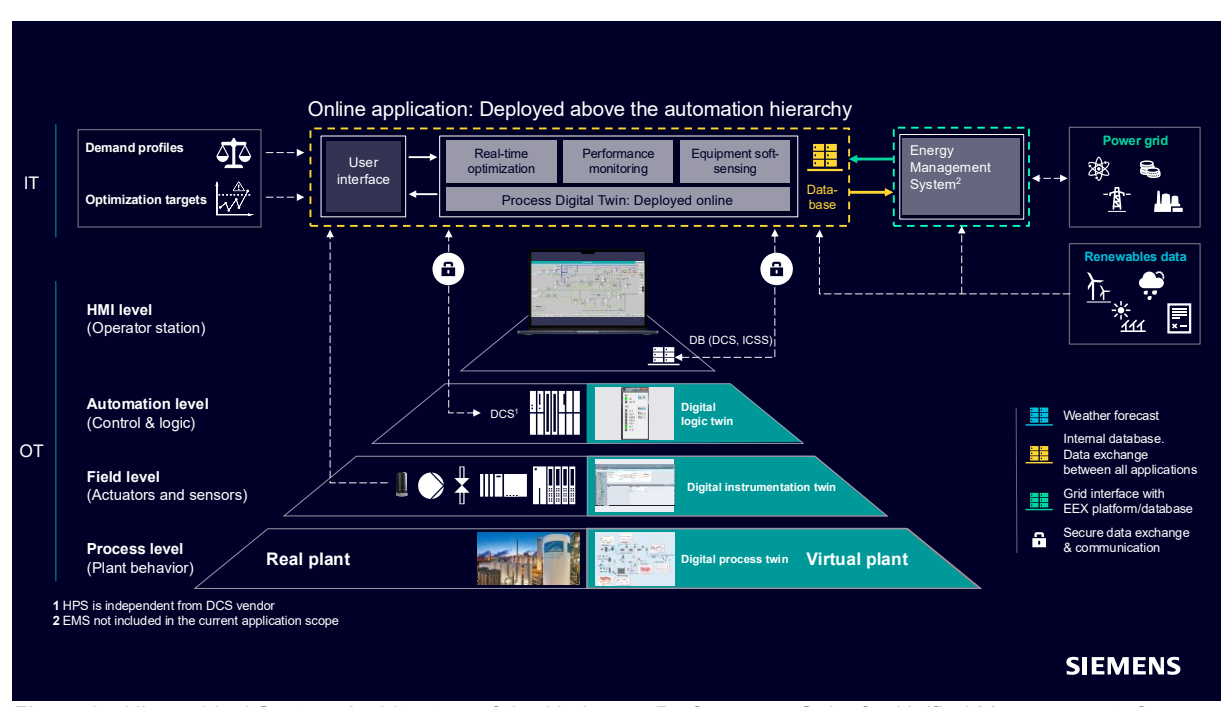


Figure 3 - Hierarchical System Architecture of the Hydrogen Performance Suite for Unified Management of Hydrogen and Power-to-X Plants, Based on the Integration of Physical Assets and Digital Twins

Overall, the integration of Digital Twin technologies into carbon capture and hydrogen production processes contributes to improved technical reliability, operational efficiency, and economic viability across all lifecycle stages.

7. Optimizing and Integrating Plant Operations

Integrating technologies such as Carbon Capture, Hydrogen Production, and Power-to-X presents a strategic opportunity to boost infrastructure performance and unlock synergies. These solutions enable the conversion of excess renewable energy into valuable fuels, chemicals, and materials, while supporting energy storage and effective CO₂ utilization.

To fully realize these benefits, optimizing and integrating plant operations becomes essential,

especially when expanding existing facilities or connecting new process units to an established infrastructure. In industrial settings, such as Power-to-X applications with carbon capture and utilization, the intelligent interconnection of processes can significantly enhance operational efficiency and sustainability.

7.1 Integration Challenges and Opportunities

Integrating carbon capture technologies with hydrogen production and downstream utilization processes presents both technical and strategic challenges but also opens significant opportunities for innovation and value creation. To ensure the efficient operation of such integrated systems, the following key aspects must be addressed:

- Technical Integration: Compatibility between diverse technologies must be ensured to enable seamless operation and minimize losses at process interfaces.
- Energy Integration: Energy flows between subsystems must be optimized to improve overall system efficiency.
- Control System Integration: Advanced control strategies are required to manage the dynamic behavior of interconnected units, focusing on system-wide performance rather than isolated optimization.
- Supply Chain Integration: Efficient logistics and material flows are critical to connect hydrogen production, CO₂ capture, and utilization pathways.

Promising opportunities lies in the use of captured CO₂ in combination with green hydrogen to produce synthetic fuels and chemicals via Power-to-X technologies. This approach supports decarbonization across multiple sectors and enables circular carbon economies.

7.2 Digital Solutions for Integration

Digital technologies are increasingly vital for integrating carbon capture systems into existing hydrogen production facilities and broader plant ecosystems. These solutions enable seamless coordination, enhance transparency, and support performance optimization and cost reduction across interconnected processes.

One of the most transformative innovations is the emergence of holistic Digital Twins. These systems integrate Energy Management Systems (EMS), real-time process simulations, and predictive, data-driven functionalities into a unified interface (Laws & Szeliga, 2025). This approach is particularly impactful in greenfield and first-of-a-kind projects, where it enables virtual commissioning, operator training, and operational optimization (Capgemini-Siemens, 2024). By consolidating these elements, holistic Digital Twins offer a streamlined and cost-effective method for improving plant performance and supporting informed decision-making (Laws & Szeliga, 2025).

A data-centric strategy further strengthens integration by establishing a unified data backbone across the entire value chain. This ensures consistent, high-quality data availability for all stakeholders, improves interoperability between systems, and accelerates the market introduction of low-carbon products (Capgemini-Siemens, 2024).

To ensure both marketability and regulatory compliance of low-carbon hydrogen, end-to-end traceability solutions are being deployed. These systems certify carbon intensity levels in accordance with recognized standards such as the EU threshold of 3.38 kg CO₂e/kgH₂ providing transparency and credibility for end users and regulatory authorities, while also contributing to profitability (Capgemini-Siemens, 2024).

7.3 Energy Flexibility and System Integration

In addition to technical and digital integration, energy flexibility plays a critical role in connecting carbon capture and hydrogen production with the broader energy system. Flexible operation strategies allow industrial plants to respond dynamically to fluctuations in energy availability and market conditions, thereby improving economic viability and supporting grid stability.

A promising model envisions carbon capture plants as flexible energy consumers, capable of adjusting their operational load based on real-time energy prices and renewable energy availability. During periods of low electricity costs or high renewable generation, these plants can ramp up their capacity. Conversely, they can reduce consumption when energy is scarce or expensive, contributing to overall system balance.

Load shifting is another viable strategy, particularly in cement plants with integrated carbon capture. Studies have shown that up to 10% of electricity consumption can be shifted without affecting core production processes, enabling responsiveness to market signals and grid demands (Eboumbou Ebongu & Sauer, 2024).

Moreover, waste heat utilization offers an effective means of improving energy efficiency. Carbon capture units can harness excess thermal and electrical energy generated in other parts of the plant, thereby reducing operational costs and enhancing sustainability.

The role of energy management systems is also crucial in hydrogen production. These systems enable the intelligent coordination of various energy sources, including grid electricity, on-site generation, and renewables, ensuring optimal energy use and supporting flexible, low-carbon operation (Capgemini-Siemens, 2024).

8. Optimizing Operations and Maintenance

Whether operated individually or in combination, hydrogen facilities, carbon capture systems, and Power-to-X (P2X) plants require optimized operation to ensure both economic efficiency and long-term viability.

8.1 Process Operations

Efficient process operations are essential for enhancing the performance and costeffectiveness of hydrogen production and carbon capture systems. Leveraging digital tools and advanced control strategies enables operators to make informed decisions in real time and adapt to dynamic operating conditions.

Dynamic real-time optimization plays a central role in aligning operations with fluctuating energy availability and market demands. In hydrogen production, this involves determining optimal production and storage schedules based on energy prices and off-taker requirements, with the aim of minimizing the levelized cost of hydrogen (Laws & Szeliga, 2025). In carbon capture, real-time optimization allows for flexible adjustment of the CO₂ capture rate in response to electricity prices and emissions targets, improving cost-efficiency and operational agility.

Soft-sensing techniques, which rely on mathematical models and live process data, estimate key variables that are not directly measurable. These virtual sensors provide continuous insights into system behavior, enabling proactive monitoring and control without relying solely on physical instrumentation (Laws & Szeliga, 2025).

Integrating process optimization with energy management systems (EMS) facilitates holistic coordination between production and energy systems. This ensures that operational

decisions consider both process efficiency and energy costs, leading to improved overall performance and resource utilization.

Recent advancements focus on the development of holistic Digital Twins that unify EMS, online process models, and predictive analytics within a single platform. These systems offer modular architectures and flexible data connectors for seamless integration, provide a comprehensive view of plant operations by merging process data, energy flows, and production metrics, and support enhanced transparency, streamlined workflows, and cost-effective decision-making.

Figure 4 illustrates a Digital Twin implementation within the Hydrogen Performance Suite. The visualization demonstrates how process data, energy flows, and production metrics are integrated into a unified interface, enabling informed decision-making in real time.



Figure 4 - Digital Twin of a Hydrogen Plant for Monitoring, Performance Analysis, and Production Optimization with the Hydrogen Performance Suite

8.2 Energy Management Strategies

Energy management is a central factor in the economic viability of carbon capture and hydrogen production facilities. In both cases, electricity costs represent a significant portion of total operating expenses. Therefore, targeted strategies to reduce energy consumption and optimize energy sourcing are essential for improving overall efficiency and cost-effectiveness.

Two main approaches can be combined to achieve this:

- Strategic Electricity Procurement: Facilities can reduce energy costs by implementing optimized purchasing strategies. This includes the use of Power Purchase Agreements (PPAs), which allow long-term access to electricity at stable prices, and the exploitation of short-term market opportunities. By actively managing procurement based on market conditions, operators can significantly lower their electricity expenses (Capgemini-Siemens, 2024).
- Deployment of Energy Management Systems (EMS): Advanced EMS enable realtime monitoring and control of energy flows within the facility. These systems help balance the use of different energy sources, such as renewable energy, grid electricity, and on-site generation, based on availability, cost, and operational needs.

EMS also support predictive planning and load optimization, contributing to more efficient energy use.

In hydrogen production plants, the integration of EMS with base load management and microgrid control solutions allows for flexible operation. These systems can adjust energy consumption dynamically, leading to electricity cost savings of up to 5% (Capgemini-Siemens, 2024). Flexibility in energy use is particularly valuable when renewable energy sources are involved, as it enables better alignment with fluctuating supply.

Carbon capture facilities can also benefit from energy flexibility. By synchronizing CO₂ capture processes with the varying load profiles of overall plant, operators can run the capture units more efficiently. This flexible operation helps reduce energy consumption during low-load periods and avoids peak electricity prices, resulting in lower overall energy costs (Eboumbou Ebongu & Sauer, 2024).

With an intelligent operations software like the Hydrogen Performance Suite from Siemens, operators can optimise hydrogen production hour by hour using real-time data on demand, renewable supply, and electricity market prices (see Figure 5). This enables up to 36% reduction in grid power usage and significantly lowers production costs (Laws & Szeliga, 2025).



Figure 5 - Siemens Hydrogen Performance Suite: Integrated Dashboard for Forecasting, Planning, and Energy Reporting

8.3 Maintenance Optimization

Optimizing maintenance strategies is essential for ensuring the long-term reliability, safety, and cost-efficiency of carbon capture and hydrogen production facilities. As these systems operate under demanding conditions and rely on complex equipment, proactive maintenance approaches are increasingly important to minimize downtime and reduce operational expenditures.

A key component is predictive maintenance, which uses real-time data from field sensors to detect early signs of wear, degradation, or malfunction. These systems continuously monitor performance parameters and can swiftly identify deviations from expected behavior. This capability helps prevent over 80% of potential shutdowns by enabling timely interventions (Capgemini-Siemens, 2024). By identifying issues before they lead to equipment failure, predictive maintenance reduces unplanned outages and costly repairs. Figure 6 provides an

example of this approach, showing how anomalies in a heat exchanger are detected and visualized to support timely maintenance decisions.

The implementation of anomaly detection and predictive maintenance technologies has been shown to significantly reduce maintenance costs and improve equipment uptime. These improvements contribute directly to lowering operational expenditures (OPEX) and enhancing the overall performance of the facility (Capgemini-Siemens, 2024).

Closely related is condition monitoring, which involves the continuous assessment of equipment health. This approach enables operators to make informed decisions about when and how to perform maintenance, rather than relying on fixed schedules. As a result, maintenance activities can be better aligned with actual equipment needs, extending asset life and improving overall system availability.

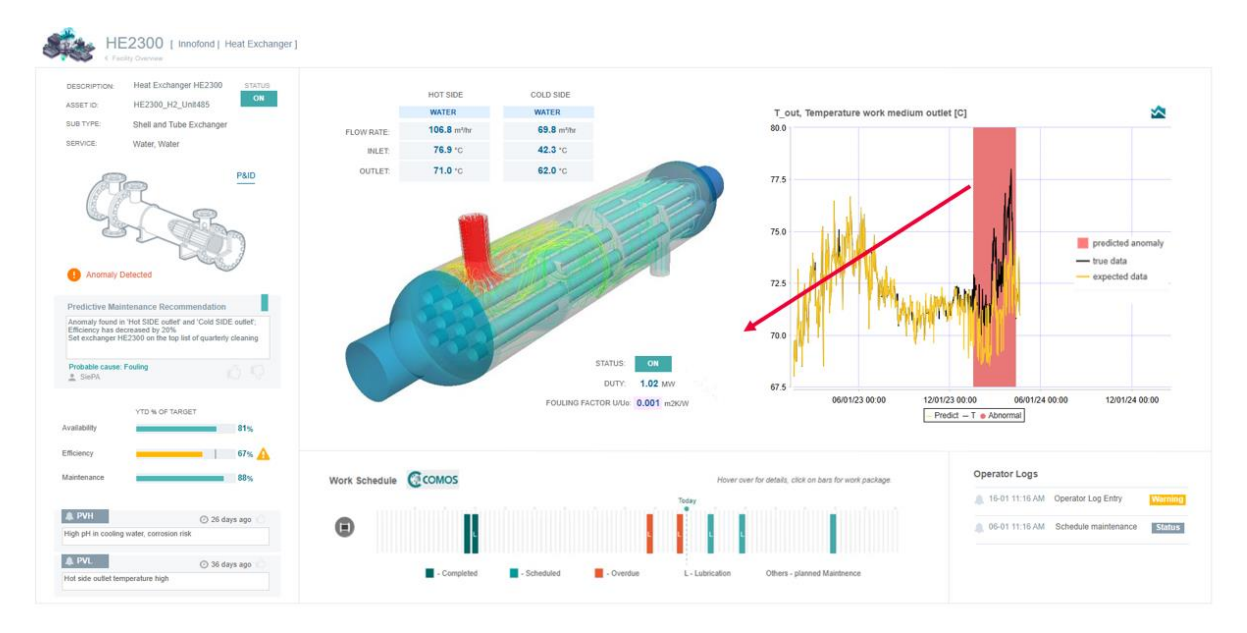


Figure 6 - Predictive Maintenance using Anomaly Detection for a Heat Exchanger

In cases where maintenance is required, digital worker solutions offer valuable support. Digital twins—virtual representations of physical assets—can guide maintenance personnel through step-by-step procedures via mobile devices. These tools can also connect technicians remotely with experts, ensuring that complex tasks are carried out correctly and efficiently (Capgemini-Siemens, 2024).

9. Economic and Environmental Impact of Optimization

The implementation of digital technologies and optimization strategies in carbon capture and hydrogen production facilities not only improves technical performance but also delivers measurable economic and environmental benefits. By enhancing energy efficiency, process control, and maintenance practices, these solutions help reduce costs, increase productivity, and support decarbonization efforts.

9.1 Cost Reduction Potential

Digital optimization offers substantial potential to reduce costs across all major areas of hydrogen production and carbon capture. Based on a reference scenario and observed benefits from comparable projects, the levelized cost of hydrogen (LCOH) can be reduced by an estimated 9% to 12% through the activation of targeted digital levers (Capgemini-Siemens, 2024).

This reduction is achieved through a combination of following measures (Capgemini-Siemens, 2024):

- CAPEX savings of up to 13% are enabled by project twins that optimize system design and support standardized asset replication.
- Electricity costs are reduced by 5% through the use of flexibility solutions, including energy management systems (EMS), base load management, and microgrid control.
- Annual OPEX, excluding electricity, is lowered by 10%, primarily through operations and maintenance twins that improve process efficiency and reduce labor-related costs.
- Production volume increases by 7%, driven by a 5% improvement in energy efficiency and a 2% gain in equipment availability enabled by predictive maintenance and anomaly detection technologies.

Similar cost reduction potential applies to carbon capture facilities, where digital optimization supports lower energy consumption and facilitates the replication of standardized designs, reducing engineering effort and implementation time.

9.2 Environmental Benefits

Beyond cost reduction, optimization of carbon capture and hydrogen production facilities offers significant environmental benefits. Optimized operations ensure that carbon capture systems operate at maximum efficiency, enabling more CO₂ to be captured per unit of energy consumed. In hydrogen production, process optimization reduces both energy and water consumption per unit of output, contributing to greater resource efficiency and lowering the environmental footprint.

Digital optimization also enhances the economic viability of these technologies, accelerating their adoption in hard-to-abate sectors such as cement and steel production. This supports faster decarbonization and helps reduce emissions in industries that are traditionally difficult to electrify. Additionally, captured CO₂ can be reused in the production of synthetic fuels, methanol, urea, and other chemicals, contributing to circular economy models and further lowering overall emissions.

Beyond operational efficiency, digital technologies support lifecycle emissions reduction by improving system design, minimizing material usage, and shortening construction timelines (Capgemini-Siemens, 2024). Advanced monitoring tools enable accurate tracking of environmental performance, ensuring regulatory compliance and increasing transparency in sustainability reporting.

Water footprint optimization also plays a critical role, particularly in hydrogen production, where reduced water consumption per unit of hydrogen is especially beneficial in water-scarce regions. Together, these measures strengthen the environmental sustainability of industrial decarbonization efforts.

10. Conclusion

Carbon capture and hydrogen production technologies are critical for achieving global climate goals. However, their successful deployment depends not only on technological innovation but also on robust policy and regulatory frameworks. Standardization of carbon intensity metrics, certification of low-carbon products, and transparent trading systems for carbon credits and low-carbon hydrogen are necessary to building trust and enabling market growth.

Digital technologies such as digital twins and advanced process optimization offer powerful

tools to address technical and economic challenges. They enable more efficient integration of carbon capture and hydrogen production and improve economic viability through flexible operational strategies.

International collaboration and harmonized regulations are key to establishing global markets for green hydrogen and carbon credits. Shared infrastructure and aligned standards can accelerate deployment and reduce costs.

An approach that integrates digital technologies from the outset, supported by robust data platforms and digital twins, can enhance efficiency, minimize risks, and accelerate the adoption of these key technologies. Especially in projects aiming for a successful Final Investment Decision (FID), digital twins strengthen investor and stakeholder confidence by providing transparency and validation of complex concepts (Laws & Szeliga, 2025).

By addressing the challenges and implementing the strategies outlined in this article, stakeholders can contribute to the development of an efficient, economical, and environmentally friendly energy ecosystem that helps meet our climate goals while supporting economic development.

References

- 1. Capgemini-Siemens (2024). WhitePaper-Capgemini-Siemens, Accelerating low-carbon hydrogen and cutting costs with digital technology
- 2. Laws, B., & Szeliga, N. (2025). US-DI-PA-GM-H2-Global-H2-Review-Jan25_original: Unlocking Plant Performance in an Uncertain World. Siemens Digital Industries.
- 3. Eboumbou Ebongu, Y., & Sauer, A. (2024). Energieflexibler Betrieb von Carbon-Capture-Anlagen in der Zementindustrie. 18. Symposium Energieinnovation, 14.-16.02.2024, Graz/Austria.
- 4. Verein Deutscher Zementwerke e.V. (VDZ). (2022). Umweltdaten der deutschen Zementindustrie: 2022. Referenced in Energieflexibler Betrieb von Carbon-Capture-Anlagen in der Zementindustrie.
- 5. IEA Publications (2022). IEA CCUS Handbook Legal and Regulatory Frameworks for CCUS
- 6. International Energy Agency (2023), Global Hydrogen Review 2023. Referenced in Hydrogen-WhitePaper-Capgemini-Siemens.original.
- 7. BNP Paribas https://cib.bnpparibas/the-future-of-carbon-capture-and-storage-strategies-and-challenges/

Operando spectroscopic techniques to investigate molecular catalysts in flow

Rucha S. Medhekar¹, Aleksander Sobolev², Martin Gerlach², Christof Hamel²,

Walter Leitner^{1,3}, Andreas J. Vorholt¹

¹Max-Planck-Institut für Chemische Energiekonversion, Mülheim a.d.Ruhr

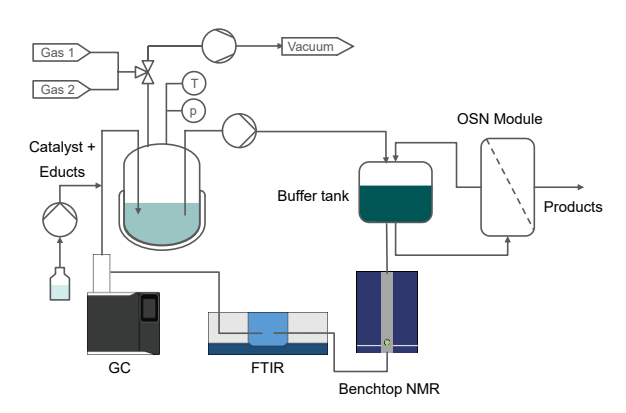
²Otto-von-Guericke-Universität Magdeburg, Magdeburg

³Institut für Technische Chemie und Makromolekulare Chemie (ITMC), RWTH Aachen University, Aachen, Germany

Abstract

High catalyst stability is an important property necessary for good catalytic performance, especially when continuous processes with physical separation steps are considered. Catalyst deactivation greatly affects the catalyst performance leading to reduced conversion and selectivity. This can result in varied product streams, reduced reaction, and higher process costs, and in general a reduced process performance. Studying the catalytic system and understanding the deactivation mechanisms, to then control the reaction conditions before the product quality actually declines, could result in more stable product qualities. Operando spectroscopy is an emerging tool for studying the catalytic system, which utilizes real-time analytical techniques, carried out under reaction conditions. [3]

In our work, operando spectroscopic techniques are used to investigate the catalytic cycle of hydroformylation of 1-decene, catalyzed by a Rh catalyst complex. For this purpose, a miniplant is set up in which the reaction mixture from the reactor is pumped through the NMR, FTIR and GC. [4] With this operando setup, it is possible to detect unstable intermediates formed during the reaction and thus analyze the catalytic cycle. In this work, the hydroformylation of 1-decene was successfully monitored. In addition, methods for prolonging and restoring catalytic activity are to be developed and used for process control, in order to obtain more stable product streams.



- [1] J. M. Dreimann, E. Kohls, H. F. W. Warmeling, M. Stein, L. F. Guo, M. Garland, T. N. Dinh, A.J. Vorholt, ACS Catalysis, 2019, 9 (5), 4308–4319.
- [2] R. H. Crabtree, Chem. Rev., 2015, 115, 127–150.
- [3] K. Köhnke, N. Wessel, J. Esteban, J. Jin, A. J. Vorholt and W. Leitner, Green Chem., 2022, 24, 1951– 1972.
- [4] N. Wessel, R. S. Medhekar, M. Sonnenberg, H. Stieber, W. Leitner, A.J. Vorholt, ACS Catal. 2024, 14, 10679-10688.

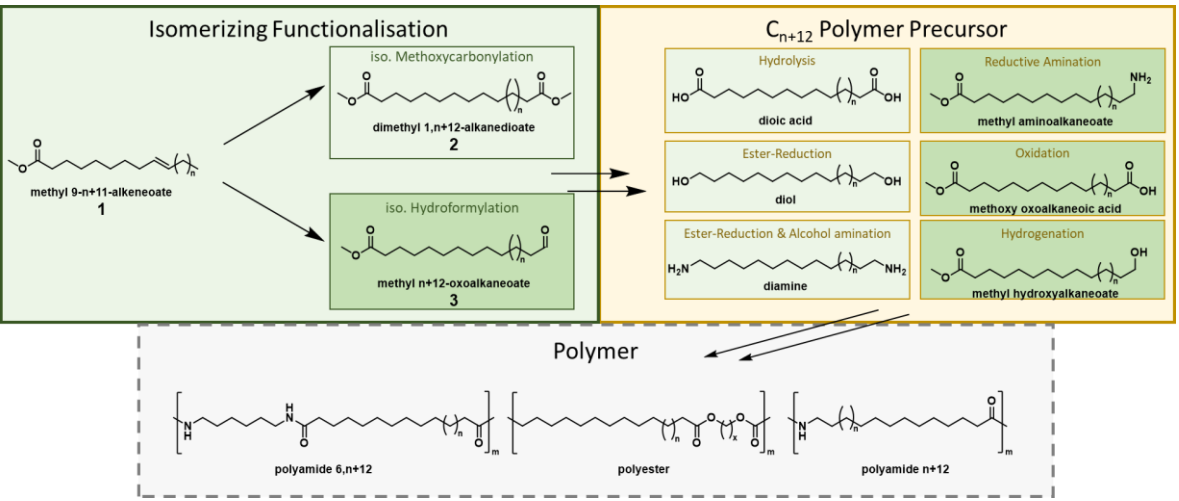
Funded by the Deutsche Forschungsgemeinschaft under project number 537105915.

Linear, Aliphatic Polymer Precursors from Local Plant Oils through Cross Metathesis and Isomerizing Functionalisation

J. Hommes, D. Vogt, T. Seidensticker TU Dortmund University, Laboratory of Industrial Chemistry, Germany

Abstract

The demand for versatile and high-performance polymers, such as polyesters or polyamides, is steadily increasing. To access those polcondensates, a diverse portfolio of C_{n+12} building blocks, such dioic acids, methyl aminoalkaneoates, and diamines, as well as many more, is required. Those building blocks are currently produced based on fossil raw materials. Here, dimethyl 1,n+12-alkanedioate (2) and methyl n+12-oxoalkaneoate (3) may serve as central platform molecules for those C_{n+12} polycondensates. Those are products of isomerizing functionalization reactions such as the isomerizing methoxycarbonylation or hydroformylation of methyl 9-alkeneoate (1). 1 can be produced *via* cross-metathesis of methyl oleate, accessible from local plant oils, and a respective alkene. Scheme 1 illustrates possible C_{n+12} polymer precursors, as well as the polymers that can be produced from 2 and 3.



Scheme 1: Isomerizing functionalisation of methyl 9-n+11-alkeneoate (1) to dimethyl 1,n+12-alkanedioate (2) via isomerizing methoxycarbonylation and to methyl n+12-oxoalkaneoate (3) via isomerizing hydroformylation, as a platform for C_{n+12} polymer precursors such as dioic acids, methyl aminoalkaneoates, diamines, etc.

The internal double bond of 1 requires a preliminary isomerization step before methoxycarbonylation or hydroformylation to obtain 2 or 3, preferably conducted using an auto-tandem catalytic system. We will primarily investigate the isomerizing hydroformylation of 1 to 3 with rhodium as catalyst metal with bidentate phosphorus ligands and the isomerizing methoxycarbonylation of 1 to 2 with palladium as catalyst metal and 1,2-DTBPMB as ligand.

[1] K. Hares, H. W. Wegener, T. F. H. Roth, R. Reichert, D. Vogt, T. Seidensticker, Catal. Sci. Technol. 2024, DOI: 10.1039/D4CY00368C.

Direct, tandem catalysis synthesis of higher alcohols from *syngas*: the influence of water on reaction rates and alcohol (regio)selectivity

F. Fiore¹, A. Rodriguez-Gomez¹, D. De Baker¹, M. Claeys², Ā. J. Vorholt³, G. Prieto¹ ITQ Instituto de Tecnología Química (UPV-CSIC), Valencia Spain

Abstract

Synthetic, high-energy-density, liquid e-fuels are expected to play a central role in the reduction of GHG emissions from hard-to-electrify, heavy-duty and long-haul transport, such as waterborne transport. Various liquid e-fuels have been proposed to replace fossil-derived diesel-type fuels, commonly produced through syngas conversion pathways such as Fischer-Tropsch synthesis, methanol synthesis, or direct dimethyl ether (DME) synthesis. The E-TANDEM project aims to enable the efficient and direct production of a new higher-oxygenate diesel-like e-fuel (HOEF) from carbon dioxide, water and renewable energy as the only inputs. The new HOEF formulation, based on heavy aliphatic alcohols and ethers (C_{5+}), is expected to combine the combustion advantages and engine/infrastructure-compatibility of paraffinic compounds with the soot reduction potential of oxygenated fuels. The tandem production of higher alcohols combines solid catalyzed, higher olefin-selective Fischer-Tropsch synthesis (FTS) with a molecular complex-catalyzed reductive hydroformylation (RHF) of FTS 1-olefins to higher alcohols in a slurry-phase with a high-boiling-point solvent (squalane). This approach contributes to overcome the operational limitations of alternative routes for the direct and selective conversion of syngas into higher alcohols [1]. Water, a major side-product of the FTS, may have multiple effects on catalytic performance, affecting the syngas conversion rate, selectivity as well as the stability of both the solid and molecular catalysts under the developed hydrothermal conditions (T=200 °C, P>150 bar). In this work, kinetic and selectivity effects of water are systematically studied by incorportating different amounts of exogenous water to the reaction medium, at the onset of batch-wise syngas conversion tests. The addition of exogenous water led to a remarkable increase of both higher alcohol selectivity and

productivity, reaching 38 C% and $mg \cdot g_{Co}^{-1} \cdot h^{-1}$, 212 respectively (**Figure 1**). Furthermore, surface hydrophobization of the FTS catalyst (via grafting with silylating agents) results in a further increase in alcohol selectivity to ca. 45 C%. Remarkably, the presence of water enhanced the linear-to-branched ratio in the higher alcohol products to 4-5, further facilitating alcohol dehydration to synthetic. aliphatic ether (e)fuels.

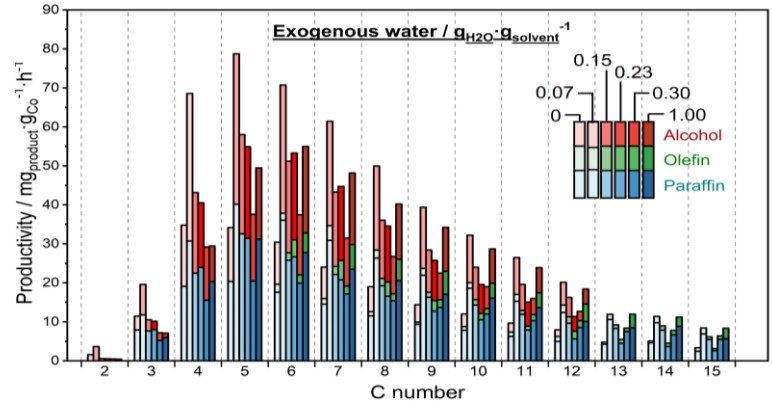


Figure 1: Evolution of the liquid product distribution for the tandem FTS-RHF syngas conversion to higher alcohols, as a function of the carbon chain length and the initial content of exogenous water.

²Catalysis Institute, Department of Chemical Engineering, University of Cape Town, Rondebosch South Africa.

³Max Planck Institute for Chemical Energy Conversion, Mülheim an der Ruhr, Germany

^[1] Direct Conversion of Syngas to Higher Alcohols via Tandem Integration of Fischer–Tropsch Synthesis and Reductive Hydroformylation, K. Jeske, T. Rösler et al., *Angew. Chem. Int. Ed.* 2022, 61.

Property-performance relationship assessment of tailored nanoparticles for alkaline water electrolysis

Tegiton Simson Sicila Mary, 1,2,3 Angelina Barthelmeß, Moritz Wolf, 2,4 Johanna Schröder Institut für Technische Chemie und Polymerchemie, Karlsruher Institut für Technologie (KIT), Karlsruhe, Germany.

- ² Institut für Katalyseforschung und -technologie (IKFT), Karlsruher Institut für Technologie (KIT), Eggenstein-Leopoldshafen, Germany
- ³ Technical University of Munich (TUM), Munich, Germany
- ⁴ Engler-Bunte-Institut, Karlsruher Institut für Technologie (KIT), Karlsruhe, Germany

Abstract

Tackling climate change is one of the major challenges nowadays asking for a reduced use and alternatives to fossil fuels. While hydrogen is currently often produced in fossil fuel reforming processes, water electrolyzers are a promising technological, electrocatalytic solution producing hydrogen (and oxygen) by splitting water electrically via renewable energy that can open up a novel, sustainable hydrogen-based energy landscape. Hydrogen can be used in hydrogen fuel cells, CO₂ reduction to form base chemicals or synthetic fuels, steel production, and many other industrial and chemical processes.

The two reactions occurring in water electrolyzers, hydrogen and oxygen evolution (HER, OER), are in mutual dependence. To overcome the slow OER process that particularly limits the overall electrolyzer efficiency, novel material designs for OER catalysts are needed. Expensive precious metals can be replaced by cheaper and less critical metals such as cobalt, iron, and nickel in alkaline electrolyzers as OER catalysts.

In contrast to state-of-the-art alkaline electrolyzers, anion-exchange membrane (AEM) electrolyzers avoid highly alkaline solutions and consist of a catalyst-membrane-catalyst assembly. Property tuning of non-precious OER catalyst materials for AEM electrolyzers is of high interest to increase the overall electrolyzer efficiency using non-critical materials supporting the development of next generation electrolyzer applications for a more sustainable energy landscape. In our contribution, we present the synthesis and characterisation of well-defined mixed (cobalt, iron, nickel) oxide or (oxy)hydroxide nanoparticles with distinct composition. The OER performance is evaluated in a rotating disk electrode (RDE) setup and correlated to the precatalyst and post-electrocatalysis properties.

Methanolation of Olefins: Versatile low-pressure synthesis of various alcohols from olefins and methanol

<u>Sebastian Stahl</u>^{1,2}, Jeroen T. Vossen^{1,2}, Jan Mädicke^{1,2}, Stephan Popp^{1,2}, Walter Leitner^{1,2}, Andreas J. Vorholt¹

¹Max Planck Institute for Chemical Energy Conversion, Mülheim an der Ruhr, Germany ²Institute for Technical and Macromolecular Chemistry, RWTH Aachen University, Aachen, Germany

Abstract

Methanol is considered a central molecular pivot between renewable energy and the chemical value chain. Such "green" methanol can be produced at sites with a large green energy capacity and transported within existing infrastructure to locations where it is in demand.[1] As a carbon source for the chemical industry, methanol can be implemented in existing processes or open opportunities for emerging applications.[2] One field that has seen little attention to date is the utilization of methanol as liquid equivalent of synthesis gas (CO/H_2). Leitner et al. showed the reversibility of the methanol synthesis from synthesis gas with a homogeneous Mn/pincer catalyst in the dehydrogenation of methanol to CO and H_2 .[3] In our recent work we paired this synthesis gas liberating reaction with the reductive hydroformylation of olefins to alcohols as this utilizes the CO/H_2 ratio of 1:2 as produced from methanol.[4]

This so-called "methanolation of olefins" formally describes the addition of methanol to olefins in a 100% atom economic manner without the need for external pressurized synthesis gas. The homogeneous Mn/pincer catalyst is combined with the Rh-based hydroformylation catalyst in one system, providing various synergistic effects. Unprecedented selectivity towards alcohols, excellent regioselectivities for the simple ligands employed and a high hydroformylation rate and TON of more than 17 121 in a single batch experiment were demonstrated with Rh concentrations in the low ppm range.

This process eliminates the need for high-pressure equipment or synthesis gas infrastructure due to the low overall reaction pressure. This drastically reduces the investment costs thus making it more accessible to a wide range of potential users on the laboratory and industrial scale and integrates "green" methanol as a sustainable synthesis gas source into the production of important intermediates and products of the present and future chemical industry. We now aim to demonstrate the broad applicability to structurally divers substrates with high demand in different branches of the chemical industry.

Literature

- [1] Olah, G. A., Goeppert, A., Prakash, G. K. S. *Beyond Oil and Gas: The Methanol Economy*; Wiley-VCH Verlag GmbH & Co. KGaA: Weinheim, **2009**.
- [2] V. Dieterich, A. Buttler, A. Hanel, H. Spliethoff, S. Fendt, *Energ. Environ. Sci.* **2020**, *13*, 3207–3252.
- [3] A. Kaithal, B. Chatterjee, C. Werlé, W. Leitner, *Angew. Chem. Int. Ed.* **2021**, *60*, 26500–26505
- [4] S. Stahl, J. T. Vossen, S. Popp, W. Leitner, A. J. Vorholt, *Angew. Chem. Int. Ed.* **2025**, *64*, e202418984.